

# Understanding cell-autonomous and non-autonomous signalling events in stomatal immunity

Janina Anna-Maria Tamborski

September 2018

A thesis submitted to the University of East Anglia for the degree of Doctor of Philosophy

This copy of the thesis has been supplied on condition that anyone who consults it is understood to recognise that its copyright rests with the author and that use of any information derived there from must be in accordance with current UK Copyright Law. In addition, any quotation or extract must include full attribution.

## Contents

Understanding cell-autonomous and non-autonomous signalling events in stomatal immunity .....	1
Abstract.....	7
List of tables .....	8
List of figures.....	9
Acknowledgements.....	11
Abbreviations .....	13
1. Introduction .....	16
1.1. The Plant's Immune System.....	16
1.1.1. Pattern-triggered Immunity (PTI).....	16
1.1.1.1. Perception of microbes at the plasma membrane by Pattern Recognition Receptors (PRRs).....	16
1.1.1.2. Perception of the bacterial MAMP flg22 by FLAGELLING SENSING 2 (FLS2) 18	
1.1.1.3. Perception of chitin through LYK5 and CERK1 .....	20
1.1.1.4. Calcium signalling in PTI.....	21
1.1.1.5. MAP Kinase cascades involved in defence.....	22
1.1.1. Effector-triggered Immunity .....	23
1.1.1.1. Pathogens secrete proteins to modulate host processes.....	23
1.1.1.2. Intracellular Immune Receptors: NLRs .....	24
1.1.1.3. Functional cooperation of NLRs to mediate effector recognition .....	25
1.1.1.4. Molecular basis of NLR activation.....	26
1.1.1.5. Activation of NLRs through Effectors.....	27
1.1.1.6. Integrated domains within NLRs.....	29
1.2. Stomata.....	30
1.2.1. Stomatal development.....	31
1.2.2. Stomatal movement .....	33
1.2.2.1. Regulation of stomatal opening.....	33
1.2.2.2. Stomatal closure .....	35
1.2.3. Stomatal closure signalling pathways.....	36
1.2.3.1. ABA-induced stomatal closure .....	36
1.2.3.2. CO <sub>2</sub> -induced stomatal closure.....	39
1.2.3.3. MAMP-induced stomatal closure .....	39
1.2.3.4. Pathogen interference with stomatal closure .....	41

1.3.	Aims and Objectives.....	43
2.	Material and Methods .....	45
2.1.	Media and Buffers:.....	45
2.1.1.	GM medium for <i>Arabidopsis thaliana</i> seedlings.....	45
2.1.2.	L medium for bacterial growth .....	45
2.1.3.	King's B medium.....	45
2.1.4.	Protein Buffers .....	46
2.1.4.1.	Plant Protein Extraction Buffer .....	46
2.1.4.2.	Loading/Sample buffer.....	46
2.1.4.3.	Kinase buffer .....	46
2.1.5.	Stomata opening buffer .....	46
2.1.6.	<i>Agrobacterium tumefaciens</i> infiltration buffer.....	46
2.1.7.	Solutions for protoplast isolation .....	46
2.1.7.1.	Enzyme solution .....	46
2.1.7.2.	PEG Solution.....	47
2.1.7.3.	W5 Solution.....	47
2.1.7.4.	MMg Solution.....	47
2.2.	Antibiotics .....	47
2.3.	Antibodies and beads used in this study .....	47
2.4.	Plant Materials.....	48
2.5.	Bacterial strains and pathogens.....	49
2.6.	Methods.....	49
2.6.1.	Plant growth conditions.....	49
2.6.1.1.	<i>Arabidopsis thaliana</i> and <i>N. benthamiana</i> seed sterilisation with chlorine gas	49
2.6.1.2.	Growing <i>Arabidopsis thaliana</i> and <i>N. benthamiana</i> seeds on plates....	49
2.6.1.3.	Growing <i>Arabidopsis thaliana</i> and <i>N. benthamiana</i> on soil .....	50
2.6.2.	Generation of transgenic plants .....	50
2.6.3.	Polymerase Chain Reaction (PCR) for cloning:.....	50
2.6.4.	Polymerase Chain Reaction (PCR) for genotyping .....	50
2.6.5.	Colony Polymerase Chain Reaction (PCR).....	51
2.6.6.	Restriction Enzyme digest .....	51
2.6.7.	Golden Gate cloning.....	51
2.6.8.	Restriction Enzyme Cloning.....	52

2.6.9.	Bacterial transformation.....	53
2.6.9.1.	Heat-shock .....	53
2.6.9.2.	Electroporation .....	53
2.6.10.	Isolation of genomic DNA .....	53
2.6.11.	Edwards method.....	53
2.6.12.	Boiling method.....	54
2.6.13.	Site-directed point mutagenesis.....	54
2.6.14.	RNA isolation using TRI reagent.....	54
2.6.15.	cDNA synthesis.....	55
2.6.16.	Protein extraction from plant samples .....	55
2.6.17.	Co-Immunoprecipitation of <i>Arabidopsis thaliana</i> proteins .....	55
2.6.18.	SDS-Page and Semi-dry Western blotting.....	56
2.6.19.	Expression and purification of recombinant proteins .....	56
2.6.20.	Transphosphorylation assay .....	57
2.6.21.	Spray infection assay.....	57
2.6.22.	Isolation and transfection of mesophyll protoplasts .....	58
2.6.23.	Isolation of guard cell-enriched samples .....	58
2.6.24.	Split-YFP assay.....	59
2.6.25.	Confocal imaging.....	59
2.6.26.	Virus-induced gene silencing (VIGS) .....	59
2.6.27.	ROS measurements.....	60
2.6.28.	Stomatal aperture measurements.....	60
2.6.29.	Generation of amiRNA constructs .....	60
2.6.30	Quantification of GFP in confocal micrographs .....	62
2.7.	Primers used in this study:.....	62
2.8.	Constructs generated in this study: .....	68
3.	Virus-induced gene silencing and guard cell-specific promoters as useful tools to study guard cell responses .....	72
3.1.	Introduction .....	72
3.2.	Results.....	74
3.2.1.	Virus-induced gene silencing does not affect guard cells in fully expanded leaves in <i>N. benthamiana</i> .....	74
3.2.2.	Guard cell-specific promoter screen in <i>Arabidopsis thaliana</i> .....	80
3.3.	Discussion.....	83

4.	Stomatal immunity involves guard cell-specific and non-autonomous signalling events	85
4.1.	Introduction .....	85
4.2.	Results.....	87
4.2.1.	Guard cell-excluding VIGS of <i>NbSERK3a/b</i> and <i>NbRBOHB</i> demonstrates guard cell autonomy .....	87
4.2.2.	Guard cell-specific complementation of RBOHD .....	89
4.2.2.1.	Generation of guard cell-specific RBOHD complementation lines in <i>Arabidopsis thaliana</i> .....	89
4.2.2.2.	<i>rboh1d/pMYB60::GFP-RBOHD</i> and <i>rboh1d/pMYB60::mCherry-RBOHD</i> plants appear to have accumulation of the cleaved tag in the tonoplast .....	89
4.2.2.3.	Guard cell-specific GFP-RBOHD plants and over-expressers show free GFP signal in Western Blot.....	91
4.2.2.4.	ROS production between transgenic lines varies strongly .....	92
4.2.3.	Guard cell-specific complementation of FLS2 in <i>Arabidopsis thaliana</i> .....	95
4.2.3.1.	Guard cell-specific complementation of FLS2 with the promoter <i>pMYB60</i>	95
4.2.3.2.	<i>pMYB60::FLS2-GFP</i> lines express FLS2-GFP to different levels.....	95
4.2.3.3.	flg22-triggered ROS production is strongly reduced in <i>fls2</i> and guard cell-specific expressers of FLS2.....	97
4.2.3.4.	MAMP recognition restricted to guard cells is sufficient to induce stomatal closure in response to flg22.....	99
4.2.3.5.	<i>pMYB60::FLS2-GFP</i> plants are not more susceptible to infection by <i>Pst</i> DC3000	99
4.2.4.	Silencing of <i>NbRBOHB</i> and pavement cell complementation with <i>AtEFR</i> and <i>AtRBOHD</i> leads to restoration of the elf18-induced stomatal closure.....	100
4.2.5.	Guard cell-specific knock-down with artificial micro-RNAs in <i>Arabidopsis thaliana</i>	103
4.2.5.1.	Generation of artificial micro RNAs (amiRNAs) against FLS2 and RBOHD	103
4.2.5.2.	Guard cell-specific knock-down of FLS2 with the use of amiRNAs under the control of <i>pMYB60</i> .....	105
4.2.5.3.	Guard cell-specific knock-down of FLS2 does not alter susceptibility to <i>Pst</i> DC3000	106
4.3.	Discussion .....	107
5.	MAMP-induced stomatal closure is mediated by SnRK2.3 and is independent of ABA biosynthesis .....	110
5.1.	Introduction .....	110

5.2.	Results.....	113
5.2.1.	MAMP-induced stomatal closure acts independent of the ABA stomatal closure pathway.....	113
5.2.1.1.	ABA biosynthesis is not required for stomatal closure in response to flg22	113
5.2.1.2.	ABA receptor mutants do not have a clear flg22 stomatal closure phenotype	115
5.2.1.3.	The dominant <i>abi1-1</i> mutant closes its stomata to flg22 treatment ..	117
5.2.1.4.	<i>ost1-3</i> and <i>ost1-4</i> knock-out mutants respond to flg22 .....	117
5.2.1.5.	OST1 kinase is not active after flg22 treatment.....	119
5.2.1.6.	<i>snrk2.2 snrk2.3 ost1-3</i> is unresponsive to flg22 treatment but can respond to H <sub>2</sub> O <sub>2</sub> treatment.....	119
5.2.1.7.	SnRK2.3 is required for MAMP-induced stomatal closure .....	119
5.2.2.	SnRK2.3 interacts with BIK1 .....	120
5.2.2.1.	OST1 and SnRK2.3 interact with FLS2, BIK1 and ABI1 in split-YFP assay	120
5.2.2.2.	SnRK2.3 interacts with BIK1 in co-IP assay in <i>Arabidopsis thaliana</i> protoplasts	123
5.2.3.	PBL1 could mediate anion channel activation in response to flg22 treatment in guard cells .....	125
5.2.3.1.	<i>pbl1</i> mutant stomata do not respond to flg22 treatment .....	125
5.2.3.2.	PBL1 activates SLAH3 anion channel in oocyte measurements .....	127
5.2.3.3.	BIK1 or PBL1 do not phosphorylate SnRK2.3, OST1, SLAH3 or SLAC1 in a recombinant kinase assay .....	127
5.3.	Discussion.....	130
6.	Discussion.....	134
6.1.	PBL1 and SnRK2.3 are novel players in MAMP-induced stomatal closure .....	134
6.2.	Several cell types mediate stomatal immunity.....	135
6.3.	Cell type-specific responses of Pattern-triggered immunity (PTI).....	137
6.4.	Cell type- and tissue-specific responses of Effector-triggered immunity (ETI)....	138
6.5.	Outlook .....	139
7.	Bibliography .....	140

## Abstract

Stomata are entry sites for bacterial pathogens and can affect the outcome of infection to the disadvantage of the pathogen. This is referred to as stomatal immunity. Guard cells can mediate certain responses in a cell-autonomous manner, but this question remains to be addressed for pathogen-induced stomatal closure.

This study reports transient and stable transgenic approaches to study guard cell responses. I employed virus-induced gene silencing and guard cell-specific promoters to investigate guard cell autonomy and non-autonomous signalling events during pathogen-induced stomatal closure. Plants that express FLAGELLIN SENSING 2 (FLS2) only in the guard cells retained stomatal closure to flg22 and wild-type-like susceptibility levels to bacterial infection. Interestingly, guard cell-specific knock-down of FLS2 did not impair stomatal closure or resistance to bacteria, suggesting that non-autonomous signalling events can mediate stomatal closure during pathogen invasion.

Screening mutants of abscisic acid (ABA) signalling components revealed that pathogen-induced stomatal closure is independent from the prototypic drought stomatal closure pathway. I showed that OPEN STOMATA 1 is not involved in pathogen-induced stomatal closure and that it was inactive after flg22 treatment. Instead, the mutant of a related kinase SUCROSE NON-FERMENTING RECEPTOR KINASE 2.3 (SnRK2.3) was impaired in its flg22 stomatal closure response suggesting that SnRK2.3 plays an important role in this response. SnRK2.3 interacted with BOTRYRIS-INDUCED KINASE 1 in split-YFP and co-immunoprecipitation assays. Interestingly, the PBS1-like 1 (PBL1) mutant was impaired in flg22-induced stomatal closure and PBL1 activated SLOW ANION CHANNEL-ASSOCIATED 1 HOMOLOGUE 3 (SLAH3) in oocyte measurements. This suggests PBL1 as major player in MAMP-induced stomatal closure.

My data reveal that aspects of stomatal immunity involve both guard cell-specific signalling events and non-symplastic cell-to-cell signalling. This work implicates independence of ABA- and pathogen-induced stomatal closure pathways and PBL1 as major regulator through direct activation of the anion channel SLAH3.

## List of tables

Table 2.2.1: Antibiotics and the concentrations used in this study.....	47
Table 2.3.1: Antibodies and beads used in this study.....	47
Table 2.4.1: <i>Arabidopsis thaliana</i> plants used in this study.....	48
Table 2.4.2: <i>Nicotiana benthamiana</i> plants used in this study.....	49
Table 2.5.1: Bacterial strains and pathogens used in this study.....	49
Table 2.7.1: Primer names and sequences used for Golden Gate Cloning.....	62
Table 2.7.2: Primer names and sequences used for genotyping of <i>Arabidopsis thaliana</i> .....	63
Table 2.7.3: Primer names and sequences used for restriction cloning.....	64
Table 2.7.4: Primer names and sequences used for Sanger sequencing.....	65
Table 2.7.5: Primer names and sequences used to generate artificial micro RNAs (amiRNAs .....	67
Table 2.8.1: Golden Gate level 0 vectors generated in this study .....	68
Table 2.8.2: Other Golden Gate vectors used in this study .....	69
Table 2.8.3: Golden Gate level 1 vectors generated in this study .....	70
Table 2.8.4: Golden Gate level 2 vectors generated in this study .....	71
Table 3.1: Information on promoters cloned for guard cell-specificity screen.....	80

## List of figures

Figure 1.1: Pattern-triggered immunity is mediated by plasma membrane-localised receptors.....	17
Figure 1.2: Domain structures of different types of plant NLRs.....	25
Figure 1.3: Illustration of cell-state transitions during stomatal development in <i>Arabidopsis thaliana</i> .....	32
Figure 1.4: Mechanisms of stomatal movement in <i>Arabidopsis thaliana</i> .....	34
Figure 1.5: Depiction of the main components of the prototypic Abscisic acid (ABA) -induced stomatal closure pathway.....	37
Figure 3.1: Confocal maximum projection micrographs of <i>pFLS2::FLS2-GFP</i> infiltrated with <i>TRV::GFP</i> .....	75
Figure 3.2: Confocal maximum projection micrographs of GFP16c infiltrated with <i>TRV::GFP</i> .....	77
Figure 3.3: Quantification of GFP intensity in silenced <i>N. benthamiana</i> plants.....	79
Figure 3.4: Confocal micrographs of 4-week-old transgenic <i>Arabidopsis thaliana</i> plants expressing free GFP under the control of different promoters in the T1 generation .....	81
Figure 3.5: Confocal micrographs of 4-week-old transgenic <i>Arabidopsis thaliana</i> plants expressing free GFP under the control of different promoters in the T2 generation .....	82
Figure 4.1: Guard cells act autonomously in MAMP-induced stomatal closure in transient assay.....	88
Figure 4.2: <i>pMYB60::GFP-RBOHD</i> and <i>pMYB60::mCherry-RBOHD</i> plants show tag accumulation in the tonoplast and surrounding cells .....	90
Figure 4.3: Generation of guard cell-specific RBOHD expression was unsuccessful .....	92
Figure 4.4: ROS signatures of <i>rbohD/pMYB60::RBOHD</i> lines in the T2 generation with different tags.....	93
Figure 4.5: Promoter <i>pMYB60</i> drives guard cell-specific expression and allows cell type-specific mutant complementation.....	96
Figure 4.6: Guard cell-specific expression of FLS2 is sufficient to induce stomatal closure to flg22 .....	98
Figure 4.7: MAMP recognition that is restricted to guard cells is sufficient for resistance to bacteria .....	100

Figure 4.8: Stomatal closure does not require guard cell ROS production or signalling via EFR .....	102
Figure 4.9: Characterisation of ROS response of transgenic plants expressing amiRNAs ...	104
Figure 4.10: Artificial micro-RNAs reduce FLS2 protein accumulation in guard cells.....	106
Figure 4.11: Guard cell-specific knock-down of FLS2 does not impair resistance to <i>Pst</i> DC3000 .....	107
Figure 5.1: MAMP-induced stomatal closure can be induced independently from ABA signalling .....	114
Figure 5.2: ABA receptor mutants do not give consistent stomatal closure phenotypes ...	116
Figure 5.3: MAMP-induced stomatal closure is mediated by SnRK2.3.....	118
Figure 5.4: OST1 interacts with BAK1, BIK1 and ABI1 in split-YFP assay in <i>Nicotiana benthamiana</i> .....	121
Figure 5.5: SnRK2.3 interacts with FLS2, BIK1, BAK1, ABI1, SnRK2.2 and OST1 in split-YFP assay in <i>Nicotiana benthamiana</i> .....	122
Figure 5.6: SnRK2.3 interacts with BIK1 in co-IP from <i>Arabidopsis thaliana</i> protoplasts....	124
Figure 5.7: PBL1 is a potential member of the flg22-induced stomatal closure pathway...	126
Figure 5.8: BIK1/PBL1 do not phosphorylate SnRK2.3, OST, SLAH3 or SLAC1 in cold kinase assay.....	129
Figure 5.9: Proposed model for PAMP-induced stomatal closure pathway.....	133

## Acknowledgements

I would like to thank my supervisor Prof. Silke Robatzek for the opportunity to do my thesis with her. I would also like to thank her for her guidance and support throughout my PhD.

Thank you also to my secondary supervisor Dr. Frank Menke, for his useful contributions during our committee meetings.

I am very grateful for the help of my Post-Doc mentor Dr. Michaela Kopischke. I appreciated all the feedback and help in the lab as well as her advice for dealing with challenging situations. All her support during the committee meetings was greatly appreciated and really made a difference to me.

I want to thank all the members of the Robatzek lab that have offered advice during lab meetings and during informal discussions. I greatly enjoyed our lunch and coffee breaks and the banter arising from them. Many of you have helped make this lab an enjoyable place to work and I am glad to have had the chance to work with you.

I am particularly thankful to my fellow Robatzek PhD students Jenna and Jelle. Thank you for all the banter, the support and understanding. Thank you, Jenna, for also being a wonderful friend outside of working hours. I have greatly enjoyed all our trips, concerts and all the other times we hung out. The PhD would have been very hard without your emotional support and understanding.

Thanks to the whole TSL student community for their collegiality and for creating such a wonderful sense of community. Although I have not been affiliated with a lab for periods of my PhD I have never truly felt alone, thanks to all of you. Special thanks to all the students in the PhD office and the many visiting students that have passed through there. You have helped create a very friendly work environment.

Big thanks go to the TSL support teams and the horticultural team. Their work and efforts have made life at TSL a lot easier and their friendly interactions have helped to make it more enjoyable. Thank you for all your help and contributions.

Thank you to Prof. Cyril Zipfel and his lab members for welcoming me in their lab during the last stretch of my PhD. I have welcomed your input and the way you integrated me into your lab.

Thank you to all the friends I have made here at TSL.

Thanks to Karen and Lynda for always having an open door for me and all your support during my parents' sickness and after my mother's death. It has helped me so much to know that you really care and I am grateful for all the help you have given me throughout the years.

Thank you to Matt for always finding a minute to talk to me when I needed advice. Thank you for mentoring me during difficult times in my PhD. Thank you for letting me babysit your kids when I needed distraction. Thank you for always listening and supporting me in whichever way you could.

Thank you to Jeoffrey, Jack, Helen and Sam. Your advice and friendship have been wonderful and I am glad to have had you around in difficult times.

I would also like to thank my family for their support throughout the years. Thanks to my father, two brothers and all the extended family.

Thank you, Mark, for your love and support. Thank you for always being there and supporting me through the hard times. Thank you for understanding my work obsession and for helping me in any way you can. I would not have made it without you.

Lastly, thanks go to my dear mother. It greatly saddens me that you are not with us anymore to see me graduate. Your love, support and your unwavering belief in me and that there is nothing I cannot achieve have gotten me here and I will continue to carry them with me.

## Abbreviations

ABA	Abscisic acid
ABI1	ABA Insensitive 1
ACA8	Autoinhibited Ca <sup>2+</sup> -ATPase, isoform 8
ACA10	Autoinhibited Ca <sup>2+</sup> -ATPase, isoform 10
AHA1	H <sup>+</sup> -ATPase 1
ALMT	Aluminium-activated anion channel
ATR1	<i>Arabidopsis thaliana</i> recognised 1
amiRNA	artificial micro-RNA
BAK1	BRI1-associated receptor kinase 1
bHLH	Basic Helix-loop-Helix
BHP	Blue light-dependent H <sup>+</sup> -ATPase Phosphorylation
BIK1	Botrytis-induced kinase 1
BLUS1	Blue light signalling 1
BRI1	BR insensitive 1
CA	Carbonic anhydrase
CBSP59	Candidate BIK1 substrate protein 59
CBL	Calcineurin B-like protein
CDPK	Calcium-dependent protein kinase
CERK1	Chitin-elicitor receptor kinase 1
CML	Calmodulin-like
CNGC	Cyclic nucleotide-gated ion channel
COI1	Coronatine-insensitive 1
COR	Coronatine
CPK	Calcium-dependent kinase
DNA	Deoxyribonucleic acid
dpi	Days post inoculation
dpg	Days post germination
EDS1	Enhanced disease resistance 1
EFR	EF-Tu Receptor
EF-Tu	Elongation factor TU
EPF	Epidermal patterning factor
ER	Endoplasmatic Reticulum
ERL	ERECTA-like
ETI	Effector-triggered Immunity
FLS2	Flagellin-sensing 2
GFP	Green Fluorescent Protein
GLR	Glutamate receptor-like channel
GMC	Guard mother cell
GSL8	Glucan Synthase 8
HMA	Heavy-metal associated
IP	Immunoprecipitation
JA	Jasmonic acid
KAT1	Potassium channel in <i>Arabidopsis thaliana</i> 1
LRR	Leucin-rich repeat
LYK5	Lysine-Motif receptor kinase 5
MAMP	Microbe-associated molecular Pattern
MAPK	Mitogen-activated protein kinase
MMCs	Meristemoid mother cells
MSL	Mechanosensitive ion channel MscS-like

NDR1	Non-race specific disease resistance 1
NLR	Nucleotide-binding leucine-rich repeat
NO	Nitric oxide
NRC	NLR Required for cell death
OSCA	Reduced hyperosmolarity-induced [Ca <sup>2+</sup> ] increase channel
OST1	Open Stomata 1
P2XR	Purigenic P2X receptor channel
PA	Phosphatidic acid
PAGE	Polyacrylamide gel electrophoresis
PBS1	AVRPPHB SUSCEPTIBLE 1
PBL1	PBS1-like 1
PBL2	PBS1-like 2
PHOT	Phototropin
PIP2;1	Plasma membrane intrinsic protein 2;1
PP2C	Type 2C protein phosphatases
PYR1	Pyrabactin-resistance 1
PYL	Pyrabactin-resistance 1-like
PM	Plasma membrane
PRR	Pattern Recognition Receptor
PRSL1	PP1 regulatory subunit2-like protein 1
PTI	Pattern-triggered Immunity
<i>Pst</i>	<i>Pseudomonas syringae</i> pv. <i>tomato</i>
RBA1	Response to the bacterial type III effector protein HopBA1
RBOHB	Respiratory Burst Oxidase Homologue B
RBOHD	Respiratory Burst Oxidase Homologue D
RBOHF	Respiratory Burst Oxidase Homologue F
RCAR	Regulatory component of ABA receptor
RIN4	RPM1-interacting protein 4
RKS1	Resistance related kinase 1
RLCK	Receptor-like cytoplasmic kinase
RLK	Receptor-like kinase
RLP	Receptor-like protein
RNA	Ribonucleic acid
RPM1	Resistance <i>Pseudomonas syringae</i> pv. <i>maculicola</i> 1
RPP1	Recognition of <i>Peronospora parasitica</i> 1
RPS2	Resistance to <i>P. syringae</i> 2
RPS4	Resistance to <i>P. syringae</i> 4
RPS5	Resistance to <i>P. syringae</i> 5
RRS1	Resistant to <i>Ralstonia solanacearum</i> 1
ROS	Reactive oxygen species
SA	Salicylic acid
SCRM	SCREAM
Ser	Serine
SERK	Somatic embryogenesis receptor kinase
SLAC1	Slow anion channel-associated 1
SLAH3	SLAC1 homologue 3
SLGCs	Stomatal-lineage ground cell
SnRK	Sucrose non-fermenting-1 related kinase
SOBIR1	Suppressor or Bir1-1
SPCH	Speechless
SUMM2	NLR Suppressor of MKK1 MKK2

T3SS	Type III secretion system
Thr	Threonine
TMM	Too many mouths
TRP	Transient receptor potential channel
VDCC	Voltage-dependent Ca <sup>2+</sup> channel
VIGS	Virus-induced gene silencing
ZAR1	HopZ-activated resistance 1
ZED1	HopZ-ETI-deficient 1

# 1. Introduction

## 1.1. The Plant's Immune System

### 1.1.1. Pattern-triggered Immunity (PTI)

#### 1.1.1.1. Perception of microbes at the plasma membrane by Pattern Recognition Receptors (PRRs)

The plant's immune system relies on each individual cell's capacity to mount a full immune response. This is achieved with every cell possessing a multitier surveillance system that recognises conserved molecular patterns that are indicative of a pathogen. These patterns are characteristic microbial molecules or host-derived molecules that arise during a pathogen attack. They are commonly referred to as microbe-associated molecular patterns (MAMPs) and host-derived damage-associated molecular patterns (DAMPs) (Gust *et al.*, 2017). Upon perception of these danger signals plant cells activate defence signalling including a number of measurable responses, for instance elevated cytosolic calcium concentrations, extracellular alkalization, production of reactive oxygen species (ROS), activation of mitogen-activated protein kinases (MAPKs), callose deposition and stomatal closure (Boller & Felix, 2009).

Perception of these patterns occurs at the plasma membrane by pattern-recognition receptors (PRRs) which are either receptor-like kinases (RLKs) or receptor-like proteins (RLPs). Plants have a largely expanded number of RLKs (Fritz-Laylin *et al.*, 2005) and RLPs compared to animals with over 600 members in *Arabidopsis thaliana*. PRRs typically consist of a unique extracellular ectodomain, a transmembrane domain and a cytoplasmic domain that, in the case of an RLK, possesses kinase activity. The cytoplasmic domains of RLPs are short and lack kinase activity so it is believed that RLPs rely on interacting kinases to relay signals to the cell's interior. The unique ectodomains participate in ligand binding and their specificity is believed to be defined by their different domain structures (Figure 1.1A). Such ectodomains are Leucin-rich repeats (LRRs), lysine motifs (LysM), lectin-type domains or EGF-like domains. LRR-RLKs and LRR-RLPs are the largest subfamily and usually bind proteins or peptides, for instance flg22 the recognised epitope from bacterial flagella, elf18 the recognised epitope from bacterial EF-Tu or endogenous AtPep peptides that arise during pathogen infection (Shiu & Blecker, 2001; Bohm *et al.*, 2014; Macho, A. P. & Zipfel, C., 2014; Macho, Alberto P. & Zipfel, Cyril, 2014). LysM, lectin-type and EFR-like domains confer perception of carbohydrate-based ligands, for example fungal chitin or bacterial

peptidoglycan, extracellular ATP, bacterial lipopolysaccharides (LPS) or oligogalacturonides that originate from plant cell-walls (Bohm *et al.*, 2014; Macho, Alberto P. & Zipfel, Cyril, 2014).

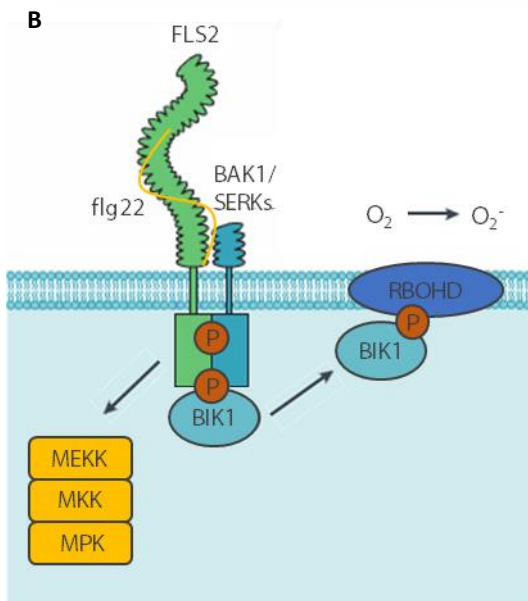
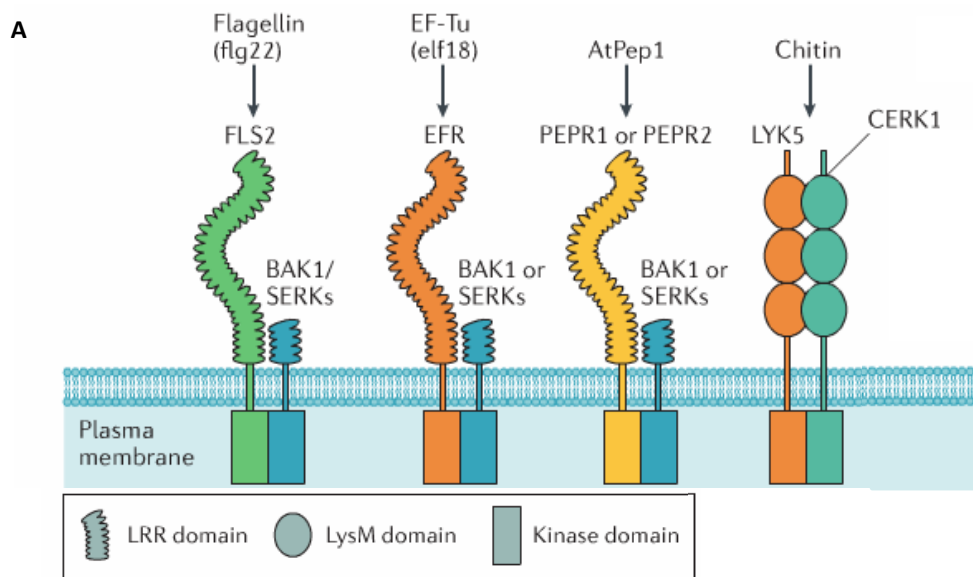


**Figure 1.1:** Pattern-triggered immunity is mediated by plasma membrane-localised receptors.

A. Domain structures of important Pattern Recognition Receptors (PRR) with their co-receptors and corresponding ligands. Leucine-rich-repeat (LRR) -type PRRs shown here are FLS2, EFR, PEPR1 with their co-receptor BAK1. In comparison displayed LysM-type PRR is LYK5 with its co-receptor CERK1.

B. Flg22-induced signalling pathway through FLS2. In *Arabidopsis thaliana* flg22 is perceived by the PRR pair FLS2 and BAK1. Binding of the ligand induces and stabilises dimerization of the co-receptors and leads to transphosphorylation events in their cytoplasmic kinase domains and onto cytoplasmic signalling partners known as

RLCKs such as BIK1. BIK1 phosphorylates and activates RBOHD, the main enzyme producing ROS in the apoplast. Subsequent signalling events include the activation of MAP-Kinase cascades and the activation of defense genes.

Figures adapted from Couto *et al.*, 2014.

Some LRR-RLKs seem to function as co-receptors through hetero-dimerization with certain LRR-RLK-type receptors and are known as somatic embryogenesis receptor kinases (SERKs) (Ma *et al.*, 2016). RLPs seem to rely on the LRR-RLK SUPPRESSOR OF BIR1-1 (SOBIR 1) as co-receptor to initiate downstream signalling (Liebrand *et al.*, 2014). Upon ligand perception receptor-like cytoplasmic kinases (RLCKs) get activated by PRRs and this subsequently

activates several parallel signalling pathways (Lin *et al.*, 2013). Downstream signalling pathways include mitogen-activated protein kinase (MAPK) cascades that mediate immune responses through direct phosphorylation of their substrates (Meng *et al.*, 2013). In the following section I will discuss examples of immune-associated RLKs and their signalling pathways in *Arabidopsis thaliana*.

#### 1.1.1.2. Perception of the bacterial MAMP flg22 by FLAGELLING SENSING 2 (FLS2)

FLS2 is one of the best characterized LRR-RLKs in plants. The ectodomain of FLS2 consists of 28 LRRs that bind the ligand, a transmembrane domain and an intracellular kinase domain (Chinchilla *et al.*, 2006). FLS2 recognizes bacterial flagellin (Gómez-Gómez & Boller, 2000) and is the main receptor mediating resistance to *Pseudomonas syringae* pv. *tomato* DC3000 (hereafter *Pst* DC3000), the virulent strain that can successfully colonise *Arabidopsis thaliana* (Zipfel *et al.*, 2004). The 22 amino acids of flagellin that participate in binding with the receptor (flg22) are commonly used to induce FLS2 signalling under laboratory conditions. Ligand binding induces FLS2 association with the regulatory LRR-RLK BRI1-ASSOCIATED RECEPTOR KINASE 1 (BAK1) (Chinchilla *et al.*, 2007). BAK1 is a member of the SERK family and with only five LRRs (Couto & Zipfel, 2016). The crystallization of the ectodomains of both receptors in complex with the ligand revealed how the interactions are formed and stabilised. In this complex, flg22 adopts a linear confirmation binding to LRR3-16 of FLS2 and to an “inner-curved loop” between Thr52 and Val54 in the N-terminus of BAK1. Since this interaction of flg22 bridges the association of FLS2 with BAK1 it is considered to act as a ‘molecular glue’ to stabilise the receptor complex (Sun *et al.*, 2013). Both FLS2 and BAK1 have an intracellular kinase domain but since FLS2 is a non-RD kinase and BAK1 is an RD-kinase their kinase activities are considerably different (Schwessinger *et al.*, 2011). Non-RD kinases carry an uncharged amino acid residue in the catalytic loop of the kinase domain, while RD kinases carry a conserved arginine residue (Dardick *et al.*, 2012). Since the FLS2 kinase activity is considerably weaker than that BAK1 (Schwessinger *et al.*, 2011) it has been suggested that the low kinase-activity of FLS2 is the reason for the association with BAK1 (Dardick *et al.*, 2012). Association of BAK1 and FLS2 is necessary for phosphorylation and activation of both proteins and strictly required to initiate downstream signalling (Lu, D. *et al.*, 2010; Sun *et al.*, 2013).

Upon perception of flg22 the receptor complex relays the extracellular danger signal to intracellular signalling partners. Receptor-like cytoplasmic kinases (RLCKs) were identified as direct substrates of PRR receptor complexes and critical for many downstream responses

(Liang & Zhou, 2018). Important RLCKs involved in flg22-induced immune signalling are BOTRYTIS-INDUCED KINASE 1 (BIK1) and AVRPPHB SUSCEPTIBLE 1-LIKE 1 (PBL1) which are part of the pre-formed FLS2-BAK1 receptor complex prior to flg22 perception (Lu, D. *et al.*, 2010; Zhang, Jie *et al.*, 2010). The *bik1 pbl1* double mutant is strongly impaired in a vast number of immune outputs including calcium influx, ROS burst, actin filament bundling, callose deposition, stomatal closure and seedling growth inhibition (Lu, Dongping *et al.*, 2010; Zhang, Jie *et al.*, 2010; Ranf *et al.*, 2014). Flg22 perception activates the receptor complex and BAK1 phosphorylates BIK1 (Zhang, J. *et al.*, 2010). BIK1 in turn phosphorylates both FLS2 and BAK1 and dissociates from the complex (Zhang, Jie *et al.*, 2010). After dissociation, BIK1 phosphorylates the RESPIRATORY BURST OXIDASE HOMOLOGUE D (RbohD), which is the NADPH oxidase predominantly producing apoplastic ROS in response to MAMPs (Nühse *et al.*, 2007; Kadota *et al.*, 2014). Additionally, RBOH enzymes are regulated by MAMP-induced elevation in cytosolic calcium as their N-terminal EF-hand motifs can bind calcium and CALCIUM DEPENDENT PROTEIN KINASEs (CDPKs) have been shown to phosphorylate RBOHD (Kobayashi *et al.*, 2007; Ogasawara *et al.*, 2008).

Another example of an RLCK acting as a positive regulator of immune signalling is BR-SIGNALING KINASE 1 (BSK1). It associates with FLS2 in *N. benthamiana* and a mutation in the gene impairs the flg22-induced ROS burst as well as resistance to several pathogens (Shi *et al.*, 2013). Many more RLCKs have recently been identified to be key signalling proteins acting in response to a vast array of different responses (Liang & Zhou, 2018) stressing their importance.

The activation of immune responses comes at the expense of growth and is therefore tightly regulated. Several regulatory mechanisms have already been uncovered that ensure a tight control on immune signalling activation and a swift switch-off when the attack has subsided. In the following section I will discuss a few examples of negative regulation of immune signalling. The prevention of interaction between inactivated receptor complex subunits is one such example. In the absence of a PTI trigger the LRR-RLK BAK1-INTERACTING RECEPTOR-LIKE KINASE 2 (BIR2), and other members of the same pseudokinase subfamily, interact with BAK1 to prevent association with FLS2 (Halter *et al.*, 2014). Consistently, in *bir2* mutants FLS2 and BAK1 show enhanced interaction (Halter *et al.*, 2014). After ligand perception BAK1 phosphorylates BIR2 and this leads to its dissociation which allows receptor complex formation (Halter *et al.*, 2014). It is therefore believed that BIR2 competes with other BAK1 interactors and prevents complex formation in the absence of a trigger.

As the phosphorylation status of PRR complexes is crucial for signalling initiation, protein phosphatases are emerging as negative regulators of PTI responses. KINASE-ASSOCIATED PROTEIN PHOSPHATASE (KAPP) is such a phosphatase with a kinase interaction (KI) domain and an N-terminal membrane anchor and directly interacts with FLS2 in Yeast-2-Hybrid assays (Gomez-Gomez *et al.*, 2001). Overexpression of KAPP renders plants insensitive to flg22 and it is suggested that KAPP dephosphorylates and thereby regulates FLS2 (Gómez-Gómez *et al.*, 2001). Another negative regulator is PROTEIN PHOSPHATASE 2A (PP2A) which interacts with BAK1 and negatively controls its phosphorylation status. Inhibition of PP2A results in enhanced disease resistance and activates PTI responses, such as ROS production and defence gene expression (Segonzac *et al.*, 2014). Furthermore, PP2C38 interacts with FLS2 and BIK1 and negatively regulates BIK1 phosphorylation and BIK1-mediated RBOHD activation (Couto *et al.*, 2016). These examples demonstrate the importance of phosphatases in the negative regulation of immune signalling.

Receptor complexes can furthermore be regulated through degradation and subsequent replenishment of newly synthesised receptors at the plasma membrane. Consistently, FLS2 is endocytosed after flg22 perception and degraded in the vacuole (Robatzek *et al.*, 2006). Endocytosis of FLS2 is clathrin-dependent and requires VPS37, a component of the ESCRT-I endosomal sorting machinery (Spallek *et al.*, 2013; Mbengue *et al.*, 2016). Recently, the E3 ligases PUB12 and PUB13 were found to polyubiquitinate FLS2 which is associated with protein degradation. Accordingly, FLS2 degradation is abolished in *pub12/13* mutants and ROS production upon flg22 treatment and resistance against *Pst* DC3000 was enhanced (Lu *et al.*, 2011). These examples illustrate the complexity of initiation and regulation of immune signalling in plants. Future studies will help us gain further insights as to how plants control immune responses.

Signalling of the LRR-RLKs EFR and PEPR1 and 2 are largely overlapping with FLS2 signalling and will not be discussed here in detail.

#### 1.1.1.3. Perception of chitin through LYK5 and CERK1

While perception of flg22, elf18 and AtPep1 largely require the same signalling partners, chitin perception is independent of some of these regulators, including BAK1. Chitin perception is mediated by the LysM domain-containing receptor complex of CHITIN ELICITOR RECEPTOR KINASE 1 (CERK1) and LYSINE MOTIF RECEPTOR KINASE 5 (LYK5) (Liu *et al.*, 2012; Cao *et al.*, 2014). LYK5 is the major chitin receptor binding chitin oligomers but also CERK1

can directly bind to chitin, but with much lower affinity than LYK5 (Petutschnig *et al.*, 2010; Cao *et al.*, 2014). This suggests a similar co-receptor dynamic where both partners are involved in ligand binding as in the FLS2/BAK1 receptor complex (Figure 1.1A). Because of the observation that CERK1 can associate with several LysM-RLKs, including LYK4, which is also involved in chitin perception, it was proposed that CERK1 acts as a regulatory receptor kinase analogous to BAK1 function (Petutschnig *et al.*, 2010; Wan *et al.*, 2012; Couto & Zipfel, 2016). This is moreover supported by the observation that LYK5 is a pseudokinase and CERK1 kinase activity is required for chitin immune signalling (Cao *et al.*, 2014). One could hypothesise that analogous to FLS2/BAK1 LYK5 associates with CERK1 because of its kinase activity. Chitin binding induces homodimerization of CERK1 and association with LYK5 (Cao *et al.*, 2014). CERK1 subsequently phosphorylates the RLCK PBL27 following its dissociation from the complex and the activation downstream signalling partners (Shinya *et al.*, 2014). PBL27 has been shown to phosphorylate MAPK kinase kinase 5 which leads to activation of MAPK kinase 4 and 5 and subsequently MAPK3 and 6 (Yamada *et al.*, 2016).

#### 1.1.1.4. Calcium signalling in PTI

Recognition of MAMPs triggers a rapid increase in the concentration of cytosolic free calcium ( $[Ca^{2+}]_{cyt}$ ), a second messenger, which is required for the activation of defence responses. This was confirmed through the use of pharmacological inhibitors in early studies (Lecourieux *et al.*, 2006). As changes in  $[Ca^{2+}]_{cyt}$  are involved in a wide range of plant responses, different stimuli are thought to induce the generation of unique spatio-temporal patterns of these calcium rises, so-called  $Ca^{2+}$  signatures. Even different MAMPs induce calcium signatures that differ in shape and intensity. BIK1 and PBL1 are required for flg22-, elf18- and AtPep1-induced calcium signatures (Ranf *et al.*, 2011). Identification of the calcium channels mediating these MAMP-induced calcium signatures remain to be identified. Genomic studies have suggested that plants do not have typical animal  $Ca^{2+}$  channels such as VOLTAGE-DEPENDENT  $Ca^{2+}$  CHANNELS (VDCCs), TRANSIENT RECEPTOR POTENTIAL (TRP) channels, PURINIC P2X RECEPTOR CHANNELS (P2XR) and cysteine loop channels. Instead, plants have expanded families of CYCLIC NUCLEOTIDE-GATED ION CHANNELS (CNGCs), MECHANOSENSITIVE ION CHANNEL MSL-LIKE (MSL) and REDUCED HYPEROSMOLARITY-INDUCED  $[Ca^{2+}]$  INCREASE CHANNELS (OSCA) (DeFalco *et al.*, 2010; Edel & Kudla, 2015; Zhu *et al.*, 2015). GLUTAMATE RECEPTOR-LIKE CHANNELS (GLRs) have been implicated in the MAMP-induced  $Ca^{2+}$  signatures as a selective calcium inhibitor impaired the calcium burst in response to flg22, elf18 and chitin (Kwaaitaal *et al.*, 2011). Interestingly, the loss of GLR3.3

lead to a hyper-susceptibility phenotype towards infection with *Pst* DC3000 (Li *et al.*, 2013). CNGC2 was shown to be a channel acting in LPS- and AtPep1-induced calcium influx (Ali *et al.*, 2007; Qi *et al.*, 2010). However, calcium signals in guard cells could not be abolished by the use of inhibitors of GLRs and CNGCs, suggesting that at least in this cell type these channels might not be involved in MAMP-induced calcium signatures (Thor & Peiter, 2014). Moreover, the study found that flg22 induces calcium oscillations in guard cells and not just a stark increase in  $[Ca^{2+}]_{cyt}$ , and these oscillations are similar to calcium oscillations in the nucleus during symbiosis (Capoen *et al.*, 2011; Thor & Peiter, 2014; Charpentier *et al.*, 2016). Indeed, AUTOINHIBITED  $Ca^{2+}$ -ATPase ISOFORM 8 (ACA8) and ACA10 associate with FLS2 and the double mutant has impaired calcium burst as well as ROS accumulation and is hypersusceptible to bacterial infection, implicating a role for these ATPases in the MAMP-induced calcium burst (Frey, N *et al.*, 2012).

#### 1.1.1.5. MAP Kinase cascades involved in defence

MITOGEN-ACTIVATED PROTEIN KINASES (MAPKs or MPKs) are universal modules of signal transduction in eukaryotes and follow a hierarchical cascade from MAP Kinase Kinase Kinases (MEKKs) that phosphorylate MAP Kinase Kinases (MKKs), which in turn phosphorylate MPKs. In this manner the signal gets forwarded and amplified at the same time, as one MEKK can activate several MKKS and so on. Plants have expanded families of MAPKs and *Arabidopsis thaliana* has 20 different MPKs that are divided into six subfamilies as well as 10 MKKs and 60 MEKKs (Zhang & Klessig, 2001). The activation motif of plant MPKs is either a Thr-Glu-Tyr or Thr-Asp-Tyr and is unique to plants (Ichimura *et al.*, 2002; Hamel *et al.*, 2006). In *Arabidopsis thaliana* two distinct MAPK cascades are involved in the MAMP-induced activation of four MAPKs. While the upstream MEKK remains to be found it is established that MAPKKs 4 and 5 activate MPK3 and MPK6 (Asai, T. *et al.*, 2002). The other cascade consists of MEKK1, MKK1 and MKK2 that activate MPK4 and MPK11 (Meszaros *et al.*, 2006; Suarez-Rodriguez *et al.*, 2007; Gao *et al.*, 2008; Bethke *et al.*, 2012). Downstream responses of MAP Kinase cascades are the activation of transcription factors that effectively reprogram transcription in favour of immune genes as well as activation of phospholipases or other substrates (Zhang & Klessig, 2001; Meng & Zhang, 2013). Inhibition of MAPK cascades reduces the expression of certain defence-associated genes (Asai, Tsuneaki *et al.*, 2002). Almost 1000 genes have found to be upregulated within 30 minutes of flg22 perception (Zipfel *et al.*, 2006, Zipfel *et al.*, 2004). A large number of those upregulated genes are RLKs, for instance the FLG22-INDUCED RECEPTOR-LIKE KINASE 1 (FRK1) (Boudsocq *et al.*, 2010).

This suggests a positive feedback loop of MAMP perception (Boller and Felix 2009). Other upregulated genes include NDR1/HIN-LIKE 10 (NHL10), PEROXIDASE 62 (PER62), WALL-ASSOCIATED KINASE 2 (WAK2) and FAD-LINKED OXIDOREDUCTASE (FOX) (Boudsocq *et al.*, 2010). Besides, there are also defence genes that can get activated independently of MPK signalling. For instance PHOSPHATE-INDUCIBLE 1 (PHI1) seems to require CALCIUM-DEPENDENT PROTEIN KINASES (CPKs) rather than MPKs (Boudsocq *et al.*, 2010).

How receptor complexes activate MAP Kinase cascades still remains elusive. Increasing evidence points towards an involvement of RLCKs in the activation of MAP Kinase cascades. The chitin-induced MAP Kinase activation strictly requires PBL27 and MKK5 was found to be a substrate of PBL27 (Shinya *et al.*, 2014; Yamada *et al.*, 2016). In addition to this it has been demonstrated that inhibition of BIK1 and related PBLs by a bacterial effector strongly inhibits flg22-induced MPK3, 4 and 6 activation (Feng, Feng *et al.*, 2012). However, the *pbl1 bik1* double mutant shows reduced AtPep1-induced MAP Kinase activity but has a wild-type-like response to flg22 (Feng, Feng *et al.*, 2012). Instead the *pcrk1 pcrk2* double mutant has slightly reduced MAP Kinase activity after flg22 trigger (Kong *et al.*, 2016). These results implicate a role for RLCKs in the activation of MAP Kinases after MAMP trigger but also indicate that there might be differential contribution of these RLCKs. In addition to the missing link between receptor complexes and MAP Kinase cascades only a small number of MPK substrates have been identified (e.g. (Pecher *et al.*, 2014). Although we know how integral MAP Kinase cascades are for immune response we still lack a thorough understanding of these important signalling modules.

### **1.1.1. Effector-triggered Immunity**

#### **1.1.1.1. Pathogens secrete proteins to modulate host processes**

Pathogens modulate host immune responses through the secretion of specialised proteins called effectors into the host cytoplasm to promote virulence. Bacteria possess a highly specialised secretion system that forms a syringe-like structure that can directly inject effectors into the cell's interior. The type III secretion system (T3SS) is essential for virulence as deletion mutants fail to successfully colonise (Buttner & He, 2009). Many devastating plant diseases are caused by gram-negative bacteria which employ this effector delivery mechanism including *Pseudomonas syringae*, *Ralstonia solanacearum* and *Xanthomonas spp.* The virulence function of the T3SS is carried out by the secreted effectors as it has been shown that expression of certain important effectors restores virulence to otherwise non-

pathogenic bacterial strains (Xin *et al.*, 2016). While suppression of host immune responses seems like an obvious task of effectors recently it emerged that another important function is the creation of an aqueous environment in the otherwise air-filled apoplast (Xin *et al.*, 2016). This function is fulfilled by the effectors HopM1 and AvrE and leads to the so-called water soaking of host leaves. Bacterial effectors are also known to interfere with PTI responses by targeting key components of the pathways. Several effectors target the phosphorylation status of receptor complexes. The *Pseudomonas syringae* effector AvrPto inhibits both FLS2 and EFR activation by acting as a general kinase inhibitor (Shan *et al.*, 2008; Xiang *et al.*, 2008). The protease effector HopB1 has recently been shown to cleave flg22-induced BAK1 to dampen PTI responses (Li *et al.*, 2016). FLS2, EFR and CERK1 are moreover degraded through the E3 ligase activity of AvrPtoB (Abramovitch *et al.*, 2006; Gohre *et al.*, 2008; Gimenez-Ibanez *et al.*, 2009). Interestingly, AvrPtoB has also been shown to negatively regulate BAK1 kinase activity (Cheng *et al.*, 2011). Another effector called HopAO1 exhibits tyrosine phosphatase activity and dephosphorylates key tyrosine residues on EFR and inhibits elf18-mediated immune responses (Macho *et al.*, 2014). RLCKs are also targets of effector interference. The *P. syringae* effector AvrPphB possesses uridylyl transferase activity and blocks the kinase activity of BIK1 and related RLCKs and thereby downstream responses mediated by BIK1 (Feng, F. *et al.*, 2012). BIK1 is also targeted by the *X. campestris* effector AvrAC and this observation led to the discovery of the decoy PBS1-LIKE 2 (PBL2) which is guarded by a cytoplasmic immune receptor (Feng & Zhou, 2012). Furthermore, the cysteine protease AvrPphB cleaves and degrades BIK1 and related RLCKs (Shao *et al.*, 2003). Other important signalling components targeted by effectors are MAP Kinase cascades. The two effectors HopAI1 and HopF2 target MAPK4 and MKK5, respectively. While HopAI1 inactivates MAPK4 through removal of phosphorylation sites, HopF2 ADP-ribosylates MKK5 to inactivate it (Zhang, J *et al.*, 2007; Wang *et al.*, 2010).

#### 1.1.1.2. Intracellular Immune Receptors: NLRs

Plants have evolved cytoplasmic immune receptors to detect secreted effectors and their virulence functions. The cytoplasmic immune receptors follow a characteristic domain structure and are called NUCLEOTIDE-BINDING LEUCINE RICH REPEAT RECEPTORS (NLRs). Most cytoplasmic immune receptors consist of a variable N-terminus, a nucleotide-binding NB-ARC domain and an LRR domain and are thus referred to as NLR proteins (Figure 1.2). NLR proteins can recognise the presence of effector proteins that have been translocated into the host cytoplasm to modulate cellular processes and to promote infection. NLRs are

part of a subfamily within the STAND (signal transduction ATPase with numerous domains) superfamily (Lukasik & Takken, 2009). The variable N-terminal domains help divide NLRs in three subclasses: TOLL-INTERLEUKIN 1 RECEPTOR (TIR domain) containing NLRs are called TNLs, those containing a coiled-coil (CC) domain are called CNLs and ones with a RPW8 domain are RNLs (Shao *et al.*, 2016). The N-terminal region is thought to determine downstream signalling partner requirements. While TNLs largely require ENHANCED DISEASE RESISTANCE 1 (EDS1) most CNLs depend on NON-RACE SPECIFIC DISEASE RESISTANCE 1 (NDR1) to activate immune signalling.

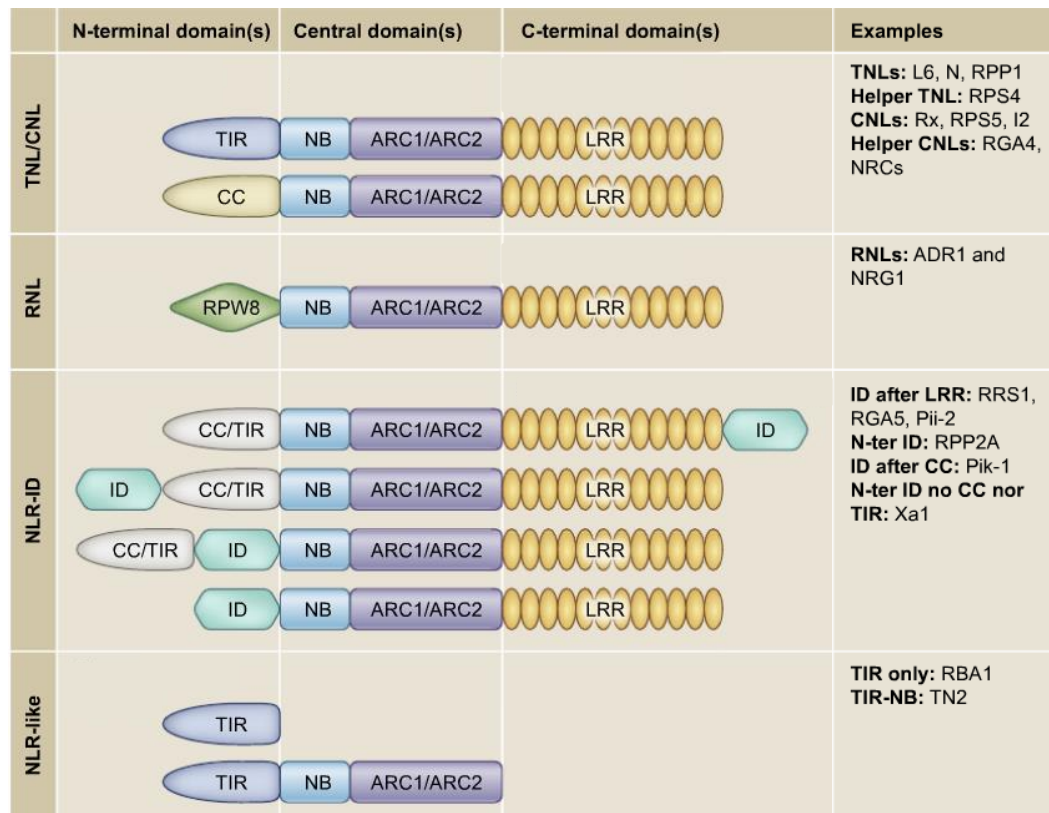


**Figure 1.2:** Domain structures of different types of plant NLRs. Most cytoplasmic immune receptors share a similar domain structures with a variable N-terminal domain, a central NB-ARC domain and an LRR domain. Special NLRs feature an addition domain originating from another host protein referred to as integrated domain (ID) or lack certain domains. CC: coiled-coil, TIR: Toll-interleukin 1 receptor, NB: nucleotide binding, ARC: Apar1, R-gene product and CED4, LRR: Leucine-rich repeat, RPW8: resistance to powdery mildew 8. Modified from (Cesari, 2018).

### 1.1.1.3. Functional cooperation of NLRs to mediate effector recognition

Research in recent years has demonstrated that some NLRs operate in functional pairs whereby one NLR acts as ‘sensor’ and the other NLR as ‘executor’ or ‘helper’. In this model the NLR dual function of recognition and signal transduction is divided into two proteins: the sensor NLR detects the pathogen and the executor NLR activates defence signalling (Cesari

*et al.*, 2014; Wu *et al.*, 2017). One such example is the NLR pair RESISTANT TO RALSTONIA SOLANACEARUM 1/RESISTANCE TO *P. SYRINGAE* 4 (RRS1/RPS4) from *Arabidopsis thaliana* that confers resistance to bacterial and fungal pathogens (Narusaka *et al.*, 2009). Other examples include Pikp-1/Pikp-2, RPP2A/RPP2B and RGA4/RGA5 (Sinapidou *et al.*, 2004; Cesari *et al.*, 2013; Maqbool *et al.*, 2015). Many of those NLR pairs are not only functionally but also genetically linked by mapping to the same locus and are usually in a head-to-head orientation, sharing transcriptional regions (Bialas *et al.*, 2018). Those linked NLR partners frequently exhibit differential domain structures stressing their specialisation in sensor and executor modules. It has been suggested that these partners have evolved together to achieve specific partnering of NLRs. This is supported by the observation that paralogous pairs only function with their genetically linked partner and cannot initiate signalling with a member of the paralogous pair (Saucet *et al.*, 2015). Recent evidence suggests that there is a large executor NLR network that regulates NLR signalling to a variety of different pathogens (Wu *et al.*, 2017). These executor NLRs transduce pathogen recognition via multiple sensors and members of the NLR REQUIRED FOR CELL DEATH (NRC) family have been identified to act in such a network structure (Wu *et al.*, 2017). Interestingly, this study revealed that some NLRs that were believed to function on their own actually require helpers (Wu *et al.*, 2017). However, there are some NLRs that have been shown to function on their own, such as MLA10 from barley (Bai *et al.*, 2012). Nonetheless, it is possible that MLA10 relies on members of a helper NLR network that have yet to be identified.

#### 1.1.1.4. Molecular basis of NLR activation

Intra- and intermolecular interactions control the signalling state of NLRs in immune signalling. NLRs are believed to cycle between an active and inactive state determined by the binding of either ADP or ATP. They are therefore regarded as molecular switches through their ability to change between these two signalling states (Takken *et al.*, 2006). When ADP is bound the NLR is in the autoinhibited or 'off' state and the N-terminal and LRR domains cooperate to prevent ADP/ATP exchange in the NB-ARC domain. Representative structural models have suggested that the positively charged LRR N-terminus associates with a negatively charged region of the NB-ARC to stabilise the inactive state (Takken & Goverse, 2012). Domains that have been implicated in maintaining the off state through domain swap and point mutation analyses are the NB, ARC2 domains and the LRR N-terminus (Rairdan & Moffett, 2006; Lukasik & Takken, 2009). Recognition of a pathogen induces conformational changes enabling the transition to the ATP- bound or 'on' state and effectively exposes the

N-terminal domain to signalling partners. The main determinant of the state is therefore the NB-ARC domain as the conformation drastically changes depending on the bound nucleotide. Intriguingly, it has been found that the exchange from ADP to ATP is not always strictly required for NLR activation. NLRs lacking the P-loop motif for ADP/ATP binding retained the ability to provide resistance to the pathogen it detects (Inoue *et al.*, 2013). In the case of the NLR pair RPS4 and RRS1 only the proposed signalling partner requires the intact P-loop while it is dispensable in the sensor NLR (Sohn *et al.*, 2014). In order to cycle back to the inactive state, NLRs require ATPase activity of the NB-ARC domain as loss of ATPase activity leads to auto-activity (Tameling *et al.*, 2006).

A recent study suggested that NLRs may constitutively cycle between the off and on state and that in unelicited cells there is a balance between both states. The 'equilibrium-based switch' model was proposed in which a recognised effector stabilises the on state thereby shifting the equilibrium towards the activated state (Bernoux *et al.*, 2016).

#### 1.1.1.5. Activation of NLRs through Effectors

How are effectors recognised by NLRs? In the following section I will discuss evidence supporting the different models of NLR activation through pathogen virulence factors.

Direct binding of the effector to the intracellular immune receptor is the simplest scenario that is also supported by Flor's gene-for-gene hypothesis (Flor, 1971). This receptor-ligand model homologous to PTI is supported by many studies which have demonstrated direct interaction between effectors and NLRs. As the LRR is highly variable and the interaction site for several MAMPs and DAMPs it is a likely candidate as effector interaction site. This is indeed the case for RECOGNITION OF PERONOSPORA PARASITICA 1 (RPP1) and Pi-ta which have been shown to interact with their respective effectors through their LRR region. Since the N-terminal portion of the LRR is also implicated in maintaining the auto-inhibited state of NLRs, that it can also interact with the effector suggests that the LRR region plays a dual role. Allelic versions of NLRs with different effector recognition ranges have enabled domain swap studies that revealed distinct interacting surfaces. RPP1 alleles NdA and Ws-B differ in their effector recognition range, with NdA having a narrow and Ws-B a broad effector recognition range of *ARABIDOPSIS THALIANA* RECOGNISED 1 (ATR1) alleles. Mutant forms of ATR1 helped identify residues that are recognised by and mediate interaction with NdA but not Ws-B. This demonstrates that different alleles of the same NLR have evolved distinct recognition mechanisms and not just differing sensitivities of the same mechanism

(Steinbrenner *et al.*, 2015). While for the association with the effector the LRR domain is sufficient, it requires further domains for defence activation (Steinbrenner *et al.*, 2015). Similar studies of the flax L5 and L6 variants revealed interaction hotspots in the LRR domain. They identified the first four and last seven repeats as mediators of interaction with the flax rust effector and therefore resistance specificity (Ravensdale *et al.*, 2012). Another interesting example is the cereal resistance gene Pm3 that directly binds and recognises Avr-Pm3. It has an unusually large LRR domain with island domains. These island regions have been shown to function in ligand recognition and mutations in the island domains of BR-INSENSITIVE 1 (BRI1) rendered it insensitive to its ligand brassinolide (Hothorn *et al.*, 2011). While interaction hotspots on Pm3 have been predicted to be between repeats 11 and 26 it is currently unknown whether island domains play a role in effector binding (Sela *et al.*, 2014).

However, other NLR domains have also been observed to interact with the AVR ligand. The tobacco resistance gene N confers resistance to Tobacco Mosaic Virus and binds the viral p50 helicase domain via its TIR domain (Burch-Smith *et al.*, 2007). Furthermore, the potato *RB* gene confers resistance to certain *P. infestans* strains through recognition of effectors of the IPI-O family through the CC domain (Chen *et al.*, 2012). Other effectors that have been found to directly interact with NLRs are Avr-Pita, AvrL567 and AvrM (Jia *et al.*, 2000; Dodds *et al.*, 2006; Catanzariti *et al.*, 2010).

Intriguingly, there are also truncated NLRs that mediate recognition without LRRs. They either consist of a TIR and NB-ARC domain in the case of T2 and only a TIR domain in the case of TX proteins. They seem to require self-association through two distinct surfaces to initiate defence signalling (Williams *et al.*, 2014; Nishimura *et al.*, 2017; Zhang *et al.*, 2017). RESISTANCE TO THE BACTERIAL TYPE III EFFECTOR HOPBA1 (RBA1) is a TIR-only that is sufficient to trigger cell death upon recognition of HopBA1 in *Arabidopsis thaliana* (Nishimura *et al.*, 2017).

Another strategy to monitor effector interference is the recognition of effector-mediated modification of host targets by NLRs. Many NLR proteins have not been observed to directly interact with their cognate effectors. This indirect recognition is summarised in the 'guard hypothesis' in which an NLR 'guards' the effector target and activates defence if the 'guardee' has been modified by an effector (Dangl & Jones, 2001). Detailed support for this strategy comes from the well-studied monitoring of RMP1-INTERACTING PROTEIN 4 (RIN4) by RESISTANCE TO PSEUDOMONAS SYRINGAE PV. MACULICOLA 1 (RPM1) and RESISTANCE

TO PSEUDOMONAS SYRINGAE 2 (RPS2). RIN4 is targeted by multiple bacterial effectors which implies that RIN4 plays a central role in plant defences. While it has been implied in several immune responses from PTI signalling to stomatal closure, its exact role is still elusive (Liu *et al.*, 2009; Liu *et al.*, 2011). RPM1 recognises AvrB- or AvrRpm1-induced phosphorylation of RIN4 while RPS2 recognises AvrRpt2-mediated protease activity and they subsequently activate immune signalling (Mackey *et al.*, 2002; Mackey *et al.*, 2003). NLR SUPPRESSOR OF MKK1 MKK2 (SUMM2) guards MPK4 and the removal of phosphorylated groups by the bacterial effector HopAI1 (Zhang *et al.*, 2012).

The guard model was taken to another level by the discovery of guarded decoys that have lost their original signalling function and serve solely as effector baits (van der Hoorn & Kamoun, 2008). These proteins may present the next step of host protein specialisation to effector perception. Such decoys include PBL2 which acts as decoy for BIK1 to prevent interference of AcrAC in BIK1-mediated responses. PBL2 is guarded by HOPZ-ACTIVATED RESISTANCE 1 (ZAR1) and the pseudokinase RESISTANCE RELATED KINASE 1 (RKS1) that specifically recruits the uridinylated PBL2 (Wang *et al.*, 2015). Interestingly, ZAR1 is also involved in the guarding of another decoy protein: HOPZ-ETI-DEFICIENT 1 (ZED1) is a pseudokinase that detects the acetylation of HopZ1a and associates and subsequently activates ZAR1 (Lewis *et al.*, 2013). These mentioned guardees can be seen as true decoys as they are functional mimics with no intrinsic protein function. However, there are also decoys that require intrinsic activities for NLR activation. The protein kinase Pto, for instance, activates the tomato NLR Prf upon perception of the effectors AvrPto and AvrPtoB and its kinase activity is required for activation of ETI responses (Mucyn *et al.*, 2006; Ntoukakis *et al.*, 2014; Saur *et al.*, 2015). Since Pto does not seem to play a crucial role in activation of PTI signalling it is nonetheless thought to be a decoy of the actual effector targets FLS2 and BAK1 (Nomura *et al.*, 2006; Shan *et al.*, 2008). The plasma membrane CNL RESISTANCE TO P. SYRINGAE 5 (RPS5) is held in the off state through direct interaction with PBS1. Cleavage of PBS1 by the effector AvrPphB activates RPS5 and is thought to protect the real target BIK1 from degradation that, unlike PBS1, plays a central role in MAMP-triggered immune responses (Ade *et al.*, 2007).

#### 1.1.1.6. Integrated domains within NLRs

Up to 10% of plant NLRs contain an atypical domain within the classical NLR domain structure. Since it is hypothesised that these domains serve as sensor domains and have evolved from a duplication and successive integration of host effector targets into the

canonical NLR structure, they are now commonly referred to as integrated domains (Figure 1.2 third panel). These integrated domains could serve as effector binding sites, to detect effector activity or to outcompete binding of the effector with the actual host target. In the case of the NLR pair RRS1/RPS4 the sensor module RRS1 has an integrated WRKY domain at its C-terminus. It has been discovered that the bacterial effectors PopP2 and AvrRps4 interact with RRS1 via the integrated WRKY domain which is also the effector's presumed host target (Le Roux *et al.*, 2015; Sarris *et al.*, 2015). It is particularly notable that an integrated heavy-metal associated (HMA) domain seems to mediate perception of three evolutionary unrelated effectors of *Mangaporthae oryzae* in rice. The sensor NLRs Pik-1 and RGA5 recognise AVR-Pik, AVR-Pia and AVR-CO39 through direct binding of the HMA domain with the effectors (Cesari *et al.*, 2013; Maqbool *et al.*, 2015; Ortiz *et al.*, 2017). This suggests that certain host proteins are predominant effector targets and therefore also more commonly integrated into NLRs.

Studies have found that some domains are more commonly integrated than others. Among the most common domains are protein kinases, WRKYs and BED domains (Kroj *et al.*, 2016; Sarris *et al.*, 2016). These are host proteins that are commonly associated with plant immune responses and present likely effector targets and have been found in NLRs with known resistance function (Yoshimura *et al.*, 1998; Brueggeman *et al.*, 2008; Narusaka *et al.*, 2009). Novel domains integrated in NLRs could offer new insight in effector targets and immunity regulators.

## 1.2. Stomata

Stomata are microscopic pores in the plant epidermis formed by a pair of guard cells that control the size of the aperture through osmotically driven water transport. They enable water transpiration and CO<sub>2</sub> uptake across the plant epidermis by opening and closing to environmental stimuli. Guard cells are able to respond and change their size and shape to a large number of stimuli and they are the only cells that can translate environmental stimuli into an active, reversible, biomechanical movement. Stimuli that induce aperture opening are for instance low CO<sub>2</sub> concentration, red and blue light and high humidity (Lange *et al.*, 1971; Shimazaki *et al.*, 2007). Conversely, stimuli that result in stomatal closure include, but are not limited to, elevated CO<sub>2</sub> concentration, drought, elevated ozone and darkness (Sheriff, 1979; Blackman & Davies, 1985; Jane *et al.*, 1997). In the following I will describe stomatal development, stomatal movements and known stomatal signalling pathways in the model plant *Arabidopsis thaliana*.

### 1.2.1. Stomatal development

Guard cells originate from protodermal cells that undergo a cellular transition to become meristemoid mother cells (MMCs). This requires the activity of the basic Helix-loop-Helix (bHLH) protein SPEECHLESS (SPCH) that is both expressed in the protoderm and stomatal lineage cells (MacAlister *et al.*, 2007; Pillitteri & Torii, 2012). The MMCs undergo asymmetric cell division which marks the initiation of the stomatal lineage. This asymmetric cell division gives rise to a smaller cell, a meristemoid and a larger cell, a stomatal-lineage ground cell (SLGC). SLGCs can have two fates: they can become a pavement cell by terminally differentiating or they can divide to a satellite meristemoid. The satellite meristemoid usually faces away from the original stoma. The meristemoids will repeatedly divide asymmetrically into sister cells in a manner that resembles stem cell-like activity, generally up to three times. These divisions serve in part to renew the meristemoid state and to increase the number of SLGCs in that particular lineage. These cells are the main source of both pavement cells and stomata (Geisler *et al.*, 2000). Eventually, meristemoids terminate cell division, undergo a transition and become a guard mother cell (GMC) and this requires the bHLH protein MUTE (Pillitteri & Torii, 2012). The GMC divides symmetrically and the two resulting cells transition into guard cells. This terminates the differentiation and guard cells do not divide any further (reviewed by (Pillitteri & Torii, 2012)). The last transitioning step is mediated by the bHLH protein FAMA that plays a dual role by inhibiting GMC cell division and promoting the transition to guard cells (Ohashi-Ito & Bergmann, 2006). All three bHLH proteins mentioned above require the partially redundant bHLH proteins SCREAM and SCREAM2 for their function. Through direct interaction with SPCH, MUTE and FAMA they are thought to promote stomatal transitions (Kanaoka *et al.*, 2008). During the differentiation and transition processes guard cells deposit cell wall material upon plasmodesmata (Wille & Lucas, 1984; Palevitz & Hepler, 1985). This requires GLUCAN SYNTHASE 8 (GSL8) which is important for callose deposition at cell plates and plasmodesmata. Loss of GSL8 results in small stomatal clusters. It is understood that the plasmodesmal truncation during differentiation is important to restrict movement of regulatory proteins and determinants (Chen *et al.*, 2009; Thiele *et al.*, 2009; Guseman *et al.*, 2010). This symplastic isolation has prompted studies investigating whether guard cell autonomy plays a role beyond stomatal development. Indeed, it was found that guard cells act autonomous in blue-light induced stomatal opening and ABA-induced stomatal closure (Cañamero *et al.*, 2006; Bauer *et al.*, 2013). Therefore, cell autonomy seems to be an important characteristic of these highly specialised cells.

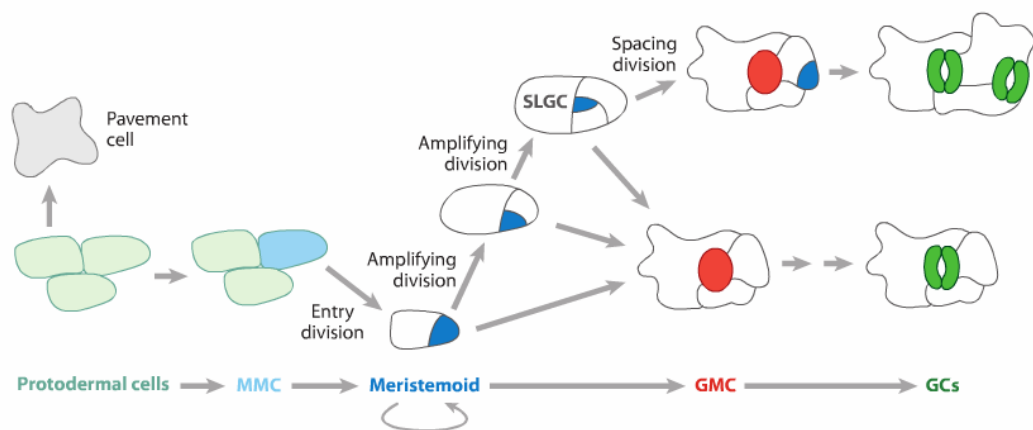


**Figure 1.3:** Illustration of cell-state transitions during stomatal development in *Arabidopsis thaliana*. Some protodermal cells undergo cell-transition and become meristemoid mother cells (MMCs, light blue) while other cells differentiate into pavement cells. MMCs enter the stomatal lineage through an asymmetrical cell division into a meristemoid (dark blue) and stomatal-lineage ground cell (SLGC). SLGCs either differentiate into a pavement cell or form a satellite meristemoid facing away from the existing stomatal precursor. Meristemoids eventually transition to become guard mother cells (GMCs, red). After one final symmetric cell division two equal guard cells are produced. Taken from Pillitteri and Torii 2012.

Gas exchange is also affected by the number and distribution of stomata across the leaf surface. This is regulated together with cell growth and division whilst also environmental conditions influence it. Across species stomata are formed following a one-cell spacing rule (Peterson *et al.*, 2010). To ensure that stomata are at least one cell apart from one another, cell-to-cell signalling components mediate the oriented divisions of SLGCs. Additionally, misplaced meristemoids can still be corrected later in the cell lineage, suggesting a short-distance signal enforcing stomatal distribution. It is hypothesised that the one-cell spacing rule is important to ensure that water and ions are rapidly available from neighbouring cells during stomatal opening and closure. This spacing distribution is proposed to be mediated by late-stomatal precursors emitting EPIDERMAL PATTERNING FACTORS (EPFs) that are recognised by ERECTA-family RLKs and form a large receptor complex with RLP co-receptor TOO MANY MOUTHS (TMM) and SERKs (Hara *et al.*, 2007; Lee *et al.*, 2012; Meng *et al.*, 2015). The RLKs ERECTA, ERL1 and ERL2 are proposed to act partially redundant and synergistically to inhibit epidermal cells from differentiating into guard cells (Shpak *et al.*, 2005). Further downstream signalling components involved in maintaining the one-cell spacing rule include YODA, MKK4/5, MPK1 and MPK3/6 (Geisler *et al.*, 2000; Bergmann *et al.*, 2004; Tamnanloo *et al.*, 2018).

## 1.2.2. Stomatal movement

### 1.2.2.1. Regulation of stomatal opening

Stomatal opening is initiated through phosphorylation of plasma membrane localised H<sup>+</sup>-ATPases in the guard cell plasma membrane. This leads to proton efflux and hyperpolarisation of the guard cell membrane (Assmann *et al.*, 1985; Shimazaki *et al.*, 1986; Haruta *et al.*, 2015; Falhof *et al.*, 2016). There are 11 plasma membrane H<sup>+</sup>-ATPases in *Arabidopsis thaliana* (AHA1 through AHA11) and they are a family of P-type ATPases with 10 transmembrane and 3 cytosolic regions. The large cytosolic domain has been shown to have auto-inhibitory function (Jahn *et al.*, 1997; Morth *et al.*, 2011). Upon phosphorylation the C-terminus interacts with 14-3-3 proteins and relocates thereby activating the pumping function (Baunsgaard *et al.*, 1998). An important regulatory phospho-site is the penultimate Thr947 in the C-terminus and is a common regulatory residue for a range of stimuli including light, salt, sucrose, auxin, gibberellin and ABA (Niittylä *et al.*, 2007; Chen *et al.*, 2010; Okumura *et al.*, 2012; Takahashi *et al.*, 2012; Hayashi *et al.*, 2014; Inoue *et al.*, 2016; Okumura *et al.*, 2016). The protein kinase phosphorylating this key residue still remains to be identified. The importance of H<sup>+</sup>-ATPases in stomatal opening is stressed by dominant mutations of AHA1 that display constitutive open stomata (Merlot *et al.*, 2007) and loss-of-function alleles that show reduced stomatal opening or a closed phenotype (Osakabe *et al.*, 2016; Yamauchi *et al.*, 2016). Furthermore, light-induced stomatal opening is enhanced through guard cell-specific overexpression of AHA2 (Wang *et al.*, 2014). Light-induced stomatal opening is generally discriminated into blue- and red light-induced opening responses. Blue light-induced opening relies on the autophosphorylation of the blue light receptors PHOTOTROPIN (PHOT) 1 and 2 that then directly phosphorylate BLUE LIGHT SIGNALLING 1 (BLUS1) (Kinoshita *et al.*, 2001; Christie, 2007; Inoue *et al.*, 2008). Further downstream signalling partners include type 1 protein phosphatase (PP1), its subunit PP1 REGULATORY SUBUNIT1-LIKE PROTEIN 1 (PRSL1) and BLUE-LIGHT-DEPENDENT H<sup>+</sup>-ATPase PHOSPHORYLATION (BHP) (Takemiya *et al.*, 2006; Takemiya *et al.*, 2013a; Takemiya *et al.*, 2013b; Takemiya & Shimazaki, 2016; Hayashi *et al.*, 2017). While the receptors and stimulus for blue light-induced stomatal opening is determined, this remains under debate for red light-induced stomatal opening. It has been suggested that red light-induced stomatal opening could be a response to reduced intracellular CO<sub>2</sub> concentrations due to photosynthetic activity of the mesophyll cells and therefore an indirect rather than light-specific response. Recent evidence, however, suggests that the red light-induced stomatal

opening response is not merely a CO<sub>2</sub> response as carbonic anhydrase double mutants of βCA1 and βCA4 exhibit red light-opening response while being hyposensitive to CO<sub>2</sub> (Matrosova *et al.*, 2015).

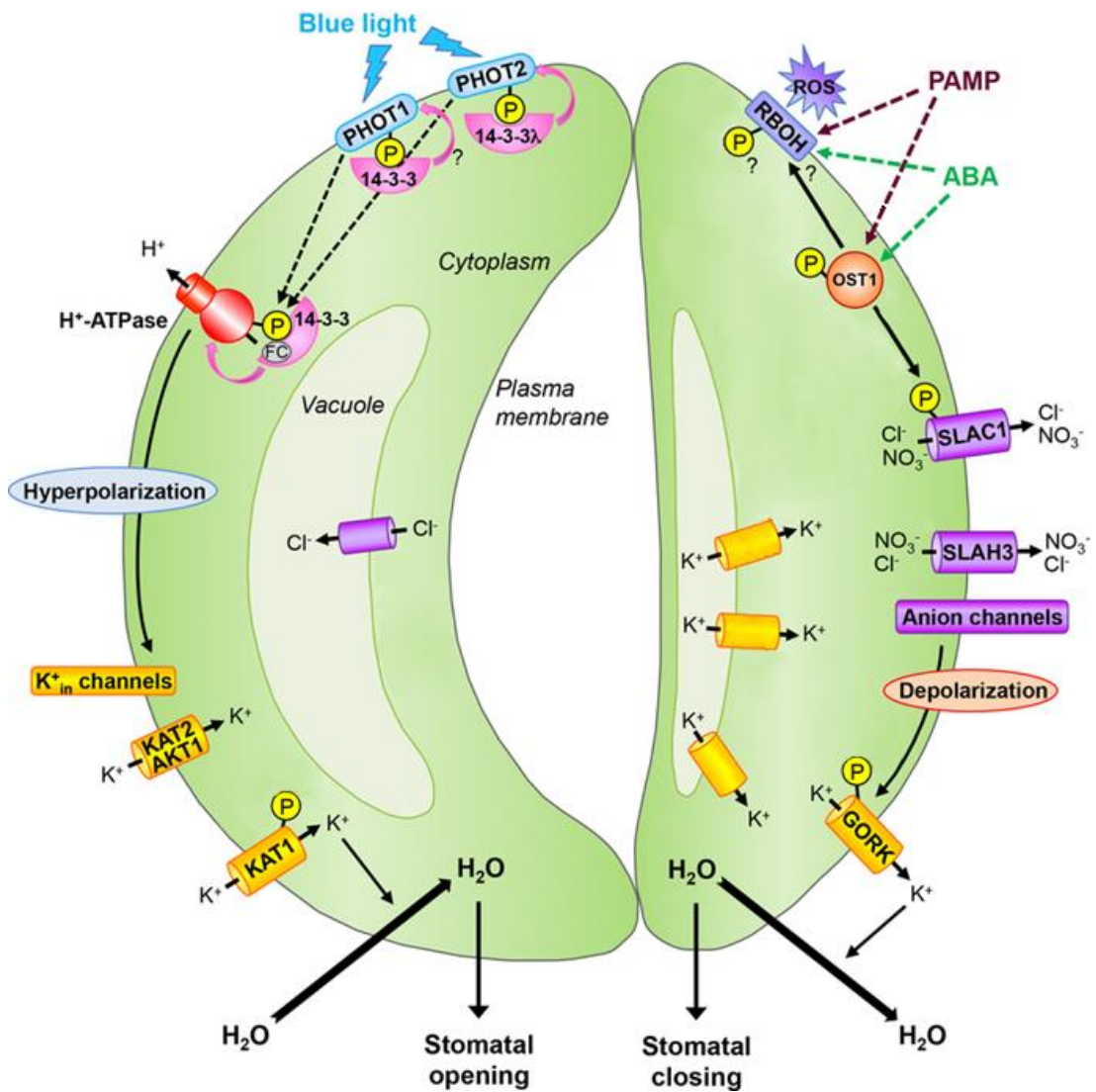


**Figure 1.4:** Mechanisms of stomatal movement in *Arabidopsis thaliana*.

Stomatal opening is initiated through the phosphorylation of plasma membrane localised H<sup>+</sup>-ATPases which leads to hyperpolarisation of the guard cell membrane. Upon phosphorylation the C-terminus of the H<sup>+</sup>-ATPases interacts with 14-3-3 proteins which activated the pumping function. The hyperpolarisation induces potassium uptake through inward rectifying potassium channels. This decreases the water potential and results in water uptake in the guard cell and its vacuole resulting in the opening of the aperture. During stomatal closure ROS is produced via NADPH oxidases at the plasma membrane. Plasma membrane localised anion channels SLAC1 and SLAH3 are activated and transport osmolytes out of the guard cells. The guard cell membrane depolarises and voltage-dependent anion channels are thereby activated. The loss of potassium and subsequent water loss leads to the loss of turgor and closure of the stomatal aperture.

Adapted from (Cotelle & Leonhardt, 2015)

Proton efflux through H<sup>+</sup>-ATPases results in hyperpolarization of the guard cell membrane and this induces K<sup>+</sup> uptake through inward rectifying K<sup>+</sup> channels KAT1 and 2, AKT1, 2 and 3 (Lebaudy *et al.*, 2008; Marten *et al.*, 2010). Inward rectifying K<sup>+</sup> channels belong to a family of shaker-like genes that form homo- and heteromeric channels in the guard cell membrane (Dreyer *et al.*, 1997). These channels are K<sup>+</sup> selective but do not determine the direction of transport, this happens via the K<sup>+</sup> gradient and the electrical potential of the membrane (Hille, 2001). The differentiation between inward and outward rectifying channels depends on their range of voltage-dependent activation (Lebaudy *et al.*, 2007). In the opening response their activation leads to the accumulation of K<sup>+</sup> and the counterions Cl<sup>-</sup>, nitrate and malate. The anions are further transported into the vacuole through tonoplast localised transporters and channels (Jossier *et al.*, 2010; De Angeli *et al.*, 2013; Andres *et al.*, 2014). This decreases the water potential in the guard cells and the vacuole and this results in water uptake and thereby guard cell inflation which opens the stomatal aperture between the guard cells.

#### 1.2.2.2. Stomatal closure

Closure-inducing stimuli activate Ca<sup>2+</sup> influx channels, outward rectifying potassium channels and Slow (S)- as well as Rapid (R)-type anion channels (Schroeder, 1989; Schroeder & Hagiwara, 1989; Hedrich *et al.*, 1990). While the calcium channels for this response remain to be identified, more is known about potassium and anion channels. Both R- and S-type anion channels are activated by membrane polarisation but their reaction time differs from milliseconds for R-type, to seconds for S-type channels (Linder & Raschke, 1992; Kolb *et al.*, 1995). Two S-type anion channels are expressed in guard cells: SLAC1 and its homolog SLAH3 (Negi *et al.*, 2008; Vahisalu *et al.*, 2008; Geiger *et al.*, 2011). SLAC1 is the major channel mediating stomatal closure in response to ozone, CO<sub>2</sub> and humidity, while both channels are required for full closure in response to ABA and MAMPs (Deger *et al.*, 2015). R-type anion channel QUAC1 is member 12 of the aluminium-activated malate transporter family (ALMT) (Dreyer *et al.*, 2012), but was renamed QUAC1 from ALMT12, as it is not activated by aluminium (Meyer *et al.*, 2010; Sasaki *et al.*, 2010). Plants lacking QUAC1 are not impaired but rather show a slower closure response to certain stimuli (Meyer *et al.*, 2010; Sasaki *et al.*, 2010). It is suggested that S-type anion channels transport nitrate and chloride while R-type channels conduct organic anions such as malate. Through the transport of anions across the guard cell membrane anion channels play an essential role in repolarising the guard cell plasma membrane which activates voltage-dependent K<sup>+</sup> efflux channels such as GORK (Ache

*et al.*, 2000; Kollist *et al.*, 2011). The loss of anions and potassium leads to water loss and a decrease in guard cell volume and this leads to the closure of the aperture between the guard cells (Hosy *et al.*, 2003). This transition from the open to the closed state requires a 2- to 3-fold decrease in volume and 30-40% decrease in surface area (Blatt, 2000; Meckel *et al.*, 2007). This guard cell volume decrease is primarily caused by a reduction in vacuolar volume and this is achieved by converting the large central vacuole into a highly convoluted structure (Bak *et al.*, 2013). Membrane trafficking seems to play an important role in this process as both exocytotic and endocytic events are crucial for guard cell movements (Homann & Thiel, 1999; Leyman *et al.*, 1999; Shope *et al.*, 2003). This process seems to require clathrin heavy chain subunits as a *chc1* mutant allele has a stomatal defect (Larson *et al.*, 2017). How exactly these membrane trafficking events are regulated still remains to be discovered. To initiate stomatal closure in sunlight conditions it is necessary to inhibit stomatal opening through the inhibition of H<sup>+</sup> efflux. This happens for instance via SLAC1 and SLAH3 who can directly bind to KAT1 and inhibit its activity (Zhang *et al.*, 2016).

In the following section I will be discussing different signalling pathways that induce stomatal closure and their core signalling components.

### **1.2.3. Stomatal closure signalling pathways**

#### **1.2.3.1. ABA-induced stomatal closure**

The most studied signal inducing stomatal closure is the hormone Abscisic acid (ABA) that is produced upon drought stress conditions. Although it is the strongest signal inducing stomatal closure and it has been discovered in the 1960s its core signalling pathway has only recently been characterized. Two groups independently identified the ABA receptors that we will refer to as PYRABACTIN-RESISTANCE 1 (PYR1)/ PYR1-LIKE (PYLs), although they are occasionally also referred to as REGULATORY COMPONENT OF ABA RECEPTOR (RCAR) (Ma *et al.*, 2009; Park *et al.*, 2009; Santiago *et al.*, 2009). There are 14 ABA receptors in *Arabidopsis thaliana* that belong to the START domain superfamily who share a conserved hydrophobic ligand-binding pocket (Iyer *et al.*, 2001; Radauer *et al.*, 2008). The 14 ABA receptors were found to share high redundancy (Park *et al.*, 2009). Several studies shed light upon the function of ABA receptors, in particular a series of crystallographic studies of PYR1, PYL1 and PYL2 (Nishimura *et al.*, 2009). PYR1 and PYL2 form homodimers who change conformation upon ABA binding. Binding of ABA to the internal cavity induces the conformational change of a lid structure (Figure 1.5). This exposes a hydrophobic surface

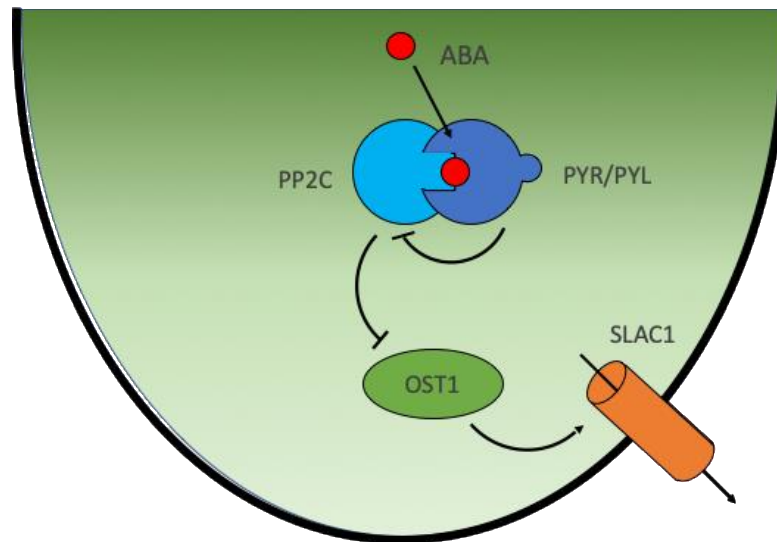


**Figure 1.5:** Depiction of the main components of the prototypic Abscisic acid (ABA) -induced stomatal closure pathway.

Upon water limiting conditions plants produce ABA which is perceived by ABA receptors PYRBACTIN-RESISTANCE 1 (PYR1) /PYR1-LIKEs (PYLs). Binding of ABA induces conformational changes that enable the ABA receptor to interact with and inhibit TYPE 2C PROTEIN PHOSPHATASES (PP2Cs) that inhibit positive regulators of stomatal closure. One of these important regulators is OPEN STOMATA 1 (OST1). Once inhibition through PP2Cs is removed, OST1 autophosphorylates and transphosphorylates SLAC1. This induces the efflux of anions which leads to the reduction of turgor and the closure of the pore between the guard cells.

that interacts with and thereby inhibits TYPE 2C PROTEIN PHOSPHATASES (PP2C) of the group A (Melcher *et al.*, 2009; Miyazono *et al.*, 2009; Yin *et al.*, 2009). This was in accordance with previous findings that ABA receptors interact with HAB1 and ABI1 in a ligand-dependent manner (Ma *et al.*, 2009; Park *et al.*, 2009). PP2C phosphatase mutants such as *abi1-1* and *abi2-1* have long been known to be negative regulators of ABA signalling (Koornneef *et al.*, 1984; Leung *et al.*, 1994; Meyer *et al.*, 1994; Roelfsema & Prins, 1995). The dominant negative *abi1-1* mutant has an amino acid exchange from Gly<sup>180</sup> to Asp which results in it being constitutively active (Leung *et al.*, 1994). PP2C phosphatases are active in the absence of ABA and dephosphorylate and inhibit the activity of positive regulators of stomatal closure. One of these regulators are Clade 2 SUCROSE NON-FERMENTING 1-RELATED KINASES (SnRKs) that are important for ABA-mediated responses and in particular stomatal closure. ABA-INSENSITIVE 1 (ABI1) has an EF-hand domain and a calcium-binding site (Allen *et al.*, 1999) that dephosphorylates Ser<sup>175</sup> in the activation loop of OPEN STOMATA1 (OST1) and thereby negatively regulates its activity (Vlad *et al.*, 2009). OST1 or SnRK2.6 is one of ten SnRK2s in *Arabidopsis thaliana* (Hrabak *et al.*, 2003) and has two close homologs: SnRK2.2 and SnRK2.3. All three homologs are major targets of PP2C phosphatases regulated by PYR1/PYLs and mediate many ABA responses throughout different tissues (Fujii *et al.*, 2007; Fujita *et al.*, 2009). Loss of all three SnRKs renders *Arabidopsis thaliana* seeds effectively

insensitive to ABA-induced seedling dormancy. OST1 is expressed in guard cells and the vasculature while SnRK2.2 and SnRK2.3 are expressed in all plant tissues (Mustilli *et al.*, 2002; Fujii *et al.*, 2007). Loss of OST1 renders guard cells highly insensitive in ABA-induced stomatal closure in response to drought (Mustilli *et al.*, 2002) and osmotic stress-induced closure, independently of ABA-signalling (Yoshida *et al.*, 2002; Yoshida *et al.*, 2006) indicating it as the prominent kinase in these pathways. Upon ABA perception the negative regulation through PP2C phosphatases is removed and OST1 gets strongly activated. OST1 can auto- and transphosphorylate and its activity is dependent on its phosphorylation status. Even though OST1 is strongly activated upon ABA treatment (Belin *et al.*, 2006) the expression level seems to be unaffected by ABA (Mustilli *et al.*, 2002). Although the expression of SnRK2.2 and SnRK2.3 is not restricted to guard cells they have been associated with guard cell-specific responses independent from OST1 (Virilouvet *et al.*, 2014). OST1 directly phosphorylates anion channels SLAC1 and QUAC1 in response to ABA but also other stimuli such as CO<sub>2</sub>, darkness and ozone (Geiger *et al.*, 2009; Lee *et al.*, 2009; Vahisalu *et al.*, 2010; Imes *et al.*, 2013). It moreover phosphorylates RBOHs in the plasma membrane to induce ROS production (Sirichandra *et al.*, 2009).

Perception of ABA induces an increase in cytosolic Ca<sup>2+</sup> (Mcainsh *et al.*, 1990; Gilroy *et al.*, 1991) but this is not essential to induce closure. It has been found that ABA signalling involves both a Ca<sup>2+</sup>-dependent and independent pathway (Levchenko *et al.*, 2005; Marten *et al.*, 2007) while transduction via PP2C phosphatases and OST1 does not require calcium elevations (Geiger *et al.*, 2009; Geiger *et al.*, 2010). Elevated calcium concentrations in the cytoplasm have been shown to induce S-type anion channel activity and SLAC1 has been shown to be activated by CALCIUM-DEPENDENT KINASES (CPK) in oocyte measurements (Geiger *et al.*, 2010; Scherzer *et al.*, 2012). ABA inhibits stomatal opening through the inhibition of H<sup>+</sup>-ATPases via ABA receptor components, H<sub>2</sub>O<sub>2</sub>, NO, phosphatidic acid (PA) and cytosolic calcium (Zhang, X *et al.*, 2007; Takemiya & Shimazaki, 2010; Hayashi & Kinoshita, 2011). Furthermore, OST1, SLAC1 and SLAH3 directly interact with KAT1 to inhibit its activity (Sato *et al.*, 2009; Zhang *et al.*, 2016). ABA has also been shown to inactivate AKS transcription factors to reduce the expression of inward rectifying K<sup>+</sup> channels and to induce KAT1 endocytosis which together decrease the amount of inward rectifying K<sup>+</sup> channels in the plasma membrane (Sutter *et al.*, 2007; Takahashi *et al.*, 2013; Takahashi *et al.*, 2016).

#### 1.2.3.2. CO<sub>2</sub>-induced stomatal closure

Guard cells respond to changes in the ambient CO<sub>2</sub> concentration to optimise efficient CO<sub>2</sub> flux for optimal photosynthesis conditions. An elevated CO<sub>2</sub> concentration induces stomatal closure whereas a reduced concentration induces opening. How CO<sub>2</sub> changes are perceived, however, is still unknown. While CO<sub>2</sub> as a lipophilic, nonpolar molecule should diffuse across membrane it has been suggested that CO<sub>2</sub> is transported into the cytoplasm via aquaporin PIP2;1 (Wang *et al.*, 2016). PIP2;1 interacts with carbonic anhydrase (CA)  $\beta$ CA4 that with other CAs converts CO<sub>2</sub> into bicarbonate (Hu *et al.*, 2010; Xue *et al.*, 2011). CO<sub>2</sub> is converted to carbonic acid, bicarbonate and protons leaving several possibilities for sensing mechanisms and how they are sensed is not understood. RHC1, a MATE family transporter, has been proposed as bicarbonate sensor that interacts with  $\beta$ CA4,  $\beta$ CA1 and HT1 to induce activation of OST1 upon elevated CO<sub>2</sub> conditions (Tian *et al.*, 2015). Another publication showed that elevated CO<sub>2</sub> concentrations activate MPKs 4 and 12 which inhibit HT1 (Horak *et al.*, 2016). In steady state conditions HT1 interacts with, phosphorylates and inhibits SLAC1 and GHR1, whether it also interacts with OST1 is under debate (Tian *et al.*, 2015; Horak *et al.*, 2016). The core signalling pathway of elevated CO<sub>2</sub>-induced stomatal closure was suggested by (Tian *et al.*, 2015). However, it was also discovered that ABA biosynthesis, ABA receptors and OST1 are required for this response, suggesting that there may be significant overlap between ABA and CO<sub>2</sub>-induced stomatal closure pathways (Chater *et al.*, 2015).

#### 1.2.3.3. MAMP-induced stomatal closure

In addition to being essential instruments regulating transpiration and gas exchange, stomata can also be exploited by pathogens to gain entry into plant tissues. As natural openings some opportunistic pathogens such as bacteria and rust fungi utilise the stomata to invade plants. Plants try to counteract this by closing their stomata upon recognition of an invading pathogen and this process is referred to as stomatal immunity. This pathogen-induced closure has been shown to be able to alter the outcome of infection to the disadvantage of the pathogen (Melotto *et al.*, 2006). Additional studies performed in grapevines support the importance of this response. Pre-closed stomata and decreased stomatal numbers were shown to impact plant susceptibility to downy mildew (Allegre *et al.*, 2009; Alonso-Villaverde *et al.*, 2011).

Recognition of an invading pathogen relies on the perception of conserved molecular patterns by Pattern-Recognition Receptors (PRRs) at the plasma membrane of guard cells.

Each PRR recognises a specific conserved microbial pattern that we refer to as Microbe-associated molecular patterns (MAMPs). Upon perception of the ligand receptors induce intracellular signalling to induce stomatal closure. Important MAMPs that induce stomatal closure include flg22, elf18 and chitin but also Danger-associated patterns (DAMPs) such as *AtPep1* induce closure (Zheng *et al.*, 2018). While it is known that powdery mildew conidia and chitosan induce stomatal closure (Maffi *et al.*, 1998; Koers *et al.*, 2011), the downstream signalling components are poorly understood. Work in our group has shown that only the *slah3* mutant is impaired in chitin-induced stomatal closure, while the *slac1* mutant shows no impairment. The work moreover suggests that the CERK1-LYK5 receptor complex phosphorylates and activates PBL27 (Shinya *et al.*, 2014) which in turn phosphorylates SLAH3 to induce stomatal closure upon chitin perception (Liu *et al.*, submitted). Flg22 and elf18 are bacterial MAMPs that are recognised by the PRRs FLAGELLIN SENSING 2 (FLS2) and EF-Tu RECEPTOR (EFR), respectively. Both receptors associate with their co-receptor BRI1-ASSOCIATED RECEPTOR KINASE1 (BAK1) upon ligand perception. The signal is transduced onto Receptor-like cytoplasmic kinases (RLCKs) such as BOTRYTIS-INDUCED KINASE1 (BIK1) through direct phosphorylation (Lu, D. *et al.*, 2010). Just like for other stimuli downstream events of ligand perception include ROS accumulation, increase in cytosolic Ca<sup>2+</sup>, NO production and activation of anion channels. For MAMP-induced stomatal closure both NADPH oxidases RBOHF and RBOHD are required, as only a double mutant is fully impaired in flg22-induced stomatal closure (Kadota *et al.*, 2014) as well as their activator BIK1 since *bik1* single and *bik1 plb1* double mutants are unresponsive to flg22 treatment (Li *et al.*, 2014). It is also known that both SLAC1 and SLAH3 are essential for a full closure response as single mutants are only partially impaired. Patch-clamp experiments in guard cells further suggest that SLAC1 is the major anion channel mediating this response (Deger *et al.*, 2015). It has been suggested that also OST1 plays a major role in MAMP-induced stomatal closure as it was shown that the *ost1-2* mutant that shows impaired stomatal closure in response to ABA also does not respond to flg22 treatment (Melotto *et al.*, 2006). Furthermore, it has been shown that this mutant is more susceptible in surface inoculations with the bacterial pathogen *Pst* DC3000<sup>cor-</sup> (Melotto *et al.*, 2006). The same publication also showed that loss of the ABA biosynthesis gene *ABA3* impairs MAMP-induced stomatal closure. It was therefore suggested that there is significant overlap between major stomatal closure pathways.

However, it has also been suggested that OST1 is not a main player in this response and that ABA biosynthesis is not required (Montillet *et al.*, 2013). This publication showed that while

OST1 is strongly activated after ABA treatment no kinase activity could be detected after flg22 treatment. Moreover, stomata of the *ost1-2* mutant show a wild-type-like stomatal closure response at higher flg22 concentrations (Montillet *et al.*, 2013). Instead they suggested an oxylipin signalling pathway, as mutants that are deficient show reduced stomatal closure to flg22 treatment (Montillet *et al.*, 2013).

Perception of AtPep1 relies on the receptor PEPR1 which shares signalling components with MAMP signalling such as BAK1 and BIK1 (Liu *et al.*, 2013). It has been suggested that AtPep1 perception serves as an amplifier of innate immunity and is a MAMP-triggered pathway (Bartels & Boller, 2015). A recent publication presented intriguing results, demonstrating that AtPep1 induces stomatal closure to the same extent as ABA, which is known as the strongest inducer of stomatal closure (Zheng *et al.*, 2018). They furthermore demonstrated that this response is independent of BIK1 and OST1 but requires both anion channels SLAC1 and SLAH3 (Zheng *et al.*, 2018).

#### 1.2.3.4. Pathogen interference with stomatal closure

Stomatal closure is an important defence mechanism for plants to fend off pathogens trying to invade the leaf interior. Several pathogens rely on natural openings such as stomata to successfully invade plant tissues. They have therefore evolved several mechanisms to prevent or reverse stomatal closure that are important virulence factors. Coronatine (COR) is a bacterial toxin produced by several strains of *P. syringae* and can reopen stomata that have closed during the infection process or through ABA (Melotto *et al.*, 2006; Zheng *et al.*, 2012). COR interacts with CORONATINE-INSENSITIVE 1 (COI1) and acts through NAC transcription factors to activate jasmonic acid (JA) signalling which in turn inhibits salicylic acid accumulation and related immune responses (Zheng *et al.*, 2012). The exact mechanism of stomatal reopening through COR remains to be elucidated. The fungal toxin fusicochin is produced by the fungal necrotroph *Fusicoccin amygdale*. It has been shown to irreversibly activate plasma membrane proton pumps by stabilising the interaction with 14:3:3 proteins (Oecking *et al.*, 1997; Baunsgaard *et al.*, 1998; de Boer & de Vries-van Leeuwen, 2012).

In addition to toxins pathogens have also evolved effectors that are able to interfere with stomatal immunity. The effector HopX1 of the wildfire pathogen *P. syringae* pv. *tabaci* seems to have an analogous function to coronatine (Gimenez-Ibanez *et al.*, 2014). HopX1 acts as a cysteine protease and degrades multiple JAZ transcriptional repressors and thereby activates the expression of JA-regulated genes (Gimenez-Ibanez *et al.*, 2014). Another effector,

HopZ1a, also targets JAZ protein, implicating JA signalling as general virulence target (Jiang *et al.*, 2013). The bacterial effector HopM1 has also been shown to interfere with stomatal closure (Lozano-Duran *et al.*, 2014). HopM1 degrades the 14-3-3 protein GROWTH-REGULATING FACTOR 8 (GRF8)/HOPM1 INTERACTING PROTEIN10 (MIN10) via the proteasomal degradation pathways along with several other host targets (Lozano-Duran *et al.*, 2014). Other effectors that suppress stomatal closure during infection include AvrB and HopF2 (Hurley *et al.*, 2014; Zhou *et al.*, 2015). Interestingly, AvrB has been found to target RIN4 and *rin4* mutants do not re-open their stomata during infection with *Pst* DC3000 (Liu *et al.*, 2009). As mentioned above (Section 1.1.2) RIN4 is a target of many bacterial effectors which suggests it plays a central role in immune responses. While the exact role of RIN4 in plant immunity still is elusive its role in stomatal reopening is better understood. RIN4 interacts with H<sup>+</sup>-ATPases AHA1 and 2 and regulates stomatal aperture to inhibit entry of bacterial pathogens (Liu *et al.*, 2009). In the presence of AvrB RIN4 is phosphorylated by RPM1-INDUCED PROTEIN KINASE (RIPK) which leads to the activation of RMP1 (Lee *et al.*, 2015).

Although it was discovered over a decade ago that stomatal closure can influence the success of bacterial invasion (Melotto *et al.*, 2006) our understanding of the signalling pathway in guard cells remains limited. While it has been established that FLS2 is the major receptor mediating this response to *Pst* DC3000 (Zipfel *et al.*, 2004) and that the anion channels SLAC1 and SLAH3 are required (Deger *et al.*, 2015), we do not understand how the signal is transduced from the receptor to the anion channels. This study was aimed at elucidating novel signalling components in the MAMP-induced stomatal closure pathway.

### 1.3. Aims and Objectives

Although the importance of optimal stomatal regulation during bacterial infection has become more apparent, we still lack thorough understanding of the signalling processes taking place in guard cells. This study aims at gaining a better understanding of the molecular mechanisms and components that are involved in MAMP-triggered stomatal closure.

It is well understood how MAMP perception activates immune signalling and what the most central regulators are. The initiation of stomatal closure is also well understood and previous studies on multiple stomatal closure pathways have offered insight into core executors. However, as of yet no direct link has been made between MAMP perception through plasma membrane localised receptors and executors of stomatal closure.

Typically, assays studying immune responses use whole leaves or even whole *Arabidopsis thaliana* rosettes with no distinction between cell types. This may have hindered the discovery of guard cell-specific regulators in MAMP-triggered stomatal closure. To this end this study aimed at providing both transient and stable transgenic tools to study guard cell responses. This study provides Virus-induced gene silencing-based transient assays in *Nicotiana benthamiana* and screened promoters to mediate guard cell-specific expression in *Arabidopsis thaliana*. These tools will empower future research into guard cell-specific responses in *N. benthamiana* and *A. thaliana*.

Guard cells have been shown to respond in an autonomous manner to multiple closure-inducing stimuli. It is currently unknown whether stomatal closure is another cell-autonomous guard cell response. Loss of FLS2 renders plants more susceptible to bacterial spray infections. It has been speculated that this may not be due to the loss of stomatal closure but to the loss of mesophyll PTI responses. I therefore expressed FLS2 in a guard cell-specific manner and investigated whether these plants retain the ability to close in response to flg22 and if so, whether this is sufficient to restore a wild-type-like susceptibility level to infection with bacteria. These experiments showed that guard cells can change the outcome of infection when no other cell types can mount flg22-induced responses.

ABA- and CO<sub>2</sub>-induced stomatal closure pathways have been shown to depend on the same central regulators. It has been proposed that ABA biosynthesis is also required for MAMP-induced stomatal closure. In addition to this, OST1 has been put forward as general convergence point of guard cell closure pathways. This was called into question when Montillet and colleagues published that an *ost1-2* point mutant can close upon higher flg22

concentrations and that OST1 is not active after flg22 treatment (Montillet *et al.*, 2013). In this study I aimed to elucidate which signalling components are required for MAMP-induced stomatal closure and whether these components overlap with central regulators of other stomatal closure pathways.

With the experiments conducted in this study I advanced our understanding of stomatal regulation during pathogen infection.

## 2. Material and Methods

### 2.1. Media and Buffers:

#### 2.1.1. GM medium for *Arabidopsis thaliana* seedlings

Recipe for 1l scale. Medium was sterilised by autoclaving.

4.30g MS salts  
0.56g MES  
0.1g Myo-inositol  
1 ml GM vitamins x1000  
pH 5.7  
0.8% Agar

##### GM vitamins x1000

0.1g Thiamine  
0.05g Pyridoxine  
0.05g Nicotinic Acid  
100 ml H<sub>2</sub>O

#### 2.1.2. L medium for bacterial growth

Recipe for 1l scale. Medium was sterilised by autoclaving.

10g Tryptone  
5g Yeast extract  
5g KCl  
1g D-Glucose

For plates 1% agar was added prior to autoclaving and plates were poured after medium cooled.

#### 2.1.3. King's B medium for *P. syringae* growth

Recipe for 1l scale. Medium was sterilised by autoclaving.

20g Proteose peptone  
10 ml Glycerol  
1.5g K<sub>2</sub>HPO<sub>4</sub>  
pH 7  
1.5% Agar

#### **2.1.4. Protein Buffers**

##### **2.1.4.1. Plant Protein Extraction Buffer**

150 mM TRIS-HCl pH 7.5  
10 mM EDTA  
150 mM NaCl  
10% Glycerol  
5 mM DTT  
1% IGEPAL CA-630 (Sigma-Aldrich)  
1 % Plant Protease Inhibitor Cocktail (Sigma-Aldrich)  
1 mM PMSF

##### **2.1.4.2. Loading/Sample buffer**

50 mM TRIS-HCl pH 6.8  
5% Glycerol  
1% SDS  
0.017% Bromophenol blue

##### **2.1.4.3. Kinase buffer**

25 mM Tris-HCl pH 7.5  
3 mM MgCl<sub>2</sub>  
3 mM MnCl<sub>2</sub>  
1 mM DTT  
10 μM ATP

#### **2.1.5. Stomata opening buffer**

50 mM KCl  
10 μM CaCl<sub>2</sub>  
10 mM MES pH 6.15  
0.01% Tween  
in H<sub>2</sub>O

#### **2.1.6. *Agrobacterium tumefaciens* infiltration buffer**

10 mM MES  
10 mM MgCl<sub>2</sub>  
100 μM Acetosyringone

#### **2.1.7. Solutions for protoplast isolation**

##### **2.1.7.1. Enzyme solution**

1-1.5 % Cellulase R10 (Yakult Honsha, Tokyo Japan)  
0.2-0.4 % Macerozyme R10 (Yakult Honsha, Tokyo Japan)

0.4 M Mannitol  
 20 mM KCl  
 20 mM MES pH 5.7  
 Solution with enzymes was heat-activated at 55°C and cooled before adding:  
 10mM CaCl<sub>2</sub>  
 0.1 % BSA  
 Enzyme solution was passed through a 0.45 nm filter

#### 2.1.7.2. PEG Solution

4g PEG 4000 (Fluka #81240)  
 0.2M Mannitol  
 0.1M CaCl<sub>2</sub>  
 3 ml H<sub>2</sub>O

#### 2.1.7.3. W5 Solution

150 mM NaCl  
 125 mM CaCl<sub>2</sub>  
 5 mM KCl  
 2 mM MES pH5.7

#### 2.1.7.4. MMg Solution

0.4 M Mannitol  
 15 mM MgCl<sub>2</sub>  
 4 mM MES pH 5.7

## 2.2. Antibiotics

Table 2.2.1: Antibiotics and the concentrations used in this study

<b>Antibiotic</b>	<b>Stock concentration</b>	<b>Working concentration</b>
Carbenicillin	100 mg/ml in H <sub>2</sub> O	100 µg/ml
Chloramphenicol	25 mg/ml in ethanol	25 µg/ml
Gentamycin	50 mg/ml in H <sub>2</sub> O	50 µg/ml
Kanamycin	50 mg/ml in H <sub>2</sub> O	50 µg/ml
Rifampicin	100 mg/ml in DMSO	50 µg/ml
Spectinomycin	100 mg/ml in H <sub>2</sub> O	100 µg/ml

## 2.3. Antibodies and beads used in this study

Table 2.3.1: Antibodies and beads used in this study

<b>Antibody</b>	<b>source</b>	<b>manufacturer</b>	<b>dilution used</b>
α-FLS2	polyclonal (rabbit)	Eurogentec	1:10.000
α-BAK1	polyclonal (rabbit)	Eurogentec	1:5.000

$\alpha$ -HA-HRP	monoclonal (rat)	Sigma-Aldrich (Roche)	1:2.000
$\alpha$ -FLAG-HRP	monoclonal (mouse)	Sigma-Aldrich	1:2.000
$\alpha$ -GORK	polyclonal (rabbit)	Agrisera	1:1.000
$\alpha$ -rabbit-HRP	polyclonal (goat)	Sigma-Aldrich	1:10.000
$\alpha$ -mouse-HRP	polyclonal (goat)	Sigma-Aldrich	1:10.000
$\alpha$ -rat-HRP	polyclonal (goat)	Sigma-Aldrich	1:10.000
$\alpha$ -FLAG Affinity Gel	monoclonal (mouse)	Sigma-Aldrich	

## 2.4. Plant Materials

Table 2.4.1: *Arabidopsis thaliana* plants used in this study

Mutant name	type	received from
<i>ost1-3</i>	SALK_008068	NASC
<i>ost1-4</i>	GK_516_B05	NASC
<i>nced3-2 nced5-2</i>	GK_129_B08/GK_328_D05	Julie Gray
<i>aba2-3</i>	EMS	NASC
<i>aba1</i>	SALK_059469	NASC
<i>aba3</i>	SAiL_576_D01	NASC
<i>snrk2.2 snrk2.3 ost1-3</i>	GK_807_G04/SALK_107315/SALK_008068	Maik Boehmer
<i>snrk2.2-1</i>	GK_807_G04	NASC
<i>snrk2.2-2</i>	SALK_096546	NASC
<i>snrk2.3</i>	SALK_107315	NASC
<i>snrk2.3</i>	SALK_107317	NASC
<i>snrk2.3</i>	SALK_096548	NASC
<i>abi1-1</i>	EMS	Rob Roelfsema
<i>pyr1 pyl1 pyl4</i>	EMS/SALK_054650/SAiL_517_C08	Sean Cutler
<i>pyr1 pyl1 pyl2 pyl4</i>	EMS/SALK_054650/GT2864/SAiL_517_C08	Sean Cutler
<i>pyr1 pyl1 pyl2 pyl4 pyl5</i>	EMS/SALK_054650/GT2864/SAiL_517_C08/SM_3_3495	Pedro Rodriguez Egea
<i>pyr1 pyl1 pyl2 pyl4 pyl5 pyl8</i>	EMS/SALK_054650/GT2864/SAiL_517_C08/SM_3_3495/SAiL_1269_A02	Pedro Rodriguez Egea
<i>crk10-1</i>	SALK_023945C	CRK consortium
<i>crk17</i>	SALK_114137	CRK consortium
<i>crk18</i>	SALK_090966C	CRK consortium

<i>crk28</i>	SALK_085178	CRK consortium
<i>fls2</i>	SALK_093905	Freddy Boutrot
<i>fls2c</i>	SAiL_691_C04	NASC

Table 2.4.2: *Nicotiana benthamiana* plants used in this study

mutant name	received from
<i>16c-GFP</i>	David Baulcombe
<i>pFLS2::FLS2-GFP</i>	Malick Mbengue

## 2.5. Bacterial strains and pathogens

Table: 2.5.1: Bacterial strains and pathogens used in this study

Strain	organism	use
DH5 $\alpha$	<i>E. coli</i>	cloning
rosetta	<i>E. coli</i>	recombinant protein expression
GV3101:pMP90	<i>A. tumefaciens</i>	transient expression in <i>N. benthamiana</i>
DC3000	<i>P. syringae</i>	infection assays in <i>A. thaliana</i>
DC3000 <sup>cor-</sup>	<i>P. syringae</i>	infection assays in <i>A. thaliana</i>

## 2.6. Methods

### 2.6.1. Plant growth conditions

#### 2.6.1.1. *Arabidopsis thaliana* and *N. benthamiana* seed sterilisation with chlorine gas

*Arabidopsis thaliana* seeds were surface sterilised in a desiccator. Chlorine gas was produced by mixing 100 ml bleach with 2.7 ml of HCl in a beaker. Seeds were incubated in the chlorine gas for at least 6 hours and dried in a sterile hood overnight.

#### 2.6.1.2. Growing *Arabidopsis thaliana* and *N. benthamiana* seeds on plates

Surface sterilised seeds were evenly distributed on GM plates under sterile conditions. If seeds were transgenic and possessed a BASTA selection cassette PPT was added at a concentration of 2 mg/ml for *N. benthamiana* and 10 mg/ml for *Arabidopsis thaliana* seeds. Plates were sealed with tape and seeds were stratified at 4°C overnight. Plates were transferred into a Sanyo Growth Chamber and grown for two weeks at 20°C with 10 hours of light at 86  $\mu\text{mol m}^{-2} \text{s}^{-1}$ . After two weeks plants were transferred to soil and grown as described below.

#### 2.6.1.3. Growing *Arabidopsis thaliana* and *N. benthamiana* on soil

*Arabidopsis thaliana* plants were grown on soil at 20°C under short day light conditions with 10 hours of light at 160  $\mu\text{mol m}^{-2} \text{s}^{-1}$ . For propagation plants were transferred to long day light conditions with 16 hours of light at 160  $\mu\text{mol m}^{-2} \text{s}^{-1}$ . Humidity was at 65% for both short and long day conditions. *Nicotiana benthamiana* plants were grown under constant long day conditions with 16 hours of light at 24°C and with 45-65% humidity at 145  $\mu\text{mol m}^{-2} \text{s}^{-1}$ .

#### 2.6.2. **Generation of transgenic plants**

Transgenic plants were generated by the Tissue Culture team at the Sainsbury Laboratory. Plants were transformed following the floral dip method. Flowering plants were dipped into *Agrobacterium tumefaciens* solutions and vacuum infiltrated.

#### 2.6.3. **Polymerase Chain Reaction (PCR) for cloning:**

For cloning purposes, the high-fidelity proof-reading polymerase Phusion (New England Biolabs) was used.

<u>reaction setup</u>	<u><math>\mu\text{l}</math></u>
5x Phusion Buffer	10
10 $\mu\text{M}$ dNTPs	1
10 $\mu\text{M}$ Primer fwd	2.5
10 $\mu\text{M}$ Primer rev	2.5
100 % DMSO	5
50 mM $\text{MgCl}_2$	0.5
Template DNA	5
Phusion	0.5
<u>H<sub>2</sub>O up to</u>	<u>50</u>

Reactions were incubated in a BIORAD PCR thermocycler following standard protocol instructions. Annealing time, elongation and cycle number were adjusted to each primer pair, template properties and fragment size. PCR products were separated on 1% Agarose gels (in TAE buffer: 40 mM Tris-HCl, 20 mM NAOAc, 1 mM EDTA, pH 7.9) and bands were imaged with a BIORAD GelDoc™ XR+ Documentation System. If DNA fragments were needed for ligation reactions desired bands were excised from agarose gels under UV light to visualise the bands. The DNA was extracted from agarose gels using the Macherey-Nagel NucleoSpin Gel and PCR Clean-Up kit following the manufacturer's instructions.

#### 2.6.4. **Polymerase Chain Reaction (PCR) for genotyping**

For genotyping the Promega GoTaq Polymerase was used.

<u>reaction setup</u>	<u>μl</u>
10x GoTaq Buffer	2
10 μM Primer fwd	0.25
10 μM Primer rev	0.25
10 μM dNTPs	0.25
25 mM MgCl <sub>2</sub>	1.25
H <sub>2</sub> O	3.95
GoTaq Polymerase	0.05
<u>genomic DNA</u>	<u>2</u>

Reactions were incubated in a BIORAD PCR thermocycler following standard protocol instructions. Annealing temperature of 48°C and 40-45 cycles were used. Elongation time was adjusted to fragment size allowing one minute per 1000 base pairs. PCR products were separated on 1% Agarose gels (in TAE buffer: 40 mM Tris-HCl, 20 mM NAOAc, 1 mM EDTA, pH 7.9) and bands were imaged with a BIORAD GelDoc™ XR+ Documentation System.

#### **2.6.5. Colony Polymerase Chain Reaction (PCR)**

Promega GoTaq Polymerase was used for colony PCRs. Reaction setup used was identical to PCR setup for genotyping except 5.95 μl of H<sub>2</sub>O was used. Bacterial colonies were picked up with a pipette tip and mixed into the PCR reaction by pipetting up and down. The pipette tip was used to spread the residual bacteria onto a new plate containing suitable antibiotics. PCR products were separated on 1% Agarose gels (in TAE buffer: 40 mM Tris-HCl, 20 mM NAOAc, 1 mM EDTA, pH 7.9) and bands were imaged with a BIORAD GelDoc™ XR+ Documentation System.

#### **2.6.6. Restriction Enzyme digest**

PCR products or plasmids were digested with restriction enzymes from New England Biolabs (NEB). Around 1 μg of DNA was digested in a 20 μl setup containing 2 μl CutSmart Buffer, 0.2 μl BSA and 0.25 μl restriction enzyme. Reactions were incubated at 37°C for at least 2 hours or overnight if required.

#### **2.6.7. Golden Gate cloning**

Golden Gate cloning was used as general cloning strategy as described previously (Engler *et al.*, 2008; Werner *et al.*, 2011; Emami *et al.*, 2013; Engler *et al.*, 2014). In this technique Type IIS restriction enzymes are utilized to develop a molecular toolbox of genes of interest, promoters, tags and terminators that can be assembled together as desired. Primers were designed to domesticate genes of interest and eliminate internal enzyme recognition sites. PCR products were separated on 1% Agarose gels and bands of the correct size were cut and

the bands were extracted using Macherey-Nagel Gel and PCR purifying kit following the manufacturer's instructions. DNA concentration was determined using a Nanodrop. 100 ng of acceptor plasmid and insert were combined in a PCR tube in relation plasmid:insert of 1:3 alongside with 1.5 µl of BSA, 1.5 µl of T4 Ligase Buffer (NEB), 1 µl *Bsal* or *Bpil*, 0.5 µl T4 ligase and water up to a 15 µl reaction. The reactions were incubated in a BIORAD PCR thermocycler (37°C for 20 seconds followed by 27 cycles of 37°C for 3 minutes, 16°C for 4 minutes followed by one cycle of 50°C for 5 minutes, 80°C for 5 minutes). Ligation products were transformed into DH5α cells using the heat-shock method and spread on plates with L medium containing appropriate antibiotics. If plasmids contained a LacZ cassette IPTG and xGAL were added to the plates to distinguish self-ligated plasmids from successful ligations. Plates were incubated at 37°C overnight and insertions confirmed either via colony PCR or restriction digest, or both. For restriction digests plasmids were isolated using the Macherey-Nagel NucleoSpin Plasmid Kit following the manufacturer's instructions. Sequences were confirmed using Sanger sequencing performed by GATC Biotech AG by combining 500 ng of plasmid DNA with 4 µl of sequencing primer (from 10 µM dilution). ABI files were analysed using the Vektor NTI software.

Promoters, coding genes, tags and terminators domesticated to exclude restriction sites are cloned into level 0 acceptors. To generate level 1 plasmids several level 0 plasmids were combined in a digestion-ligation reaction and assembled into an expression cassette with Promoter, Gene of interest, fluorescent tag, if required, and terminator. Several level 1 expression cassettes were assembled together to create level 2 vectors. Level 2 vectors with plant selection cassettes were used for generation of transgenic plants.

#### **2.6.8. Restriction Enzyme Cloning**

Primers for restriction enzyme cloning were designed by Thomas DeFalco and Janina Tamborski (Table 2.6.3.). Inserts were amplified by PCR using the proofreading ThermoFisher Phusion Polymerase. Vectors were isolated from bacterial *E. coli* cells using the Macherey-Nagel NucleoSpin Plasmid Kit as recommended by the manufacturer. Vectors and PCR products (26µl) were digested in the CutSmart Buffer (New England Biolabs, 3 µl) with appropriate restriction enzymes (0.5 µl each) for at least 2h at 37°C. Vectors were additionally dephosphorylated by adding 1 µl of Roche Shrimp Alkaline Phosphatase and incubating at 37°C for 10 minutes. Phosphatase was inactivated by incubating at 65°C for 15 minutes. All digests were loaded onto 1% agarose gels in TAE buffer and separated via electrophoresis. Bands of the correct size were excised with the help of UV visualisation. PCR

products and vectors were extracted using the Macherey-Nagel Gel and PCR purification kit following the manufacturer's instructions. DNA concentration was determined using a NanoDrop™ 8000 Spectrophotometer (Thermo Fisher Scientific) and ligation reactions set up as follows: 1 µl of 10x T4 ligase Buffer (New England Biolabs), 1 µl vector, 0.5 µl T4 Ligase (New England Biolabs), insert in a relation of 3:1 to the vector and water to 10 µl. Reactions were incubated overnight at room temperature and on the next day the T4 ligase was inactivated by incubating at 65°C for 10 minutes before transforming reactions into DH5α by heat-shock.

### **2.6.9. Bacterial transformation**

#### **2.6.9.1. Heat-shock**

Plasmids or ligation reactions were added to 100 µl of DH5α chemically competent E. coli cells. Bacteria and DNA were incubated on ice for 30 minutes before subjecting the cells to heat-shock treatment at 42°C for 90 seconds. Bacteria were left to recover on ice for 2 minutes and 900 µl of L medium was added and the cells left to recover at 37°C for at least an hour. After recovery 50-200 µl were plated on L plates containing appropriate antibiotics and incubated over-night at 37°C.

#### **2.6.9.2. Electroporation**

Electroporation cuvettes were cooled on ice prior to transformation. Bacteria were thawed on ice before adding 10ng - 1 µg of plasmid DNA. Bacteria with plasmids were transferred to pre-cooled electroporation cuvettes. Electroporation was performed with a Biorad MicroPulser™ Electroporation system at the "Agr" setting for *Agrobacterium tumefaciens* provided by the manufacturer. Bacterial cells were subsequently transferred to a 1.5 ml centrifuge tube with 1 ml of L medium. Cells were incubated at 28°C for 2h. After recovery 50-200 µl were plated on L plates containing appropriate antibiotics and incubated for two days at 28°C.

### **2.6.10. Isolation of genomic DNA**

#### **2.6.11. Edwards method**

One fully expanded leaf of one 4-5-week-old Arabidopsis plant was harvested into a 1.5 ml centrifuge tube containing two metal beads and 400 µl of Edwards Buffer (200 mM Tris-HCl pH 7.5, 250 mM NaCl, 25 mM EDTA, 0.5% SDS). Tissue was ground in a Qiagen Tissue Lyser for 2 Min at full speed. The tubes were spun in an Eppendorf tabletop centrifuge for 5 min

at 13,000 *g* for 5 min and 300  $\mu$ l of the supernatant were transferred to a new 1.5 ml centrifuge tube. 300  $\mu$ l of Isopropanol were added, the tubes were inverted and incubated for a short period at room temperature. The samples were centrifuged for 5 minutes at 16,000 *g* and the supernatant was taken off with a vacuum pump. The pellet was washed with 300  $\mu$ l of 70% ethanol and dried before it was resuspended in 100  $\mu$ l of Millipore water.

#### **2.6.12. Boiling method**

A small piece of one *Arabidopsis thaliana* plant was cut and placed in a 96-well PCR plate containing 60  $\mu$ l of Extraction Solution (100 mM Tris-HCl pH 8, 250 mM KCl, 10 mM EDTA, adjusted to pH 9.3). Samples were incubated at 95°C for 15 min and cooled to 16 °C for 10 min. The extraction solution was transferred into a fresh 96-well PCR plate taking care not to transfer any leaf material. DNA was diluted by adding 200  $\mu$ l Dilution Solution (1 % BSA adjusted to pH 7.6 with 1 M KOH) and stored at 4°C until used for PCR.

#### **2.6.13. Site-directed point mutagenesis**

Primers were designed to be 30-40 base pairs long and to harbour the desired point mutation in their middle. Melting temperature was adjusted to be higher than 78°C. Plasmids that were to be mutated were used as template for the 50  $\mu$ l PCR reaction that was setup as follows: 2.5  $\mu$ l of each forward and reverse primer, 10  $\mu$ l Phusion Buffer for GC-rich templates, 4  $\mu$ l of 10 mM dNTPs, 1.5  $\mu$ l DMSO and 1  $\mu$ l Phusion Polymerase. A control reaction was setup that did not include primers but only the template plasmid. The samples were incubated in a BIORAD PCR thermocycler with the following cycle conditions: 20 cycles of 98°C for 10 seconds, 58-65°C for 30 seconds, 72°C for 60 seconds per 1 kilobase. Polymerase was heat-inactivated at 72°C for 15 minutes. The template plasmid was digested by adding 1  $\mu$ l of DpnI (New England Biolabs) enzyme and incubating at 37°C for at least 2 hours. 10  $\mu$ l of the reaction were transformed into the DH5 $\alpha$  *E.coli* strain using the heat-shock method and spread on plates containing appropriate antibiotics. Plates were incubated overnight at 37°C. Mutations were verified by Sanger sequencing.

#### **2.6.14. RNA isolation using TRI reagent**

3 leaf discs of 4-5-week-old *Arabidopsis thaliana* plants were harvested into a 1.5 ml centrifuge tube and snap frozen in liquid nitrogen. Tissue was ground on ice into a fine green powder. 900  $\mu$ l of TRI reagent were added and the solution was vortexed vigorously. Subsequently 200  $\mu$ l chloroform were added and again vortexed vigorously. The tubes were centrifuged for 20 min at max speed at 4°C in an Eppendorf table top centrifuge. 550  $\mu$ l of

the upper phase were transferred to a fresh 1.5 ml centrifuge tube and the same volume of isopropanol was added, the tubes were inverted and incubated at room temperature for 10 min. The tubes were centrifuged at max speed at 4°C. The supernatant was discarded and the pellet washed with 500 µl of 70% ethanol. The supernatant was discarded and the pellet dried before dissolving the RNA in 26 µl Millipore water. To digest any residual genomic DNA the extraction was treated with DNase (Applied Biosystems TURBO DNA-free kit) following the manufacturer's instructions. 0.1 volume of 10x TURBO DNase Buffer and 1 µl TURBO DNase were added to the extracted RNA and gently mixed. The mixture was incubated at 37°C for 20-30 minutes. After incubation 0.1 volume of DNase inactivation reagent was added and incubated at 24 °C for 5 minutes. The tubes were centrifuged at 10,000 *g* for 1.5 minutes and the supernatant transferred to a fresh 1.5 ml centrifuge tube. RNA concentration was determined with a Nanodrop instrument (Thermo Fisher Scientific).

#### **2.6.15. cDNA synthesis**

cDNA was transcribed using the Invitrogen SuperScript II reverse transcriptase following the manufacturer's instructions. 1 ng to 5 µg of RNA were mixed with 1 µl Oligo dTs, 1µl of 10 mM dNTPs and incubated at 65°C for 5 minutes. Samples were chilled on ice and 4 µl of 5x First Strand buffer, 2 µl DTT and 1 µl RNaseOUT were added and incubated at 42°C for 5 minutes. Enzymes were inactivated at 70 µl for 15 minutes and the reactions filled up to 60 µl and stored at -20°C until use.

#### **2.6.16. Protein extraction from plant samples**

*Arabidopsis thaliana* leaf material from 4-5-week-old plants was harvested into a 1.5 ml centrifuge tube and snap frozen in liquid nitrogen. The leaf material was ground on ice until it was a fine powder. Protein extraction buffer was added to frozen ground leaf material (2:1 w/v) or protoplasts and incubated at 4°C for at least 30 minutes. Samples were centrifuged at 16,000 *g* for 20-30 minutes at 4°C and the supernatant was transferred to a new centrifuge tube. Loading buffer was added and the sampled boiled at 95°C for 10 minutes. Boiled samples were centrifuged at 16,000 *g* for 1 minute to spin down any precipitated SDS. Samples were loaded onto acrylamide gels and run in SDS buffer at 120 V for 1-2 hours.

#### **2.6.17. Co-Immunoprecipitation of *Arabidopsis thaliana* proteins**

*Arabidopsis thaliana* protoplasts were transfected with suitable expression vectors to express proteins of interest as described below (2.5.20). Protoplasts were snap frozen in liquid nitrogen and proteins were extracted as described above (2.5.14). For 500 µl of

protoplasts 1 ml of extraction buffer (2.1.4.1) was added. After extraction 100 µl of sample was transferred to a new centrifuge tube, snap frozen and stored at -80°C as input sample. All work was performed under 4°C. Anti-FLAG Affinity Gel was prepared by centrifuging at 100-500x *g* at 4°C. The supernatant was discarded and exchanged with 1 ml of extraction buffer. The wash step was repeated and the beads incubated for 30 minutes in the extraction buffer. After incubation 30 µl of bead slurry was added to plant extracts and incubated for 2-3 hours while shaking. Subsequently the mixtures were centrifuged at 200 *g* for 1 minute and the supernatant was discarded. The beads were washed three times with extraction buffer before sample buffer was added, the samples were boiled for 10 minutes at 95°C and stored at -80°C until further processed.

#### **2.6.18. SDS-Page and Semi-dry Western blotting**

Bisacrylamide gels were prepared as previously described (Laemmli 1970). Acrylamide percentage was varied according to protein size. Boiled protein samples with sample buffer were loaded onto stacking gels as well as PageRuler™ Plus Protein Ladder (Thermo Fisher Scientific). Polyacrylamide Gel Electrophoresis (PAGE) was run with SDS-running buffer (25 mM Tris-HCl, 250 mM glycine, 0.1% SDS, pH8) in a BIORAD Mini-PROTEAN® Tetra Vertical Electrophoresis Cell at 90 V until proteins passed the stacking gel and subsequently at 120 V until the desired protein separation was achieved. Acrylamide gels were incubated for 30 minutes in transfer buffer (20% methanol) while a PVDF membrane was activated in methanol for 1 minute. Proteins were transferred from the gel onto the activated PVDF membrane using the semi-dry method in the BIORAD Trans-Blot® SD Transfer Cell at 25 V for 1.15 hours. Whatman Papers were soaked well in transfer buffer and placed onto the Trans-Blot® SD Transfer Cell as follows (bottom to top): thick Whatman Paper, two thin Whatman Papers, PVDF membrane, acrylamide gel, two thin Whatman Papers, thick Whatman Paper. Special care was taken to avoid air bubbles trapped between gel and membrane to ensure an even transfer across the whole membrane.

#### **2.6.19. Expression and purification of recombinant proteins**

Expression vectors were transformed into Rosetta cells using the heat-shock method. Colonies were picked into liquid L medium containing suitable antibiotics and chloramphenicol and grown overnight at 37°C. On the next day a larger culture of 500 ml of L medium with antibiotics and chloramphenicol was inoculated with 5 ml from the overnight culture and grown for 2-3 hours at 37°C. Protein expression was induced by adding 0.1 mM

IPTG to the bacterial culture and incubating the cells at 18°C overnight. Subsequently bacterial cells were centrifuged for 15 minutes at 4,000 *g* speed. The bacterial pellet was resuspended in extraction buffer (50 mM Tris pH 7.5, 500 mM NaCl, 5% glycerol, 0.5-1 mM DTT and Mini Protease Inhibitor; for HA-tagged proteins add 3 mM imidazole) and frozen in liquid nitrogen until further processed.

To purify proteins frozen bacterial pellets were thawed in warm water and lysed via sonication. Cell fragments were centrifuged for 20 minutes at 20,000 *g* at 4°C. The supernatant was transferred to a 50 ml centrifuge tube and GSH- or Ni-agarose resin was added to enrich for tagged recombinant proteins. The mixtures were left to incubate for 30-60 minutes at 4°C ensuring constant shaking. Samples were centrifuged at 500 *g* for 1 minute and the supernatant was taken off with a vacuum pump. The resin pellet was washed four to five times with 20 ml of wash buffer (50 mM Tris-HCl pH7.5, 500 mM NaCl, 5% glycerol; for HA-tagged proteins add 30 mM imidazole). After the final wash was removed the proteins were eluted from the resin with elution buffer (50 mM Tris-HCl pH7.5, 500 mM NaCl, 5% glycerol; add 10 mM reduced GSH for GST-tagged proteins and 300 mM imidazole for HA-tagged proteins) and incubated on ice for 3 minutes. The resin was spun down at 500 *g* for 1 minute and the protein solutions were transferred to a new 15 ml centrifuge and stored at -80°C until processed further. To assess whether proteins were produced 10 µl of protein sample with 5 µl of sample buffer were boiled at 95°C for 10 minutes and separated on a 13% bisacrylamide gel. The gel was stained in Coomassie Brilliant Blue Solution (0.5% Coomassie brilliant blue R-250, 50% methanol and 7.5% glacial acetic acid) for 1 hour and de-stained for several hours (de-stain solution: 40% methanol, 20% acetic acid).

#### **2.6.20. Transphosphorylation assay**

Proteins were produced in *E.coli* rosetta cells and expressed and purified as described above. Recombinant proteins were incubated together in kinase buffer (2.1.4.3 on p. 42) with 1 µg of kinase and substrate each for 30 minutes at 30°C. Sample buffer was added, the samples boiled at 95°C for 10 minutes and stored at -80°C until processed further.

#### **2.6.21. Spray infection assay**

*Arabidopsis thaliana* plants were grown for 4-5 weeks under short day conditions (see 2.6.1.3). The evening before spraying, the plants are watered and covered with a propagator lid to maintain high humidity for ideal infection conditions. Two days before spraying bacteria were grown on KB medium containing appropriate antibiotics at 28°C over-night.

The next day, a small number of bacteria was resuspended in 100 µl of 10 mM MgCl<sub>2</sub> and spread on a new KB plate with antibiotics and grown over-night at 28°C. Bacterial cells were resuspended in 15 ml of 10 mM MgCl<sub>2</sub> and set to the appropriate OD<sub>600</sub>. Just before spraying, 40 µl of Silwet was added to 100 ml of bacterial solution. Bacteria were sprayed evenly on the upper and lower side of the plant leaves. Plants remained covered for 1 day when sprayed with *Pst* DC3000 and three days when sprayed with *Pst* DC3118. Three days after spraying three leaf discs per plant were harvested into a 1.5 ml centrifuge tube containing 200 µl of 10 mM MgCl<sub>2</sub> and 2 metallic beads. Plant tissue was homogenised using a Tissue Lyser by shaking at 30 1/s for 4 minutes. Ground tissue was diluted 1:10 to 1:100000 and 10 µl was plated on KB plates and grown at 28°C for two days. After two days bacterial dilutions were counted and analysed.

#### **2.6.22. Isolation and transfection of mesophyll protoplasts**

*Arabidopsis thaliana* plants were grown for 4-5 weeks at short-day conditions. Fully expanded leaves were excised and placed next to each other on masking tape with the lower side facing upwards. The lower epidermis of the leaves was removed with scotch tape and the leaves without epidermis were placed facing down into a petri dish containing 15 ml of enzyme solution (see section 2.1.7.1 on p. 42) and shaken at 500 rpm for 1-2 hours. After two hours the tape was removed and 15 ml of W5 solution (see section 2.1.7.3 on p. 43) was poured over the leaves to release more protoplasts. Protoplasts were filtered through a 50 µm filter and collected in a 14 ml round bottom tube on ice. Protoplasts were spun down at 500g for 1 min at 4°C. The supernatant was discarded and the pellet resuspended in 10 ml W5 solution. Protoplasts were incubated on ice for 30 minutes. Protoplasts were centrifuged again and resuspended in MMg solution (see section 2.1.7.4 on p. 43) to the desired dilution.

Plasmid DNA was added to the protoplasts and incubated for 1 min. PEG solution was added to the protoplasts in relation 1:1 and incubated for 7 minutes. Transfection was stopped by adding at least two volumes of W5 solution. Protoplasts were spun down and resuspended in W5 solution. Protoplasts were incubated at room temperature over-night, frozen in liquid nitrogen and stored at -80°C until protein extraction.

#### **2.6.23. Isolation of guard cell-enriched samples**

*Arabidopsis thaliana* plants were grown for 4-5 weeks on soil under short-day conditions as described above. Leaves were cut off and the mid-rib was excised with a razor blade until 1-1.5 g of leaf material per genotype was collected. The cut leaves were transferred to a

Warring blender with 250 ml Milli-Q water and a handful of crushed ice. The mixtures were blended for 1 minute on the High setting. The sample was filtered through a mesh filter of 100 nm size and the epidermal peels were collected in the middle of the filter. The peels were transferred back to the blender together with 250 ml Milli-Q water and a handful of crushed ice. The sample was blended for 1 minute on the high setting and filtered again. Blending and filtering were repeated another time before the epidermal peels were collected from the filter and transferred to a 1.5 ml centrifuge tube, snap frozen in liquid nitrogen and stored at -80°C until processed further.

#### **2.6.24. Split-YFP assay**

Expression vectors were transformed into *Agrobacterium tumefaciens* *GV3103:pMMP90* cells via electroporation as described above. Bacterial cells were grown overnight in liquid L culture with suitable antibiotics at 28°C shaking at 1 *g*. In the morning cells were collected via centrifugation at 3,400 *g* for 15 minutes and resuspended in infiltration buffer (see section 2.1.6). Complementary constructs were combined in solution to a final OD<sub>600</sub>=0.1 and infiltrated together. Two fully expanded leaves of five-week-old *N. benthamiana* plants were infiltrated and the infiltrated areas marked with a waterproof marker pen. Two days after infiltration leaf discs from the infiltrated areas were harvested and imaged with a Leica SP5 Confocal Laser-scanning Microscope.

#### **2.6.25. Confocal imaging**

For cell biological assays we used the Leica SP5 Confocal Laser-scanning Microscope. All images were taken with the 63x water immersion objective. GFP fluorescence was excited with an Argon Laser set to 488 nm and was detected with the Hy-D detector set to the wavelength of 500-550 nm. YFP was excited at 514 nm and detected from 520-570 nm.

#### **2.6.26. Virus-induced gene silencing (VIGS)**

Three days before infiltration bacteria were streaked on LB plates containing appropriate antibiotics and incubated at 28°C for two days. Subsequently, liquid LB cultures with antibiotics were inoculated from the plates and shaken at 1 *g* and 28°C over-night. In the morning bacterial cultures were transferred to a centrifuge tube and spun at 1,900 *g* for 15 minutes. The supernatant was discarded and the bacterial pellet resuspended in *Agrobacterium tumefaciens* infiltration buffer. The construct containing the RNA1 *Tobacco Rattle Virus* (TRV) was mixed with the RNA2 constructs targeting the gene of interest to a final OD<sub>600</sub> of 0.4 and 0.2, respectively. *N. benthamiana* plants were infiltrated at either 2 or

5 weeks of age, depending on the silencing distribution that was desired. 2-week-old plants were used for even silencing throughout all cell types, whereas 5-week-old plants were used when trying to exclude guard cells from silencing. Plants were infiltrated with either *Tobacco Rattle Virus (TRV)* alone or *TRV::GFP* as control. *TRV::NbRBOHB* and *TRV::SERK3a/b* were used to silence components required for MAMP-triggered stomatal closure. When two-week-old plants were used experiments were performed 2 weeks after infiltration, in 5-week-old plants 6 days post infiltration. When five-week-old plants were silenced the area that was infiltrated was marked with a marker and the same area was used for further experiments.

#### **2.6.27. ROS measurements**

*N. benthamiana* or *Arabidopsis thaliana* plants were grown in soil for five weeks (see section 2.6.1. for details). Leaf discs were harvested the evening before into 96-well plates containing 200  $\mu$ l of H<sub>2</sub>O with a 4 mm leaf punch and left to rest at room temperature overnight. Before the measurement the water was carefully removed from the wells and replaced with 100  $\mu$ l of 200 nM Luminol and Peroxidase either without MAMP addition, 10 nM flg22 or 5 nM elf18. Luminescence was measured with an ICCD photon-counting camera for 45 minutes. Total photon counts were calculated from the luminescence measurements.

#### **2.6.28. Stomatal aperture measurements**

All plants used for stomatal closure experiments were grown in soil for five weeks. In the morning of the experiment leaf discs were harvested with a 4 mm leaf punch into stomata opening buffer (SOB, see section 2.1.5.) and incubated in a plant growth cabinet with white light for 2 hours. After two hours some leaf discs were transferred to SOB containing 10 M flg22, elf18 or ABA while the remaining leaf discs remained in the stomata opening buffer without MAMPs. Mock treatment was imaged 3 hours after harvesting and flg22 treated plants were imaged 2 hours post treatment with a Leica DM5500 light microscope. Stomatal aperture was measured using ImageJ. At least 60 stomata per treatment were measured and averaged.

#### **2.6.29. Generation of amiRNA constructs**

The amiRNAs were designed following the instructions on the WMD webpage (<http://wmd2.weigelworld.org>). The sequences for the amiRNAs were provided by the webpage and generated through overlapping PCR from the template plasmid pRS300 which

contains the endogenous *Arabidopsis thaliana* miR319a precursor in a pBlueScript SK backbone. The webpage provides 4 oligonucleotides (I, II, III and IV) to replace the 20mer sequence of miR319a and requires to additional generic oligos that hybridize to the pRS300 plasmid outside of the miR319a sequence. I added Bpil restriction sites to the generic oligos (oligo A and B) to make them compatible for Golden Gate cloning.

The PCR reactions were carried out with the high-fidelity proof-reading polymerase Phusion (New England Biolabs) following this setup:

Reaction	Forward oligo	Reverse oligo	template	length of PCR product
(a)	A	IV	pRS300	272 bp
(b)	III	II	pRS300	171 bp
(c)	I	B	pRS300	298 bp
(d)	A	B	(a) + (b) + (c)	701 bp

<u>reaction setup (a), (b), (c)</u>	<u>μl</u>	<u>PCR conditions</u>
5x Phusion Buffer	4	95°C 2 min
10 μM dNTPs	0.4	95°C 30 sec
10 μM Primer fwd	1	52°C 30 sec
10 μM Primer rev	1	72°C 40 sec
100% DMSO	0.2	24 to 40 cycles
50 mM MgCl <sub>2</sub>	0.2	<u>72°C 7 min</u>
Template DNA	1	
Phusion	0.2	
<u>H<sub>2</sub>O up to</u>	<u>15</u>	

<u>reaction setup (d)</u>	<u>μl</u>	<u>PCR conditions</u>
5x Phusion Buffer	4	95°C 2 min
10 μM dNTPs	0.4	95°C 30 sec
10 μM Primer fwd	1	55°C 30 sec
10 μM Primer rev	1	72°C 90 sec
100% DMSO	0.2	24 to 40 cycles
50 mM MgCl <sub>2</sub>	0.2	<u>72°C 7 min</u>
purified gel fragments (a, b, c)	1.5	
Phusion	0.2	
<u>H<sub>2</sub>O up to</u>	<u>15</u>	

Sequences were verified using Sanger sequencing (GATC Biotech AG). Expression cassettes were generated using the Golden Gate Cloning strategy as described above.

## 2.6.30 Quantification of GFP in confocal micrographs

Confocal maximum projection images were converted to show luminance in ImageJ. Regions of interest were drawn within ImageJ including either only pavement cells or only guard cells. Raw Intensity Density of area of interest was measured using ImageJ. Values were normalised to surface area measured. Ten representative images were measured for every combination of genotype and time point.

## 2.7. Primers used in this study:

Table 2.7.1: Primer names and sequences used for Golden Gate Cloning

For Golden Gate cloning	
pMYB60_fwd	AGAAGACaaGGAGCACAAGGACACAAGGACATATGGT
pMYB60_rev	AGAAGACaaCATTCTTTCTCTCTCTCTCTCCTCTAGATCTC
pCYP86A2_fwd1	AGAAGACaaGGAGAAGGTAACACATGTATATATATGTCACATA
pCYP86A2_rev1	AGAAGACaaGCTCTCTCTCTTTTACATTTGTTTTTCCTT
pCYP86A2_fwd2	AGAAGACaaGAGCAGAAAGGTCTAACTAAACCTAAAGAGTCA
pCYP86A2_rev2	AGAAGACaaCATTATCAATGAATATGAAATGATACTAAAATG
OST1_fwd1	aGAAGACaaAATGGATCGACCAGCAGTGAGTGGT
OST1_rev1	aGAAGACaaCTCGCTGAAGCGGCCTGCATT
OST1_fwd2	aGAAGACaaGAGGACGAGGTTGTTCTCTCTTTTTT
OST1_rev2	aGAAGACaaATCTTCTCCATATCGTCATCTATGTCC
OST1_fwdf3	AGAAGACaaACACCAAATTTGCTCTGCTTTGCTTTA
OST1_rev3	AGAAGACaaGTGTTCCATAAAAATCAATCAATTTTGTA
OST1_fwd4	aGAAGACaaAGATTTAGAGAGCGACCTTGATGATCTT
OST1_rev4	aGAAGACaaCGAAggCATTGCGTACACAATCTCTCCG
pCPK13_fwd1	aGAAGACaaGGAGTGGATGGTTTACGAGGAATCACTAGT
pCPK13_rev1	aGAAGACaaGCTCCTTGGTTTCTTTTTCTTTTTGAAAAATG
pCPK13_fwd2	aGAAGACaaGAGCCCAAATTATGATTGAGTTTTACAAAATA
pCPK13_rev2	aGAAGACaaATCTCTTTTGAGTTTTTGATATTTATTTAAT
pCPK13_fwd3	aGAAGACaaAGATCTCTCTCTCTCTCTCTCTCTCTCTCGCTACTCTCATC
pCPK13_rev3	aGAAGACaaCATTCACTGTGTGTAGCTCTGATGAGGGGT
pKCS1_fwd1	aGAAGACaaGGAGACATTTTCAATATCGAATTCGTAGTTG
pKCS1_rev2	aGAAGACaaGTGTTTCGTTAAGACGTTTGTATATAAGGG
pKCS1_fwd2	aGAAGACaaACACAGCAAATTTATAAATGACAATGACTAC
pKCS1_rev2	aGAAGACaaCATTGAGTATAGTTTTGGGTCGAAATATTC
ABI1_fwd1	aGAAGACaaAATGGAGGAAGTATCTCCGGCGATCGC

ABI1_rev1	aGAAGACaaGCCTTCTTCCACAAATCGAAGTGAAACCA
ABI1_fwd2	aGAAGACaaAGGCCAGAGATGGAAGATGCTGTTTCGAC
ABI1_rev2	aGAAGACaaCGAAggGTTCAAGGGTTTGCTCTTGAGTTT
SnRK2.2_fwd1	aGAAGACaaAATGGATCCGGCGACTAATTCA
SnRK2.2_rev1	aGAAGACaaTGACTGAAGAAAAGAAACGCAT
SnRK2.2_fwd2	aGAAGACaaGTCACTGTCTTTCATTCCCAACCA
SnRK2.2_rev2	aGAAGACaaATCTCATGGCCTTACCTTGCCATCA
SnRK2.2_fwd3	aGAAGACaaAGATCAATTCCTCTGTCTAGAGTT
SnRK2.2_rev3	aGAAGACaaCGAAggGAGAGCATAAACTATCTCTC
SnRK2.3_fwd1	aGAAGACaaATGACTTTGAATATCCAAAATCACAAATTTTAAATCGAG GAGCAGGA
SnRK2.3_rev1	aGAAGACaaTCATCTGTTCTTCATTACAACCAAAGTCAACTGTTGG

Table 2.7.2 Primer names and sequences used for genotyping of *Arabidopsis thaliana*

For Genotyping		Mutant
SALK_059469_LP	GATGTTGGTGGTGAAAAATG	<i>aba1</i>
SALK_059469_RP	ACGTTCAAGAGCATCGTCATC	
aba2-3_fwd2	ACCATTGTAGTTTTGTGGCCC	<i>aba2-3</i>
aba2-3_rev2	AGGAGTGGTTAGTGCAAGTGA	
SAIL_576_D01_LP	CTTCTTGTTTTCGGCTGATG	<i>aba3</i>
SAIL_576_D01_RP	TTGGGCCTGATTTATGTGAAG	
SALK_093905_fwd	AACATCAACGCCTCTGATCTAA	<i>fls2</i>
SALK_093905_rev	AATAGAGTCCCCGAGTTCCATA	
SAIL_691_C04_LP	ACATGTCCGGTACTATCGCAG	<i>fls2c</i>
SAIL_691_C04_RP	TCCATCAAGACAGCTAATGAGC	
GK_129_B08_fwd	GGATTTCAAGACAGGACACTCTTG	<i>nced3-2</i>
GK_129_B08_rev	CTTCCTAAAACGGCTGATCCTA	
GK_328_D05_fwd	ACTAAACCAAGACGCCGTAAACT	<i>nced5-2</i>
GK_328_D05_rev	ATCTCCGACGCATCTTTA	
SALK_008068_LP	CATATCTTTAGACGAGGGGCC	<i>ost1-3</i>
SALK_008068_RP	GTGAGTGGTCCAATGGATTTG	
GK_516_B05_fwd	ATTTCTAAAACTACAGGCCCAT	<i>ost1-4</i>
GK_516_B05_rev	AAGAAAAACCTCGCCTAC	
GK_807_G04_fwd	AGATCCTCGATATTAGATGGCGAC	<i>snrk2.2</i>
GK_807_G04_rev	GTGGAGAACTTTATGAGCGGATTT	

SALK_096546_LP	GGTTTTGAGTGTTCTGCTTTTG	<i>snrk2.2</i>
SALK_096546_RP	ACATCTGCAATCTGGTAACCG	
SALK_107315_LP	TGCTTTTGAGTGCTTTTAATGTG	<i>snrk2.3</i>
SALK_107315_RP	ACATCTGCAATCTGGTAACCG	
SALK_107317_LP	TGCTTTTGAGTGCTTTTAATGTG	<i>snrk2.3</i>
SALK_107317_RP	ACATCTGCAATCTGGTAACCG	
SALK_096548_LP	ACCACAGGTCACTAAGGCATC	<i>snrk2.3</i>
SALK_096548_RP	ACAGCATTCAAGGTGATATCCG	
pyr1-1_geno_fwd	CCTTCGGAGTTAACACCAGAAG	<i>pyr1-1</i>
pyr1-1_geno_rev	CACGTGAAAAAATCTTATCCCCATG	
SALK_054640_LP	TGCCAATTTTCAGACATTAAGC	<i>pyl1-1</i>
SALK_054640_RP	AACCATGCCTTCCGATTTAAC	
GT_2864_fwd	ACCACCAGTTCGAACCAGAC	<i>pyl2-1</i>
GT_2864_rev	TTCCTCTGTGTTCCCTCGG	
SAIL_517_C08_LP	TTCCAATCGTTCCAAATATCG	<i>pyl4-1</i>
SAIL_517_C08_RP	TAAGACTCGACAACGACGGTC	
SM_3_3495_LP	AAACACAAAGCCTTCACATCC	<i>pyl5</i>
SM_3_3495_RP	AAGTTTTGTGAATCCCCAAC	
SAIL_1269_A02_LP	AGAGAGTGGAACCCCATGATC	<i>pyl8</i>
SAIL_1269_A02_RP	TTCTTCTTCTTCCTTCATGCG	
rbohd_fwd	ATGAAAATGAGACGAGGCAATTC	Torres <i>et al.</i> , 2002
rbohd_rev	GGATACTGATCATAGGCGTGGCTCCA	Torres <i>et al.</i> , 2002
rbohf_fwd	CTCCGATATCCTTCAACCAACTC	Torres <i>et al.</i> , 2002
rbohf_rev	GAGATTGCCTTTATACTATAAGTG	Torres <i>et al.</i> , 2002
dSpm11	GGTGCAGCAAACCCACACTTTTACTTC	Tissier <i>et al.</i> , 1999
dSpm1	CTTATTTCAAGAGTGTGGGGTTTTGG	Tissier <i>et al.</i> , 1999

Table 2.7.3: Primer names and sequences used for restriction cloning

<b>For restriction cloning</b>		for vector
SnRK2.3_Sall-f	<b>TAGTCGACTC</b> ATGGATCGAGCTCCGGTG	pGEX4T1
SnRK2.3_NotI-r	<b>TAGCGGCCGCTT</b> AGAGAGCGTAAACTATC	
SnRK2.3_NdeI-f	<b>TACATATG</b> GATCGAGCTCCGGTGAC	pET28a
SnRK2.3_BaMHI-r	<b>TAGGATCCTT</b> AGAGAGCGTAAACTATC	
SnRK2.6_Sall-f	<b>TAGTCGACTC</b> ATGGATCGACCAGCAGTG	pGEX4T1
SnRK2.6_NotI-r	<b>TAGCGGCCGCTT</b> ACATTGCGTACACAATCTC	

SnRK2.6_NdeI-f	<b>TACATATG</b> GATCGACCAGCAGTGAG	pET28a
SnRK2.6_BaMHI-r	<b>TAGGATCCTTA</b> CATTGCGTACACAATCTC	
SLAH3_NdeI-f	<b>TACATATG</b> GAGGAGAAACCAAAC	pET28a
SLAH3_251_BaMHI-r	<b>TAGGATCCTTA</b> CTTTTTATCATTGGTAG	
SLAH3_563_Sall-f	<b>TAGTCGACTC</b> CACGCCTTTGTCCTCCGAG	pGEX4T1
SLAH3_NotI-r	<b>TAGCGGCCGCTTA</b> TGATGAATCACTCTCTTG	
SLAC1_NdeI-f	<b>TACATATG</b> GAGAGGAAACAGTCAAATG	pET28a
SLAC1_181_BaMHI-r	<b>TAGGATCCTTA</b> TTGCTCCTCTTTTGAAG	
SLAC1_496_Sall-f	<b>TAGTCGACTC</b> CACGCCTTTGTCTGGC	pGEX4T1
SLAC1_NotI-r	<b>TAGCGGCCGCTTA</b> GTGATGCGACTCTTCC	
ABF2_Sall-f	<b>TAGTCGACTc</b> ATGGATGGTAGTATGAATTTG	pGEX4T1
ABF2_NotI-r	<b>TAGCGGCCGCTTA</b> CCAAGTCCCGACTCTGTC	

Table 2.7.4 Primer names and sequences used for Sanger sequencing

<b>For Sequencing</b>	
BASTA_seq_rev1	GTACGGAAGTTGACCGTGCT
BASTA_seq_fwd1	GAAATTTGTAAGTTTGAATGAGCC
CYP86A2_seq_fwd1	GCAGTTGCAGCGTACACAAG
CYP86A2_seq_rev1	GTTAGACCTTTCTGGTCTCTCTCTC
CYP86A2_seq_fwd2	GGGTACACTCTCTCAACAATCCA
CYP86A2_seq_rev2	GTTTAAGGAATATGAAATGGTGTTC
FLS2_seq_fwd1	GTAACCATTTAACTGGTTTCGAT
FLS2_seq_rev1	CTGTAAGTTCAAGAGATTTCCAAAATCTCTCG
FLS2_seq_fwd2	GTGTGGCAGATAACAACTTAACAGGAACTC
FLS2_seq_rev2	CAAATCTTTCAGATCCCGATTTCTCGAGG
FLS2_seq_fwd3	GGTGTCTTGGATCTCTCTAGTAACAATCT
FLS2_seq_rev3	GGCGTTGATGTTTTTGAACACCCC
FLS2_seq_fwd4	CTGGATATGGTTTTCCCATCGTTCATTG
FLS2_seq_rev4	GTGCTTCCATCTTCGCGGAAA
FLS2_seq_fwd5	GCTTTGTTTGTCTGTACAAGCTCTAGAC
FLS2_seq_rev5	CGCTTTCCTCTAAGTTTCATCAGATG
Term_seq_fwd1	GAGAAGCCTATGATCGCATGATA
Term_seq_rev1	ATAAAAATACGATAGTAACGGGTG
pMYB60_seq_fwd1	CAGATCGCTGCAAGAATTC
pMYB60_seq_rev1	AGGGAACGTAAGAAGAGACAAAT

---

pMYB60_seq_fwd2	GTAACATAGCTTGTGACTCTTCTTC
pMYB60_seq_rev2	TTGCTTAATTTGGAACATTCG
OST1_seq_fwd	CCTTAGGATTGCTTCAGGTTATATT
OST1_seq_rev	CTTTCTTCACCAAAATTCTTGAAG
p35S_seq_fwd	GATTCCATTGCCAGCTAT
p35S_seq_rev	CGTCAGTGGAGATGTCACATC
PIP1;4_seq_fwd	TGTTTCATGCTCTGTTTGACC
PIP1;4_seq_rev	AACCGGGGAAATTCGATC
OST1_seq_fwd2	CCAGCAACTCATTTCCAGGAGT
OST1_seq_rev2	TTTGTGTTGTCTCACCTGTGAG
PEN1_seq_fwd	GATTGAGGGAGCTTATCTCGT
PEN1_seq_rev	TCCAGAGATCAATTCAGCTCT
RBOHD_seq_fwd1	TCCGCCGCGTGTCT
RBOHD_seq_rev1	GCAGAGAGTAAGAGGCCGTT
RBOHD_seq_fwd2	GGTGGACAAAGATGAAGATGGGC
RBOHD_seq_rev2	CCATTTTGTCTGTTCCACATGAAGTTAATATATTGATG
RBOHD_seq_fwd3	ATCTCGACAATGGGTGGTT
RBOHD_seq_rev3	AATAGCAACATTTCCAAGTTTTTC
RBOHD_seq_fwd4	ATCTCGACAATGGGTGGTTAGTGG
RBOHD_seq_rev4	GCTTGTAATAGCAACATTTCCAAGTTTTTCGATC
RBOHD_seq_fwd5	ACGGTCCATACGGTGCT
RBOHD_seq_rev5	CCTCGTACACACTCGTGCAA
mCherry_seq_fwd	GGCCCCGTAATGCAGAA
mCherry_seq_rev	TGGCCGCCGTCCTT
GFP_seq_fwd	AGGAGCGCACCATCTTCTT
GFP_seq_rev	GATGTTGCCGTCCTCCTT
pGC1_fwd1	GTGTCACAATGTCTGAACTAAGAGA
pGC1_rev1	CTACAATTCTACATCGTCAATTCC
3xFLAG_fwd_seq	GGACCATGACGGAGACTA
3xFLAG_rev_seq	CACTTATCGTCATCGTCCT
SnRK2.2_seq_fwd1	GAGCAGTGTTCTTGCAACTTACTTGAAC
SnRK2.2_seq_rev1	CAATGTATTTCCAGCTTCAGATCCCGAT
SnRK2.2_seq_fwd2	CCACTGATTTTAAAACGCAGAGAATCCTTAG
SnRK2.2_seq_rev2	GTAAAACCTTACTGTTGCCGGATCAGC

---

SnRK2.3_seq_fwd1	CCGGTTTCCTTATGGTTTGATCTCTTC
SnRK2.3_seq_rev1	CAGTCCATAGGCTCCATGAAACAGATT
SnRK2.3_seq_fwd2	CACCTGAATGCTGTCATCTTATTTCAAGAATCT
SnRK2.3_seq_rev2	CTGGTATGCTTATTCTCTGTAACAAACAACATC
pUBQ10_seq_fwd1	GCTGCAGGTCAACGGAT
pUBQ10_seq_rev1	CACTCGTGTTCAAGTCCAATGA
pUBQ10_seq_fwd2	CGTGACCTAGTCGTCCTC
pUBQ10_seq_rev2	CGCACAAACTAGAAACTAACACC
YFPc_seq_fwd	AGGCTACGTCCAGGAGCGCA
YFPc_seq_rev	GCCGTTTACGTCGCCGTCCA
YFPn_seq_fwd	GCGAGGGCGATGCCACCTAC
YFPn_seq_rev	GTGCGCTCCTGGACGTAGCC
BIK1_seq_rev1	CAAACCGTTCCAGGTTTAGTCG
BIK1_seq_fwd2	GATGTGTACAGTTTCGGAGTT
BIK1_seq_rev2	ATCCAACGCTCGCTTACCAGATA
BAK1_seq_rev1	CTAATAATCTATGATAATGC
BAK1_seq_fwd1	GGTGTATGTGGGATGTTA
BAK1_seq_rev2	GACGCCTAACCACCAATAC
BAK1_seq_fwd2	CGACAGGTGAAAGGGTTGTT
BAK1_seq_rev3	GCTAGACCACATCTACTTAC

Table 2.7.5: Primer names and sequences used to generate artificial micro RNAs (amiRNAs)  
For generation of amiRNAs in R vector

OligoA_amiRNA	aGAAGACaaAATGCTGCAAGGCGATTAAGTTG
OligoB_amiRNA	aGAAGACaaAGCGCGGATAACAATTTACACAG
amiRNA_FLS2_1_I	gaTAACCGAGACTACATGTCCGTtctctctttgtattcc
amiRNA_FLS2_1_II	gaACGGACATGTAGTCTCGGTTAtcaaagagaatcaatga
amiRNA_FLS2_1_III	gaACAGACATGTAGTGTGCGTTTTcacaggtcgtgatatg
amiRNA_FLS2_1_IV	gaAAACCGACTACTACATGTCTGTtctacatatattcct
amiRNA_FLS2_2_I	gaTCAATTACAGTGTGTAACGGtctctctttgtattcc
amiRNA_FLS2_2_II	gaCCGTTACGACTGTAATTGAtcaaagagaatcaatga
amiRNA_FLS2_2_III	gaCCATTACGACTCTAATTGTtcaaggtcgtgatatg
amiRNA_FLS2_2_IV	gaACAATTAGAGTGTGTAATGGtctacatatattcct
amiRNA_FLS2_3_I	gaTAAATGAATTCGCTTTCCTGtctctctttgtattcc
amiRNA_FLS2_3_II	gaCAGGCAAAGCGAATTCATTTAtcaaagagaatcaatga

amiRNA_FLS2_3_III	gaCAAGCAAAGCGAAATCATTTTTcacaggtcgtgatatg
amiRNA_FLS2_3_IV	gaAAAATGATTCGCTTTGCTTGtctacatatatattcct
amiRNA_RBOHD_1_I	gaTTCTACAATCGAATACGGCGTtctctcttttgattcc
amiRNA_RBOHD_1_II	gaACGCCGTATTCGATTGTAGAAAtcaaagagaatcaatga
amiRNA_RBOHD_1_III	gaACACCGTATTCGAATGTAGATtcacaggtcgtgatatg
amiRNA_RBOHD_1_IV	gaATCTACATTCGAATACGGTGTtctacatatatattcct
amiRNA_RBOHD_2_I	gaTATGCGAATACCAAAGGCGAtctctcttttgattcc
amiRNA_RBOHD_2_II	gaTCGCCTTTTGGTATTCGCATAtcaaagagaatcaatga
amiRNA_RBOHD_2_III	gaTCACCTTTTGGTAATCGCATTtcacaggtcgtgatatg
amiRNA_RBOHD_2_IV	gaAATGCGATTACCAAAGGTGAtctacatatatattcct
amiRNA_RBOHD/F_1_I	gaTGAAGTCCGCTTTTACGGCCAtctctcttttgattcc
amiRNA_RBOHD/F_1_II	gaTGGCCGTAAAAGCGGACTTCAtcaaagagaatcaatga
amiRNA_RBOHD/F_1_III	gaTGACCGTAAAAGCCGACTTCTtcacaggtcgtgatatg
amiRNA_RBOHD/F_1_IV	gaAGAAGTCCGCTTTTACGGTCAtctacatatatattcct
amiRNA_RBOHD/F_2_I	gaTGAAGTCCGCTTTTACGCCGtctctcttttgattcc
amiRNA_RBOHD/F_2_II	gaCGGCGGTAAAAGCGGACTTCAtcaaagagaatcaatga
amiRNA_RBOHD/F_2_III	gaCGACGGTAAAAGCCGACTTCTtcacaggtcgtgatatg
amiRNA_RBOHD/F_2_IV	gaAGAAGTCCGCTTTTACCGTCGtctacatatatattcct
amiRNA_RBOHF_1_I	gaTTCTACAATCGAATACGGCGTtctctcttttgattcc
amiRNA_RBOHF_1_II	gaACGCCGTATTCGATTGTAGAAAtcaaagagaatcaatga
amiRNA_RBOHF_1_III	gaACACCGTATTCGAATGTAGATtcacaggtcgtgatatg
amiRNA_RBOHF_1_IV	gaATCTACATTCGAATACGGTGTtctacatatatattcct
amiRNA_RBOHF_2_I	gaTTATCGGAAGTATATACACGCtctctcttttgattcc
amiRNA_RBOHF_2_II	gaGCGTGTATATACTCCGATAAtcaaagagaatcaatga
amiRNA_RBOHF_2_III	gaGCATGTATATACTACCGATATtcacaggtcgtgatatg
amiRNA_RBOHF_2_IV	gaATATCGGTAGTATATACATGCtctacatatatattcct

## 2.8. Constructs generated in this study:

Table 2.8.1: Golden Gate level 0 vectors generated in this study

Golden Gate level 0 vectors				
Promoters				
ID	Gene name	Gene ID	Backbone	Resistance
CJT01	pCYP86A2	At4g00360	pICH41295	Spec (100)

CJT04	pMYB60	At1g08810	pICH41295	Spec (100)
CJT17	pCPK13	At3g51850	pICH41295	Spec (100)
CJT19	pKCS1	At1g01120	pICH41295	Spec (100)
CJT15	pMYB60 (for N-tag)	At1g08810	pICSL01008	Spec (100)
<b>Protein Coding Genes</b>				
ID	gene name	Gene ID	Backbone	Resistance
CJT09	OST1 (genomic)	At4g33950	pICSL01005	Spec (100)
CJT162	ABI1 (genomic)	At4g26080	pICSL01005	Spec (100)
CJT164	amiRNA-FLS2(1)	At5g46330	pICH41308	Spec (100)
CJT165	amiRNA-FLS2(2)	At5g46330	pICH41308	Spec (100)
CJT166	amiRNA-FLS2(3)	At5g46330	pICH41308	Spec (100)
CJT167	amiRNA-RBOHD(1)	At5g47910	pICH41308	Spec (100)
CJT168	amiRNA-RBOHD(2)	At5g47910	pICH41308	Spec (100)
CJT169	amiRNA-RBOHD/F(1)	At5g47910/At1g64060	pICH41308	Spec (100)
CJT170	amiRNA-RBOHD/F(2)	At5g47910/At1g64060	pICH41308	Spec (100)
CJT120	RBOHD (genomic)	At5g47910	pICH41308	Spec (100)
CJT261	SnRK2.2 (genomic)	At3g50500	pICSL01005	Spec (100)
CJT163	SnRK2.3 (CDS)	At5g66880	pICSL01005	Spec (100)

Table 2.8.2: Other Golden Gate vectors used in this study:

ID	gene name	Gene ID	Resistance	generated by
<b>Promoters</b>				
pICH51277	short p35S + $\Omega$		Spec (100)	Synbio TSL
pICSL12015	pAtUBQ10		Spec (100)	Synbio TSL
pICSL13005	pAtUBQ10 for (N-tag)		Spec (100)	Synbio TSL
<b>Protein Coding Genes</b>				
pICSL50008	GFP as C-tag		Spec (100)	Synbio TSL
pICSL30006	GFP as N-tag		Spec (100)	Synbio TSL
pICSL50004	mCherry as C-tag		Spec (100)	Synbio TSL
pICSL50007	3xFLAG as C-tag		Spec (100)	Synbio TSL
pICSL50003	YFPc as C-tag		Spec (100)	Synbio TSL
pICSL50002	YFPn as C-tag		Spec (100)	Synbio TSL
pICH41531	GFP ORF		Spec (100)	Synbio TSL
CZLp1778	BAK1	At4g33430	Spec (100)	Freddy Boutrot

CZLp1566	BIK1	At2g39660	Spec (100)	Christoph Buecherl
<b>Terminators</b>				
pICH41432	t <i>AtuOcs</i>		Spec (100)	Synbio TSL
<b>Backbone vectors</b>				
ID	Description		Resistance	generated by
pICSL01008	Level 0 for Pro+5'UTR with Ntags		Spec(100)	Synbio TSL
pICH41295	Level 0 acceptor promoter+5'UTR		Spec(100)	Synbio TSL
pICH41308	Level 0 for CDS		Spec(100)	Synbio TSL
pICSL01005	Level 0 acceptor CDS no Stop		Spec(100)	Synbio TSL
pICH47742	Level 1 pos2		Carb (50)	Synbio TSL
pAGM31171	Level 2 RB corr low copy in Agro LacZ sel		Kan (50)	Synbio TSL
<b>Expression cassettes</b>				
ID	Description		Resistance	generated by
pICSL11013	Level 1 pos1 Bar plant resistance		Carb (50)	Synbio TSL
pICSL11015	Level 1 pos1 pFAST-Red selection cassette		Carb (50)	Synbio TSL

Table 2.8.3: Golden Gate level 1 vectors generated in this study

<b>Golden Gate level 1 vectors</b>				
ID	construct	Backbone	Resistance	use
CJT284	<i>p35S::FLS2-YFPn</i>	pICH47742	Carb (50)	split-YFP
CJT285	<i>p35S::BIK1-YFPc</i>	pICH47742	Carb (50)	split-YFP
CJT286	<i>p35S::BAK1-YFPc</i>	pICH47742	Carb (50)	split-YFP
CJT287	<i>p35S::SnRK2.2-YFPc</i>	pICH47742	Carb (50)	split-YFP
CJT288	<i>p35S::SnRK2.2-YFPn</i>	pICH47742	Carb (50)	split-YFP
CJT289	<i>pUBQ10::SnRK2.2-3xFLAG</i>	pICH47742	Carb (50)	Co-IP
CJT290	<i>p35S::SnRK2.3-YFPn</i>	pICH47742	Carb (50)	split-YFP
CJT291	<i>p35S::SnRK2.3-YFPc</i>	pICH47742	Carb (50)	split-YFP
CJT292	<i>pUBQ10::SnRK2.3-3xFLAG</i>	pICH47742	Carb (50)	Co-IP
CJT293	<i>p35S::OST1-YFPc</i>	pICH47742	Carb (50)	split-YFP
CJT294	<i>p35S::OST1-YFPn</i>	pICH47742	Carb (50)	split-YFP
CJT295	<i>p35S::ABI1-YFPc</i>	pICH47742	Carb (50)	split-YFP

CJT322	<i>p35S::BRI1-YFPn</i>	pICH47742	Carb (50)	split-YFP
CJT323	<i>p35S::BRI1-YFPc</i>	pICH47742	Carb (50)	split-YFP
CJT148	<i>pUBQ10::OST1-3xFLAG</i>	pICH47742	Carb (50)	Co-IP

Table 2.8.4: Golden Gate level 2 vectors generated in this study

<b>Golden Gate level 2 vectors</b>				
ID	construct	Backbone	Resistance	plant Selection
CJT281	<i>pUBQ10::GFP-RBOHD</i>	pAGM31171	Kan (50)	pFAST-Red
CJT282	<i>pUBQ10::mCherry-RBOHD</i>	pAGM31171	Kan (50)	pFAST-Red
CJT283	<i>pUBQ10::3xFLAG-RBOHD</i>	pAGM31171	Kan (50)	pFAST-Red
CJT187	<i>pMYB60::GFP-RBOHD</i>	pAGM31171	Kan (50)	pFAST-Red
CJT188	<i>pMYB60::3xFLAG-RBOHD</i>	pAGM31171	Kan (50)	pFAST-Red
CJT280	<i>pMYB60::mCherry-RBOHD</i>	pAGM31171	Kan (50)	pFAST-Red
CJT203	<i>pMYB60::MIFLS2 I</i>	pAGM31171	Kan (50)	pFAST-Red
CJT190	<i>pMYB60::MIFLS2 II</i>	pAGM31171	Kan (50)	pFAST-Red
CJT226	<i>pMYB60::MIRBOHD I</i>	pAGM31171	Kan (50)	pFAST-Red
CJT227	<i>pMYB60::MIRBOHD II</i>	pAGM31171	Kan (50)	pFAST-Red
CJT228	<i>pMYB60::MIRBOHD/F I</i>	pAGM31171	Kan (50)	pFAST-Red
CJT229	<i>pMYB60::MIRBOHD/F II</i>	pAGM31171	Kan (50)	pFAST-Red
CJT204	<i>pUBQ10::MIFLS2 I</i>	pAGM31171	Kan (50)	pFAST-Red
CJT191	<i>pUBQ10::MIFLS2 II</i>	pAGM31171	Kan (50)	pFAST-Red
CJT233	<i>pUBQ10::MIFLS2 III</i>	pAGM31171	Kan (50)	pFAST-Red
CJT234	<i>pUBQ10::MIRBOHD I</i>	pAGM31171	Kan (50)	pFAST-Red
CJT235	<i>pUBQ10::MIRBOHD II</i>	pAGM31171	Kan (50)	pFAST-Red
CJT236	<i>pUBQ10::MIRBOHD/F I</i>	pAGM31171	Kan (50)	pFAST-Red
CJT237	<i>pUBQ10::MIRBOHD/F II</i>	pAGM31171	Kan (50)	pFAST-Red
CJT034	<i>pMYB60::FLS2-GFP</i>	pAGM4723	Kan (50)	BASTA

### 3. Virus-induced gene silencing and guard cell-specific promoters as useful tools to study guard cell responses

#### 3.1. Introduction

Stomata are vital cellular structures that enable plants to adapt to a constantly changing environment. They are formed of highly specialised cells in the plant epidermis that can translate a chemical stimulus into a biomechanical, reversible response. Stomata originate from pavement cells that undergo a series of cell divisions and cell-state transitions and these changes are accompanied by dramatic changes in morphology. Part of these morphological changes are depositions of cell wall material upon plasmodesmata that connect a differentiating guard cell to surrounding tissues. Once fully differentiated, guard cells are symplastically isolated as their plasmodesmata are effectively truncated (Wille & Lucas, 1984; Palevitz & Hepler, 1985). This is also essential to prevent translocation of essential cell-fate determinants, such as bHLH transcription factors *SPEECHLESS*, *MUTE* and *FAMA* to surrounding cells (reviewed by (Pillitteri & Torii, 2012)). In addition to these determinants, guard cells possess a number of highly specialised proteins that are either exclusively, or predominantly, expressed there because of their specific function. One example is the kinase *OPEN STOMATA 1* which localises to guard cells and the vasculature (Mustilli *et al.*, 2002) and plays a predominant role in mediating stomatal closure to a number of different stimuli (Mustilli *et al.*, 2002; Melotto *et al.*, 2006; Chater *et al.*, 2015). Other examples are channels, such as anion channel *SLAC1* and potassium channel *GORK1*, which are predominantly expressed in guard cells. Not only specialised cell types have proteins whose localisation correlates with their function. This is also true of specialised organs or tissues. It is known from root cell imaging that certain proteins are only expressed in a subset of root cells. Their promoters are therefore also suitable to drive tissue-specific gene expression. For instance the promoter *pLBD16* drives expression in the pericycle and *pSCR* drives expression in endodermal initial cells, the quiescent centre and the endodermal cell lineage and have been used in studies for their cell type-specificity (DiLaurenzio *et al.*, 1996; Goh *et al.*, 2012; Wyrsh *et al.*, 2015).

Constitutive promoters are the most commonly used promoters in the generation of transgenic plants for either laboratory or field purposes. But with an increasing understanding of the differences between plant cell types and their role in specific physiological responses comes the necessity for more precise tools to enable us to

differentiate input from differing cell types to an overall phenotype. Moreover, one might wish to express target proteins in only a subset of cells if one wishes to alter only specific responses that are cell type- or tissue-specific. To improve water use efficiency or drought tolerance, for instance, it makes sense to target only the guard cells as demonstrated in a study using a chimeric promoter (Na & Metzger, 2014). For applications such as this it is useful to have information on promoter expression patterns readily available, for instance in a database (Smirnova *et al.*, 2012). Furthermore, direct comparisons of promoters with similar expression patterns can help to make informed decisions about the most suitable promoter for a proposed application.

A number of promoters have been published to be guard cell-specific and were put forward as research tools to study guard cell-specific responses (Galbiati *et al.*, 2008; Yang *et al.*, 2008; Rusconi *et al.*, 2013). In addition to these published promoters I identified two further proteins whose localisation patterns provided an incentive to investigate whether their promoters could be suitable to drive guard cell-specific expression (Gray *et al.*, 2000; Ronzier *et al.*, 2014). Most of these studies used Promoter-GUS fusions to understand expression distribution. Only one of these studies compared their identified promoters with other guard cell-specific promoters (Yang *et al.*, 2008).

Guard cells are unique cells that differ from other cells in their shape, their capacity to change their shape in response to chemical stimuli and also their protein composition. To truly understand guard cell responses during immunity I aimed at establishing tools to study immune outputs only from guard cells without interference from surrounding cells. To this end I established a transient system in *N. benthamiana* to specifically reduce protein abundance in pavement cells. In addition to this I screened guard cell-specific promoters to identify the most specific and reliable promoter for guard cell-specific expression of proteins.

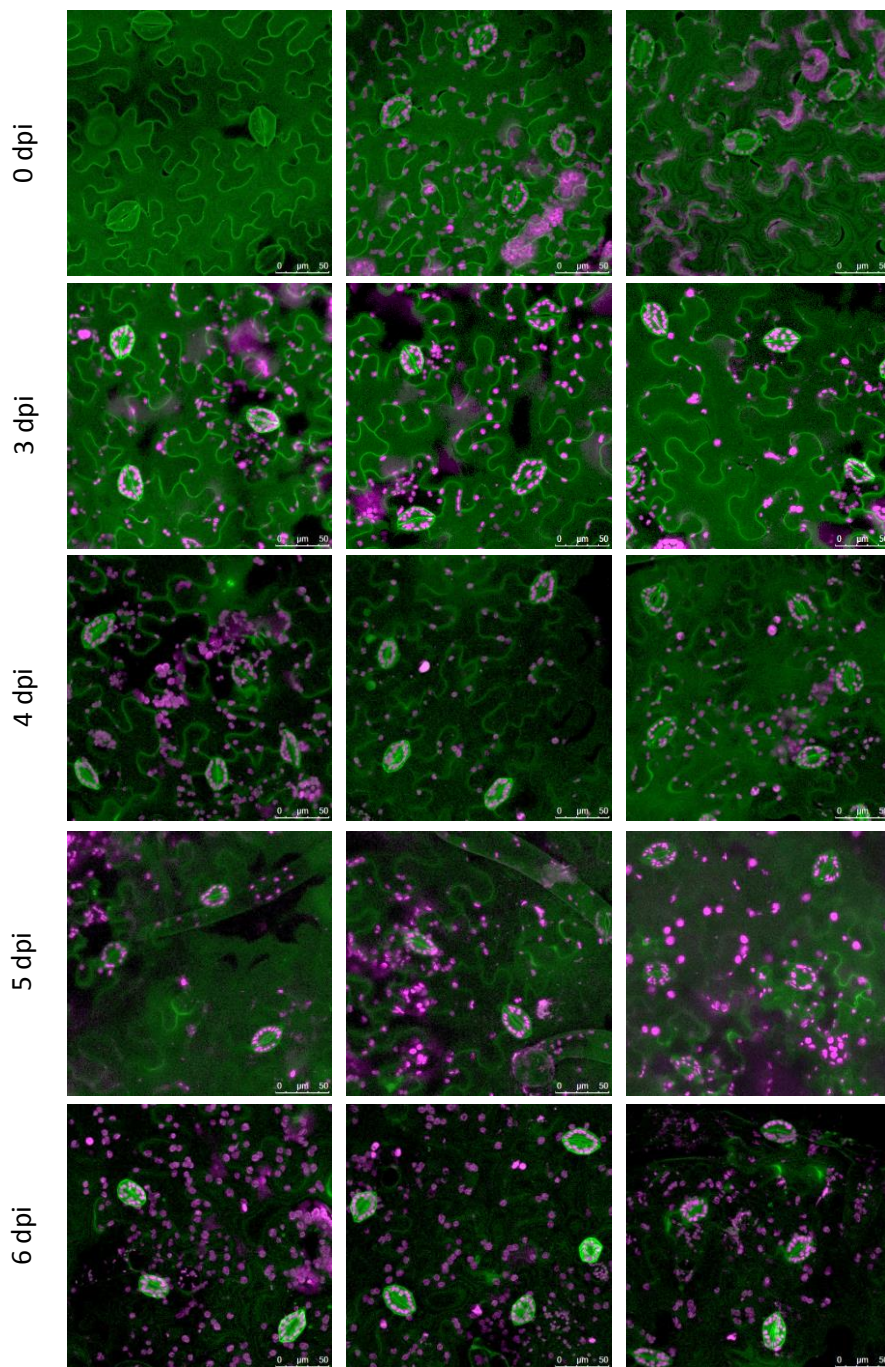
Here, I demonstrate transient and stable transgenic approaches to study guard cell responses. Making use of stable transgenic *N. benthamiana* plants expressing fluorescent proteins, I was able to visualise gradual silencing in pavement cells while guard cell protein accumulation was unaffected. I show that age and developmental stages of leaves are crucial for the outcome and distribution of virus-induced gene silencing (VIGS). Furthermore, I report a comprehensive side by side comparison of guard cell-specific promoter activities to investigate their specificity. I identify *pMYB60* as the most specific and suitable promoter to express proteins in a guard cell-specific manner.

## 3.2. Results

### 3.2.1. Virus-induced gene silencing (VIGS) does not affect guard cells in fully expanded leaves in *N. benthamiana*

Viruses rely on plasmodesmata for local cell-to-cell movement (reviewed by (Benitez-Alfonso *et al.*, 2010)). I therefore reasoned that one could exploit virus-induced gene silencing (VIGS) to silence all cell types except guard cells when applying it at the right developmental stage of the leaf. I therefore infiltrated silencing constructs into *N. benthamiana* leaves at differing developmental stages. To follow silencing progression, I decided to utilise stable transgenic *N. benthamiana* plants expressing fluorescent proteins that I could visualise with a confocal laser-scanning microscope. To this end, I infiltrated *pFLS2::FLS2-GFP* and GFP16c plants (Ruiz *et al.*, 1998) with the silencing construct targeting GFP (*TRV::GFP*). I infiltrated leaves of different developmental stages and evaluated the GFP signal in the infiltrated leaf and distal leaves. To achieve silencing throughout all cell types VIGS constructs are usually infiltrated in 2-week-old leaves. I started with these conditions and increased the age of infiltrated plants and which leaves to infiltrate until I reached the desired silencing distribution. Leaves were imaged with a confocal laser-scanning Microscope (Leica SP5). Figure 3.1 and Figure 3.2 show the silencing progression from day three to day six after infiltration in the transgenic plants. Figure 3.1 shows confocal maximum projections from the transgenic plant *pFLS2::FLS2-GFP*. All pictures were taken at the same time of day with the same microscope settings. Uninfiltrated leaves exhibit a strong FLS2-GFP signal at the plasma membrane (Figure 3.1 0 days). At three days after infiltration the GFP signal is undiminished in all cell types. At four days, however, the GFP signal seems to be slightly reduced. This trend progresses to day five and peaks at day six when the GFP signal in the pavement cells is visibly reduced, whereas the guard cell FLS2-GFP signal is not visibly altered. At day six also distal leaves were evaluated to determine whether the virus had also already reached systemic leaves. However, these leaves showed a strong and GFP signal at the plasma membrane indistinguishable from uninfiltrated leaves. This suggests that at six days after infiltration the silencing can only spread locally in the infiltrated leaf to silence pavement cells. This is supported by the observations made by imaging the infiltrated GFP16c plants. This plant expresses a GFP-tagged protein localising to the endoplasmatic reticulum (ER) and consistently, I observed a reticulate structure typical of proteins localising to the ER (Figure3.2). The overall GFP signal appears a lot stronger than in the FLS2-GFP plant indicating a higher level of expression of the protein. This is most likely due to the different

GFP/autofluorescence merge



Systemic leaf

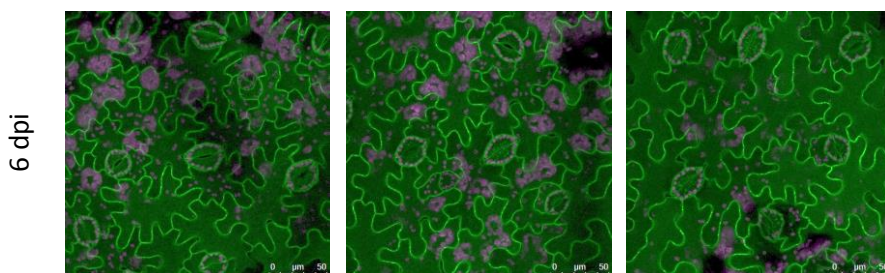
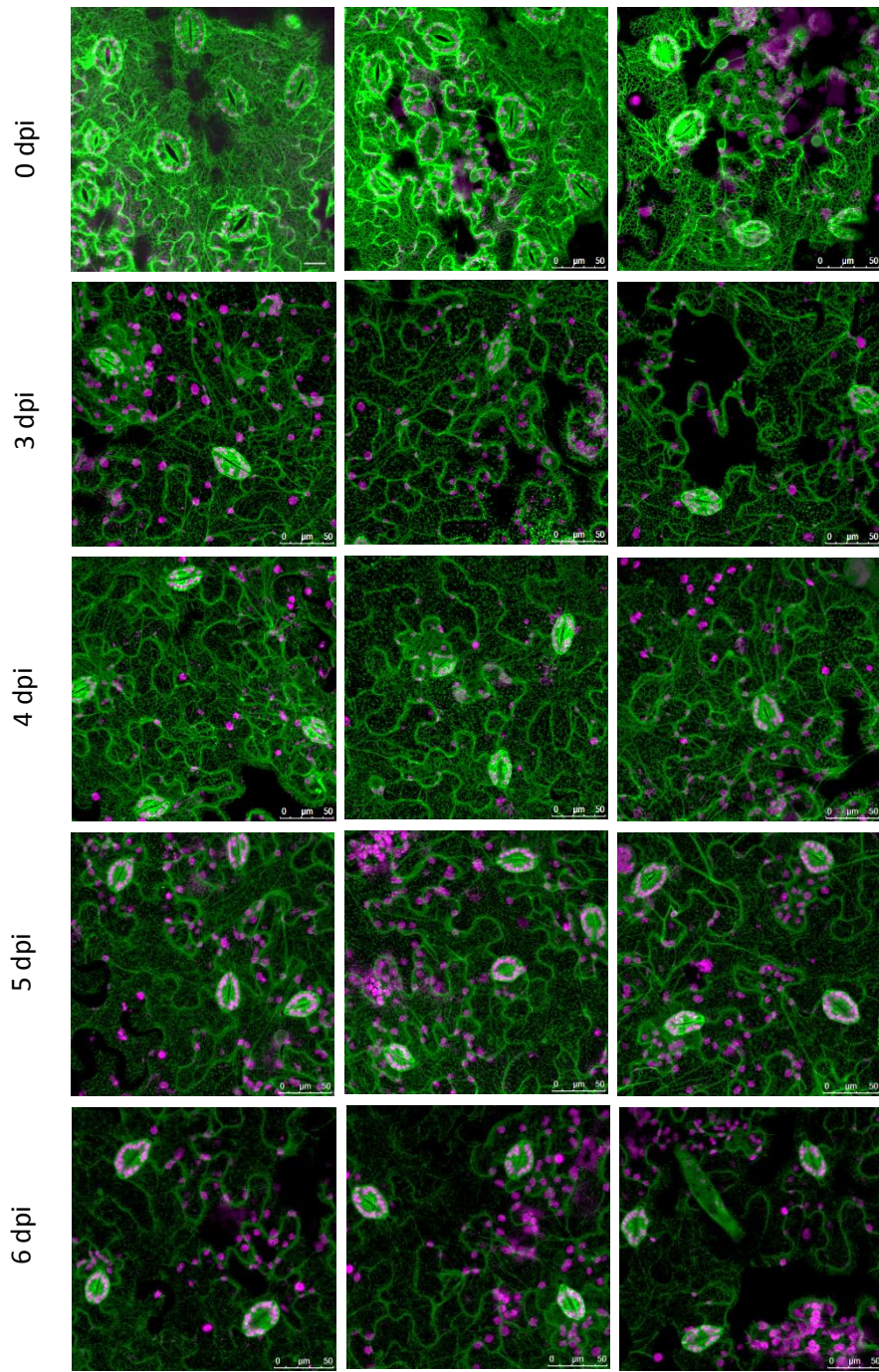


**Figure 3.1:** Confocal maximum projection micrographs of *pFLS2::FLS2-GFP* infiltrated with *TRV::GFP*. GFP signal continuously decreases in pavement cells in plants infiltrated with VIGS constructs targeting GFP while GFP in guard cells remains unaltered. Five-week-old *N. benthamiana* plants were infiltrated with *TRV::GFP* in fully expanded leaves. Leaf discs were taken at 0, 3, 4, 5 and 6 dpi. At 6 dpi GFP signal in infiltrated leaves were compared to systemic, uninfiltrated leaves. Pictures show maximum projection images taken with a Leica SP5 confocal microscope and bars indicate 50  $\mu$ m. Each picture corresponds to an independent leaf, with each time point showing images from three separate leaves. Green signal corresponds to GFP and magenta to autofluorescence.

strengths of the promoters as the *p35S* promoter is known to drive strong overexpression. Consistent with the observations made in Figure 3.1 I could observe a gradual reduction of GFP signal in pavement cells and the lowest signal was reached at six days after infiltration. However, at six days I still observed a weak GFP signal in pavement cells, predominantly at the cell periphery, while the intracellular net-like structure was profoundly reduced. Systemic leaves were unaffected, suggesting that the virus silencing had not yet moved to systemic tissues. This suggests that VIGS is not able to completely silence highly expressed genes or that the turnaround time for the GFP-tagged protein in the GFP16c plant is a lot higher than for FLS2. These observations were confirmed in two additional repeats.

To verify that GFP intensity decreases more in the pavement cells than the guard cells I converted the confocal micrographs into greyscale images (using function luminance in ImageJ) to quantify the brightness intensity in ImageJ. I selected ten representative images for each time point for quantification. In order to measure only pavement or guard cell GFP intensity I drew areas of interest in the selected images that included either only pavement or guard cells (see Figure 3.3C and D for example images). I subsequently normalised the intensity output against the size of the measured area to receive intensity per pixel. I averaged the data for the ten images for each time point and plotted the data in Figure 3.3A and B. Figure 3.3A shows the data from the intensity measurement of the genotype GFP16c. Black bars correspond to the intensity per pixel in pavement cells and white bars to the intensity in guard cells. In the GFP16c plant the intensity per pixel in pavement cells was significantly decreased at 3 dpi and continued to decrease through 4 and reached a 7-fold decrease at 6 dpi. Overall intensity per pixel was almost four times as high in guard cells as compared to pavement cells. This suggests that this protein may be accumulating to higher amounts in the guard cells. This intensity per pixel in guard cells was significantly decreased at 3 dpi and reached a 2-fold decrease at 6 dpi. The intensity per pixel was significantly lower in systemic leaves at 6 dpi in both pavement and guard cells. This could indicate that younger

GFP/autofluorescence merge



Systemic leaf

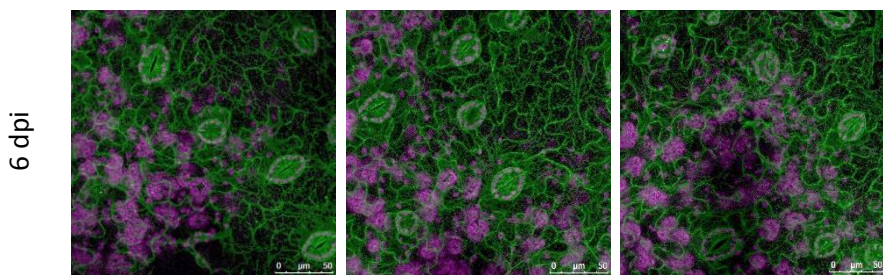


**Figure 3.2:** Confocal maximum projection micrographs of GFP16c infiltrated with *TRV::GFP*. GFP signal continuously decreases in pavement cells in plants infiltrated with VIGS constructs targeting GFP while GFP in guard cells remains unaltered. Five-week-old *N. benthamiana* plants were infiltrated with *TRV::GFP* in fully expanded leaves. Leaf discs were taken at 0, 3, 4, 5 and 6 dpi. At 6 dpi GFP signal in infiltrated leaves were compared to systemic, uninfiltrated leaves. Pictures show maximum projection images and bars indicate 50  $\mu$ m. Each picture corresponds to an independent leaf, with each time point showing images from three separate leaves.

leaves generally have a lower abundance of the 16c fusion protein or that virus-induced silencing affected accumulation of this protein in systemic leaves. Overall, I conclude that in the GFP16c plant silencing in the pavement cells was a lot stronger than in the guard cells, but still detectable in guard cells. Intensity measurement of images obtained from pFLS2::FLS2-GFP plants are shown in Figure 3.3.B. Intensity per pixel in pavement cells at 0 dpi is comparable to the intensity measured in GFP16c plants at 0 dpi. GFP intensity significantly decreased in the pavement cells starting at 3 dpi and reaching a 12-fold decrease at 6 dpi. The intensity per pixel in the systemic leaf at 6 dpi was indistinguishable to the intensity found at 0 dpi, suggesting that in this genotype there does not seem to be a difference in fusion protein accumulation between leaves. Intensity per pixel in guard cells was not significantly different in any of the time point or in the systemic leaf. This suggests that in this phenotype virus-induced silencing does not affect guard cell protein accumulation but significantly decreases protein accumulation in the pavement cells. The intensity measured in systemic leaves was indistinguishable to 0 dpi in both pavement and guard cells. Taken together this data shows that silencing evolves differently across phenotypes and depends on the protein observed. In fully expanded leaves virus-induced gene silencing affects guard cells to a lesser extent than pavement cells and in the case of FLS2-GFP not at all. Since the components I wished to silence are more comparable to FLS2 than the 16c protein in localisation and function I decided that this approach was suitable for my chosen application. I used this silencing protocol for further experiments to address guard cell autonomy in Chapter 2.

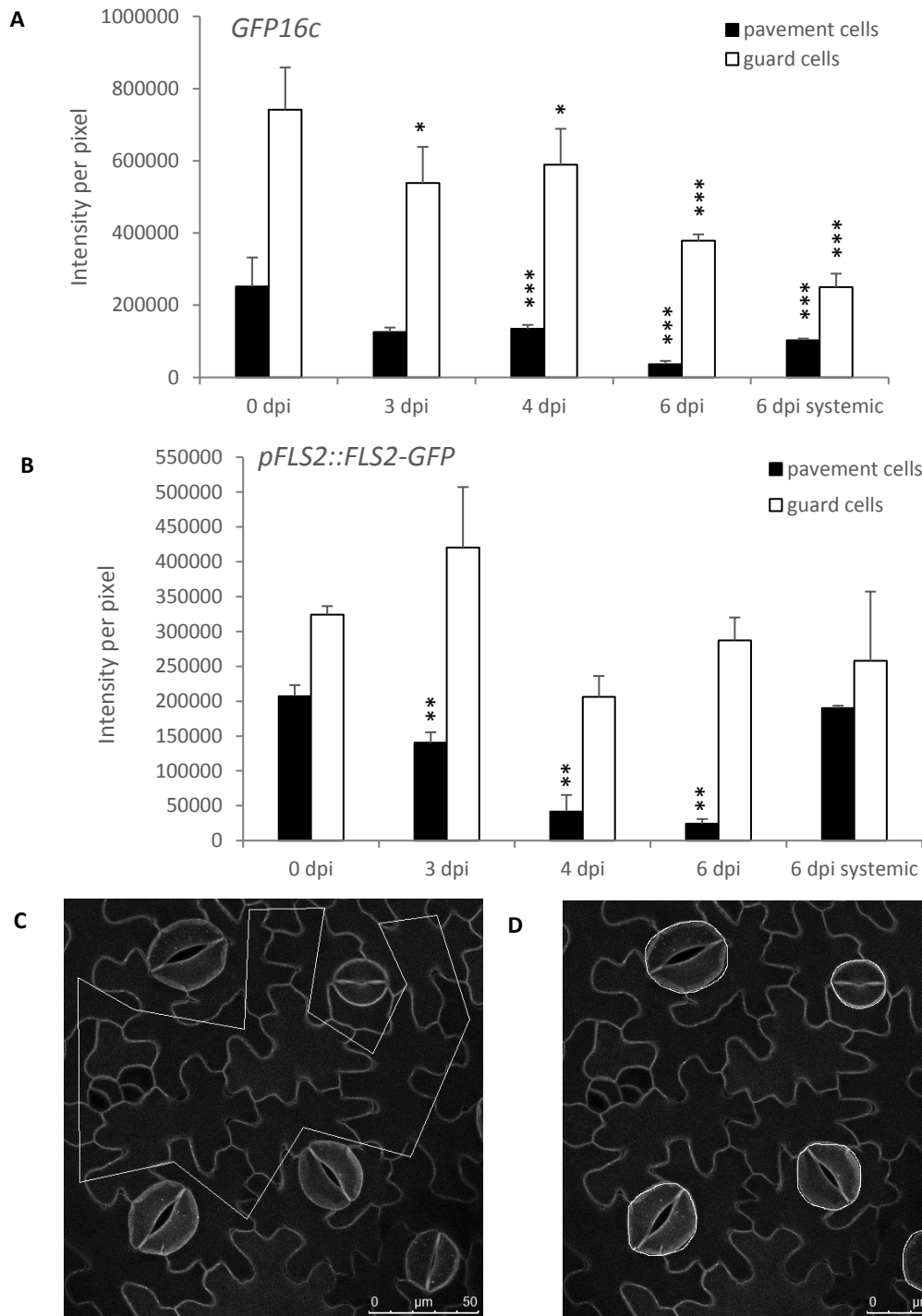


**Figure 3.3:** Quantification of GFP intensity in silenced *N. benthamiana* plants. A. GFP intensity in epidermal cells and stomata of *16cGFP* plants decrease during silencing in infiltrated and systemic leaves. B. GFP intensity in epidermal cells of *pFLS2::FLS2-GFP* plants decreases while stomatal GFP intensity remains unaffected. C. Example images showing selected pavement cell area for intensity measurement. D. Example images showing selected guard cells for intensity measurement. Confocal maximum projection images were converted to show luminance in ImageJ. Raw Intensity Density of area of interest was measured using ImageJ. Values were normalised to surface area measured. Ten representative images were measured for every combination of genotype and time point. Images are from one representative experiment. Experiment was repeated twice with similar results. Error bars indicate SD from mean. Asterisks indicate significant differences from 0 dpi (student's t-test, \*  $p < 0.05$ , \*\*  $p < 0.01$ , \*\*\*  $p < 0.001$ ). Bars indicate 50  $\mu\text{m}$ .

### 3.2.2. Guard cell-specific promoter screen in *Arabidopsis thaliana*

In addition to a transient setup I also aimed at establishing a stable transgenic setup in *Arabidopsis thaliana* to investigate guard cell autonomy. To this end I identified five candidate promoters from the literature to drive guard cell-specific expression of our proteins of interest. To evaluate their suitability and specificity I created stable transgenic *Arabidopsis thaliana* plants expressing free GFP under the control of these promoters. Transgenic plants were selected and screened for their GFP distribution with a confocal laser-scanning microscope. Consequently, I screened twenty individual T1 plants. Representative maximum projection images were chosen and are presented in Figure 3.4. Both the *pCYP86A2* and *pMYB60* promoters show a strong GFP signal in guard cells and a weak signal in surrounding pavement cells. The other three promoters, *pCPK13*, *pKCS1* and *pGC1*, do not show any GFP signal in the T1 generation.

**Table 3.1:** Information on promoters cloned for guard cell-specificity screen. All promoters were cloned from genomic DNA isolated from *Arabidopsis thaliana*. All promoters were domesticated into a level 0 acceptor plasmid for use in the Golden Gate system.

Promoter	publication	cloned from	region cloned
<i>pGC1</i>	Yang <i>et al.</i> , 2008	gDNA <i>Arabidopsis thaliana</i>	-1716 to 0
<i>pKCS1</i>	Gray <i>et al.</i> , 2000	gDNA <i>Arabidopsis thaliana</i>	-2180 to 0
<i>pCPK13</i>	Ronzier <i>et al.</i> , 2014	gDNA <i>Arabidopsis thaliana</i>	-2291 to 0
<i>pMYB60</i>	Rusconi <i>et al.</i> , 2013	gDNA <i>Arabidopsis thaliana</i>	-1307 to 0
<i>pCYP86A2</i>	Galbiati <i>et al.</i> , 2008	gDNA <i>Arabidopsis thaliana</i>	-1256 to 0

Further characterisation of expression patterns driven by candidate promoters was done after propagation in the T2 generation. Dr. Michaela Kopischke and Dr. Ben Petre had already characterised the *pGC1* promoter and found it to drive stronger, but not exclusive expression in guard cells (unpublished) and therefore I did not include these plants with this promoter for further analyses. The GFP localisation pattern from at least two independent transgenic events were analysed. Figure 3.5 shows confocal maximum projection micrographs of the four analysed promoters at 16 and 26 days post germination (dpg). The promoter *pKCS1* showed a stronger accumulation of GFP in guard cells than in pavement cells but did not appear to be very specific since there I could still detect a GFP signal at the pavement cell periphery. The expression pattern driven by *pKCS1* does not depend on the developmental stage, as it is the same for both 16 and 26 dpg. I therefore conclude that this promoter is not suitable for our purposes. Both *pMYB60* and *pCYP86A2* appeared to have a high specificity

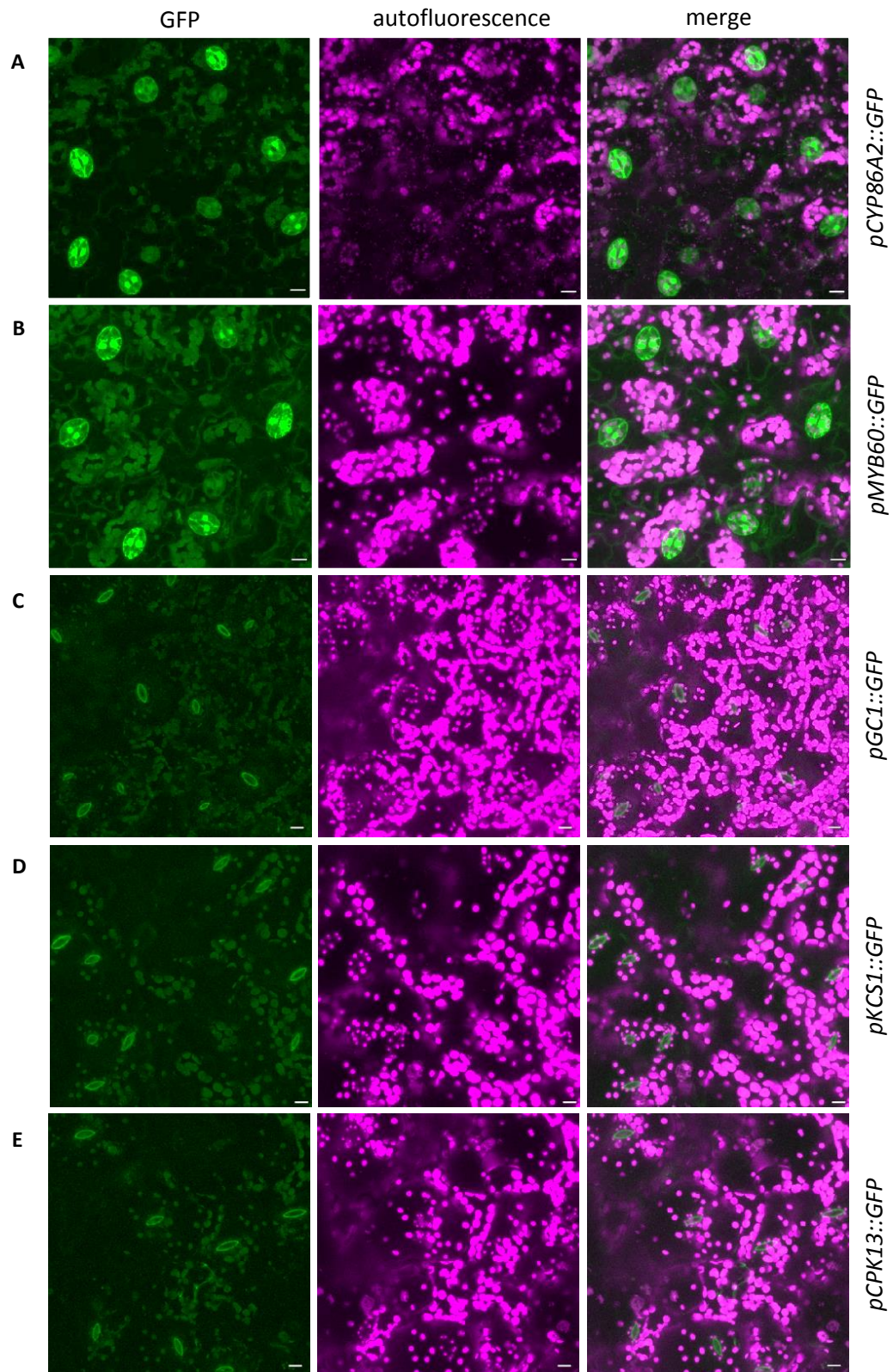


**Figure 3.4:** Confocal micrographs of 4-week-old transgenic *Arabidopsis thaliana* plants expressing free GFP under the control of different promoters in the T1 generation. A. Expression pattern of the *pCYP86A2* promoter is restricted to guard cells. B. Expression pattern of *pMYB60* promoter is stronger in, but not restricted to, guard cells. C., D. and E. The promoters *pGC1*, *pKCS1* and *pCPK13* show no GFP expression in the T1 generation. 20 individual T1 plants were screened. Images show selected, representative maximum projection images and bars indicate 10  $\mu$ m.

for guard cells as little to no GFP signal was observed in pavement cells but a strong signal was present in guard cells. This was true for both 16 and 26 dp. Another factor I took into account was the correlation between BASTA-positive plants and detectable GFP expression. In the case of *pCYP86A2* only a quarter (25%) of the BASTA-positive transgenic lines showed detectable GFP signal by confocal imaging, suggesting a low GFP expression rate in three quarters (75%) of the transgenic plants. In comparison, the *pMYB60* BASTA-positives showed a much higher expression rate, with 85% of positively selected plants exhibiting an observable GFP signal with the confocal microscope. The promoter *pCPK13* showed a strong and specific GFP signal in guard cells at 16 dp. However, at 26 dp I could not observe a strong guard cell GFP signal, but instead a high accumulation of GFP in the epidermal cells. When taking into account both the expression strength and distribution I conclude that the most suitable promoter for guard cell-specific expression is the *pMYB60* promoter.

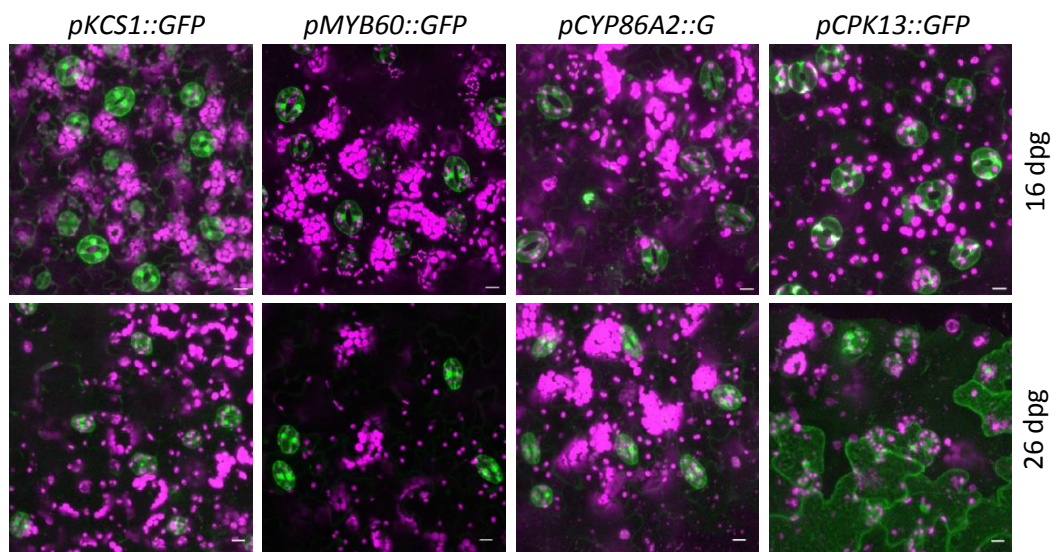


**Figure 3.5:** Confocal micrographs of 4-week-old transgenic *Arabidopsis thaliana* plants expressing free GFP under the control of different promoters in the T2 generation.

The strongest, most guard cell-specific signal is achieved with the *pMYB60* promoter. Expression pattern of the *pKCS1*, *pCYP86A2*, *pMYB60* promoters do not differ between 16 and 26 days post germination (dpg). Expression pattern of *pCPK13* is no longer restricted to guard cells at 26 dp. Images show selected, representative maximum projection images and bars indicate 10  $\mu$ m.

### 3.3. Discussion

While the generation of stable transgenic plants takes several weeks or months to complete, transient assays require little preparation time and can be performed as soon as vectors are completed. For this reason, I endeavoured to set up a transient expression system to study guard cell autonomy in *N. benthamiana*. The transient silencing application I describe here can be used to transiently test guard cell-specific responses in a fast, high-throughput manner. Figures 3.1 and 3.2 show that when applied at the right developmental stage silencing affects cell types differentially. The quantification of GFP intensity in the confocal maximum projection images confirmed this (Figure 3.3). GFP intensity in the pavement cells was strongly reduced in both tested genotypes. Interestingly, whether guard cell GFP intensity was affected by silencing differed between the phenotypes. While the GFP intensity in the guard cells of *16cGFP* plants significantly decreased after infiltration it was unaffected in the *pFLS2::FLS2-GFP* plants. This could be due to the differences between fusion proteins. The 16c fusion protein is localised to the ER and seems to be expressed to higher amounts in the guard cells as the intensity was almost four times as high as compared to the pavement cells. It is possible that the stress of infiltration with *Agrobacterium* expressing the silencing constructs affects accumulation of this protein throughout the whole plant as also uninfiltreated, systemic leaves showed a reduction in GFP intensity. It is also conceivable that this is due to the high amount of variation I observed between plants and leaves of this genotype. In contrast, the GFP intensity in guard cells was unaffected in the *pFLS2::FLS2-GFP* plants and only the pavement cell intensity significantly decreased. Also, systemic leaves were unaffected at 6 dpi in this phenotype suggesting that the decrease in GFP intensity in systemic tissues observed in *16cGFP* plants is not a common trend and probably not due to the virus-induced silencing construct. As FLS2 is plasma membrane localised and involved in defence activation it is more similar to the components I want to silence in pavement cells than the ER localised 16c protein. I therefore conclude that this silencing approach is suitable to silence defence components in pavement cells while leaving guard cells unaffected.

Previous studies have identified and promoted promoters as guard cell-specific and useful research tools. In this study I directly compared cell type-specific promoters side by side. Comparisons in T1 plants proved impossible as many plants did not show any GFP accumulation at all (Figure 3.4), as all T1 are hemizygous for the transgene. However, after propagation I was able to compare all promoters in the T2 generation. Through confocal microscopy on several T2 plants per promoter I was able to determine that some of the previously published promoter are not suitable to drive guard cell-specific expression (Figure

3.5). The differences between my observations and the published results can be explained through the difference in techniques used to assess guard cell-specificity. Four out of five of those studies exclusively used *Promoter::GUS* fusions to evaluate promoter specificity (Gray *et al.*, 2000; Galbiati *et al.*, 2008; Rusconi *et al.*, 2013; Ronzier *et al.*, 2014). One study also included *Promoter::YC3.60* constructs to image calcium signalling in guard cells and evaluated the expression pattern by confocal microscopy (Yang *et al.*, 2008). The same study compared the expression strength of the *pGC1* promoter with *pMYB60* and *pKAT1* based on guard cell-specific micro-array data. They concluded that *pGC1* is the strongest promoter and have shown successful silencing of GFP in guard cells when driving an antisense GFP construct with this promoter. However, we could not reproduce their results that this promoter was very specific expression in guard cells. Localisation experiments with transgenic plants by confocal microscopy performed by Ben Petre and Michaela Kopschke indicated this promoter to be leaky. Differences observed could be due to the different microscopes used or excitation wavelengths. (Yang *et al.*, 2008) used a GFP excitation wavelength of 440 nm, while our lab commonly uses 488 nm. We concluded that this promoter was unsuitable for our desired application which requires a guard cell-specific promoter. We chose microscopy as the optimal method to determine specificity, because it allows for high-throughput screening, as well as having high sensitivity. Differences in expression patterns between our study and studies using *Promoter::GUS* fusions can be explained by differences in sensitivity between assays.

There are already several useful resources for researchers to determine expression patterns of proteins between tissues, upon certain stimuli and during development. Such an example is the eFP browser (<http://bar.utoronto.ca/efp/cgi-bin/efpWeb.cgi>) that offers such information for both *Arabidopsis thaliana* and *Oryza sativa*. Another example is the Genevestigator (<https://genevestigator.com/gv/>) that offers curated expression data for several organisms, including ten plant species. While these are useful tools, they can only be considered starting points and the responsibility to verify these results still lie with the researchers conducting experiments based on data obtained from these websites. Especially if one wants to draw conclusions regarding responses of only one cell type or tissue. In this study, I provide this useful information on specificity for guard cell expression. This study will therefore be a useful resource for future scientists to identify a suitable promoter for guard cell-specific expression.

## 4. Stomatal immunity involves guard cell-specific and non-autonomous signalling events

### 4.1. Introduction

Plants have evolved complex and highly regulated molecular signalling pathways to respond to the plethora of stresses to which they are exposed. Despite the considerable progress that led to a conceptual understanding of these regulatory pathways and unravelled key molecular components underlying plant responses, our understanding remains limited. With global warming, an increasing population and an increasing number of invading pathogens, it has become even more important to understand and deploy those mechanisms. According to estimates yield losses due to abiotic stresses such as drought, salinity and extreme temperatures can reach more than 50% for major crop plants (Boyer, 1982; Harrison *et al.*, 2014). In addition to abiotic stresses plants also suffer from biotic stresses. Especially plant diseases pose a great challenge for agriculture. Some diseases are considered a great threat to our food security and the most severe diseases have been compiled in the list of “The Big 7”(AAAS, 1998). Wheat stem rust, for instance, can cause yield losses greater than 40% to the global harvest.

An important tool for the plant to respond to these abiotic and biotic stimuli are the stomata. Formed by a pair of guard cells that control the size of the aperture by means of osmotically driven water transport, stomata enable active control over water loss and gas exchange, but also respond to pathogens trying to gain access into plant tissues through natural openings. Bacteria are one group of such opportunistic pathogens that rely on access into the leaf interior to establish a successful infection. The ability to close the stomata upon recognition of a pathogen and to change the outcome of infection to the disadvantage of the pathogen is referred to as stomatal immunity (Melotto *et al.*, 2006). This is mediated by Pattern Recognition Receptors (PRRs) that perceive Microbe-Associated Molecular Patterns (MAMPs) at the plasma membrane and are primary sensors of the plant’s immune system. FLS2 is the major PRR mediating immunity against *Pst* DC3000 (Zipfel *et al.*, 2004). Upon MAMP perception FLS2 associates with its co-receptor BAK1 (Chinchilla *et al.*, 2007) and the associated kinase BIK1 initiates ROS production via RBOHD (Kadota *et al.*, 2014), as one of the earliest measurable responses. Subsequently MAP-Kinase cascades lead to the activation of further immune responses (Boller & Felix, 2009). While plant immune responses have

been widely studied, only few studies have taken differences between cell types into account.

Once fully differentiated, guard cells are symplastically isolated as cell wall material is deposited upon plasmodesmatal connections during the differentiation process (Wille & Lucas, 1984; Palevitz & Hepler, 1985). This isolation and their unique ability of reversibly changing their shape has led to the hypothesis that guard cells act autonomously when initiating opening or closure. Consequently, studies have been conducted that showed that guard cells mediate blue light-induced opening and ABA-induced closure in an autonomous manner (Cañamero *et al.*, 2006; Bauer *et al.*, 2013). Whether this remains true for other stimuli has yet to be shown. Furthermore, it has never been studied whether other cell types have the capacity to signal to guard cells and alter the size of aperture when guard cells cannot respond.

To understand whether stomatal closure is an autonomous guard cell response or whether pavement cells are able to induce closure, I developed genetic resources that either lead to a guard cell-specific complementation or guard cell-specific gene knock-down. To this end I employed the guard cell-specific promoter *pMYB60* (Rusconi *et al.*, 2013 and Chapter 3) to complement knock-out mutants only in guard cells. In parallel, I designed artificial micro RNAs that can be expressed under this promoter for a cell type-specific knock-down of genes.

In this study I show that MAMP-induced stomatal closure is mediated by both autonomous and non-autonomous signalling events. Guard cell-excluding silencing of RBOHB and SERK3 in *Nicotiana benthamiana* leaves stomata responsive to MAMP treatment, although to a lesser extent than the wild-type. Transgenic *Arabidopsis thaliana* plants that express FLS2 in a guard cell-specific manner close their stomata in response to MAMP treatment in a wild-type-like manner. This guard cell-specific recognition is furthermore sufficient for resistance against bacterial pathogens. Through *Agrobacterium*-mediated transformation, I complemented EFR and RBOHD only in pavement cells and show that pavement cells can induce stomatal closure in response to elf18 in *Nicotiana benthamiana*. Expression of amiRNAs targeting FLS2 under the control of a constitutive promoter rendered guard cells unresponsive to flg22 treatment. The same amiRNAs were expressed under the control of the guard cell-specific promoter *pMYB60* and transgenic plants remained wild-type-like stomatal closure responses to flg22 treatment and susceptibility to *Pst* DC3000. Together, I show that both cell-type specific and non-autonomous signalling events occur to mediate MAMP-induced stomatal closure.

## 4.2. Results

### 4.2.1. Guard cell-excluding VIGS of *NbSERK3a/b* and *NbRBOHB* demonstrates guard cell autonomy

In chapter three I demonstrated that virus-induced gene silencing can silence genes in pavement cells while leaving guard cells unaffected when applied at the right developmental stage of the leaf. To investigate guard cell autonomy in MAMP-triggered stomatal closure, I silenced components in pavement cells that are known to be important for this response. Previous studies have demonstrated that ROS production via RESPIRATORY BURST OXIDASE HOMOLOGUE D (RBOHD) is crucial for MAMP-induced stomatal closure (Kadota *et al.*, 2014) and that BRI1-ASSOCIATED RECEPTOR KINASE (BAK1) is necessary for defence initiation via FLS2 (Chinchilla *et al.*, 2007). I therefore silenced ROS production by targeting the *N. benthamiana* homolog of *AtRBOHD*, the primary NADPH oxidase after MAMP perception (*TRV::NbRBOHB*) and BAK1, the co-receptor of FLS2 (*TRV::NbSERK3a/b*) (Heese *et al.*, 2007; Segonzac *et al.*, 2011). I infiltrated the GFP-targeting silencing construct into wild-type *N. benthamiana* as a control as this plant does not express GFP. This allowed me to determine whether the infiltration of a silencing construct has an effect on either of the performed assays. Six days after the silencing constructs were infiltrated, I conducted ROS and stomatal closure assays to characterise the autonomy of guard cells.

Uninfiltrated *Nicotiana benthamiana* wild-type leaves and leaves infiltrated with the control construct *TRV::GFP* show a strong ROS burst in response to flg22 trigger (Figure 4.1A). Both leaves silenced for *NbRBOHB* or *NbSERK3a/b* show strongly reduced ROS production compared to controls in response to flg22, demonstrating that silencing was indeed successful. Leaf discs from the same leaves were also subjected to a stomatal closure assay. Leaf discs were harvested in the morning of the experiment and incubated in stomata opening buffer under constant light to induce opening of all stomata. Two hours later the MAMP treatment was applied for two hours before the apertures were imaged and measured using ImageJ. Uninfiltrated wild-type *N. benthamiana* leaves show a significantly reduced stomatal aperture after flg22 treatment, as does the *TRV::GFP* control construct (Figure 4.1B). Leaves that had silenced pavement cells for ROS production or MAMP perception showed less closure to flg22 trigger ( $p < 0.05$ ). As in this transient setup guard cells were not silenced and remained the only cells with full capacity for producing ROS and initiating defence signalling, these results provide evidence that guard cells can initiate stomatal closure in an autonomous manner. However, the stomatal closure response is not

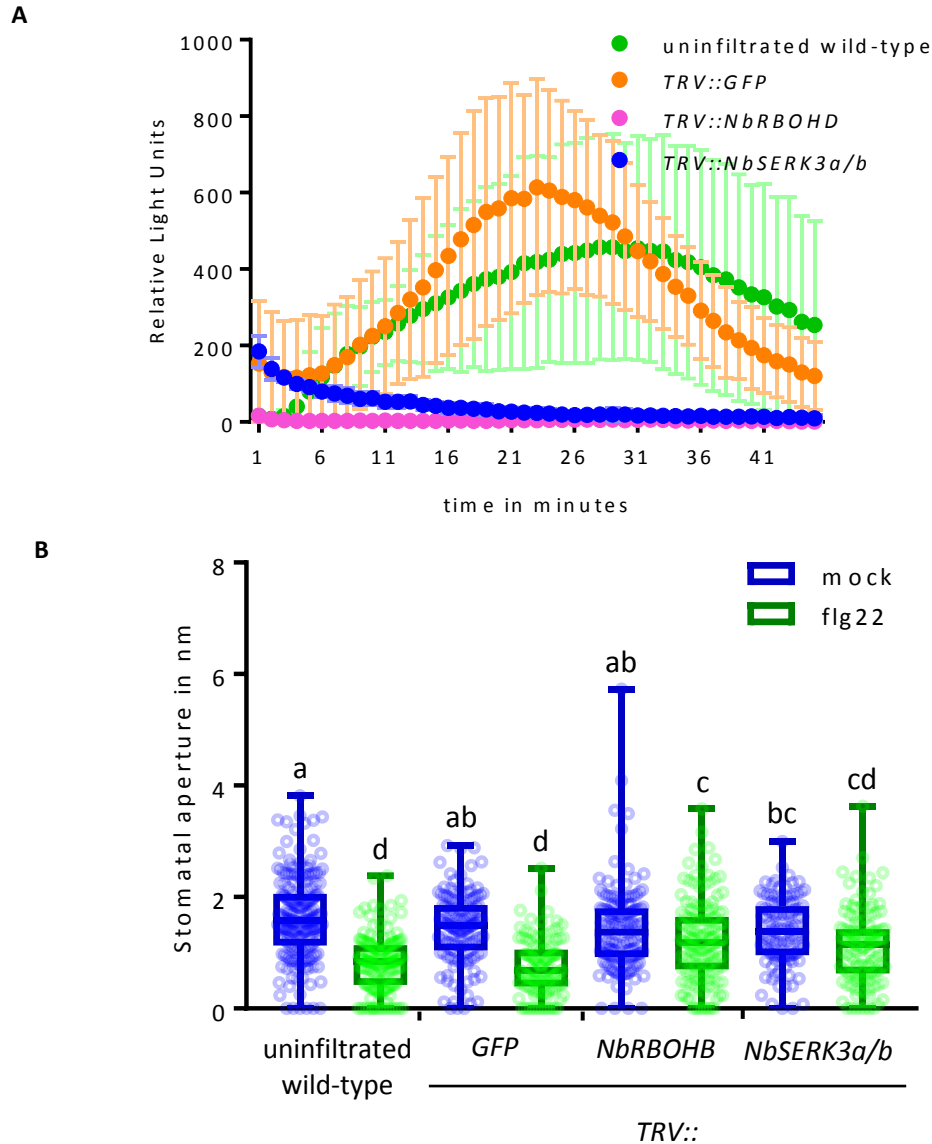


**Figure 4.1:** Guard cells act autonomously in MAMP-induced stomatal closure in transient assay. 5-week-old *N. benthamiana* plants were infiltrated with *TRV::GFP* as control or *TRV::NbRBOHD* or *TRV::NbSERK3a/b*.

A. Flg22-induced ROS production is strongly reduced in silenced *N. benthamiana* leaves. Graph shows flg22-induced ROS burst on 48 leaves from 6 plants per treatment. Data show mean from one independent experiment (n=3 independent experiments). Error bars indicate SD from mean.

B. Guard cell closure in silenced *N. benthamiana* plants is reduced but not abolished. Graph shows flg22-induced stomatal closure on 3 leaves from 3 plants per treatment in per cent. mock: stomata opening buffer. At least 60 stomata per combination of genotype and treatment were measured in Image J. Graph shows data from one representative experiment. Experiment was performed three times with similar results. Error bars indicate SD from mean of each genotype and treatment combination. Letters indicate significance levels (two-way ANOVA followed by Tukey's test,  $p < 0.05$ ).

as pronounced as in control leaves. This could be a limitation of the transient expression approach and further experiments were conducted to verify these results in stable transgenic plants.

## 4.2.2. Guard cell-specific complementation of RBOHD

### 4.2.2.1. Generation of guard cell-specific RBOHD complementation lines in *Arabidopsis thaliana*

The NADPH oxidases RBOHD and RBOHF generate ROS in the apoplast. ROS production is important for flg22-induced stomatal closure as the *rboh*d *rboh*f double mutant is insensitive to flg22 in stomatal closure assays (Kadota *et al.*, 2014). Since ROS is produced in the apoplast it could originate from many cell-types it is not known which cell type is the primary source of ROS that leads to induction of stomatal closure. To see whether the generation of ROS by two single guard cells is sufficient, I generated *Arabidopsis thaliana* expressing RBOHD under the control of the guard cell-specific promoter pMYB60 (as described in chapter one) in the *rboh*d null-mutant. The Golden Gate compatible AtRBOHD was synthesised by ENSA and I cloned it into a level1 expression cassette with the guard cell-specific promoter pMYB60. To visualise RBOHD localisation it was N-terminally tagged with GFP or mCherry. Transgenic lines were generated by the TSL Tissue Culture Team using the floral dip method and positive transformants identified by the red seed coat from the pFAST-Red plant selection cassette (Shimada *et al.*, 2010). This selection method makes use seed-specific promoter that drives expression of an oil body membrane protein fused to RFP. The marker is only expressed in dry seeds during dormancy making it easy to screen seeds to only grow transformed plants (Shimada *et al.*, 2010). Positive transformants were propagated and characterised in the T2 generation.

### 4.2.2.2. *rboh*d/pMYB60::GFP-RBOHD and *rboh*d/pMYB60::mCherry-RBOHD plants appear to have accumulation of the cleaved tag in the tonoplast

pFAST-Red-positive transgenic plants were grown on soil under short day conditions (section 2.6.1.3) and their expression pattern of tagged RBOHD was evaluated using a confocal Laser-Scanning Microscope (Leica SP5). Plants expressing mCherry-tagged RBOHD showed a strong signal of mCherry in the guard cells that wraps around the chloroplasts, indicative of tonoplast localisation (confocal micrographs are shown in Figure 4.2B). While GFP-RBOHD plants show a weaker signal, upon closer inspection the GFP signal can also be observed in the tonoplast (confocal micrographs in Figure 4.2A). This suggests that fusion tags are cleaved from RBOHD or that the whole fusion protein is degraded in the vacuole.

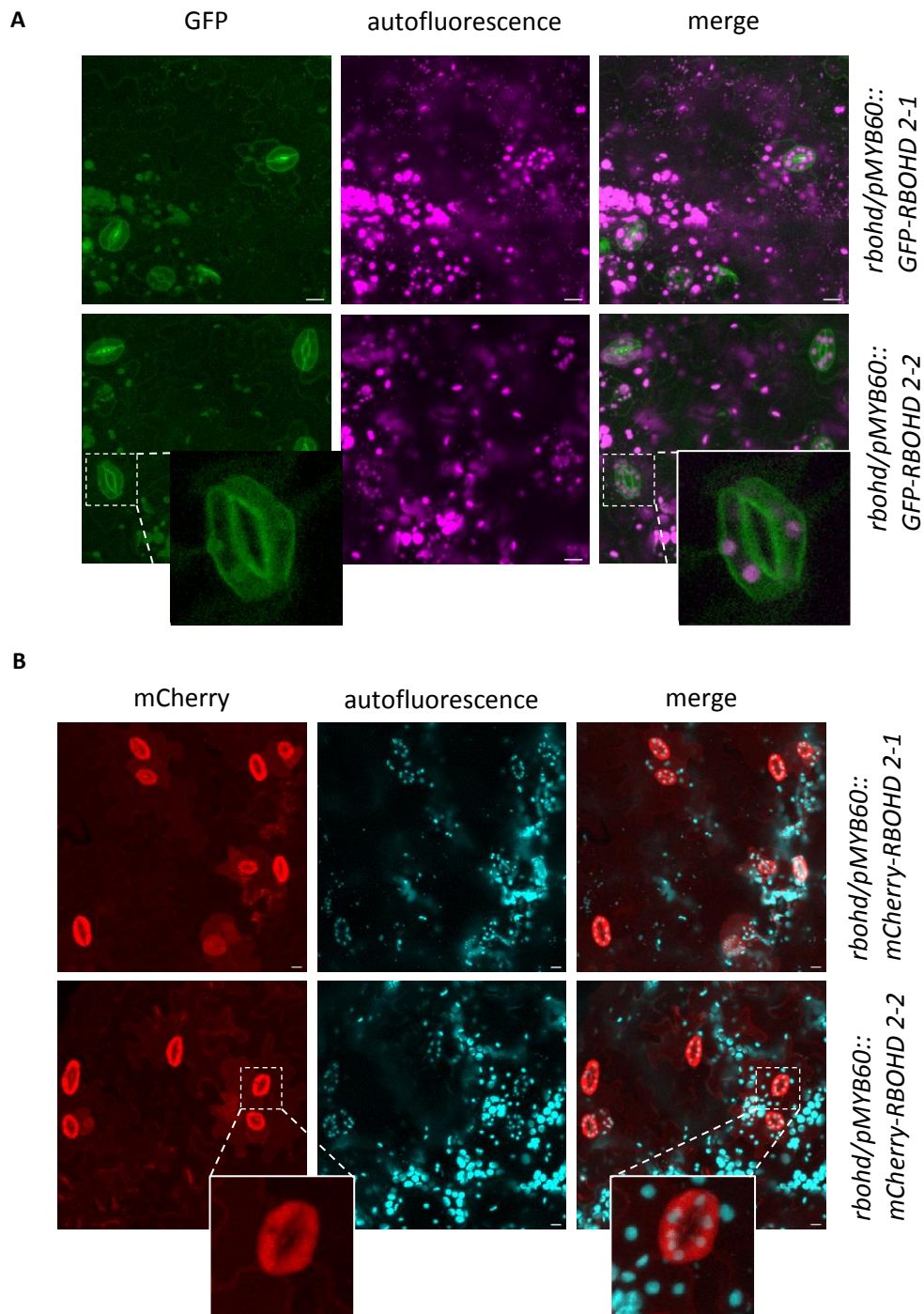


**Figure 4.2:** *pMYB60::GFP-RBOHD* and *pMYB60::mCherry-RBOHD* plants show tag accumulation in the tonoplast and surrounding cells.

A. Confocal micrographs of *rboh/pMYB60::GFP-RBOHD* plants show leaky expression and GFP accumulation in the tonoplast. Leaf discs from five-week-old *Arabidopsis thaliana* transgenic plants grown in soil under short day conditions were harvested and observed with a confocal laser-scanning microscope (Leica SP5). Squares indicate magnified region. Connected images are single slices magnified 28.5 times from the shown maximum projection. Bars indicate 10  $\mu$ m. Micrographs are shown from one experiment. Similar results were observed across 20 independent T2 plants.

B. Confocal micrographs of *rboh/pMYB60::mCherry-RBOHD* plants show leaky expression and mCherry accumulation in the tonoplast of guard and surrounding cells. Leaf discs from five-week-old *Arabidopsis thaliana* transgenic plants grown in soil under short day conditions were harvested

and imaged with a confocal laser-scanning microscope (Leica SP5). Squares indicate magnified region. Connected images are single slices magnified 28.5 times from the shown maximum projection. Bars indicate 10  $\mu\text{m}$ . Micrographs are shown from one experiment. Similar results were observed across 20 independent T2 plants.

#### 4.2.2.3. Guard cell-specific GFP-RBOHD plants and over-expressers show free GFP signal in Western Blot

Next, I performed protein extractions and Western Blot analysis probing with the anti-GFP antibody. Transgenic T2 lines, wild-type and *rbohd* mutants were grown in soil for five weeks under short day conditions. One full leaf was snap frozen in liquid nitrogen, ground to a fine powder and proteins were extracted before they were fractionated by SDS-PAGE and blotted onto PVDF membrane using the semi-dry method. No GFP signal could be detected in transgenic lines expressing *pMYB60::GFP-RBOHD* plants while the over-expresser line *pUBQ10::GFP-RBOHD* showed a positive fusion-protein band (data not shown). I therefore performed guard cell-enrichments before extracting proteins. For this, 1g of leaf material was repeatedly blended with crushed ice and ultrapure water until mainly epidermal peels remained intact. The destroyed mesophyll cells and their contents were filtered and the epidermal peels collected and snap frozen in centrifuge tubes following protein extraction. Crude extracts were performed alongside the guard cell enrichments and loaded together on gels and blots to directly compare the samples. Wild-type Col-0 plants do not show a GFP-RBOHD or free GFP band as they were not transformed and do not express any GFP-fusion protein (Figure 4.3). The over-expresser *rbohd/pUBQ10::GFP-RBOHD* line has a strong band at 130 kDa corresponding to the size of the GFP-RBOHD fusion protein under short and long exposure times in both crude and guard cell-enriched extractions. This is consistent with the *pUBQ10* promoter being a strong promoter in all cell types. However, the over-expressing line and two guard cell-specific lines show free GFP at 25 kDa under short exposure as do all lines under long exposure. Lines 1-8, 1-9, 1-15 and 1-16 show very low GFP-RBOHD accumulation, as the band can only be detected after very long exposure of the membrane. No bands corresponding to GFP-RBOHD can be detected in line 1-6 crude or guard cell-enriched samples. Protein concentrations between crude and guard cell-enriched extractions were adjusted using Bradford protein quantification. Since guard cells have lower photosynthetic rates than mesophyll cells, the band corresponding to rubisco is reduced in guard cell-enriched samples, compared to crude extracts in the Coomassie Brilliant Blue staining (Figure 4.3). However, there seems to be a guard cell-specific band of an unknown protein between 35 and 25 kDa that is stronger in guard cell-enriched samples indicating that

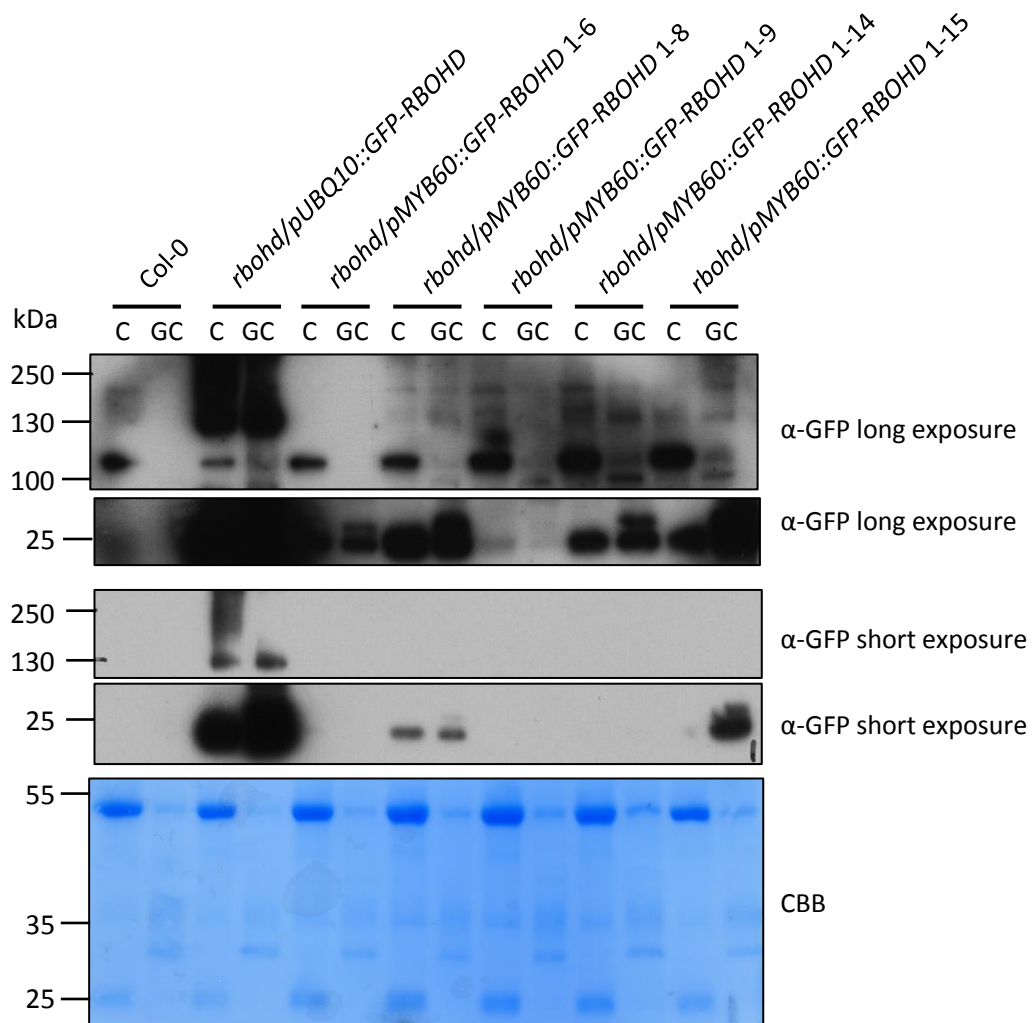


**Figure 4.3:** *pMYB60::GFP-RBOHD* plants show very low fusion protein expression and a high amount of free, cleaved GFP. Whole leaves from 5-week-old soil-grown *Arabidopsis thaliana* were used for crude extractions and 1g of leaf material from five T2 plants were used for guard cell enrichment. For guard cell enrichments leaves without central veins were blended for 60 seconds in a kitchen blender with 250 ml ultrapure water and crushed ice. Epidermal peels were collected through filtering and blending was repeated twice. Epidermal peels were snap frozen in liquid nitrogen and proteins were extracted as described in section 2.6.16. C: crude extract; GC: Guard cell enrichment; CBB: Coomassie Brilliant Blue.

guard cell-enrichment was indeed successful. Together, these results suggest that GFP-RBOHD accumulation is very low and a high amount of GFP-tag is cleaved in transgenic lines generated in this study.

#### 4.2.2.4. ROS production between transgenic lines varies strongly

To further characterise the transgenic plants, I performed luminol-based ROS assays on leaf discs of five-week-old soil-grown plants in the T2 generation. Figure 4.4 shows the apoplastic ROS accumulation of selected lines. Wild-type shows a strong transient production of ROS

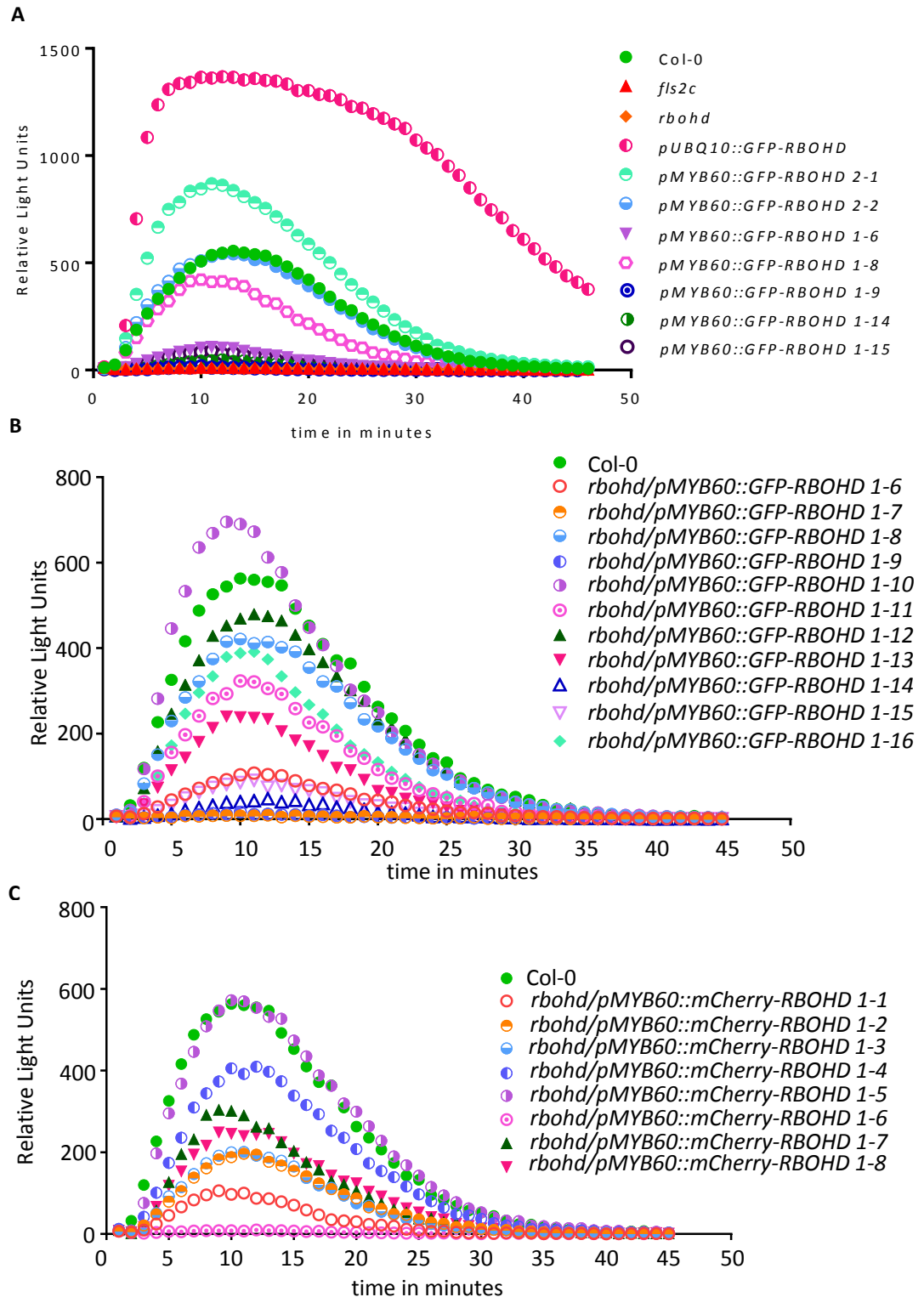


**Figure 4.4:** ROS signatures of *rbohD/pMYB60::RBOHD* lines in response to flg22 in the T2 generation with different tags.

A. *rbohD/pMYB60::GFP-RBOHD* plants have ROS signatures that vary in intensity. B. The ROS signature of several transgenic plants expressing *rbohD/pMYB60::GFP-RBOHD* varies strongly. C. Transgenic lines expressing mCherry-RBOHD guard cell-specifically have very different ROS signatures.

In a luminol-based assay, leaf discs of 5-week-old transgenic *A. thaliana* plants were imaged for 45 minutes by an ICCD photon-counting camera. Leaf discs were harvested on the evening before the assay and left to rest over night. Graph shows data from one experiment.

upon flg22 treatment while *rboh*d mutant plants do not show any ROS production (Figure 4.4A). ROS production in wild-type and transgenic plants increases until it peaks at 10 minutes after MAMP treatment and declines thereafter until it reaches basal levels between 35 and 40 minutes post treatment. The over-expressing plant expressing GFP-RBOHD under the constitutive *pUBQ10* promoter shows a very strong ROS accumulation that exceeds the wild-type response. Guard cell-specific transgenic lines 2-1 and 2-2 that showed a GFP signal detectable with the confocal Laser Scanning Microscope show wild-type-like and stronger than wild-type ROS accumulation, respectively. Line 1-8 has a slightly reduced ROS accumulation compared to wild-type, while lines 1-6, 1-9, 1-14 and 1-15 have a strongly reduced ROS response. Although lines 1-14 and 1-15 seem to have the strongest GFP-RBOHD band this does not reflect in their capacity to accumulate apoplastic ROS.

As a consequence of the high variance in ROS phenotypes, I evaluated the response of 40 different T2 plants originating from two independent transgenic events. I could not observe any correlation between transgenic events, the fusion-protein accumulation and the ROS response. To illustrate the broad range of responses by both GFP-RBOHD and mCherry-RBOHD complemented plants these are shown in Figures 4.4A, B and C. The ROS responses range from *rboh*d-like, to wild-type-like to over-expresser-like. Taken together with the observation that the majority of the GFP- and mCherry-tag is cleaved off in the transgenic plants, I decided not to characterise these plants any further.

### 4.2.3. Guard cell-specific complementation of FLS2 in *Arabidopsis thaliana*

#### 4.2.3.1. Guard cell-specific complementation of FLS2 with the promoter *pMYB60*

To assess whether the perception of a ligand by only guard cells is sufficient to mount the full closure response, I complemented *fls2* receptor knock-out mutants with constructs driving expression exclusively in guard cells. Making use of the *pMYB60*, I created plants that express FLS2 only in guard cells and can therefore only perceive flg22 in these cells. To visualise the expression pattern of the promoter, FLS2 was tagged with GFP and the transgenic plants were examined with a confocal laser-scanning microscope. Confocal micrographs in Figure 4.5A show that FLS2-GFP signals can only be observed in guard cells in two independent transgenic lines in the T2 generation. The GFP signal can be detected at the plasma membrane and I could not observe any GFP signal in cytoplasm or tonoplast that would suggest cleavage of the tag as was the case for the GFP- and mCherry-RBOHD transgenics. Plants whose expression pattern was confirmed using confocal microscopy were used for further assays.

#### 4.2.3.2. *pMYB60::FLS2-GFP* lines express FLS2-GFP to different levels

Since the guard cell-specific RBOHD lines generated in this study proved unsuitable due to the cleavage and possible degradation of the tag and the protein, I decided to examine protein expression for the guard cell-specific FLS2 transgenics. To this end I extracted proteins from five-week-old soil-grown *Arabidopsis thaliana* plants and performed a Western Blot making use of the  $\alpha$ -FLS2 antibody. As a control, I included Col-0 wild-type, two *fls2* null-mutants and a transgenic plant generated in our lab that has both the FLS2 wild-type protein and a FLS2-3xMyc-GFP fusion protein (*Col-0/pFLS2::FLS2-3xMyc-GFP*). Wild-type Col-0 shows a single band at around 170 kDa that corresponds to the wild-type FLS2 protein (Figure 4.6A). Both *fls2* null-mutants do not show a band at either short or long exposure of the film. The transgenic plant *Col-0/pFLS2::FLS2-3xMyc-GFP* shows two bands, the lower one corresponding to the FLS2 wild-type protein and the higher band corresponding to the FLS2-3xMyc-GFP fusion protein. All the guard cell-specific transgenic plants show a single band with a molecular weight between that of the wild-type FLS2 and the FLS2-3xMyc-GFP proteins, as it is lacking the 3xMyc tag and is therefore slightly smaller. The *pMYB60::FLS2-GFP* transgenics also show a lower signal of the protein than wild-type or transgenic plants. The transgenic plant expresses the fusion protein under its native promoter

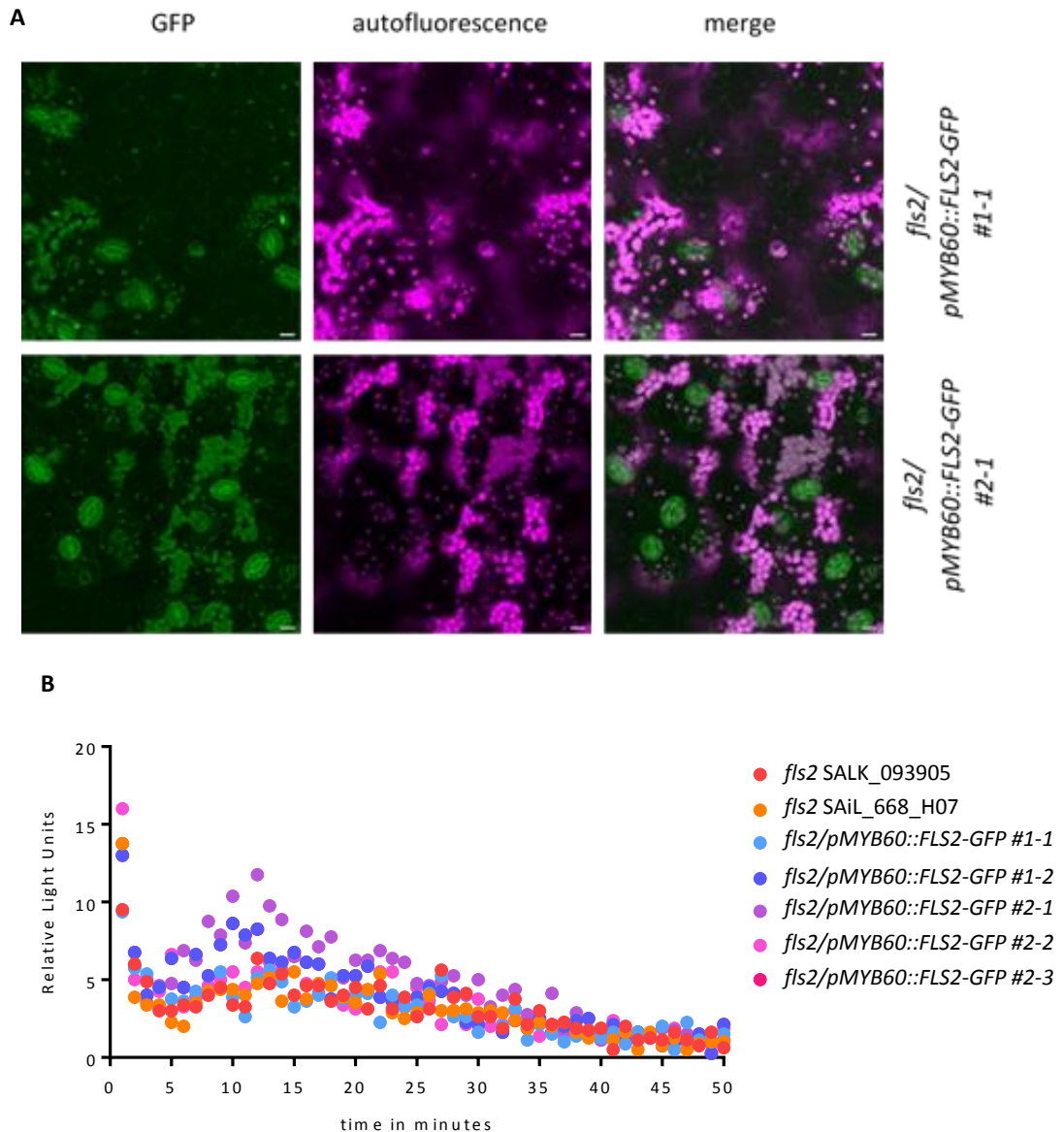


**Figure 4.5:** Promoter *pMYB60* drives guard cell-specific expression and allows cell type-specific mutant complementation.

A. Confocal micrographs of 2 independent 5-week-old transgenic *A. thaliana* plants expressing *pMYB60::FLS2-GFP*. Transgenic *Arabidopsis thaliana* expressing *fls2/pMYB60::FLS2-GFP* plants show GFP localisation at the plasma membrane of guard cells. *fls2* (SALK\_093905) knock-out mutants were stably transformed to express FLS2-GFP only in guard cells making use of the guard cell-specific promoter *pMYB60*. Pictures show confocal micrographs of two independent transgenic lines in the T2 generation. Bars indicate 10  $\mu$ m. Experiment was performed three times with similar results (n=3 independent experiments).

B. Transgenic plants expressing *pMYB60::FLS2-GFP* show only little ROS burst to flg22. elf18-induced ROS burst is like wild-type. In a luminol-based assay leaf discs of 5-week-old transgenic *A. thaliana* plants were imaged for 45 minutes by an ICCD photon-counting camera. Graph shows data from one representative experiment. Experiment was performed three times with similar results (n=3 independent experiments). Graph shows data from T3 plants.

that is expressed in all cell types. In plants that express FLS2 only in guard cells, the protein is much more diluted in the protein extractions as compared to the plants that express FLS2 in all cell types. As I could only observe a single band that runs higher than the wild-type FLS2 protein it appears that the GFP-tag is not cleaved, but that the whole fusion-protein accumulates in guard cells (Figure 4.6A). While all transgenic lines express FLS2-GFP, the protein accumulation between transgenics varies. The strongest expresser seems to be line 2-2, while 1-1 is the weakest expresser. Together with the results from the ROS assays, I conclude that the transgenic plants generated that express FLS2 only in guard cells are suitable for further experiments.

#### 4.2.3.3. flg22-triggered ROS production is strongly reduced in *fls2* and guard cell-specific expressers of FLS2

ROS production is an important early immune response and required for induction of stomatal closure. I therefore performed luminol-based ROS assays with our transgenic plants to evaluate their capacity to produce ROS in response to MAMPs. Wild-type Col-0 shows a strong ROS accumulation after flg22 and elf18 treatment, but to a lesser extent for the case of elf18. Mutants that lack FLS2 do not produce ROS in response to flg22 but show a wild-type-like response to elf18 treatment (Figure 4.5B). Transgenic plants expressing FLS2 in guard cells show low ROS production to flg22 trigger compared to wild-type plants. ROS production in response to elf18 is unaltered from the wild-type response. Figure 4.5B shows the ROS accumulation of the guard cell-specific expressers of FLS2 in detail, compared to the *fls2* knock-out mutants. While the response of the guard cell-specific FLS2 expressers is very low, a distinguishable peak can be observed at 10 minutes for lines 1-2 and 2-1. Since the complementation occurred only in guard cells, ROS production across the whole well from the whole leaf disc is not sufficient to be detected by this assay. This is in line with our observation that ABA-induced ROS production that occurs only in guard cells is almost undetectable in this assay in our hands. This demonstrates that the expression of FLS2 by the *pMYB60* promoter is specific enough to ensure that only guard cells produce ROS.

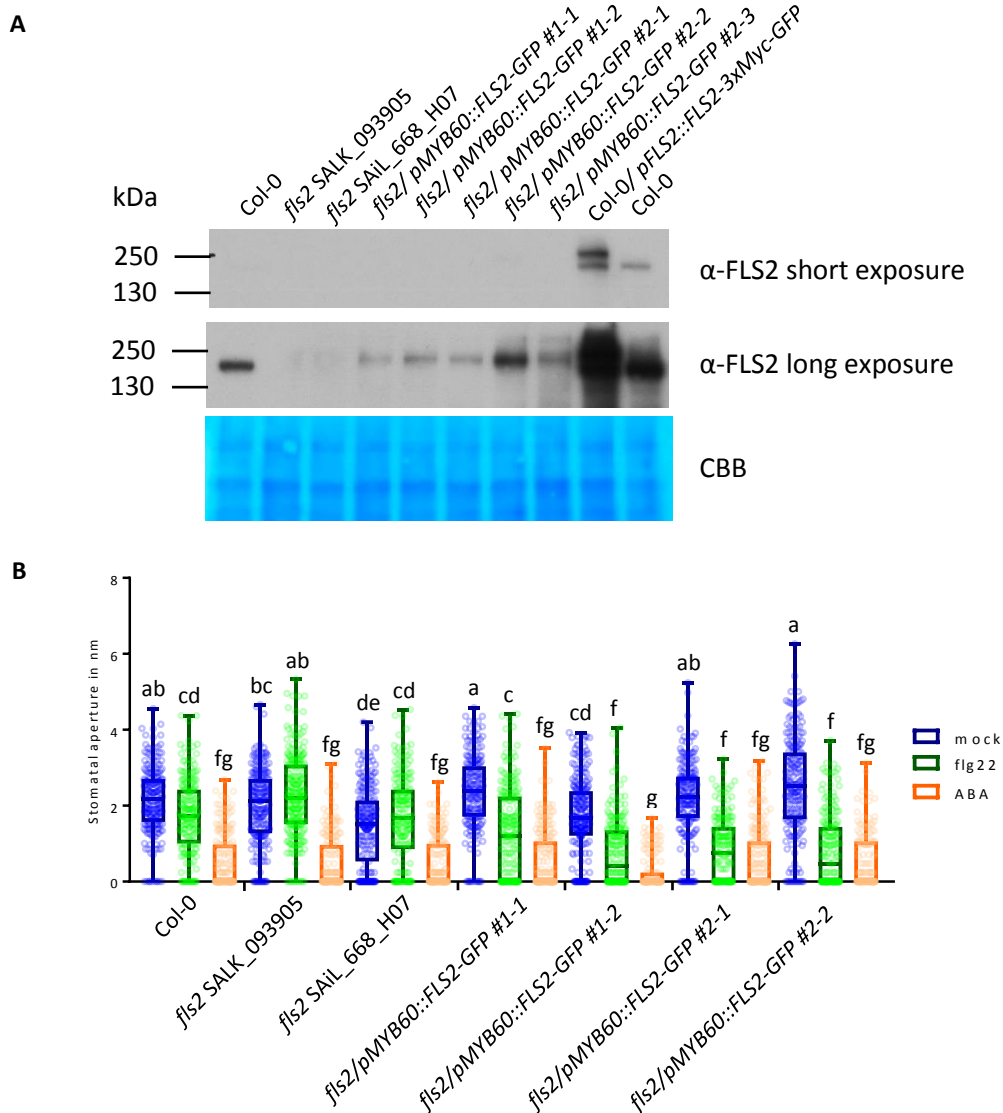


**Figure 4.6:** Guard cell-specific expression of FLS2 is sufficient to induce stomatal closure to flg22. A. Transgenic *fls2/pMYB60::FLS2-GFP* plants express fusion protein to different levels. Whole leaf protein extracts of five-week-old soil-grown *Arabidopsis thaliana* plants were blotted with the FLS2 antibody. CBB: Coomassie Brilliant Blue. Experiment was performed three times with similar results (n=3 independent experiments). Experiment was performed on plants in the T3 generation. B. MAMP-induced stomatal closure is enhanced in plants expressing FLS2 in guard cell-specific manner. Leaf discs from 5-week-old *Arabidopsis thaliana* plants were harvested in the morning and incubated for 2 hours in Stomata Opening Buffer in the light. After two hours MAMP or ABA treatment was applied to leaf discs. Two hours after treatment leaf discs were imaged and stomatal aperture was measured using ImageJ. Genotypes were hidden until after measurements to avoid unconscious bias. At least 150 stomata were measured per combination of genotype and treatment. Graph shows data from one representative experiment performed on plants in the T3 generation. Experiment was performed three times with similar results (n=3 independent experiments). Error bars indicate SD from mean. Letters indicate significance levels (two-way ANOVA followed by Tukey's test,  $p < 0.05$ ).

#### 4.2.3.4. MAMP recognition restricted to guard cells is sufficient to induce stomatal closure in response to flg22

The perception of MAMPs by cell-surface receptors leads to stomatal closure. To test whether this response can be autonomously induced by guard cells, I subjected plants that express FLS2 only in guard cells to MAMP treatment and evaluated their stomatal response. Wild-type Col-0 shows a significant reduction of stomatal aperture in response to flg22 and ABA treatment (Figure 4.6B). Plants lacking the *fls2* receptor do not close their stomata in response to flg22 but have a wild-type-like ABA closure response (Figure 4.6B). I therefore conclude that guard cell-specific perception of flg22 is sufficient for a full stomatal closure response to the MAMP.

#### 4.2.3.5. *pMYB60::FLS2-GFP* plants are not more susceptible to infection by *Pst* DC3000

To test whether expression of FLS2 in guard cells is sufficient for immunity to bacteria, I surface inoculated the transgenic plants with two strains of the bacterium *Pseudomonas syringae* pv. *tomato* (*Pst*) that is able to establish successful infection on *Arabidopsis thaliana*. I tested their response to the highly virulent *Pst* DC3000 strain and a strain of *Pst* DC3000<sup>cor-</sup> that lacks coronatine, which renders this strain less virulent (Mittal & Davis, 1995). Plants in the T3 generation were grown for five weeks on soil under short day conditions. Plants were watered and covered to induce opening of stomata a day prior to inoculation and bacteria were sprayed evenly on the abaxial and adaxial sides of leaves. Leaf tissue was harvested three days after inoculation. Leaf tissue was ground, diluted and spread on King's B plates containing appropriate antibiotics. Two days later colony forming units (cfu) were counted which correspond to the ability of the bacteria to gain access and proliferate in the leaf tissue. In spray inoculations both *fls2* knock-out strains are more susceptible to both strains of bacteria (Figure 4.7A and B). Plants expressing FLS2 in guard cells specifically are not hypersusceptible but show wild-type-like infection rates by *Pst* DC3000. This experiment was performed four times in total with similar results. Some guard cell-specific expressers of FLS2 were more susceptible than the wild-type to infection with *Pst* DC3000<sup>cor-</sup> (one-way ANOVA,  $p < 0.05$ ). The plants that were more susceptible than the wild-type are also the ones that showed the lowest accumulation of FLS2 (Figure 4.6A). This suggests that susceptibility to *Pst* DC3000<sup>cor-</sup> depends on the expression level of FLS2 in guard cells. When sufficient FLS2 is expressed in guard cells the induced FLS2 signalling response is enough to lead to wild-type-like susceptibility levels. I therefore conclude that guard cells can act autonomously to induce MAMP-mediated stomatal closure.

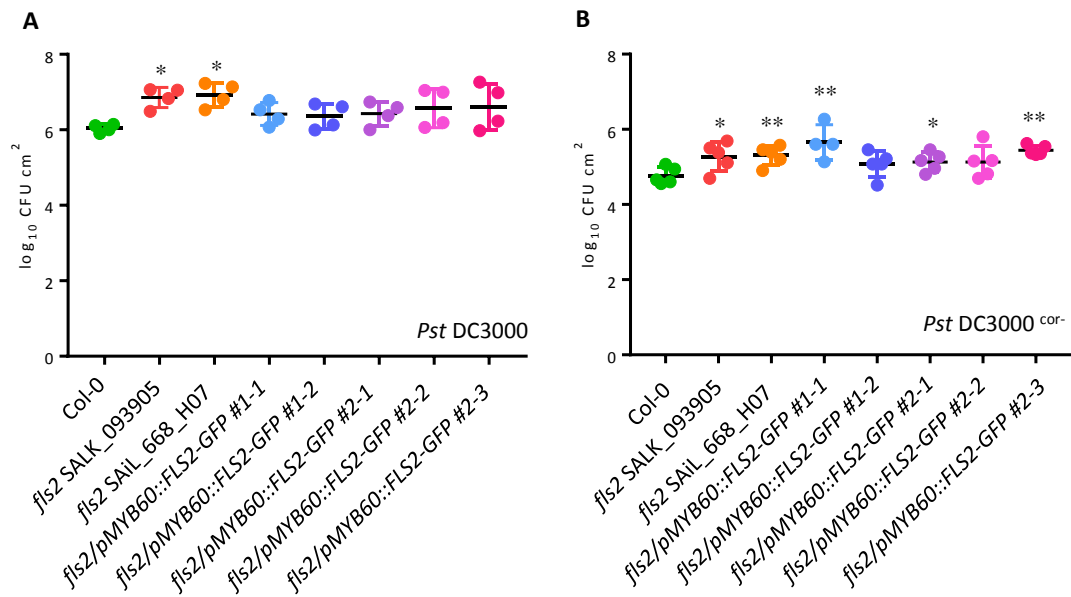


**Figure 4.7:** MAMP recognition that is restricted to guard cells is sufficient for resistance to bacteria. A. *pMYB60::FLS2-GFP* plants are as susceptible as wild-type to the virulent strain *Pst* DC3000. Both *fls2* knock-out mutants are significantly more susceptible than wild-type. Five-week-old plants were spray inoculated with *Pst* DC3000 at an OD<sub>600</sub>=0.2. Samples were ground 3 days after inoculation and colony forming units per square cm<sup>2</sup> determined. Graph shows data from four independent experiments. Six plants per genotype were sprayed and three leaf discs per plant harvested in each independent experiment. Error bars indicate SD from mean and asterisks indicate significant differences from wild-type (one-way ANOVA, \*p < 0.05). Infection assays were performed on plants in the T3 generation. B. Five-week-old plants were spray inoculated with *Pst* DC3000<sup>cor-</sup> at an OD<sub>600</sub>=0.2. Samples were ground 2 days after inoculation and colony forming units per square cm<sup>2</sup> determined. Graph shows data from three independent experiments. Six plants per genotype were sprayed and three leaf discs per plant harvested in each independent experiment. Error bars indicate SD from mean and asterisks indicate significant differences from wild-type (student's t-test, \*p < 0.05, \*\*p < 0.01). Infection assays were performed on plants in the T3 generation.

#### 4.2.4. Silencing of *NbRBOHB* and pavement cell complementation with *AtEFR* and *AtRBOHD* leads to restoration of the *elf18*-induced stomatal closure

I demonstrated by using transient and stable transgenic approaches that guard cells possess the ability to execute stomatal closure in response to MAMPs without input from surrounding pavement cells. However, this does not address the question of whether pavement cells have the ability to signal to guard cells and induce closure when guard cells cannot respond.

To address this question, I conducted a transient experiment in *N. benthamiana* in which only guard cells can not respond to a MAMP stimulus. To this end, I first silenced whole leaves by using the same silencing constructs as before but applying them at an earlier

developmental stage of the tissue. At this stage, guard cells are not yet differentiated and therefore still connected to the symplast, allowing the virus to silence all cells evenly. Leaves were then complemented by Agrobacterium-mediated transformation, which is unable to transform guard cells (unpublished). I silenced ROS production by infiltrating the leaves with the construct *TRV::NbRBOHB*. Two weeks later leaves were infiltrated with complementation constructs from *Arabidopsis thaliana* that are unaffected by the applied silencing construct. To introduce MAMP perception to elf18, I introduced EF-TU RECEPTOR (*AtEFR*) as it is not naturally present in *N. benthamiana* and to re-introduce ROS production I complemented with *AtRBOHD*.

As control plants, I used transgenic *N. benthamiana* plants expressing *p35S::EFR*, since wildtype *N. benthamiana* plants have no EFR receptor and are blind to elf18. Figure 4.8A shows elf18-induced ROS production in uninfiltrated and leaves infiltrated with silencing and complementation constructs. Upon elf18 treatment leaves from *p35S::EFR* shows strong ROS accumulation, whereas leaves silenced for *NbRBOHB* and complemented with either *AtRBOHD* or *AtEFR* have strongly reduced ROS production compared to wild-type. Leaves silenced for *NbRBOHD* and complemented with both *AtEFR* and *AtRBOHD* show stronger ROS accumulation than the plants complemented with only one component. This demonstrates that silencing of *NbRBOHB* was successful and that complementation of both *AtEFR* and *AtRBOHD* is necessary to see a ROS response to elf18. While this ROS response is significantly lower than the plant over-expressing EFR through the *p35S* promoter, it resembles the ROS response induced by flg22 in *N. benthamiana* (Figure 4.1A). I therefore conclude that complementation with RBOHD and EFR was successful in restoring the response leading to ROS accumulation to MAMPs. Leaf discs from the same plants were also subjected to stomatal closure assays, as described above. Control plants significantly closed their stomata to elf18 treatment (Figure 4.8B). Only the plants that were complemented with both EFR and RBOHD showed a stomatal response to elf18 and significantly reduced their aperture. Plants that had only one component complemented were either lacking the MAMP receptor, or the ROS-producing enzyme. This shows that *N. benthamiana* is, indeed, insensitive to elf18 and that ROS production is essential for the elf18-mediated stomatal closure response. As in this experiment guard cells were silenced and only pavement cells were complemented, I hereby demonstrate that non-autonomous signalling events occur during MAMP-triggered stomatal closure in *N. benthamiana*.

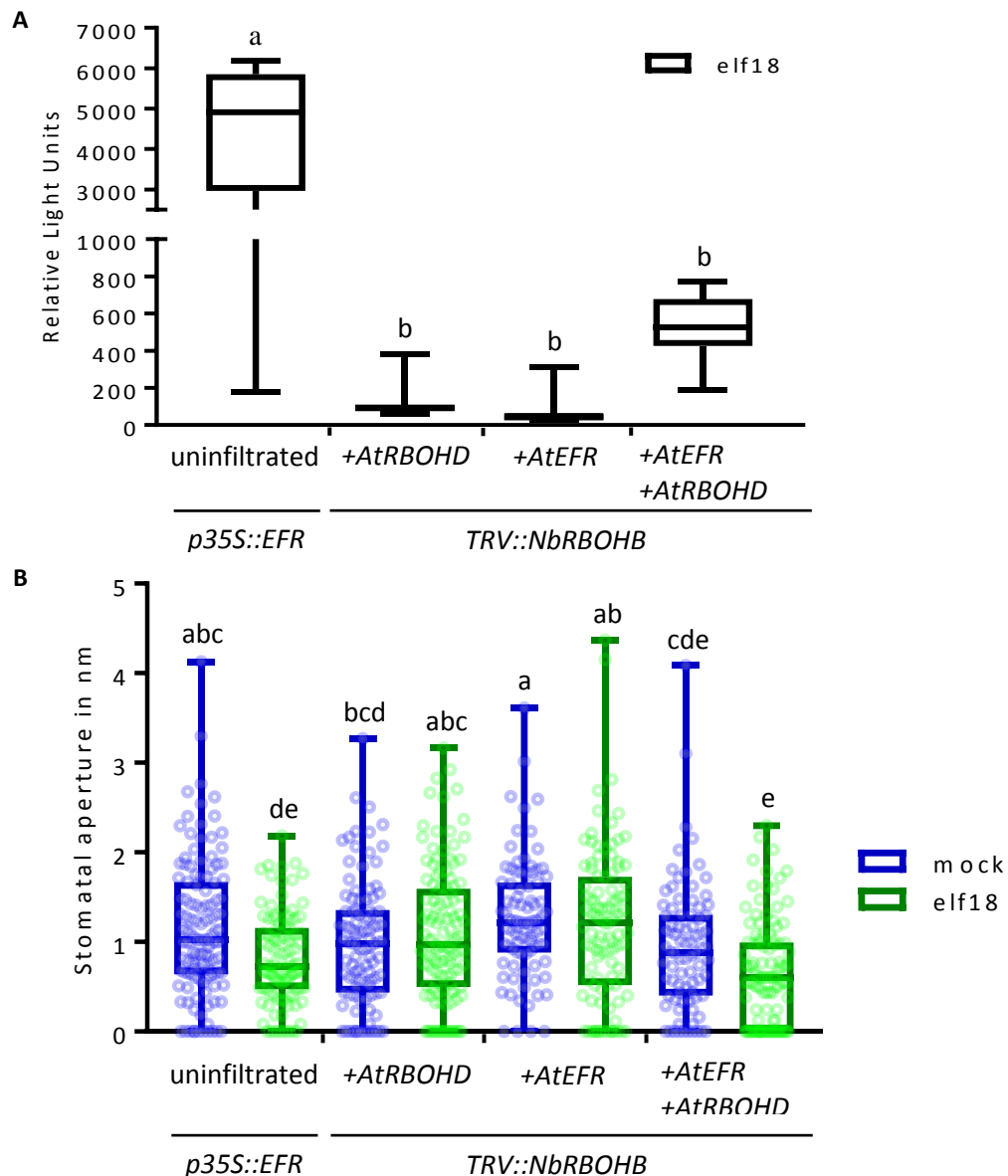


**Figure 4.8:** Stomatal closure does not require guard cell ROS production or signalling via EFR. A. Pavement cell complementation with *AtEFR* and *AtRBOHD* wild-type-like ROS response to elf18. Graph shows elf18-induced ROS burst on 24 leaves from 3 plants per treatment. Error bars indicate SD. Graph shows mean from one representative experiment. Experiment was performed twice with similar results (n=2 independent experiments). Letters indicate significance levels (one-way ANOVA,  $p < 0.01$ ). Bars indicate SD from mean. B. Pavement cell complementation of *EFR* and *RBOHD* is sufficient to induce stomatal closure in response to elf18. Graph shows elf18-induced stomatal closure on 3 leaves from 3 plants per treatment. Graph shows mean from one representative experiment. Experiment was performed twice with similar results (n=2 independent experiments). At least 60 stomata were measured per combination of genotype and treatment. Bars indicate SD from mean. Letters indicate significance levels (two-way ANOVA followed by Tukey's test,  $p < 0.05$ ). 2-week-old *N. benthamiana* plants were infiltrated with *TRV::NbrBOHB*. Two to three weeks later they were infiltrated with either *AtEFR* or *AtRBOHD* alone or together. Transgenic plants expressing *p35S::AtEFR* were used as control.

#### 4.2.5. Guard cell-specific knock-down with artificial micro-RNAs in *Arabidopsis thaliana*

##### 4.2.5.1. Generation of artificial micro RNAs (amiRNAs) against FLS2 and RBOHD

The transient assay indicated that pavement cells have the capacity to signal to guard cells. To test this in a stable transgenic plant I decided to express artificial micro-RNAs (amiRNAs) expressed under the control of the guard cell-specific promoter. I designed the amiRNAs with the Web MicroRNA Designer ([wmd3.weigelworld.org](http://wmd3.weigelworld.org)) choosing FLS2, RBOHD and RBOHF as targets of silencing. I chose three different sequences to silence FLS2, two to silence RBOHD and two to silence both RBOHD and RBOHF. I generated the amiRNAs following the instructions provided on the website and verified the sequences via sequencing. To evaluate the amiRNAs for their silencing capacity I expressed them under the constitutive *pUBQ10* promoter and screened the T2 plants for their ROS response to flg22 (this work was carried out in association with my internship student Sabine Engel). Figure 4.9A shows the ROS responses of all tested transgenic plants. Across all amiRNAs I obtained 144 pFAST-Red positive T1 plants. Each amiRNA construct was dipped twice independently and we included both transgenic events in the screen. Of each T1 parent I screened three T2 plants for their ROS accumulation. The ROS data from each transgenic event was combined to normalise for differential expression strengths across T1 individuals. This way I sought to get a true sense of silencing efficiency independent of the location of the transgene insertion. Col-0 wild-type showed strong accumulation of ROS following flg22 treatment. All three amiRNAs against FLS2 reduced a flg22-induced ROS accumulation strongly, while amiRNA-FLS2 (3) showed the least reduction and (1) and (2) were about the same. This demonstrates that overexpression of these amiRNAs leads to silencing of FLS2 and therefore a reduction in flg22 signalling outputs, such as ROS production. Unfortunately, neither of the tested amiRNAs targeting RBOHD, or both RBOHD and RBOHF, showed a strong reduction in ROS production in overexpressing transgenic plants. This suggests that silencing of RBOHD by the amiRNAs was not very efficient and I decided not to pursue these transgenic lines any further.

To validate the silencing efficiency of amiRNAs against FLS2, I repeated the experiments with those transgenic lines that showed a strongly reduced ROS signature in the first screen of both amiRNA-FLS2 (1) and (2). Wild-type Col-0 plants showed ROS production after flg22 and elf18 treatment while the *fls2c* null-mutant only produced ROS in response to elf18. The plants overexpressing amiRNAs against FLS2 all showed a wild-type-like ROS burst in response to elf18 treatment, demonstrating the specificity of the silencing amiRNAs. Indeed, in response to flg22 treatment all amiRNA-FLS2 over-expressing lines showed a reduced ROS

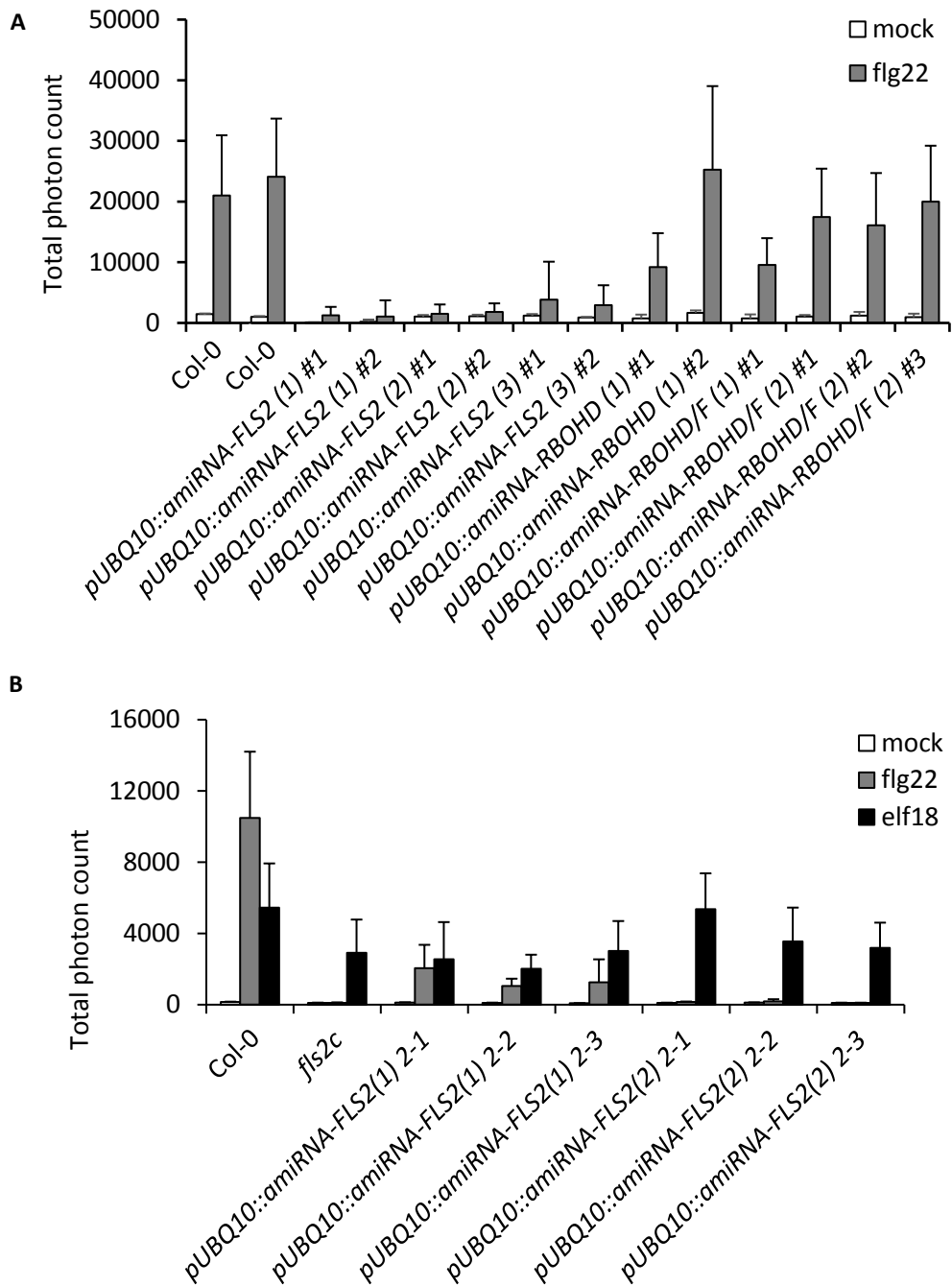


**Figure 4.9:** Characterisation of ROS response of transgenic plants expressing amiRNAs  
A. Plants expressing artificial micro-RNAs under the control of the constitutive pUBQ10 promoter show reduced ROS accumulation after flg22 treatment. Graph shows means pooled from two experiments from plants in the T2 generation in Col-0 background. Error bars indicate SD from mean. Experiment was performed once on at least 20 plants per genotype.  
B. Overexpression of amiRNAs targeting FLS2 leads to a strong reduction in ROS production after flg22 treatment, but not elf18 treatment. Graph shows mean from one independent experiment. Experiment was performed three times with similar results. Error bars indicate SD from mean.  
In a luminol-based assay leaf discs of 5-week-old transgenic *A. thaliana* plants were imaged for 45 minutes by an ICCD photon-counting camera. Leaves were harvested the evening before the experiment and left to rest in water over-night.

signature. While the transgenic plants overexpressing amiRNA-FLS2 (1) still showed a residual ROS response, transgenics overexpressing amiRNA-FLS2 (2) showed an almost undetectable ROS signature and strongly resemble the *fls2c* null-mutant (Figure 4.9B). I therefore conclude that amiRNA-FLS2 (2) has the highest silencing efficiency and leads to a strong reduction of FLS2-mediated signalling outputs.

#### 4.2.5.2. Guard cell-specific knock-down of FLS2 with the use of amiRNAs under the control of *pMYB60*

I generated plants expressing the amiRNAs under the control of the guard cell-specific promoter *pMYB60* to assess their stomatal response to MAMP treatment. These plants would have flg22-insensitive stomata which could not mount FLS2-mediated responses. Since I showed in Figure 4.9A that expression in whole plants strongly reduced the FLS2-mediated signalling outputs, expression in guard cells was predicted to reduce FLS2 accumulation only in the guard cells. To test whether this is indeed the case I performed crude and guard cell-enriched protein extractions from five-week-old soil-grown *Arabidopsis thaliana* plants of the T2 generation and probed them with the FLS2 antibody. Figure 4.10 shows crude and guard cell-enriched extractions side by side for each genotype. Wild-type Col-0 plants have almost equal amounts of FLS2 receptor in whole leaf extracts and guard cell-enrichments. The *fls2* null-mutant has no FLS2 and the over-expresser of amiRNA-FLS2 (2) shows very low amounts of the FLS2 protein in either extractions (Figure 4.10, top panel). The transgenic plants shown in Figure 4.10 were chosen for reduced FLS2 accumulation in guard cells but normal accumulation in crude extracts, demonstrating that expression of amiRNAs under the control of the *pMYB60* promoter indeed only silences FLS2 expression in guard cells. Protein amounts were normalised before blotting using the Bradford protein quantification assay. As in Figure 4.3 guard cell enrichments showed a weaker band corresponding to Rubisco in Coomassie Brilliant Blue Staining (Figure 4.10 lower panel) since guard cells have lower amounts of this protein. Just as can be seen in Figure 4.3 there is accumulation of an unknown protein between 25 and 35 kDa, presumably corresponding to a guard cell-specific protein. In summary, this result demonstrates that guard cell-specific silencing of FLS2, by expression of amiRNAs under a guard cell-specific promoter, was successful and these plants were therefore selected for further assays.

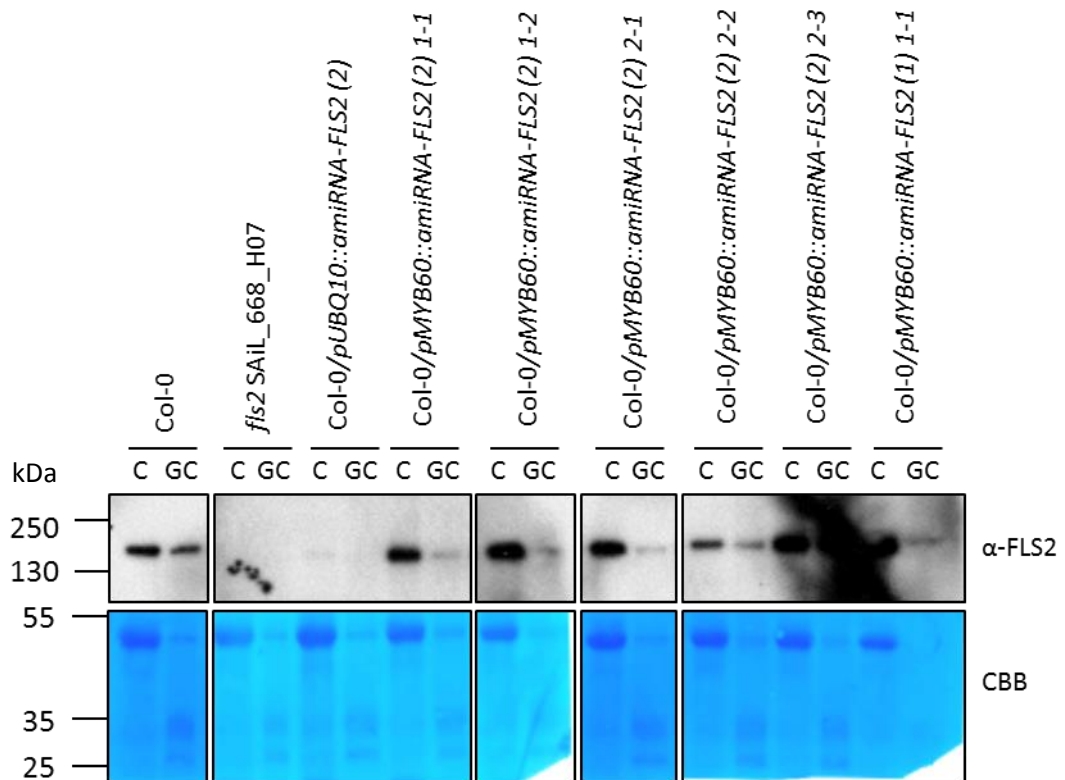


**Figure 4.10:** Artificial micro-RNAs reduce FLS2 protein accumulation in guard cells. *Col-0/pMYB60::amiRNA-FLS2* plants show reduced FLS2 accumulation in guard cells compared to whole leaf extracts. Whole leaves from five-week-old soil-grown *Arabidopsis thaliana* were used for crude extractions and 1g of leaf material from five T2 plants were used for guard cell enrichment. For guard cell enrichments leaves without central veins were blended for 60 seconds in a kitchen blender with 250 ml ultrapure water and crushed ice. Epidermal peels were collected through filtering and blending was repeated twice. Epidermal peels were snap frozen in liquid nitrogen and proteins were extracted as described in section 2.6.16. C: crude extract; GC: Guard cell enrichment; CBB: Coomassie Brilliant Blue.

#### 4.2.5.3. Guard cell-specific knock-down of FLS2 does not alter susceptibility to *Pst* DC3000

I subjected the transgenic amiRNA lines with reduced FLS2 accumulation in guard cells (Figure 4.10) to spray infection with a virulent bacterial strain *Pst* DC3000. Experimental conditions were the same as described in section 4.2.3.5. The knock-out mutant *fls2c* was more susceptible to infection with *Pst* DC3000 than wild-type Col-0 (Figure 4.11, one-way ANOVA,  $p < 0.05$ ). The overexpressing line *pUBQ10::amiRNA-FLS2* (2) also seems more susceptible in some, but not all replicates (three out of four). More experiments should be conducted to address whether the overexpressing line is more susceptible than wild-type under our experimental conditions. The transgenic lines expressing the amiRNAs targeting FLS2 in guard cells are as susceptible to *Pst* DC3000 infection as wild-type. Since FLS2 accumulation was strongly reduced in guard cells in these plants they were not able to initiate immune responses through FLS2. Nonetheless, their susceptibility phenotype does

not differ from wild-type plants. This suggests that other cell types are able to signal to guard cells and induce stomatal closure during infection.

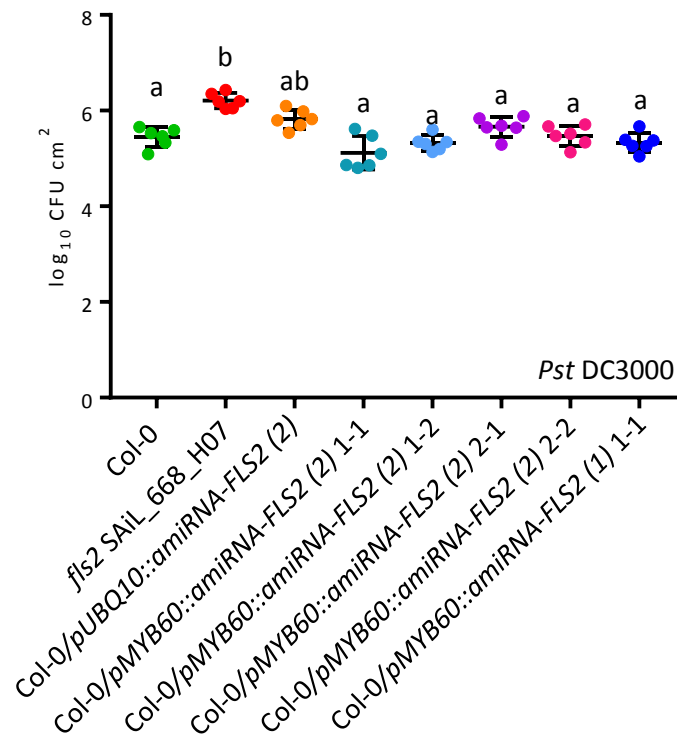


**Figure 4.11:** Guard cell-specific knock-down of FLS2 does not impair resistance to *Pst* DC3000. *pMYB60::amiRNA-FLS2* plants are as susceptible as wild-type to the virulent strain *Pst* DC3000. The *fls2* knock-out mutant is significantly more susceptible than wild-type. Five-week-old plants were spray inoculated with *Pst* DC3000 at an  $\text{OD}_{600}=0.2$ . Samples were ground 3 days after inoculation and colony forming units per square  $\text{cm}^2$  determined. Graph shows data from four independent experiments. Six plants per genotype were sprayed and three leaf discs per plant harvested in each independent experiment. Error bars indicate SD and letters indicate significance levels (one-way ANOVA,  $*p < 0.05$ ).

### 4.3. Discussion

Through a transient silencing approach and the use of a guard cell specific promoter I have demonstrated that MAMP-induced stomatal closure can be executed by guard cells in a cell-autonomous manner. The stomatal response in the transient assay in Figure 4.1 is not a full closure response to the same extent as the uninfiltated wild-type and the control-silencing plants show. As I did not quantify the silencing through qPCR and only used flg22-induced ROS accumulation as read-out. While the absence of ROS accumulation as seen in Figure 4.1A suggests that silencing was very efficient, it would be necessary to perform additional experiments to draw conclusions on the extent of the silencing in guard cells. I can therefore not exclude that some guard cells may not have been silenced, which could explain the

reduced closure response in Figure 4.1B. As this was a limitation of the transient approach I generated stable transgenic plants in *Arabidopsis thaliana* to draw more definitive conclusions. To assess whether guard cell ROS production is sufficient for the induction of stomatal closure in response to PAMPs I tried generating plants that express RBOHD only in guard cells. Unfortunately, it appeared that tagging of the protein was unsuccessful and was cleaved off (Figure 4.2 and 4.3). The GFP and mCherry signals in the confocal micrographs seemed to localise to the tonoplast and in the Western Blot I found free GFP in all transgenic plants and after both protein extraction methods. Furthermore, the protein abundance of GFP-RBOHD I was able to detect in the Western Blot was extremely low. A possible explanation is that the tagged protein might be degraded in the vacuole. This seems to be independent of the tag as I observed the tonoplast localisation with both GFP and mCherry tags. Although this protein has been tagged successfully before (Hao *et al.*, 2014), I used a different cloning method, that enables seamless tagging. It is possible that RBOHD requires a longer linker region. Complementation of the flg22 receptor FLS2 with a guard cell-specific promoter, however, proved sufficient to restore flg22-induced ROS burst (Figure 4.5B), flg22-induced stomatal closure (Figure 4.6B) and resistance to infection with bacterial pathogens (Figure 4.7). Although ROS production in guard cell-specific expressers of FLS2 was non-significant (Figure 4.5B), the ABA-induced ROS burst that only occurs in stomata is also not detectable in this assay in our hands (data not shown). However, that these plants showed a positive guard cell closure response to flg22 (Figure 4.6B) and ROS accumulation is required for stomatal closure suggests that guard cells are indeed producing ROS. The results of these two experiments taken together suggest that our promoter is not leaky, as we would have otherwise seen a much stronger ROS response. These results together show that the ability to respond autonomously is shared by the ABA and flg22 signalling pathways and even blue light-induced stomatal opening (Cañamero *et al.*, 2006; Bauer *et al.*, 2013). Although the perception of these stimuli differs dramatically from each other they all can be mediated by guard cells in an autonomous manner. This suggests that autonomy is a common feature of guard cells irrespective of the stimulus. I have furthermore shown that this is sufficient for resistance to a virulent bacterial strain *Pst* DC3000. This demonstrates that guard cell closure in response to MAMPs is an important component of the plant immune response. This is the first comprehensive study investigating bacterial immunity at the level of guard cells and adds significantly to our knowledge of stomatal immunity. Engineering of water use efficiency has already made use of a chimeric guard cell-specific stress-inducible promoter (Na & Metzger, 2014) or manipulating stomatal density (Caine *et al.*, 2018). The knowledge

that resistance to certain bacterial pathogens can be mediated by guard cells autonomously, may lead to novel engineering approaches of disease control.

In addition to demonstrating cell-autonomy I have shown by a transient expression in *N. benthamiana* that pavement cells have the capacity to initiate stomatal closure when guard cells cannot respond. The transgenic *Arabidopsis thaliana* plants expressing amiRNAs to reduce FLS2 accumulation in guard cells also support this observation. The Western Blot shown in Figure 4.10 shows that these transgenic plants indeed show a lower accumulation of FLS2 in guard cells than wild-type plants. Nevertheless, these plants showed unaltered susceptibility levels to bacterial infection, suggesting that pavement cells can influence stomatal aperture during infection. Since the experiments were performed in T2 not all plants in this infection assay would be homozygous, which explains why my transgenic plant overexpressing the amiRNA targeting FLS2 under the control of the constitutive promoter is not significantly more susceptible. This experiment should be repeated in the T3 generation. As the stomatal response in the transient assay in *N. benthamiana* was dependent on ROS production through *NbRBOHB* in *N. benthamiana*, I hypothesise that apoplastic ROS production can be sensed and serve as a local signal to guard cells. The ROS from neighbouring cells could be transported into the guard cells by aquaporins as suggested previously (Rodrigues *et al.*, 2017). Alternatively, cysteine-rich kinases (CRKs) that have been shown to be important for stomatal closure, in response to flg22, could act as ROS sensors (Bourdais *et al.*, 2015). Some CRKs are expressed to a higher extent in guard cells than pavement cells and show a normal ROS response, but do not close their stomata in response to flg22.

Taken together, my data show that there are both autonomous and non-autonomous signalling events involved in MAMP-induced stomatal closure. This is the first study to demonstrate that epidermal cells have the capacity to influence stomatal aperture, adding an important new layer to our understanding of the regulation of stomatal closure.

## 5. MAMP-induced stomatal closure is mediated by SnRK2.3 and is independent of ABA biosynthesis

### 5.1. Introduction

As sessile organisms, plants have a particularly demanding job in adapting to a changing environment. Due to their nature plants are sophisticated organisms that have acquired a vast array of mechanisms to actively adapt and thrive. For efficient photosynthesis under such challenging conditions, plants are required to control water loss and gas exchange tightly. This happens via leaf pores called stomata at the leaf surface that are actively regulated by the plant following different stimuli. But they are also major entry sites for certain pathogens such as bacteria and rust fungi who exploit natural openings to gain access into plant tissues. Bacteria invade through hydathodes, wounds and stomata. Plants try to counteract such invasion by closing their stomata upon recognition of a pathogen and this can alter the outcome of infection to the disadvantage of a pathogen (Melotto *et al.*, 2006). Perception of an invading pathogen at the cell-surface level is mediated by Pattern-Recognition Receptors (PRRs). Important PRRs recognising bacterial epitopes are FLAGELLIN-SENSING 2 (FLS2) and EF-Tu RECEPTOR (EFR), with FLS2 being the major receptor for resistance against *Pseudomonas syringae* pv. *tomato* DC3000 (Zipfel *et al.*, 2004). Upon ligand perception, PRRs associate with their co-receptor BRI1-associated kinase 1 (BAK1) and together phosphorylate the receptor-like cytoplasmic kinase Botrytis-induced kinase 1 (BIK1) and its close homolog PBS1-like 1 (PBL1). BIK1 and PBL1 are two highly homologous receptor-like cytoplasmic kinases (RLCKs). They associate with the inactive FLS2 receptor and other PRRs and become phosphorylated upon flg22 perception (Lu, Dongping *et al.*, 2010; Zhang, Jie *et al.*, 2010). They phosphorylate the respiratory burst oxidase homolog H (RBOHD), which induces apoplastic ROS production and this is required to induce stomatal closure. In addition to BIK1, PBL1 and RBOHD flg22-induced stomatal closure also requires ROS production through RBOHF, as only the double *rbohD rbohF* mutant is completely impaired in stomatal closure. The anion channels SLOW ANION CHANNEL-ASSOCIATED 1 (SLAC1) and SLAC1 HOMOLOGUE 3 (SLAH3) are required for MAMP-induced stomatal closure and it has been proposed that OST1 phosphorylates and thereby activates them following MAMP perception (Deger *et al.*, 2015). However, this and a link between perception of the ligand and the plasma membrane, has yet to be demonstrated.

The ABA or drought-induced stomatal closure pathway is very well understood (Figure 1.5) and offers a potential for engineering plants for areas where water is scarce or infrequent. Upon water limiting conditions plants produce the hormone ABA that is perceived by receptors of the PYR-family (Nishimura *et al.*, 2009; Park *et al.*, 2009). ABA binds to the receptor resulting in conformational changes that enables the receptors to bind and inhibit the activity of PP2C phosphatases that negatively regulate kinases such as OST1. One of these negative regulators is the PP2C phosphatase ABI1 that was identified together with ABI2, HAB1 and PP2A. Identification of the *abi1-1* mutant which has an amino acid exchange from Gly<sup>180</sup> to Asp which results in it being constitutively active (Leung *et al.*, 1994), has been a major step in understanding OST1 regulation. ABI1 was further characterised as a PP2C with an EF-hand domain and a calcium-binding site (Allen *et al.*, 1999) that dephosphorylates Ser<sup>175</sup> in the activation loop of OST1 and thereby regulates its activity (Vlad *et al.*, 2009). Without the negative regulation, OST1 autophosphorylates and phosphorylates its downstream targets which include SLAC1, RBOHF and ABA-responsive transcription factors (Furihata *et al.*, 2006; Geiger *et al.*, 2009; Sirichandra *et al.*, 2009). Even though OST1 is strongly activated upon ABA treatment (Belin *et al.*, 2006) the expression level seems to be unaffected by ABA (Mustilli *et al.*, 2002).

OST1 is a member of the family of sucrose non-fermenting 1-related kinases (SnRKs) which are serine/threonine kinases. There are 38 SnRKs in *Arabidopsis thaliana* and they can be divided into clades taking into account their sequence and domain similarities: SnRK1 to 3 (Hrabak *et al.*, 2003). SnRK1 kinases are the most similar to the yeast kinases whereas SnRK2 and 3 seem to be plant specific (Halford & Hardie, 1998). Clade 2 SnRKs are important for the transduction of abiotic stress signals through ABA mediated signalling pathways and in particular stomatal closure. OST1 or SnRK2.6 is one of ten SnRK2s in *Arabidopsis thaliana* (Hrabak *et al.*, 2003). OST1 is expressed in guard cells and the vasculature and is therefore an example of a protein whose expression pattern correlates with its specific function (Mustilli *et al.*, 2002). OST1 has been shown to be involved in abiotic stress-induced stomatal closure, such as ABA-induced stomatal closure in response to drought (Mustilli *et al.*, 2002) and osmotic stress-induced closure, independently of ABA-signalling (Yoshida *et al.*, 2002; Yoshida *et al.*, 2006). The mutant allele *ost1-2* was characterised in a screen for mutants with a reduced leaf temperature due to impaired ability to close stomata in response to drought stress. The *ost1-2* mutation is a point mutation in the ATP-binding pocket that renders the protein inactive and the guard cells insensitive to ABA (Belin *et al.*, 2006). OST1 is one of three closely related cytoplasmic kinases. Its homologs are SnRK2.2 and SnRK2.3 and they

are also strongly activated after ABA treatment (Boudsocq *et al.*, 2004) and required for ABA responses in seeds and roots (Fujii *et al.*, 2007). They are expressed in all plant tissues and not just restricted to the guard cells (Fujii *et al.*, 2007) but are required for the transcriptional memory in guard cells during repetitive dehydration stress requires SnRK2.2 and 2.3 independently of OST1 (Virlovet & Fromm, 2015).

Recently it emerged that some central regulators are shared between ABA, CO<sub>2</sub>- and ozone-induced stomatal closure (Merilo *et al.*, 2013; Chater *et al.*, 2015). It was shown that ABA biosynthesis, ABA receptors and OST1 are necessary for stomatal closure in response to elevated CO<sub>2</sub> concentrations, ozone and reduction of air humidity. OST1 was shown to also play a role in flg22-induced stomatal closure (Melotto *et al.*, 2006) and OST1 was subsequently proposed as general convergence point of stomatal closure pathways. Moreover, the *aba2* ABA biosynthesis mutant was shown to be impaired in flg22-induced stomatal closure (Melotto *et al.*, 2006). However, this has also been disputed by Montillet and colleagues (Montillet *et al.*, 2013) who found that while the overall aperture size differs between *aba2* and wild-type its stomata still close to flg22 treatment.

The involvement of OST1 in flg22-induced stomatal closure has been under debate as contradictory results have been reported. While Melotto and colleagues found that the *ost1-2* mutant does not close stomata in response to flg22 treatment and is more susceptible to *Pst* DC3000<sup>cor</sup> spray infection than wild-type, Montillet and colleagues found that it shows a concentration-dependent phenotype and responds like wild-type to higher flg22 concentrations. They furthermore show that OST1 kinase activity is strongly activated after ABA treatment, and it remains inactive after flg22 treatment, raising questions about the involvement of OST1 in the flg22-induced stomatal closure pathway (Melotto *et al.*, 2006; Montillet *et al.*, 2013).

Here I show that OST1 is not necessary for MAMP-induced stomatal closure. I demonstrate that *ost1* knock-out mutants are responsive to flg22 and no activation of the kinase is detectable after MAMP treatment. The *snrk2.2 snrk2.3 ost1-3* triple mutant as well as the *snrk2.3* single mutant are insensitive to flg22 treatment in stomatal aperture assays. Furthermore, I show that this response is independent from ABA biosynthesis because all our tested mutants respond to flg22 treatment as the wild-type. The PP2C phosphatases that mediate ABA-induced stomatal closure do not seem to play a role in MAMP-induced stomatal closure as the dominant *abi1-1* mutant has a wild-type-like stomatal closure response to flg22 treatment. I show that BIK1 interacts with SnRK2.3 in both split-YFP and

co-immunoprecipitation assays. However, I could not detect transphosphorylation of BIK1 or PBL1 to SnRK2.3, or vice versa. In oocyte measurements our collaborators demonstrated that PBL1 strongly activates SLAH3 but not SLAC1. I therefore hypothesise that there are two pathways acting additively to induce stomatal closure in response to MAMPs: SLAH3 activation through RLCKs and a SnRK-dependent pathway.

## 5.2. Results

### 5.2.1. MAMP-induced stomatal closure acts independent of the ABA stomatal closure pathway

#### 5.2.1.1. ABA biosynthesis is not required for stomatal closure in response to flg22

The ABA biosynthesis pathway has been very well characterised and other stimuli, such as CO<sub>2</sub> and ozone make use of the same core signalling components. As there has been debate over the extent of overlap between the ABA and flg22 stomatal closure pathway, I decided to test mutants for central components of the ABA stomatal closure pathway. As ABA biosynthesis is required for both guard cell responses to drought and elevated CO<sub>2</sub>-concentrations I tested ABA biosynthesis mutants for their stomatal response to flg22. *Arabidopsis thaliana* plants were grown for five weeks in soil under short-day conditions. I harvested leaf discs into Stomata Opening Buffer to induce opening of all stomata. Two hours later I applied either MAMP, ABA or H<sub>2</sub>O<sub>2</sub> and measured stomata two hours after treatment was applied. Stomatal apertures were measured using ImageJ. I tested the *aba1* and *aba3* biosynthesis mutants that have been shown to have 17% and 10% of wild-type ABA levels, respectively (Koornneef *et al.*, 1982; Leon-Kloosterziel *et al.*, 1996). Col-0 ecotype was used as wild-type control throughout all experiments. As shown in Figure 5.1A Col-0 closes its stomata in response to flg22 and even stronger in response to ABA treatment (two-way ANOVA following Tukey's test,  $p < 0.05$ ). Both *aba1* (Figure 5.1B) and *aba3* (Figure 5.1A) respond to flg22 and ABA with a significant closure response. It has been reported that the *aba2-1* mutant retained the ability to respond to flg22 (Montillet *et al.*, 2013) so I decided to test the *aba2-3* mutant for its response to ABA and flg22. In accordance with the published results I found that also the *aba2-3* mutant responds to flg22 and ABA in a wild-type like manner. Since all three mutants have a residual amount of ABA left, I decided to test the *nced3-2 nced5-2* mutant. This double mutant lacks two guard cell-expressed isoforms of 9-cis-epox-y-carotenoid dioxygenase that catalyses the first committed step in ABA biosynthesis

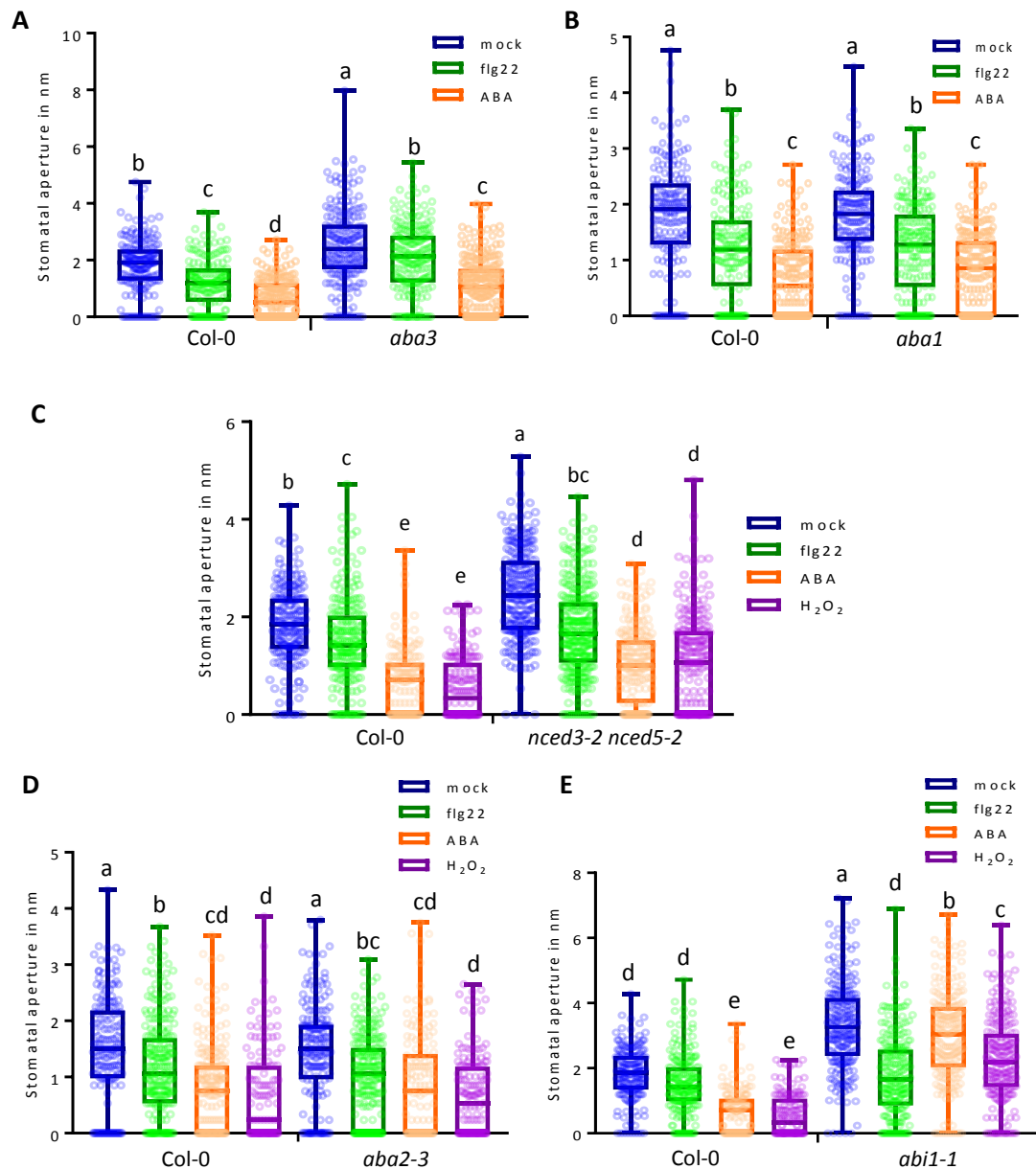


**Figure 5.1:** MAMP-induced stomatal closure can be induced independently from ABA signalling.

A. The *aba3* single mutant responds to flg22 and ABA like wild-type. Graph shows data from one experiment (n=1 independent experiment). B. The *aba1* single mutants closes its stomata to flg22 and ABA like wild-type. Graph shows data from one representative experiment. Experiment was performed twice with similar results (n=2). C. The *nced3-2 nced5-2* double mutant responds to flg22, ABA and H<sub>2</sub>O<sub>2</sub> in a wild-type-like manner. Graph shows data from one representative experiment. Experiment was performed four times with similar results (n=4). D. The *aba2-3* single mutants closes its stomata to flg22 and ABA like wild-type. Graph shows data from one representative experiment. Experiment was performed four times with similar results (n=4). E. The dominant *abi1-1* allele closes its stomata to flg22 and H<sub>2</sub>O<sub>2</sub> but not ABA treatment. Graph shows data from one experiment (n=1 independent experiment).

Leaf discs from 5-week-old *Arabidopsis thaliana* plants were harvested in the morning and incubated for 2 hours in Stomata Opening Buffer in the light. After two hours MAMP or ABA treatment was applied to leaf discs. Two hours after treatment leaf discs were imaged and stomatal aperture was measured using ImageJ. Genotypes were hidden to avoid unconscious bias. At least 150 stomata were measured for each combination of genotype and treatment. Error bars indicate SD from mean. Letters indicate significance levels (two-way ANOVA followed by Tukey's test, p < 0.05).

(Frey, A *et al.*, 2012; Bauer *et al.*, 2013). In accordance with the other ABA biosynthesis mutants the *nced3-2 nced5-2* closes its stomata in response to flg22, ABA and H<sub>2</sub>O<sub>2</sub>. Taken together these data suggest that ABA biosynthesis is not required for MAMP-induced stomatal closure.

#### 5.2.1.2. ABA receptor mutants do not have a clear flg22 stomatal closure phenotype

I showed that ABA biosynthesis is not required for flg22-induced stomatal closure, but I was also interested to see whether other components of the ABA core pathway could be involved. I therefore tested ABA receptor triple and quadruple mutants *pyr1 pyl1 pyl2* and *pyr1 pyl1 pyl2 pyl4* that previously have been shown to be unresponsive to elevated CO<sub>2</sub> concentrations (Chater *et al.*, 2015). However, these mutants did not show a consistent response to flg22 treatment (Figure 5.2A and B), as in three replicates they responded to flg22 treatment and in three replicates they failed to close their stomata in response to flg22. The triple mutant responds to ABA treatment in a wild-type-like manner while the *pyr1 pyl1 pyl2 pyl4* mutant has a reduced stomatal closure response to ABA treatment in accordance with published results. I therefore decided to acquire higher-order mutants and requested the quintuple and sextuple mutants *pyl1 pyl2 pyl5 pyl4* and *pyr1 pyl1 pyl2 pyl5 pyl8*. In these experiments, I included both a wild-type and a FLS2 receptor null-mutant control that does not respond to flg22 treatment. The wild-type closes stomata in response to flg22 and ABA treatment while the *fls2c* mutant does not close its stomata following flg22 treatment but is only responsive to ABA. Unfortunately, I was also unable to obtain a robust response from these higher order ABA receptor mutants. While the quintuple mutant closed its stomata to flg22 treatment in three replicates (Figure 5.2C and 2D) the sextuple mutant did not respond in two replicates out of four performed. Since the negative control *fls2c* closed its stomata in response to flg22 ( $p < 0.05$ ) in three out of four replicates with the sextuple mutant, more replicates need to be performed to come to a definitive conclusion about the involvement of ABA receptors in flg22-induced stomatal closure.

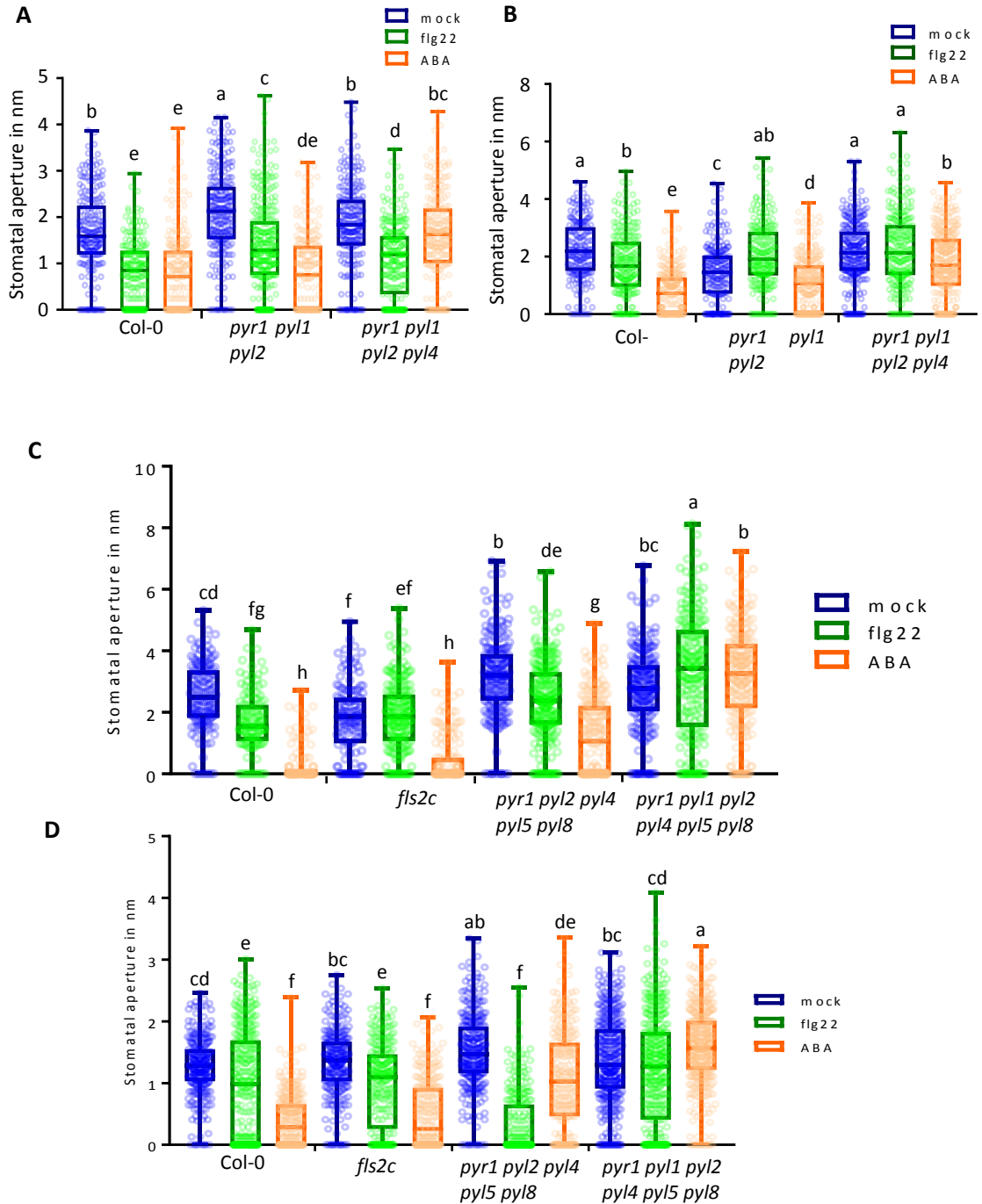


**Figure 5.2:** ABA receptor mutants do not give consistent stomatal closure phenotypes.

A. ABA receptor triple and quadruple mutants close their stomata in response to flg22 treatment. Graph shows data from one representative experiment (n=3 independent experiments). B. ABA receptor triple and quadruple mutants do not close their stomata to flg22 treatment. Graphs show data from one representative experiment (n=3 independent experiments). C. & D. ABA receptor quintuple mutant is responsive to flg22 in stomatal closure assay whereas the sextuple mutant is not. Graphs show data from one representative experiment (n=2 independent experiments). Leaf discs from 5-week-old *Arabidopsis thaliana* plants were harvested in the morning and incubated for 2 hours in Stomata Opening Buffer in the light. After two hours MAMP or ABA treatment was applied to leaf discs. Two hours after treatment leaf discs were imaged and stomatal aperture was measured using ImageJ. Genotypes were hidden to avoid unconscious bias. At least 150 stomata were measured for each combination of genotype and treatment. Error bars indicate SD from mean. Letters indicate significance levels (two-way ANOVA followed by Tukey's test,  $p < 0.05$ ).

#### 5.2.1.3. The dominant *abi1-1* mutant closes its stomata to flg22 treatment

PP2C phosphatases play an important regulatory role in ABA-induced stomatal closure. It has been proposed that they are not involved in MAMP-induced stomatal closure as the dominant mutant *abi1-1* can still close its stomata in response to flg22 (Deger *et al.*, 2015). I wanted to confirm this result under my own conditions. The *abi1-1* mutant has a point mutation that makes the protein unable to interact with ABA receptors and therefore constitutively active (Leung *et al.*, 1994). Under my experimental conditions, Col-0 wild-type shows significant stomatal closure to flg22, ABA and H<sub>2</sub>O<sub>2</sub> treatment and the *abi1-1* did not respond to ABA treatment but closed in a wild-type-like manner to flg22 and H<sub>2</sub>O<sub>2</sub> treatment (Figure 5.1E). I therefore conclude that MAMP-induced stomatal closure does not require the PP2C phosphatases of the ABA stomatal pathway.

#### 5.2.1.4. *ost1-3* and *ost1-4* knock-out mutants respond to flg22

PP2C phosphatases negatively regulate OST1 in the absence of an ABA trigger. OST1 is a central component of stomatal closure pathways and has been proposed to also be involved in MAMP-induced stomatal closure. Studies implicating OST1 in MAMP-induced stomatal closure have mostly used the *ost1-2* point-mutant. To unmask any phenotypes the inactive OST1-2 protein might conceal, I decided to test knock-out mutants for their stomatal response to MAMP treatment. I therefore subjected *ost1-3* and *ost1-4* knock-out mutants to stomatal closure assays. Figure 5.3A shows that Col-0 wild-type closes its stomata in response to both flg22 and ABA treatment and that the *ost1-3* and *ost1-4* mutant alleles largely respond to our tested flg22 concentration but not to ABA treatments ( $p < 0.05$ ). This suggests that the kinase-inactive OST1-2 protein has a dominant-negative effect on the MAMP-triggered stomatal closure in accordance with the concentration-dependency shown by Montillet and colleagues (Montillet *et al.*, 2013).

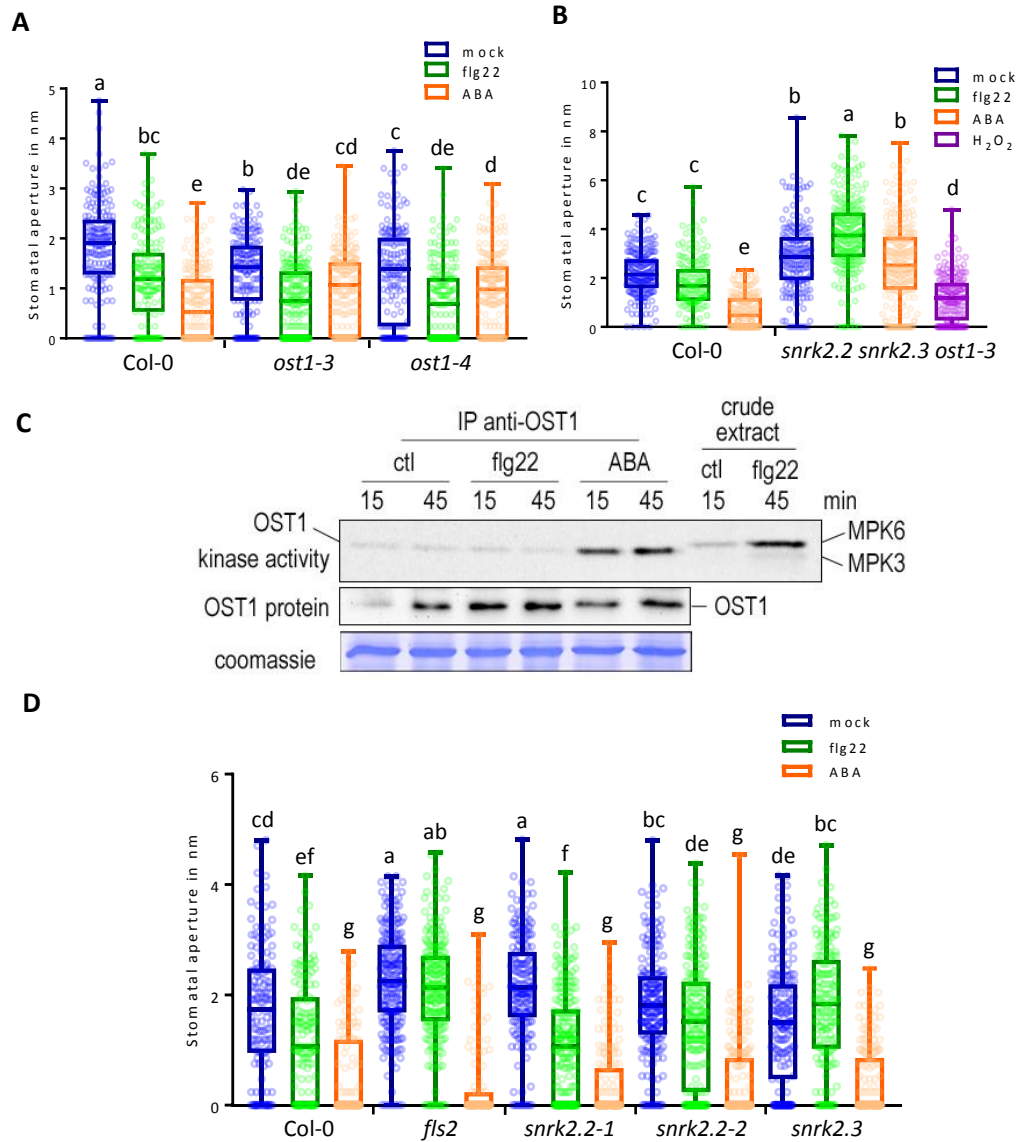


**Figure 5.3:** MAMP-induced stomatal closure is mediated by SnRK2.3.

A. Single *ost1* knock-out mutants can respond to flg22 but are impaired in ABA-induced stomatal closure. Graph shows data from one representative experiment (n=3 independent experiments). B. Stomata of triple mutant *snrk2.2 snrk2.3 snrk2.6* do not close after 2 hours of flg22 treatment. Graph shows data from one representative experiment (n=1 independent experiment). C. OST1 kinase assay performed by Dr. Marie Boudsocq. OST1 kinase is strongly activated after ABA treatment but inactive after flg22 treatment. OST1 from whole leaf samples was immunoprecipitated with the anti-OST1 antibody. To ensure flg22 treatment was successful MAP-Kinase activation was used as control. D. *snrk2.3* is required for flg22-induced stomatal closure. Graph shows data from one representative experiment (n=2 independent experiments). A., B. and D. Leaf discs from 5-week-old *Arabidopsis thaliana* plants were harvested in the morning and incubated for 2 hours in Stomata Opening Buffer in the light. After two hours MAMP or ABA treatment was applied to leaf discs. Two hours after treatment leaf discs were imaged and stomatal aperture was measured using ImageJ. At least 150 stomata were measured for each combination of genotype and treatment. Error bars indicate SD from mean. Letters indicate significance levels (two-way ANOVA followed by Tukey's test,  $p < 0.05$ ).

#### 5.2.1.5. OST1 kinase is not active after flg22 treatment

Together with the *ost1-2* mutant showing a concentration-dependent response, it was shown that OST1 kinase is not active after flg22 treatment (Montillet *et al.*, 2013). However, it is strongly activated after ABA treatment (Belin *et al.*, 2006), casting further doubt on its involvement. To shed light on this controversy our collaborator Dr. Marie Boudsocq (Institute of Plant Sciences Paris-Saclay) performed kinase assays on purified untagged OST1 proteins with the anti-OST1 antibody from *Arabidopsis thaliana* leaf tissues treated with a high concentration of flg22. Figure 5.3C confirms the published result, namely that OST1 can be found to be strongly activated after ABA treatment but inactive after flg22 treatment (Montillet *et al.*, 2013). MAP-Kinases were simultaneously isolated and can be seen to have been activated by the flg22 treatment, demonstrating that MAMP treatment was effective. This suggests OST1 might not be actively involved in the MAMP-induced stomatal closure pathway.

#### 5.2.1.6. *snrk2.2 snrk2.3 ost1-3* is unresponsive to flg22 treatment but can respond to H<sub>2</sub>O<sub>2</sub> treatment

OST1 is one of three closely related cytoplasmic SnRKs. As I have shown that OST1 is not required for stomatal closure in response to flg22 I wanted to assess whether other related SnRKs might act in the flg22 stomatal closure pathway. I tested the *snrk2.2 snrk2.3 ost1-3* triple mutant response to flg22, ABA and H<sub>2</sub>O<sub>2</sub>. Col-0 wild-type closes its stomata in response to flg22, ABA and H<sub>2</sub>O<sub>2</sub> ( $p < 0.05$ ). The triple mutant *snrk2.2 snrk2.3 ost1-3* is insensitive to ABA and flg22 treatment but can respond in a wild-type-like manner to H<sub>2</sub>O<sub>2</sub> treatment (Figure 5.3B). This shows that the triple mutant is not generally impaired in stomatal closure but is specifically impaired in its response to ABA and flg22 treatment. I therefore conclude that SnRKs are required for MAMP-induced stomatal closure.

#### 5.2.1.7. SnRK2.3 is required for MAMP-induced stomatal closure

As I concluded that SnRKs are required for flg22-induced stomatal closure because the *snrk2.2 snrk2.3 ost1-3* triple mutant guard cells were irresponsive to MAMP treatment. I therefore aimed to investigate which of the three SnRKs could be involved in this response. I furthermore ruled out the involvement of OST1, so I tested single mutants of the closely related homologs SnRK2.2 and SnRK2.3. Figure 5.3D shows that both *snrk2.2* mutants respond to flg22 in a wild-type-like manner, but *snrk2.3* does not respond. Taken together

with the results that *ost1-3* and *ost1-4* close their stomata to flg22, but not ABA, I conclude that SnRK2.3 and not OST is required for MAMP-induced stomatal closure.

## 5.2.2. SnRK2.3 interacts with BIK1

### 5.2.2.1. OST1 and SnRK2.3 interact with FLS2, BIK1 and ABI1 in split-YFP assay

SnRK2.3 is required for MAMP-induced stomatal closure, but it is not yet known how the signal is transduced from the cell surface to SnRK2.3 and potential downstream targets. It is known that OST1 interacts with and is phosphorylated by BAK1 (Shang *et al.*, 2016). I therefore wanted to check whether SnRK2.3 also associates with BAK1. I generated split-YFP constructs to test for possible interactions of SnRKs with each other and known components of the larger receptor complex. All constructs were generated in the same vector backbone with the same *p35S* promoter and corresponding N- or C-terminal parts of YFP. All constructs were infiltrated into fully expanded leaves of four to five-week-old *N. benthamiana* plants mixed together at the final OD<sub>600</sub> = 0.1. FLS2 interacts with BIK1 but not BAK1 prior to flg22 treatment in accordance with published results. YFP was reconstituted in all tested combinations with OST1, confirming its known interactions with BAK1 and ABI1 and implicating FLS2 and BIK1 as novel possible interactors. It has been shown that the closely related SnRK kinases form heterocomplexes with each other (Waadt *et al.*, 2015). I therefore tested whether OST1 and SnRK2.3 can interact with each other in split-YFP assays and I could detect YFP re-constitution, confirming the published interactions (Figure 5.4 and 5.5 (Waadt *et al.*, 2015)). SnRK2.3 furthermore interacts with FLS2, BAK1, BIK1, ABI1 and SnRK2.2 in the split-YFP assay in *N. benthamiana* (Figure 5.5). These results have to be considered cautiously because the split-YFP has affinity to re-constitute in a non-reversible manner, since the re-constituted YFP cannot dissociate again. Many of the tested proteins have been shown to interact with one another which makes it likely that they are in close proximity to each other through interaction with another protein and this could lead to false positive results. From the results acquired from the split-YFP assay, I speculate that one or several members of the receptor complex directly interact with and phosphorylate SnRK2.3 to induce stomatal closure upon flg22 perception.

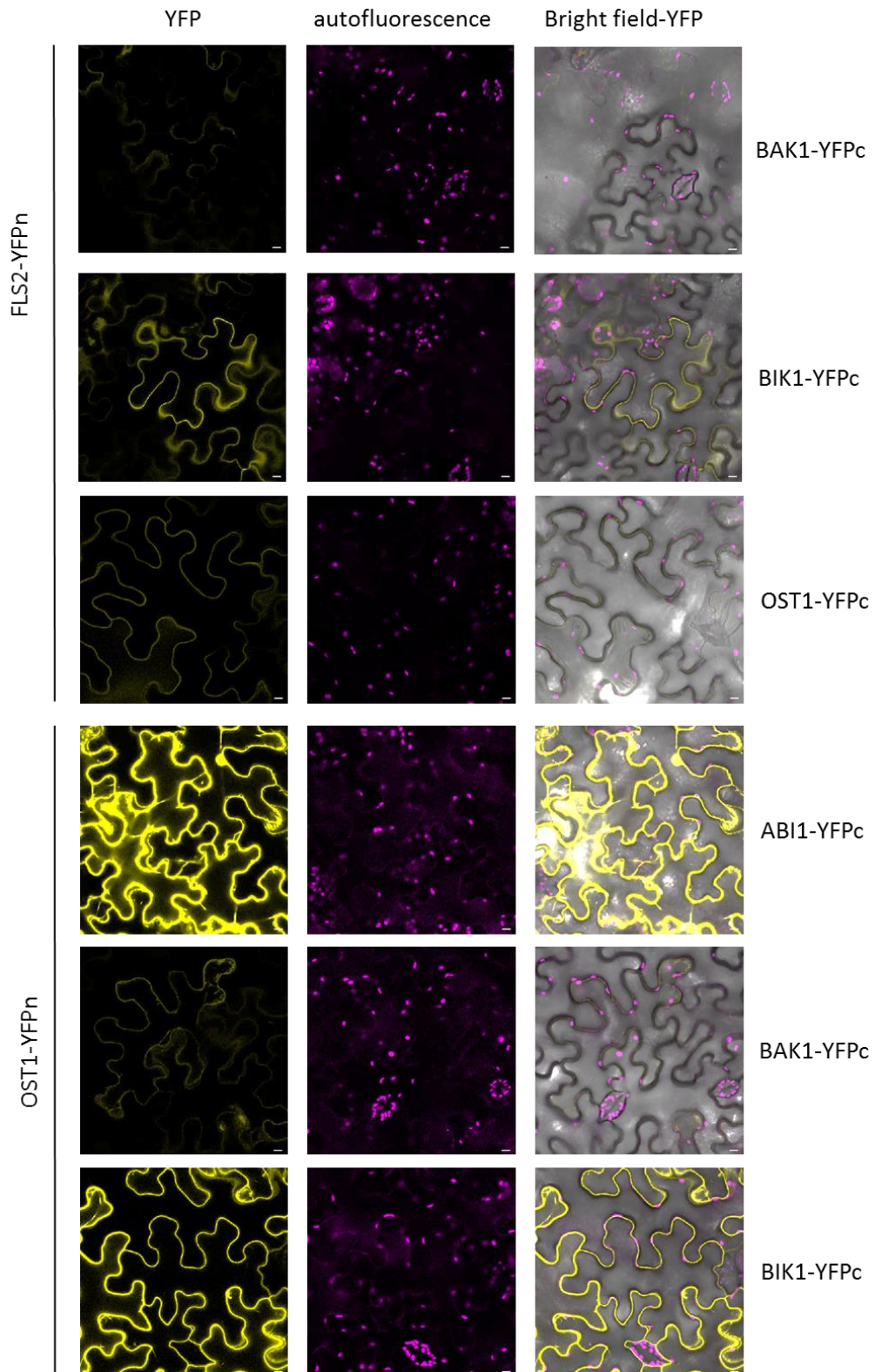


**Figure 5.4:** OST1 interacts with BAK1, BIK1 and ABI1 in split-YFP assay in *Nicotiana benthamiana*. Four-week-old *N. benthamiana* plants were infiltrated with *Agrobacterium* mixtures of split-YFP constructs ( $OD_{600}=0.1$ ). All constructs drove expression with the *p35S* promoter and were in the pICH47742 Golden Gate vector. Leaves were imaged by confocal microscopy two days after infiltration. Pictures are shown from one representative experiment. Bars indicate 10  $\mu$ m. Experiment was performed twice with similar results.

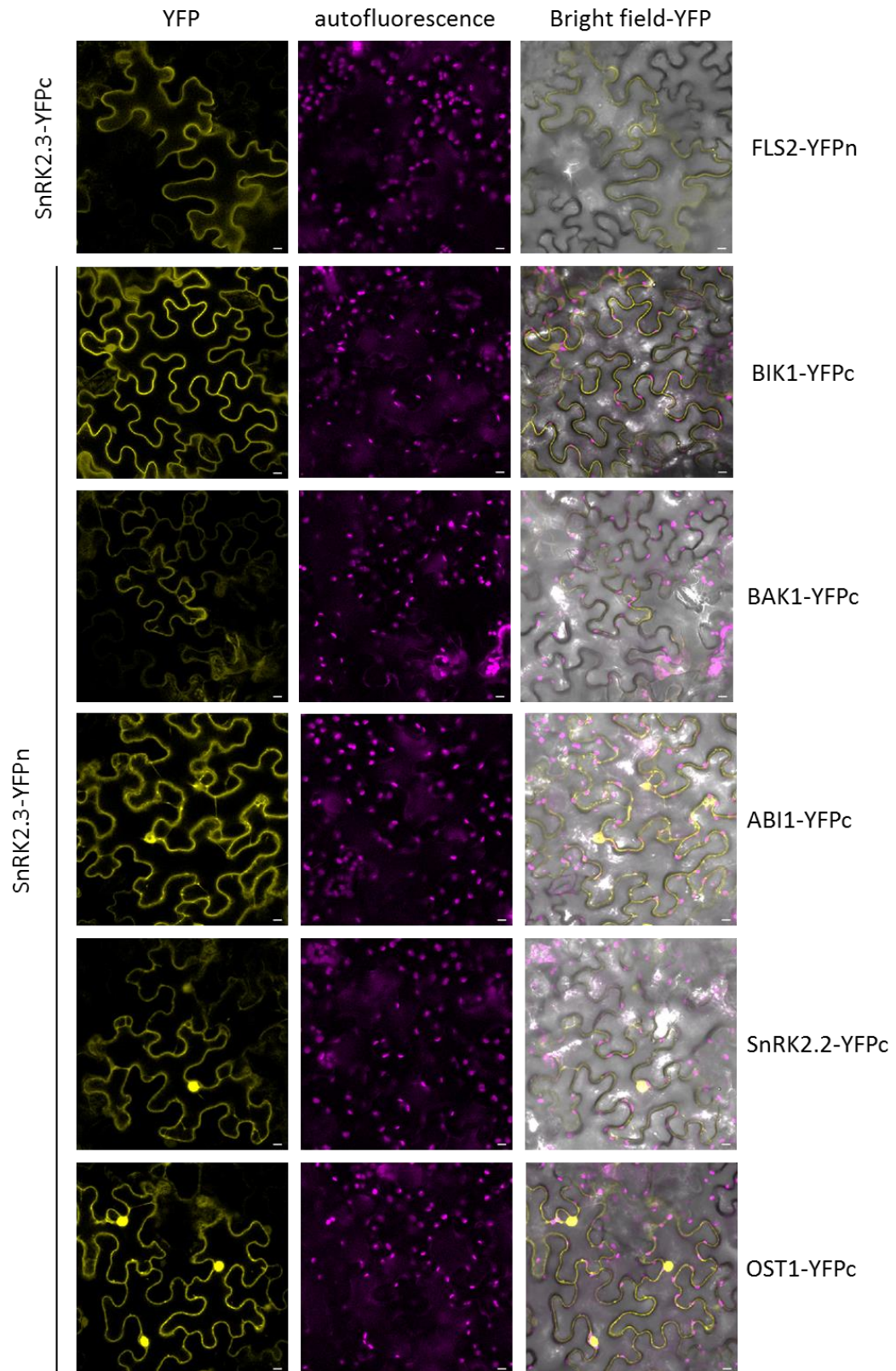
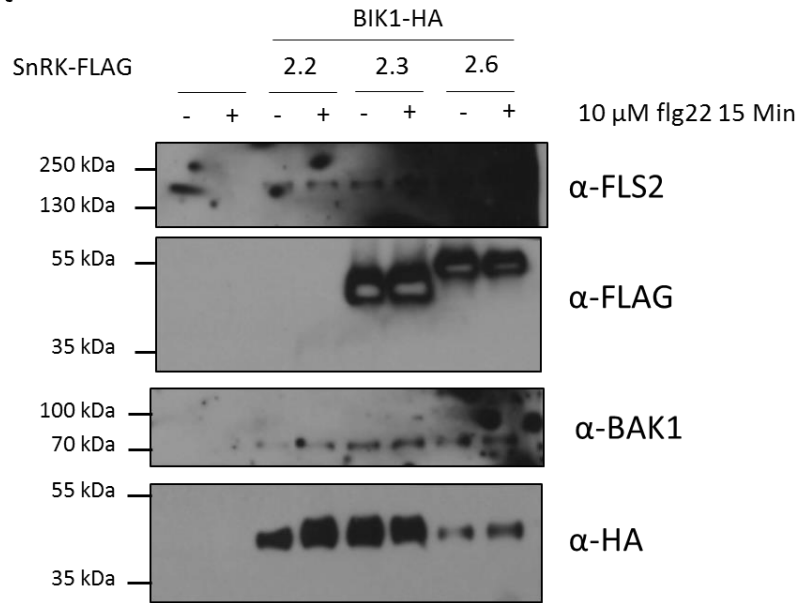


**Figure 5.5:** SnRK2.3 interacts with FLS2, BIK1, BAK1, ABI1, SnRK2.2 and OST1 in split-YFP assay in *Nicotiana benthamiana*. Four-week-old *N. benthamiana* plants were infiltrated with *Agrobacterium* mixtures of split-YFP constructs ( $OD_{600}=0.1$ ). All constructs drove expression with the *p35S* promoter and were in the pICH47742 Golden Gate vector. Leaves were imaged by confocal microscopy two days after infiltration. Pictures are shown from one representative experiment. Bars indicate 10  $\mu$ m. Experiment performed twice with similar results.

#### 5.2.2.2. SnRK2.3 interacts with BIK1 in co-IP assay in *Arabidopsis thaliana* protoplasts

To confirm the interactions found through split-YFP assays in *N. benthamiana*, I transfected *Arabidopsis thaliana* protoplasts with 3xFLAG-SnRKs, treated them with 10  $\mu$ M flg22 for 15 minutes, and then performed a co-immunoprecipitation assay. I could show that BIK1 interacts with SnRK2.3 but not with OST1/SnRK2.6 (Figure 5.6). Notably, the interaction seems to decrease upon flg22 treatment suggesting that the complex is pre-formed and might dissociate after flg22 perception. Unfortunately, the endogenous levels of FLS2 and BAK1 were too low to be detected on the Western Blots and we can therefore not draw a conclusion regarding these interactions. In this experiment SnRK2.2 does not seem to have been expressed successfully in mesophyll protoplasts. The co-IP assay needs to be repeated with overexpression of FLS2 and BAK1 as well as ensuring that the SnRK2.2-3xFLAG construct is successfully expressed in protoplasts. This suggests that one of the kinases in the complex might phosphorylate SnRK2.3 to induce stomatal closure.

### Input



### IP: $\alpha$ -FLAG

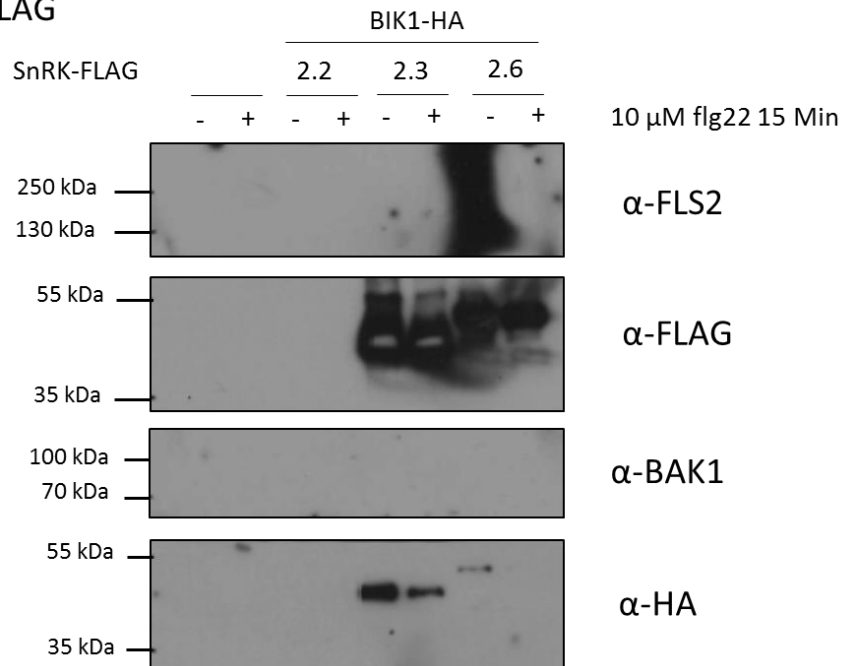


**Figure 5.6:** SnRK2.3 interacts with BIK1 in co-IP from *Arabidopsis thaliana* protoplasts. Mesophyll protoplasts were transfected with *p35S::BIK1-HA* and either *p35S::SnRK2.2-3xFLAG*, *p35S::SnRK2.3-3xFLAG* or *p35S::SnRK2.6-3xFLAG*. Proteins were extracted and IP performed with FLAG-affinity beads to enrich for 3xFLAG-SnRKs. Extracts and IP samples were separated on SDS-PAGE and a Western Blot was performed. Antibodies were applied as indicated. Experiment was performed once.

### 5.2.3. PBL1 could mediate anion channel activation in response to flg22 treatment in guard cells

#### 5.2.3.1. *pbl1* mutant stomata do not respond to flg22 treatment

PBL1 is a close homolog of BIK1 and is redundant in all flg22 responses tested to date (Lu, Dongping *et al.*, 2010; Zhang, Jie *et al.*, 2010). While it has been published that *bik1* and *bik1 pbl1* mutant stomata do not close in response to flg22 treatment (Zhang, J. *et al.*, 2010), it is unknown whether the loss of its close homolog PBL1 shows the same stomatal phenotype. As BIK1 is able to interact with SnRK2.3 it is possible that BIK1 and its homolog positively act in the MAMP-induced stomatal closure pathway. To investigate this possibility, I tested the *pbl1* single mutant for its stomatal response to flg22 to establish whether PBL1 plays a role in flg22-mediated stomatal closure. Figure 5.7A shows that Col-0 wild-type closes its stomata in response to flg22 and ABA ( $p < 0.05$ ), while the *fls2c* mutant is impaired in flg22-induced stomatal closure but has a wild-type-like response to ABA. *pbl1* does not show stomatal closure to flg22 treatment but has a wild-type-like response to ABA. I also tested the *pbl27* mutant because our lab has shown that PBL27 activates SLAH3 to mediate chitin-induced stomatal closure (Liu *et al.*, revision submitted). This seems to be a chitin-specific response, because *pbl27* shows a wild-type-like stomatal closure response to flg22 and ABA. This would suggest that PBL1 could also play an active role in flg22-mediated stomatal closure. As I only have one replicate of this experiment, this needs to be repeated to come to a definitive conclusion.

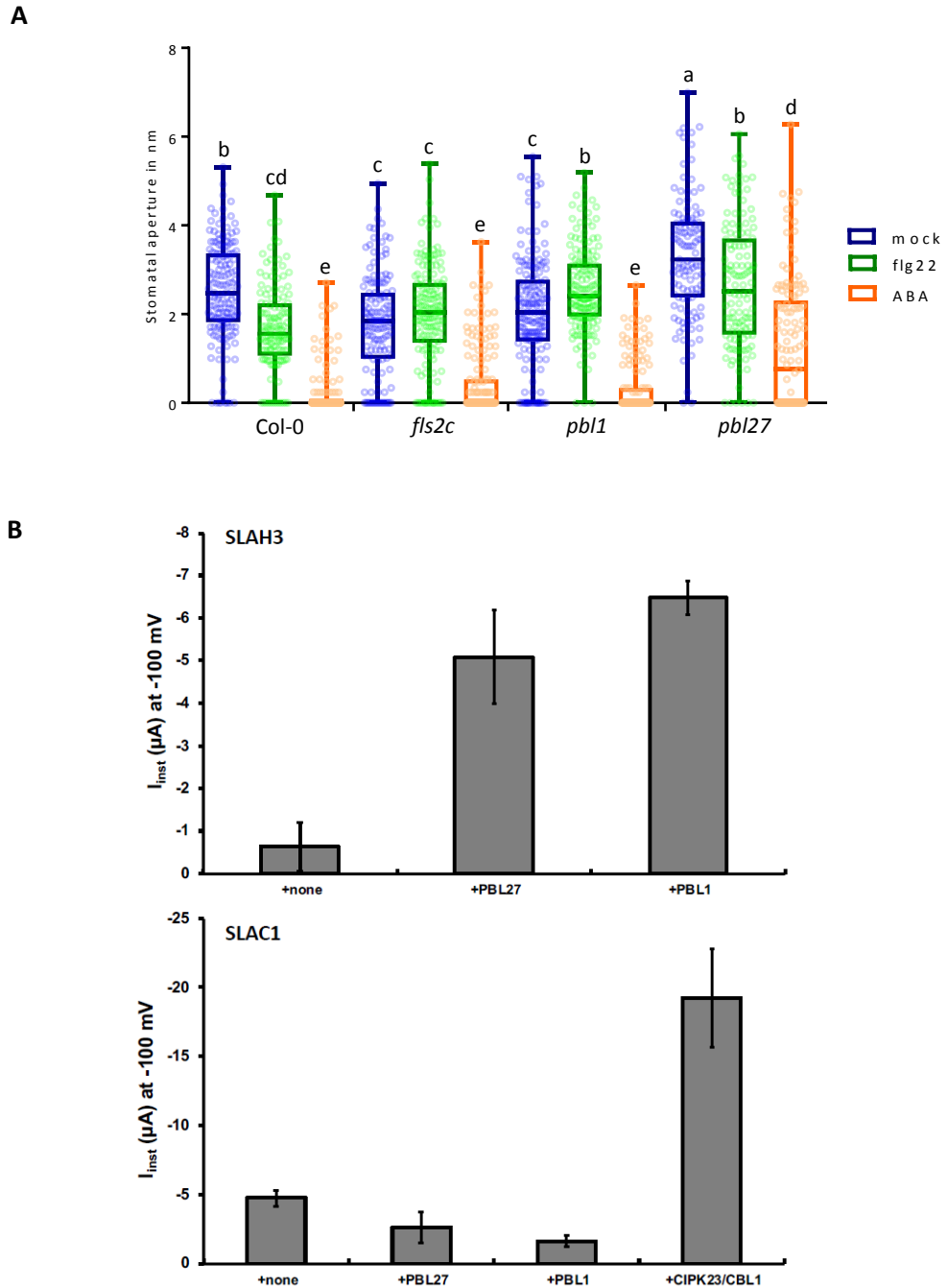


**Figure 5.7:** PBL1 is a potential member of the flg22-induced stomatal closure pathway

A. Stomata of the *pbl1* single mutant are unresponsive to flg22 treatment. Leaf discs from 5-week-old *Arabidopsis thaliana* plants were harvested in the morning and incubated for 2 hours in Stomata Opening Buffer in the light. After two hours MAMP or ABA treatment was applied to leaf discs. Two hours after treatment leaf discs were imaged and stomatal aperture was measured using ImageJ. Genotypes were hidden until after measurements to avoid unconscious bias. Graph shows data from one independent experiment. Experiment was performed three times with similar results. At least 150 stomata were measured for each combination of genotype and treatment. Error bars indicate SD from mean. Letters indicate significance levels (two-way ANOVA followed by Tukey's test,  $p < 0.05$ ).

B. PBL1 activates SLAH3 but not SLAC1 in oocyte measurements. *Xenopus* oocyte measurements were performed by Dr. Tobias Maierhofer at the University of Würzburg. Instantaneous currents ( $I_{inst}$ ) at -100 mV recorded from oocytes expressing SLAH3 (top) or SLAC1 (bottom) alone or co-expressing with the indicated kinases in the presence of 100 mM nitrate ( $n > 3$ , mean  $\pm$  SD).

#### 5.2.3.2. PBL1 activates SLAH3 anion channel in oocyte measurements

Oocytes present a useful tool to examine whether two proteins interact and is especially useful to test anion channel activation by another protein. It was previously published that SLAC1 and SLAH3 are necessary for flg22-induced stomatal closure (Deger *et al.*, 2015) and therefore our collaborators Dr. Tobias Maierhofer (Rainer Hedrich, University of Würzburg) tested whether RLCKs involved in the flg22 signalling pathway can directly activate these anion channels. They were able to show that BIK1 is unable to induce anion channel currents by either SLAH3 or SLAC1 (data not shown). Figure 5.7B shows that both PBL1 and PBL27 strongly activate SLAH3 in *Xenopus* oocytes. This suggests that PBL1 and PBL27 may play homologous roles in flg22- and chitin-induced stomatal closure. SLAC1 is not activated by either RLCK but as both channels are important in the flg22-mediated stomatal closure response this suggests that there may be two separate pathways working alongside one another to induce stomatal closure in response to MAMPs.

#### 5.2.3.3. BIK1 or PBL1 do not phosphorylate SnRK2.3, OST1, SLAH3 or SLAC1 in a recombinant kinase assay

Because I observed direct interaction between BIK1 and SnRK2.3 in split-YFP and co-immunoprecipitation assays, I decided to test whether SnRKs can be phosphorylated by BIK1. I also included anion channels and PBL1 in this assay, because our collaborators demonstrated that PBL1 can activate SLAH3 in oocyte measurements. I cloned the proteins and channel subunits with an N-terminal GST tag into a vector suitable for expression of recombinant protein in *E.coli* Rosetta cells (Novagen). I expressed and purified the proteins from *E.coli* and conducted a transphosphorylation assay. Additional replicates and blots were performed by Dr. Thomas DeFalco (University of Zurich). Proteins were incubated together at 30°C for 2.5 hours. GST was included as an artificial substrate to distinguish between phosphorylation on the tag and the protein. Protein blots were probed with a 1:1 mixtures of general anti-phosphothreonine and anti-phosphoserine antibodies. CANDIDATE BIK1 SUBSTRATE PROTEIN 59 (CBSP59) is strongly phosphorylated by BIK1 (unpublished, personal communication) and was included as positive control. In order to be able to distinguish between auto- and transphosphorylation activity, all SnRK kinases were provided as inactive mutant forms which is indicated by the asterisks (Cai *et al.*, 2014). Neither SnRK2.3\* nor SnRK2.6 were observed to be transphosphorylated by BIK1 or PBL1 (Figure 5.8). We could also not detect any transphosphorylation on anion channel subunits by BIK1 and PBL1 (Figure 5.8). All active kinases showed positive phosphoserine and phosphothreonine signals in the

blots and all substrates could be detected in the Coomassie Brilliant Blue staining of the membranes (Figure 5.8, lower panel). However, we could also not detect any phosphorylation on the positive control CBSP59. This protein was found to be strongly phosphorylated by BIK1 in <sup>32</sup>P kinase assays, which suggests that this assay is more sensitive. As all kinases were active and all substrates expressed this suggests that this assay is not sensitive enough to detect transphosphorylation by BIK1 or PBL1. Additional assays will have to be performed to clarify whether PBL1 can phosphorylate SLAH3 and whether BIK1 phosphorylates SnRK2.3.

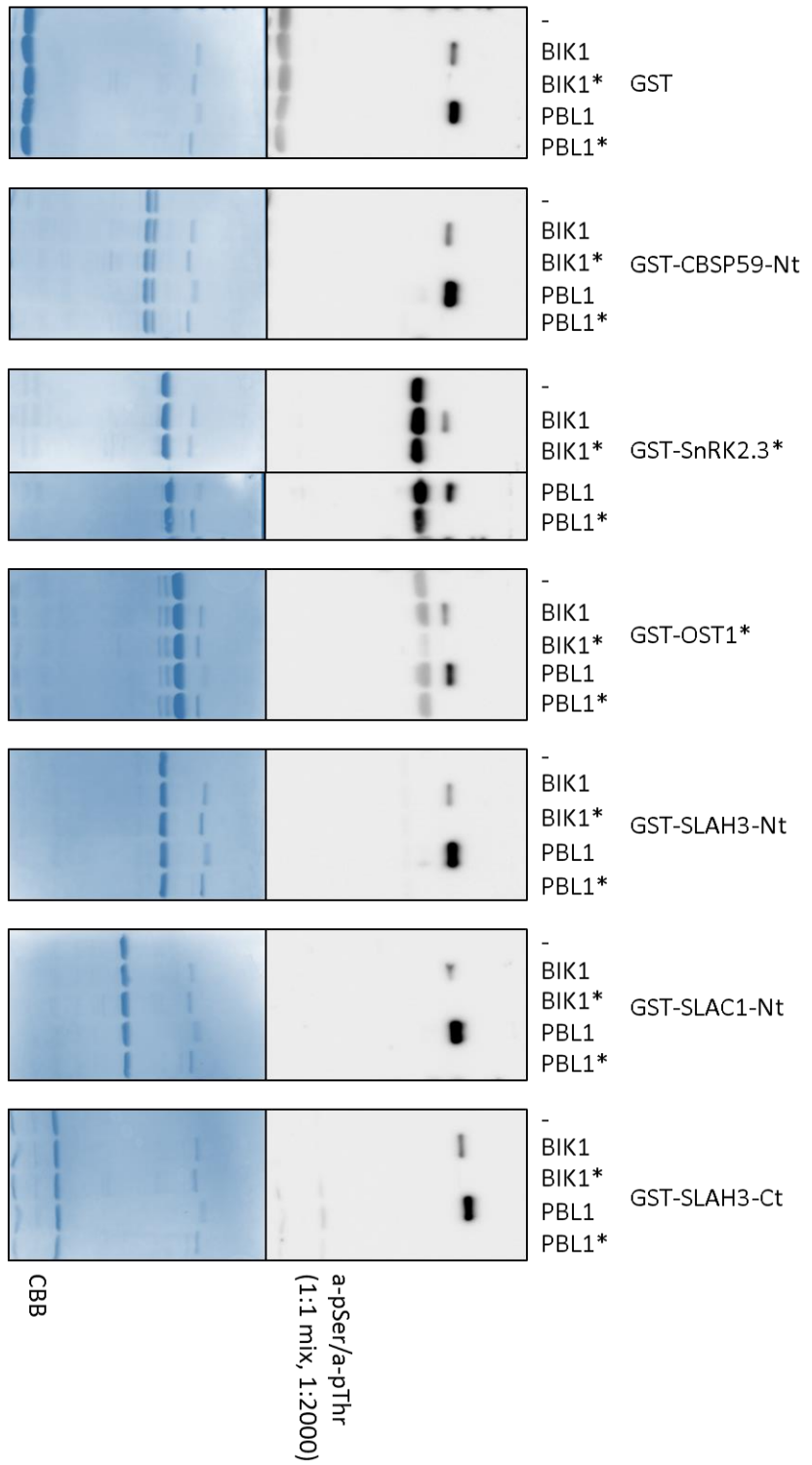


**Figure 5.8:** BIK1/PBL1 do not phosphorylate SnRK2.3, OST, SLAH3 or SLAC1 in cold kinase assay. Transphosphorylation from RLCKs onto substrates could not be detected in the cold kinase assay. CBSP59 was used as positive control for BIK1 transphosphorylation but could not be detected with this assay. Cold kinase assays were performed from recombinant protein purifications. Reactions were performed at 30°C for 2.5 hours. Protein blots were probed with a 1:1 mixture anti-phosphothreonine (Cell Signaling Technology P-Thr-Polyclonal #9381, 1:2000) and anti-phosphoserine (Abcam #ab93332, 1:2000) in the same blocking solution. Cold kinase assays were performed by Dr. Thomas Defalco (University of Zurich). CSP59 = CANDIDATE BIK1 SUBSTRATE PROTEIN 59.

### 5.3. Discussion

Recent evidence has suggested that stomatal closure pathways largely overlap and depend on mostly the same central regulators (Melotto *et al.*, 2006; Chater *et al.*, 2015). The same central regulators are required to induce stomatal closure to several different stimuli, such as ABA or elevated CO<sub>2</sub> concentration (Deger *et al.*, 2015). By testing the stomatal closure responses of four different ABA biosynthesis mutants (Figure 5.1A, B, C and D), ABA receptor mutants (Figure 5.2) and a PP2C phosphatase mutant (Figure 5.1E) I present strong evidence that ABA and MAMP-induced stomatal closure signalling pathways are distinct from each other. It is still unknown whether ABA receptors are required for the flg22 stomatal closure response since I was unable to get conclusive results from the mutants I tested. Although these plants were genotyped before the assay as we received them from a collaborator, their response to flg22 was not consistent. This could be due to varying conditions in the growth chambers or changing water conditions. While many abiotic stimuli inducing stomatal closure all involve ABA biosynthesis, ABA receptors and OST1 this study suggests that this is not the case for flg22-induced stomatal closure (Mustilli *et al.*, 2002; Merilo *et al.*, 2013; Chater *et al.*, 2015). The overlap between biotic and abiotic stress-activated signalling pathways in guard cells therefore seems much smaller than previously assumed. Only the anion channels SLAC1 and SLAH3 have also been shown to be involved in flg22-induced stomatal closure suggesting that convergence of the pathways occurs downstream at the level of the executors (Deger *et al.*, 2015).

OST1 is a central executor of stomatal closure in response to several different stimuli. Previous evidence provided a direct link from OST1 to known downstream requirements for stomatal closure, including RBOHF, SLAC1 and GORK1. The involvement of OST1 in flg22-induced stomatal closure, however, has been under discussion. Melotto *et al.*, 2006 demonstrated that *ost1-2* does not close its stomata in response to flg22, while Mustilli *et al.*, 2012 showed a concentration-dependent phenotype. Previous studies have almost exclusively used the *ost1-2* mutant, that has a point mutation in the ATP-binding pocket of the kinase (Mustilli *et al.*, 2002) rendering it unable to bind ATP and therefore constitutively inactive (Belin *et al.*, 2006). Here, I provide evidence that not OST1 but SnRK2.3 mediate stomatal closure in response to flg22. The *ost1-3* and *ost1-4* mutants consistently closed their stomata in response to flg22 (Figure 5.3A) while *snrk2.3* was unresponsive (Figure 5.3D). I hypothesise that the constitutively inactive OST1-2 protein could have a dominant-negative effect on SnRK2.3 and thereby flg22-induced stomatal closure. This is consistent with the concentration dependent phenotype of *ost1-2* demonstrated previously whereby *ost1-2*

responds to flg22 in a wild-type-like manner when treated with higher concentrations of flg22 (Montillet *et al.*, 2013) and the observation that SnRK2.3 and OST1 directly interact with each other as shown by (Waadt *et al.*, 2015) and in this study (Figure 5.5). Taken together these data demonstrate that flg22-induced stomatal closure is independent of OST1 and I propose a novel player – SnRK2.3 - in this pathway. However, how SnRK2.3 plays a role in this pathway still remains elusive. There is no current link between receptor complex members and SnRK2.3 and it is not able to activate SLAC1 in oocyte measurements (Geiger *et al.*, 2009). It has been suggested that SnRK2s require activation by an upstream kinase (Boudsocq *et al.*, 2007) and GSK3-like kinases have been shown to phosphorylate SnRK2.2 and SnRK2.3 to modulate ABA signalling (Cai *et al.*, 2014). I tried to connect SnRK2.3 to the receptor complex through split-YFP assays and pull downs as well as kinase assays. All tested combinations of receptor complex members (FLS2, BAK1, BIK1) with SnRK2.3 showed a positive YFP reconstitution in the split-YFP assay (Figure 5.5) but only the interaction between SnRK2.3 and BIK1 could be confirmed in the co-immunoprecipitation assay (Figure 5.6). Since the split-YFP has the inherent affinity to reconstitute to the complete fusion protein and cannot disassemble once reconstituted the results suggests that SnRK2.3 is most likely in close proximity to the receptor complex members. The results from the split-YFP assay should therefore be interpreted very cautiously. Although we detected interaction between SnRK2.3 and BIK1 in co-immunoprecipitation assays (Figure 5.6), we could not detect phosphorylation of SnRK2.3 by BIK1 in cold kinase assays (Figure 5.8). However, as we could also not detect transphosphorylation on our positive control CBSP59 that was shown to be phosphorylated by BIK1 in <sup>32</sup>P phosphorylation assays (unpublished), the cold kinase assay might not be sensitive enough to detect transphosphorylation by BIK1. Whether SnRK2.3 is activated by flg22 treatment and what its downstream signalling partners are, remain important questions that need to be addressed in order to understand how SnRKs are involved in MAMP-induced stomatal closure.

RLCKs have recently emerged as important signalling modules of RLK complexes. PBL1 and BIK1 are members of the RLCK-VII family and are redundant in many FLS2-mediated defence functions, for instance phosphorylation and activation of RBOHD to induce ROS production upon MAMP perception (Kadota *et al.*, 2014). While it has been shown that *bik1* and *bik1 pbl1* mutants have flg22-insensitive stomata, I now show that the *pbl1* mutant also has flg22-insensitive stomata (Figure 5.7A). This suggests that both BIK1 and PBL1 could play an important role in mediating flg22-induced stomatal closure. As BIK1 does not activate either SLAH3 or SLAC1, it is possible that BIK1 has an indirect role in MAMP-induced stomatal

closure by mediating ROS production through RBOHD, which is required for this response. In contrast, PBL1 activates SLAH3 in oocyte measurements (Figure 5.7B) suggesting an active role of PBL1 in this response. Moreover, this demonstrates a direct link between receptor complex components and anion channel activation in flg22 signalling. However, because induction of stomatal closure in response to MAMPs requires both SLAC1 and SLAH3 (Deger *et al.*, 2015) it is still unknown how SLAC1 is activated after flg22 treatment. I hypothesise that SnRK2.3 may be acting in an alternative pathway that acts hand in hand with direct interaction and activation of SLAH3 by PBL1. It will be important to demonstrate whether PBL1 can phosphorylate SLAH3 and to identify the required phosphosites.

Interestingly, a recent study demonstrated that AtPep1-induced stomatal closure acts independently of OST1 and requires BIK1 and both SLAC1 and SLAH3 (Zheng *et al.*, 2018). It is conceivable that biotic stimuli use a stomatal closure pathway that is distinct from that activated by abiotic stimuli. Current evidence would therefore suggest that, during MAMP-induced stomatal closure, anion channels are activated by PRR complex-associated RLCKs independently from the prototypic ABA signalling pathway.

I propose the following model for flg22-induced stomatal closure (Figure 5.9). Upon flg22-perception FLS2 associates with its co-receptor BAK1 and the cytoplasmic kinases PBL1 and BIK1 are phosphorylated and activated. BIK1 and PBL1 subsequently phosphorylate and activate RBOHD which leads to the accumulation of ROS in the apoplast. I propose that activated PBL1 phosphorylates and activates SLAH3 to induce stomatal closure. The involvement OST1 and SnRK2.3 and how SLAC1 is activated remains to be demonstrated.

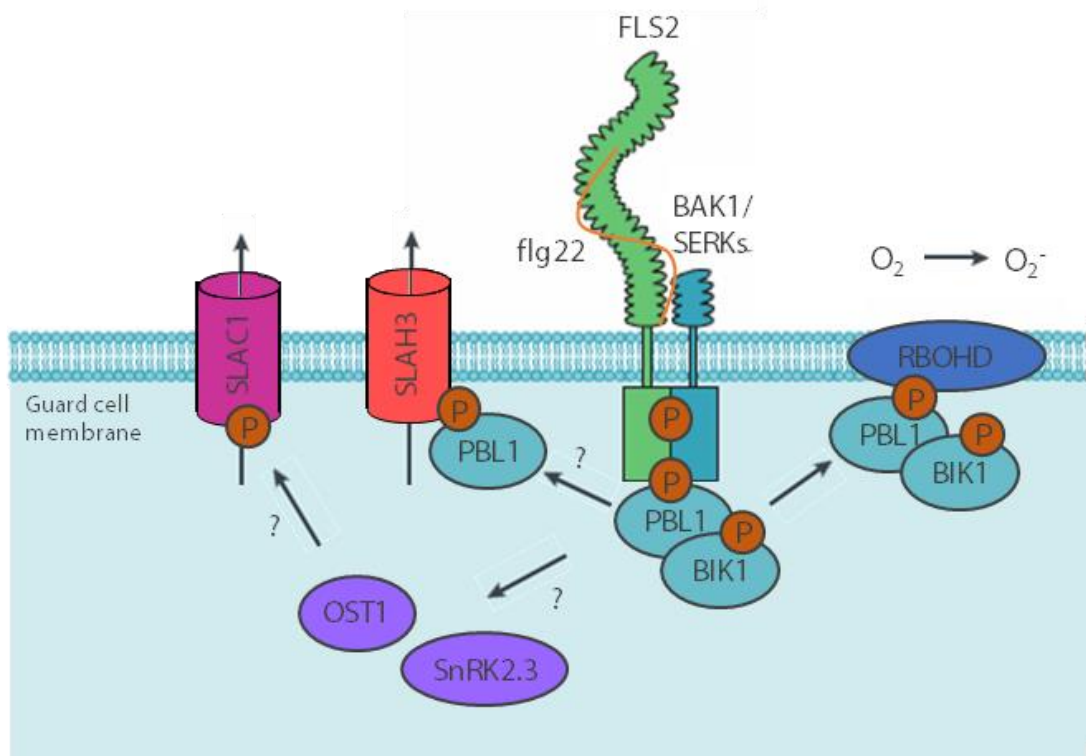


**Figure 5.9:** Proposed model for PAMP-induced stomatal closure pathway. Upon flg22-perception FLS2 associates with its co-receptor BAK1 and the cytoplasmic kinases PBL1 and BIK1 are phosphorylated and activated. BIK1 and PBL1 subsequently phosphorylate and activate RBOHD which leads to the accumulation of ROS in the apoplast. We propose that activated PBL1 phosphorylates and activates SLAH3 to induce stomatal closure. Whether OST1 and SnRK2.3 are involved in this pathway remains to be shown. How SLAC1 is activated during flg22-induced stomatal closure remains unknown.

## 6. Discussion

### 6.1. PBL1 and SnRK2.3 are novel players in MAMP-induced stomatal closure

Although a number of molecular components were described in MAMP-induced stomatal regulation, there has been some opposing findings and the molecular link between receptor complex activation and regulators of stomatal apertures have remained largely unknown. In this study I propose two novel regulators of MAMP-induced stomatal closure that have not previously been associated with guard cell-specific responses.

This study supports the hypothesis that PBL1 is a major regulator of MAMP-induced stomatal closure. Together with its close homolog BIK1, PBL1 is an important regulatory component of MAMP responses and known to be part of the larger PRR receptor complex at the plasma membrane (Lu, Dongping *et al.*, 2010; Zhang, Jie *et al.*, 2010). Both BIK1 and PBL1 act largely redundant in all immune outputs tested to date, including the activation of ROS production by RBOHD, calcium burst, seedling growth inhibition, callose deposition and MAP Kinase activation (Zhang, J. *et al.*, 2010; Li *et al.*, 2014; Ranf *et al.*, 2014). Here I demonstrate the first distinct function of PBL1. The single *pbl1* mutant is impaired in flg22-induced stomatal closure and PBL1 activates SLAH3 in oocytes (Figure 5.7). BIK1 has not been found to activate SLAC1 or SLAH3 (Liu *et al.*, 2018, revision submitted), indicating that this signalling role is not shared between the two otherwise redundant RLCKs. RLCKs have emerged as a major class of signalling proteins that mediate RLK-associated outputs and this study has provided more evidence supporting their important signalling function (Liang & Zhou, 2018).

Since ROS and calcium are such crucial messengers to initiate stomatal closure and require BIK1 and PBL1, it has been hypothesised that BIK1 and PBL1 mediate stomatal closure by mediating ROS production and calcium burst (Li *et al.*, 2014; Ranf *et al.*, 2014). Interestingly, *AtPep1*-induced stomatal closure has been reported to be independent of ROS production by RBOHD and RBOHF and furthermore independent of BIK1 (Zheng *et al.*, 2018). This would suggest that not all stomatal closure pathways depend on ROS production.

In this study I provide evidence that not OST1/SnRK2.6 is mediating stomatal closure in response to MAMPs (Figure 5.3A&C). Instead, I show that the *snrk2.3* single mutant is impaired in stomatal closure (Figure 5.3D). Furthermore, I demonstrate that ABA signalling is not required for this response (Figure 5.1 and 5.2). This suggests that although stomatal

closure in response to ABA, CO<sub>2</sub> and ozone make use of the same central regulators, this is not the case for flg22-induced stomatal closure. I therefore propose that stomatal closure pathways converge on the level of anion channels and that there are at least two distinct stomatal closure signalling pathways. Although SnRK2.3 is expressed throughout all plant tissues it has been shown to play a role in stomatal responses in drought stress memory (Virilouvet & Fromm, 2015). It is interesting that also SnRK2.3 seems to have a previously unknown guard cell-specific function, namely in the execution of MAMP-induced stomatal closure. Future research will have to address whether SnRK2.3 is activated by flg22 treatment and how it acts in the flg22-induced stomatal closure pathway.

While this study has provided novel components involved in MAMP-induced stomatal closure, many questions remain unanswered. It is still not clear how these two different players integrate into a common stomatal closure response. While PBL1 can strongly activate SLAH3 in oocyte measurements, neither PBL1 nor SnRK2.3 can activate SLAC1 and both anion channels are required for MAMP-induced stomatal closure (Deger *et al.*, 2015). It has been shown that anion channels require phosphorylation at their N-termini for activation (Geiger *et al.*, 2009; Geiger *et al.*, 2010; Geiger *et al.*, 2011; Brandt *et al.*, 2012; Maierhofer *et al.*, 2014). Intriguingly, SLAH3 can also be activated in the absence of an activating kinase and ligand if it associates with the modulatory subunit SLAH1 (Cubero-Font *et al.*, 2016). One might therefore hypothesise, that in response to flg22 SLAC1 might not get activated through phosphorylation but by a yet unknown mechanism. Future studies addressing the gating mechanisms of these anion channels could address this question and offer insight into SLAC1-dependency in flg22-induced stomatal closure.

I propose that during flg22-induced stomatal closure FLS2 and BAK1 activate PBL1 which in turn activates SLAH3 (Figure 5.9). This leads to the induction of stomatal closure and stomatal immunity. This is homologous to the chitin-induced stomatal closure model suggested by Liu *et al.*, revision submitted. After chitin perception by LYK5 and CERK1 the RLCK PBL27 gets activated and phosphorylates SLAH3 at Ser127 and Ser189. It will be interesting to see whether PBL1 phosphorylates SLAH3 at the same phosphosites or whether there is distinction between biotic stimuli.

## 6.2. Several cell types mediate stomatal immunity

Guard cells have been shown to act as autonomous units in ABA-induced stomatal closure and blue-light induced stomatal opening (Cañamero *et al.*, 2006; Bauer *et al.*, 2013). This

study demonstrates that this is also true for MAMP-induced stomatal closure. Expression of a PRR restricted to guard cells is sufficient for wild-type-like stomatal closure responses and resistance to bacteria (Figure 4.6B and 4.7A&B). This supports the previous assumption that guard cells are fully autonomous and require no signalling input from surrounding cells to initiate closure.

However, it has also long been hypothesised that mesophyll cells are able to influence the stomatal aperture to ensure optimal conditions for photosynthesis (Lawson *et al.*, 2014). This hypothesis stems from the observed correlation between mesophyll photosynthesis and stomatal conductance (Wong *et al.*, 1979). Here I report that non-autonomous signalling events occur to initiate stomatal closure homologous to the proposed “mesophyll signal” (Mott *et al.*, 2008; Mott, 2009). Transient assays performed in *N. benthamiana* imply that this response is dependent on ROS production by NADPH oxidase *NbrBOHB* (Figure 3.1). ROS is produced in the apoplast which makes it the most likely candidate for such a systemic signal as compared with other proposed systemic signals, such as a  $Ca^{2+}$  wave which requires symplastic connections (Choi *et al.*, 2014). Apoplastic ROS has been reported to be recognised and propagated by cells to generate a systemic ROS wave (Miller *et al.*, 2009) and this could be a potential non-autonomous signal generated by pavement cells to induce stomatal closure. Interestingly, a LRR-RLK kinase HYDROGEN PEROXIDE-RESISTANT 1 (GHR1) is required for flg22-induced stomatal closure and has been shown to interact with and phosphorylate SLAC1 (Hua *et al.*, 2012). Furthermore, CYSTEINE-RICH KINASES (CRKs) which present potential ROS sensors due to their cysteine-rich nature (Wang *et al.*, 2012). Evidence suggests that CRKs play a regulatory role in stomatal closure as several *crk* mutants are impaired in stomatal closure to different stimuli (Bourdais *et al.*, 2015). Aquaporins have also been proposed to transport  $H_2O_2$  into the cytoplasm of guard cells and this is required for stomatal closure (Rodrigues *et al.*, 2017). Current evidence therefore supports the hypothesis of ROS acting as a non-autonomous signal for the induction of stomatal closure in response to MAMPs.

The existence of both autonomous and non-autonomous triggers that induce stomatal closure upon recognition of an invading pathogen seems like an elegant way to increase robustness of stomatal immunity. This would enable the first cell that comes into contact with a pathogen to alert nearby guard cells to an imminent invasion and to induce stomatal closure before the pathogen comes in contact with the actual guard cells. Guard cells would therefore be able to close the aperture in a preventive manner rather than just as a reactive

response to bacterial invasion. It would be interesting to investigate whether these non-autonomous signals are a local response only affecting adjacent stomata or whether this is a leaf-wide systemic response.

### 6.3. Cell type-specific responses of Pattern-triggered immunity (PTI)

BIK1 and PBL1 have been described as redundant RLCKs with largely overlapping function (Zhang, J. *et al.*, 2010; Li *et al.*, 2014; Ranf *et al.*, 2014). SnRK2.3 and SnRK2.2 are major mediators of ABA responses in diverse plant tissues (Fujii *et al.*, 2007; Fujita *et al.*, 2009). This work describes a novel function for both PBL1 and SnRK2.3 that is restricted to a specific cell type: the guard cells. This brings forward the general concept that immune responses may not be identical across all cell types and tissues. Since plants do not have specialised immune cells like animals it has been assumed that each cell has the ability to mount a full immune response. While this is mostly true it does not necessarily mean that the immune response is identical in each cell. Different cell types and tissues are specialised to fulfil a specific function and as such may come into touch with different pathogens or require different immune outputs. Indeed, stomatal closure is such a unique response that requires guard cell-specific regulators that it does not come as a complete surprise that unique regulators are required to execute this response. It is intriguing that this guard cell-specific response does not seem to be regulated by proteins with a specific localisation but by regulators expressed in all tissues and cell types. This implies that to fully understand plant immunity we have to discriminate immune responses of different tissues and cell types.

Previous studies support this as it has been shown that immune responses of the leaf differ from root responses – a clear example of tissue-specific immunity. While wild-type *Arabidopsis thaliana* roots can induce a ROS burst and MAP Kinase activation following flg22 perception they are unable to do so in response to elf18 (Wyrsh *et al.*, 2015). The study also describes FLS2 expression under the control of tissue-specific promoters and found that MAMP perception and sensitivity depends on the tissue in which the receptor was expressed (Wyrsh *et al.*, 2015). This also demonstrated that not only the tissue but also the cell type strongly influences PTI responses. Additionally, one study suggested that roots are more sensitive to DAMPs than MAMPs, suggesting that different tissues are specialised towards detecting different danger signals (Poncini *et al.*, 2017).

Future research trying to understand PTI is going to have to take both tissue and cell type identities into consideration. Moreover, cell type-specific analyses are necessary to tease

these differences in PTI signalling apart. It will be exciting to see more studies investigating what these differences are, how they are regulated and what their significance for whole plant health is.

#### 6.4. Cell type- and tissue-specific responses of Effector-triggered immunity (ETI)

Could ETI exhibit cell type- and tissue-specific responses similar to PTI? It has been shown that NLR genes are differentially expressed across different tissues in chickpea, suggesting that this may indeed be the case (Sharma *et al.*, 2017). This appears to be also true for NLRs in *Arabidopsis thaliana* (Tan *et al.*, 2007). However, I could not find any studies specifically addressing the question of cell type-specific expression of NLRs within different tissues. It would be interesting to analyse whether NLRs are differentially expressed within a tissue and whether certain cell types show higher expression than others.

While it has been shown that effectors interfere with stomatal closure and that effectors can translocate into the guard cells, they do so at a much lower rate than into pavement cells (Henry *et al.*, 2017). This could be due to the reinforced cell wall of guard cells that are necessary to enable them to withstand the drastic volume and shape changes they undergo during stomatal movement. One could hypothesise that targeting of the stomata by certain pathogens may therefore be a means of avoiding detection by the plant before infection is successfully established.

If effector translocation into guard cells happens at such a low rate, how can effectors successfully interfere with stomatal closure? This study has provided evidence for both cell autonomy and non-autonomous signalling events associated with MAMP-induced stomatal closure. One may hypothesise that there are not only non-autonomous signalling events inducing stomatal closure but also interfering with stomatal closure. It has been shown that guard cell-specific and guard cell-excluding expression of RIN4 enabled RPM1-mediated hypersensitive responses across the whole leaf (Henry *et al.*, 2017). This indicates that there are also non-autonomous signalling events associated with ETI. It is therefore conceivable that effector interference with stomatal closure is not only mediated by guard cells but also other cell types.

## 6.5. Outlook

Many questions remain and future research into cell type-specific responses will greatly enhance our understanding of plant immunity. There are already many tools established and promoters identified that enable such studies. There are many protocols to isolate guard cell-enriched samples or guard cell purification that enable cell type-specific transcriptomic analyses (Obulareddy *et al.*, 2013; Jalakas *et al.*, 2017). Cell type-specific promoters in combination with cell sorting make it possible to isolate virtually any cell type. Comparative transcriptomics between different cell types are needed to elucidate differential NLR expression and potentially differential immune responses. We have all the tools available at hand to investigate cell type-specific immune responses. It will be exciting to see what future research in this area will bring to the table.

## 7. Bibliography

- AAAS. 1998.** Armed and Dangerous, The Big 7. *Science News* **153**(9): 137-137.
- Abramovitch RB, Janjusevic R, Stebbins CE, Martin GB. 2006.** Type III effector AvrPtoB requires intrinsic E3 ubiquitin ligase activity to suppress plant cell death and immunity. *Proc Natl Acad Sci U S A* **103**(8): 2851-2856.
- Ache P, Becker D, Ivashikina N, Dietrich P, Roelfsema MR, Hedrich R. 2000.** GORK, a delayed outward rectifier expressed in guard cells of *Arabidopsis thaliana*, is a K(+)-selective, K(+)-sensing ion channel. *FEBS Lett* **486**(2): 93-98.
- Ade J, DeYoung BJ, Golstein C, Innes RW. 2007.** Indirect activation of a plant nucleotide binding site-leucine-rich repeat protein by a bacterial protease. *Proc Natl Acad Sci U S A* **104**(7): 2531-2536.
- Ali R, Ma W, Lemtiri-Chlieh F, Tsaltsas D, Leng Q, von Bodman S, Berkowitz GA. 2007.** Death don't have no mercy and neither does calcium: *Arabidopsis* CYCLIC NUCLEOTIDE GATED CHANNEL2 and innate immunity. *Plant Cell* **19**(3): 1081-1095.
- Allegre M, Heloir MC, Trouvelot S, Daire X, Pugin A, Wendehenne D, Adrian M. 2009.** Are grapevine stomata involved in the elicitor-induced protection against downy mildew? *Mol Plant Microbe Interact* **22**(8): 977-986.
- Allen GJ, Kuchitsu K, Chu SP, Murata Y. 1999.** *Arabidopsis* *abi1-1* and *abi2-1* phosphatase mutations reduce abscisic acid-induced cytoplasmic calcium rises in guard cells. *The Plant cell*.
- Alonso-Villaverde V, Boso S, Santiago JL, Gago P, Martinez MC. 2011.** Variability of the stomata among 'Albarino' (*Vitis vinifera* L.) clones and its relationship with susceptibility to downy mildew. *Vitis* **50**(1): 45-46.
- Andres Z, Perez-Hormaeche J, Leidi EO, Schlucking K, Steinhorst L, McLachlan DH, Schumacher K, Hetherington AM, Kudla J, Cubero B, et al. 2014.** Control of vacuolar dynamics and regulation of stomatal aperture by tonoplast potassium uptake. *Proc Natl Acad Sci U S A* **111**(17): E1806-1814.
- Asai T, Tena G, Plotnikova J, Willmann MR, Chiu W-LL, Gomez-Gomez L, Boller T, Ausubel FM, Sheen J. 2002.** MAP kinase signalling cascade in *Arabidopsis* innate immunity. *Nature* **415**(6875): 977-983.
- Asai T, Tena G, Plotnikova J, Willmann MR, Chiu WL, Gomez-Gomez L, Boller T, Ausubel FM, Sheen J. 2002.** MAP kinase signalling cascade in *Arabidopsis* innate immunity. *Nature* **415**(6875): 977-983.
- Assmann SM, Simoncini L, Schroeder JI. 1985.** Blue-Light Activates Electrogenic Ion Pumping in Guard-Cell Protoplasts of *Vicia-Faba*. *Nature* **318**(6043): 285-287.
- Bai S, Liu J, Chang C, Zhang L, Maekawa T, Wang Q, Xiao W, Liu Y, Chai J, Takken FL, et al. 2012.** Structure-function analysis of barley NLR immune receptor MLA10 reveals its cell compartment specific activity in cell death and disease resistance. *PLoS Pathog* **8**(6): e1002752.
- Bak G, Lee EJ, Lee Y, Kato M, Segami S, Sze H, Maeshima M, Hwang JU, Lee Y. 2013.** Rapid structural changes and acidification of guard cell vacuoles during stomatal closure require phosphatidylinositol 3,5-bisphosphate. *Plant Cell* **25**(6): 2202-2216.
- Bartels S, Boller T. 2015.** Quo vadis, Pep? Plant elicitor peptides at the crossroads of immunity, stress, and development. *J Exp Bot* **66**(17): 5183-5193.

- Bauer H, Ache P, Lautner S, Fromm J, Hartung W, Al-Rasheid KA, Sonnewald S, Sonnewald U, Kneitz S, Lachmann N, et al. 2013.** The stomatal response to reduced relative humidity requires guard cell-autonomous ABA synthesis. *Current biology : CB* **23**(1): 53-57.
- Baunsgaard L, Fuglsang AT, Jahn T, Korthout HAAJ, de Boer AH, Palmgren MG. 1998.** The 14-3-3 proteins associate with the plant plasma membrane H<sup>+</sup>-ATPase to generate a fusicoccin binding complex and a fusicoccin responsive system. *Plant Journal* **13**(5): 661-671.
- Belin C, de Franco P-OO, Bourbousse C, Chaignepain S, Schmitter J-MM, Vavasseur A, Giraudat J, Barbier-Brygoo H, Thomine S. 2006.** Identification of features regulating OST1 kinase activity and OST1 function in guard cells. *Plant physiology* **141**(4): 1316-1327.
- Benitez-Alfonso Y, Faulkner C, Ritzenthaler C, Maule AJ. 2010.** Plasmodesmata: gateways to local and systemic virus infection. *Mol Plant Microbe Interact* **23**(11): 1403-1412.
- Bergmann DC, Lukowitz W, Somerville CR. 2004.** Stomatal development and pattern controlled by a MAPKK kinase. *Science* **304**(5676): 1494-1497.
- Bernoux M, Burdett H, Williams SJ, Zhang XX, Chen CH, Newell K, Lawrence GJ, Kobe B, Ellis JG, Anderson PA, et al. 2016.** Comparative Analysis of the Flax Immune Receptors L6 and L7 Suggests an Equilibrium-Based Switch Activation Model. *Plant Cell* **28**(1): 146-159.
- Bethke G, Pecher P, Eschen-Lippold L, Tsuda K, Katagiri F, Glazebrook J, Scheel D, Lee J. 2012.** Activation of the Arabidopsis thaliana Mitogen-Activated Protein Kinase MPK11 by the Flagellin-Derived Elicitor Peptide, flg22. *Molecular Plant-Microbe Interactions* **25**(4): 471-480.
- Bialas A, Zess EK, De la Concepcion JC, Franceschetti M, Pennington HG, Yoshida K, Upson JL, Chanclud E, Wu CH, Langner T, et al. 2018.** Lessons in Effector and NLR Biology of Plant-Microbe Systems. *Mol Plant Microbe Interact* **31**(1): 34-45.
- Blackman PG, Davies WJ. 1985.** Root to shoot communication in maize plants of the effects of soil drying. *Journal of experimental botany* **36**(1): 39-48.
- Blatt MR. 2000.** Cellular signaling and volume control in stomatal movements in plants. *Annu Rev Cell Dev Biol* **16**: 221-241.
- Bohm H, Albert I, Fan L, Reinhard A, Nurnberger T. 2014.** Immune receptor complexes at the plant cell surface. *Curr Opin Plant Biol* **20**: 47-54.
- Boller T, Felix G. 2009.** A renaissance of elicitors: perception of microbe-associated molecular patterns and danger signals by pattern-recognition receptors. *Annual review of plant biology*.
- Boudsocq M, Barbier-Brygoo H, Lauriere C. 2004.** Identification of nine sucrose nonfermenting 1-related protein kinases 2 activated by hyperosmotic and saline stresses in Arabidopsis thaliana. *J Biol Chem* **279**(40): 41758-41766.
- Boudsocq M, Droillard MJ, Barbier-Brygoo H, Lauriere C. 2007.** Different phosphorylation mechanisms are involved in the activation of sucrose non-fermenting 1 related protein kinases 2 by osmotic stresses and abscisic acid. *Plant Mol Biol* **63**(4): 491-503.

- Boudsocq M, Willmann MR, McCormack M, Lee H, Shan L, He P, Bush J, Cheng S-HH, Sheen J. 2010.** Differential innate immune signalling via Ca(2+) sensor protein kinases. *Nature* **464**(7287): 418-422.
- Bourdais G, Burdiak P, Gauthier A, Nitsch L, Salojarvi J, Rayapuram C, Idanheimo N, Hunter K, Kimura S, Merilo E, et al. 2015.** Large-Scale Phenomics Identifies Primary and Fine-Tuning Roles for CRKs in Responses Related to Oxidative Stress. *PLoS Genet* **11**(7): e1005373.
- Boyer JS. 1982.** Plant productivity and environment. *Science (New York, N.Y.)* **218**(4571): 443-448.
- Brandt B, Brodsky DE, Xue SW, Negi J, Iba K, Kangasjarvi J, Ghassemian M, Stephan AB, Hu HH, Schroeder JI. 2012.** Reconstitution of abscisic acid activation of SLAC1 anion channel by CPK6 and OST1 kinases and branched ABI1 PP2C phosphatase action. *Proceedings of the National Academy of Sciences of the United States of America* **109**(26): 10593-10598.
- Brueggeman R, Druka A, Nirmala J, Cavileer T, Drader T, Rostoks N, Mirlohi A, Bennypaul H, Gill U, Kudrna D, et al. 2008.** The stem rust resistance gene Rpg5 encodes a protein with nucleotide-binding-site, leucine-rich, and protein kinase domains. *Proc Natl Acad Sci U S A* **105**(39): 14970-14975.
- Burch-Smith TM, Schiff M, Caplan JL, Tsao J, Czymmek K, Dinesh-Kumar SP. 2007.** A novel role for the TIR domain in association with pathogen-derived elicitors. *PLoS biology* **5**(3): 501-514.
- Buttner D, He SY. 2009.** Type III protein secretion in plant pathogenic bacteria. *Plant Physiol* **150**(4): 1656-1664.
- Cai Z, Liu J, Wang H, Yang C, Chen Y, Li Y, Pan S, Dong R, Tang G, Barajas-Lopez Jde D, et al. 2014.** GSK3-like kinases positively modulate abscisic acid signaling through phosphorylating subgroup III SnRK2s in Arabidopsis. *Proc Natl Acad Sci U S A* **111**(26): 9651-9656.
- Caine RS, Yin X, Sloan J, Harrison EL, Mohammed U, Fulton T, Biswal AK, Dionora J, Chater C, Coe RA, et al. 2018.** Rice with reduced stomatal density conserves water and has improved drought tolerance under future climate conditions. *New Phytologist*.
- Cañamero RC, Boccalandro H, Casal J, Serna L. 2006.** Use of confocal laser as light source reveals stomata-autonomous function. *PLoS one* **1**.
- Cao YR, Liang Y, Tanaka K, Nguyen CT, Jedrzejczak RP, Joachimiak A, Stacey G. 2014.** The kinase LYK5 is a major chitin receptor in Arabidopsis and forms a chitin-induced complex with related kinase CERK1. *Elife* **3**.
- Capoen W, Sun J, Wysham D, Otegui MS, Venkateshwaran M, Hirsch S, Miwa H, Downie JA, Morris RJ, Ane JM, et al. 2011.** Nuclear membranes control symbiotic calcium signaling of legumes. *Proceedings of the National Academy of Sciences of the United States of America* **108**(34): 14348-14353.
- Catanzariti AM, Dodds PN, Ve T, Kobe B, Ellis JG, Staskawicz BJ. 2010.** The AvrM Effector from Flax Rust Has a Structured C-Terminal Domain and Interacts Directly with the M Resistance Protein. *Molecular Plant-Microbe Interactions* **23**(1): 49-57.
- Cesari S. 2018.** Multiple strategies for pathogen perception by plant immune receptors. *New Phytol* **219**(1): 17-24.

- Cesari S, Bernoux M, Moncuquet P, Kroj T, Dodds PN. 2014.** A novel conserved mechanism for plant NLR protein pairs: the "integrated decoy" hypothesis. *Front Plant Sci* **5**: 606.
- Cesari S, Thilliez G, Ribot C, Chalvon V, Michel C, Jauneau A, Rivas S, Alaux L, Kanzaki H, Okuyama Y, et al. 2013.** The rice resistance protein pair RGA4/RGA5 recognizes the *Magnaporthe oryzae* effectors AVR-Pia and AVR1-CO39 by direct binding. *Plant Cell* **25**(4): 1463-1481.
- Charpentier M, Sun JH, Martins TV, Radhakrishnan GV, Findlay K, Soumpourou E, Thouin J, Very AA, Sanders D, Morris RJ, et al. 2016.** Nuclear-localized cyclic nucleotide-gated channels mediate symbiotic calcium oscillations. *Science* **352**(6289): 1102-1105.
- Chater C, Peng K, Movahedi M, Dunn JA, Walker HJ, Liang Y-KK, McLachlan DH, Casson S, Isner JC, Wilson I, et al. 2015.** Elevated CO<sub>2</sub>-Induced Responses in Stomata Require ABA and ABA Signaling. *Current biology : CB*.
- Chen P, Song ZL, Qi YH, Feng XF, Xu NQ, Sun YY, Wu X, Yao X, Mao QY, Li XL, et al. 2012.** Molecular Determinants of Enterovirus 71 Viral Entry CLEFT AROUND GLN-172 ON VP1 PROTEIN INTERACTS WITH VARIABLE REGION ON SCAVENGE RECEPTOR B 2. *Journal of Biological Chemistry* **287**(9): 6406-6420.
- Chen XY, Liu L, Lee E, Han X, Rim Y, Chu H, Kim SW, Sack F, Kim JY. 2009.** The Arabidopsis Callose Synthase Gene GSL8 Is Required for Cytokinesis and Cell Patterning. *Plant physiology* **150**(1): 105-113.
- Chen Y, Hoehenwarter W, Weckwerth W. 2010.** Comparative analysis of phytohormone-responsive phosphoproteins in Arabidopsis thaliana using TiO<sub>2</sub>-phosphopeptide enrichment and mass accuracy precursor alignment. *Plant Journal* **63**(1): 1-17.
- Cheng W, Munkvold KR, Gao H, Mathieu J, Schwizer S, Wang S, Yan YB, Wang J, Martin GB, Chai J. 2011.** Structural analysis of *Pseudomonas syringae* AvrPtoB bound to host BAK1 reveals two similar kinase-interacting domains in a type III Effector. *Cell Host Microbe* **10**(6): 616-626.
- Chinchilla D, Bauer Z, Regenass M, Boller T, Felix G. 2006.** The Arabidopsis receptor kinase FLS2 binds flg22 and determines the specificity of flagellin perception. *The Plant cell* **18**(2): 465-476.
- Chinchilla D, Zipfel C, Robatzek S, Kemmerling B, Nürnberger T, Jones JD, Felix G, Boller T. 2007.** A flagellin-induced complex of the receptor FLS2 and BAK1 initiates plant defence. *Nature* **448**(7152): 497-500.
- Choi WG, Toyota M, Kim SH. 2014.** Salt stress-induced Ca<sup>2+</sup> waves are associated with rapid, long-distance root-to-shoot signaling in plants. *Proceedings of the ...*
- Christie JM. 2007.** Phototropin blue-light receptors. *Annual review of plant biology* **58**: 21-45.
- Cotelle V, Leonhardt N. 2015.** 14-3-3 Proteins in Guard Cell Signaling. *Front Plant Sci* **6**: 1210.
- Couto D, Niebergall R, Liang X, Bucherl CA, Sklenar J, Macho AP, Ntoukakis V, Derbyshire P, Altenbach D, Maclean D, et al. 2016.** The Arabidopsis Protein Phosphatase PP2C38 Negatively Regulates the Central Immune Kinase BIK1. *PLoS Pathog* **12**(8): e1005811.

- Couto D, Zipfel C. 2016.** Regulation of pattern recognition receptor signalling in plants. *Nat Rev Immunol* **16**(9): 537-552.
- Cubero-Font P, Maierhofer T, Jaslan J, Rosales MA, Espartero J, Diaz-Rueda P, Muller HM, Hurter AL, AL-Rasheid KAS, Marten I, et al. 2016.** Silent S-Type Anion Channel Subunit SLAH1 Gates SLAH3 Open for Chloride Root-to-Shoot Translocation. *Current Biology* **26**(16): 2213-2220.
- Dangl JL, Jones JDG. 2001.** Plant pathogens and integrated defence responses to infection. *Nature* **411**(6839): 826-833.
- Dardick C, Schwessinger B, Ronald P. 2012.** Non-arginine-aspartate (non-RD) kinases are associated with innate immune receptors that recognize conserved microbial signatures. *Current opinion in plant biology* **15**(4): 358-366.
- De Angeli A, Zhang J, Meyer S, Martinoia E. 2013.** AtALMT9 is a malate-activated vacuolar chloride channel required for stomatal opening in Arabidopsis. *Nat Commun* **4**: 1804.
- de Boer AH, de Vries-van Leeuwen IJ. 2012.** Fusicocanes: diterpenes with surprising biological functions. *Trends in plant science* **17**(6): 360-368.
- DeFalco TA, Bender KW, Snedden WA. 2010.** Breaking the code: Ca<sup>2+</sup> sensors in plant signalling. *Biochemical Journal* **425**: 27-40.
- Deger AG, Sönke S, Maris N, Justyna K, Hannes K, Mikael B, Serpil U, Marie B, Rainer H, Roelfsema MRG. 2015.** Guard cell SLAC1-type anion channels mediate flagellin-induced stomatal closure. *New Phytologist* **0**.
- DiLaurenzio L, WysockaDiller J, Malamy JE, Pysh L, Helariutta Y, Freshour G, Hahn MG, Feldmann KA, Benfey PN. 1996.** The SCARECROW gene regulates an asymmetric cell division that is essential for generating the radial organization of the Arabidopsis root. *Cell* **86**(3): 423-433.
- Dodds PN, Lawrence GJ, Catanzariti AM, Teh T, Wang CIA, Ayliffe MA, Kobe B, Ellis JG. 2006.** Direct protein interaction underlies gene-for-gene specificity and coevolution of the flax resistance genes and flax rust avirulence genes. *Proceedings of the National Academy of Sciences of the United States of America* **103**(23): 8888-8893.
- Dreyer I, Antunes S, Hoshi T, Muller-Rober B, Palme K, Pongs O, Reintanz B, Hedrich R. 1997.** Plant K<sup>+</sup> channel alpha-subunits assemble indiscriminately. *Biophys J* **72**(5): 2143-2150.
- Dreyer I, Gomez-Porrás JL, Riano-Pachon DM, Hedrich R, Geiger D. 2012.** Molecular evolution of slow and quick anion channels (SLACs and QUACs/ALMTs). *Frontiers in plant science* **3**.
- Edel KH, Kudla J. 2015.** Increasing complexity and versatility: How the calcium signaling toolkit was shaped during plant land colonization. *Cell Calcium* **57**(3): 231-246.
- Emami S, Yee M-CC, Dinneny JR. 2013.** A robust family of Golden Gate Agrobacterium vectors for plant synthetic biology. *Frontiers in plant science* **4**: 339.
- Engler C, Kandzia R, Marillonnet S. 2008.** A one pot, one step, precision cloning method with high throughput capability. *PLoS one* **3**(11).
- Engler C, Youles M, Gruetzner R, Ehnert T-MM, Werner S, Jones JD, Patron NJ, Marillonnet S. 2014.** A Golden Gate Modular Cloning Toolbox for Plants. *ACS synthetic biology*.

- Falhof J, Pedersen JT, Fuglsang AT, Palmgren M. 2016.** Plasma Membrane H<sup>+</sup>-ATPase Regulation in the Center of Plant Physiology. *Molecular Plant* **9**(3): 323-337.
- Feng F, Yang F, Rong W, Wu X, Zhang J, Chen S, He C, Zhou J-MM. 2012.** A Xanthomonas uridine 5'-monophosphate transferase inhibits plant immune kinases. *Nature* **485**(7396): 114-118.
- Feng F, Yang F, Rong W, Wu X, Zhang J, Chen S, He C, Zhou JM. 2012.** A Xanthomonas uridine 5'-monophosphate transferase inhibits plant immune kinases. *Nature* **485**(7396): 114-118.
- Feng F, Zhou JM. 2012.** Plant-bacterial pathogen interactions mediated by type III effectors. *Curr Opin Plant Biol* **15**(4): 469-476.
- Flor HH. 1971.** Current Status of the Gene-For-Gene Concept. *Annual review of phytopathology* **9**: 275-296.
- Frey A, Effroy D, Lefebvre V, Seo M, Perreau F, Berger A, Sechet J, To A, North HM, Marion-Poll A. 2012.** Epoxy-carotenoid cleavage by NCED5 fine-tunes ABA accumulation and affects seed dormancy and drought tolerance with other NCED family members. *Plant J* **70**(3): 501-512.
- Frey N, Mbengue M, Kwaaitaal M, Nitsch L, Altenbach D, Haweker H, Lozano-Duran R, Njo MF, Beeckman T, Huettel B, et al. 2012.** Plasma Membrane Calcium ATPases Are Important Components of Receptor-Mediated Signaling in Plant Immune Responses and Development. *Plant physiology* **159**(2): 798-+.
- Fritz-Laylin LK, Krishnamurthy N, Tor M, Sjolander KV, Jones JD. 2005.** Phylogenomic analysis of the receptor-like proteins of rice and Arabidopsis. *Plant Physiol* **138**(2): 611-623.
- Fujii H, Verslues PE, Zhu JK. 2007.** Identification of two protein kinases required for abscisic acid regulation of seed germination, root growth, and gene expression in Arabidopsis. *Plant Cell* **19**(2): 485-494.
- Fujita Y, Nakashima K, Yoshida T, Katagiri T, Kidokoro S, Kanamori N, Umezawa T, Fujita M, Maruyama K, Ishiyama K, et al. 2009.** Three SnRK2 Protein Kinases are the Main Positive Regulators of Abscisic Acid Signaling in Response to Water Stress in Arabidopsis. *Plant and Cell Physiology* **50**(12): 2123-2132.
- Furihata T, Maruyama K, Fujita Y, Umezawa T, Yoshida R, Shinozaki K, Yamaguchi-Shinozaki K. 2006.** Abscisic acid-dependent multisite phosphorylation regulates the activity of a transcription activator AREB1. *Proceedings of the National Academy of Sciences of the United States of America* **103**(6): 1988-1993.
- Galbiati M, Simoni L, Pavesi G, Cominelli E, Francia P, vavasseur A, Nelson T, Bevan M, Tonelli C. 2008.** Gene trap lines identify Arabidopsis genes expressed in stomatal guard cells. *The Plant Journal* **53**(5): 750-762.
- Gao MH, Liu JM, Bi DL, Zhang ZB, Cheng F, Chen SF, Zhang YL. 2008.** MEKK1, MKK1/MKK2 and MPK4 function together in a mitogen-activated protein kinase cascade to regulate innate immunity in plants. *Cell Research* **18**(12): 1190-1198.
- Geiger D, Maierhofer T, AL-Rasheid KAS, Scherzer S, Mumm P, Liese A, Ache P, Wellmann C, Marten I, Grill E, et al. 2011.** Stomatal Closure by Fast Abscisic Acid Signaling Is Mediated by the Guard Cell Anion Channel SLAH3 and the Receptor RCAR1. *Science signaling* **4**(173).

- Geiger D, Scherzer S, Mumm P, Marten I, Ache P, Matschi S, Liese A, Wellmann C, Al-Rasheid KAS, Grill E, et al. 2010.** Guard cell anion channel SLAC1 is regulated by CDPK protein kinases with distinct Ca<sup>2+</sup> affinities. *Proceedings of the National Academy of Sciences of the United States of America* **107**(17): 8023-8028.
- Geiger D, Scherzer S, Mumm P, Stange A, Marten I, Bauer H, Ache P, Matschi S, Liese A, Al-Rasheid KA, et al. 2009.** Activity of guard cell anion channel SLAC1 is controlled by drought-stress signaling kinase-phosphatase pair. *Proceedings of the National Academy of Sciences of the United States of America* **106**(50): 21425-21430.
- Geisler M, Nadeau J, Sack FD. 2000.** Oriented asymmetric divisions that generate the stomatal spacing pattern in Arabidopsis are disrupted by the too many mouths mutation. *Plant Cell* **12**(11): 2075-2086.
- Gilroy S, Fricker MD, Read ND, Trewayas AJ. 1991.** Role of Calcium in Signal Transduction of Commelina Guard-Cells. *Plant Cell* **3**(4): 333-344.
- Gimenez-Ibanez S, Boter M, Fernandez-Barbero G, Chini A, Rathjen JP, Solano R. 2014.** The Bacterial Effector HopX1 Targets JAZ Transcriptional Repressors to Activate Jasmonate Signaling and Promote Infection in Arabidopsis. *PLoS biology* **12**(2).
- Gimenez-Ibanez S, Hann DR, Ntoukakis V, Petutschnig E, Lipka V, Rathjen JP. 2009.** AvrPtoB targets the LysM receptor kinase CERK1 to promote bacterial virulence on plants. *Curr Biol* **19**(5): 423-429.
- Goh T, Joi S, Mimura T, Fukaki H. 2012.** The establishment of asymmetry in Arabidopsis lateral root founder cells is regulated by LBD16/ASL18 and related LBD/ASL proteins. *Development* **139**(5): 883-893.
- Gohre V, Spallek T, Hawecker H, Mersmann S, Mentzel T, Boller T, de Torres M, Mansfield JW, Robatzek S. 2008.** Plant pattern-recognition receptor FLS2 is directed for degradation by the bacterial ubiquitin ligase AvrPtoB. *Curr Biol* **18**(23): 1824-1832.
- Gomez-Gomez L, Bauer Z, Boller T. 2001.** Both the extracellular leucine-rich repeat domain and the kinase activity of FSL2 are required for flagellin binding and signaling in Arabidopsis. *Plant Cell* **13**(5): 1155-1163.
- Gómez-Gómez L, Bauer Z, Boller T. 2001.** Both the extracellular leucine-rich repeat domain and the kinase activity of FSL2 are required for flagellin binding and signaling in Arabidopsis. *The Plant cell* **13**(5): 1155-1163.
- Gómez-Gómez L, Boller T. 2000.** FLS2: an LRR receptor-like kinase involved in the perception of the bacterial elicitor flagellin in Arabidopsis. *Molecular cell* **5**(6): 1003-1011.
- Gray JE, Holroyd GH, van der Lee FM, Bahrami AR, Sijmons PC, Woodward FI, Schuch W, Hetherington AM. 2000.** The HIC signalling pathway links CO<sub>2</sub> perception to stomatal development. *Nature* **408**(6813): 713-716.
- Guseman JM, Lee JS, Bogenschutz NL, Peterson KM, Virata RE, Xie B, Kanaoka MM, Hong Z, Torii KU. 2010.** Dysregulation of cell-to-cell connectivity and stomatal patterning by loss-of-function mutation in Arabidopsis chorus (glucan synthase-like 8). *Development (Cambridge, England)* **137**(10): 1731-1741.
- Gust AA, Pruitt R, Nurnberger T. 2017.** Sensing Danger: Key to Activating Plant Immunity. *Trends Plant Sci* **22**(9): 779-791.
- Halford N, Hardie DG. 1998.** SNF1-related protein kinases: global regulators of carbon metabolism in plants? *Plant molecular biology* **37**(5): 735-748.

- Halter T, Imkamp J, Mazzotta S, Wierzba M, Postel S, Bücherl C, Kiefer C, Stahl M, Chinchilla D, Wang X, et al. 2014.** The leucine-rich repeat receptor kinase BIR2 is a negative regulator of BAK1 in plant immunity. *Current biology : CB* **24**(2): 134-143.
- Hamel LP, Nicole MC, Sritubtim S, Morency MJ, Ellis M, Ehltng J, Beaudoin N, Barbazuk B, Klessig D, Lee J, et al. 2006.** Ancient signals: comparative genomics of plant MAPK and MAPKK gene families. *Trends in plant science* **11**(4): 192-198.
- Hao H, Fan L, Chen T, Li R, Li X, He Q, Botella MA, Lin J. 2014.** Clathrin and Membrane Microdomains Cooperatively Regulate RbohD Dynamics and Activity in Arabidopsis. *Plant Cell* **26**(4): 1729-1745.
- Hara K, Kajita R, Torii KU, Bergmann DC, Kakimoto T. 2007.** The secretory peptide gene EPF1 enforces the stomatal one-cell-spacing rule. *Genes & development* **21**(14): 1720-1725.
- Harrison MT, Tardieu F, Dong ZS, Messina CD, Hammer GL. 2014.** Characterizing drought stress and trait influence on maize yield under current and future conditions. *Global Change Biology* **20**(3): 867-878.
- Haruta M, Gray WM, Sussman MR. 2015.** Regulation of the plasma membrane proton pump (H<sup>+</sup>-ATPase) by phosphorylation. *Current opinion in plant biology* **28**: 68-75.
- Hayashi M, Inoue S, Ueno Y, Kinoshita T. 2017.** A Raf-like protein kinase BHP mediates blue light-dependent stomatal opening. *Scientific Reports* **7**.
- Hayashi M, Kinoshita T. 2011.** Crosstalk between blue-light- and ABA-signaling pathways in stomatal guard cells. *Plant Signal Behav* **6**(11): 1662-1664.
- Hayashi Y, Takahashi K, Inoue S, Kinoshita T. 2014.** Abscisic Acid Suppresses Hypocotyl Elongation by Dephosphorylating Plasma Membrane H<sup>+</sup>-ATPase in Arabidopsis thaliana. *Plant and Cell Physiology* **55**(4): 845-853.
- Hedrich HJ, Fangmann J, Reetz IC, Kloting I, Hansen AK, Wonigeit K. 1990.** Genetic-Characterization of Different Diabetes-Prone and Diabetes-Resistant Bb-Rat Strains with Special Reference to Rt6. *Transplantation Proceedings* **22**(6): 2570-2571.
- Heese A, Hann DR, Gimenez-Ibanez S, Jones AM, He K, Li J, Schroeder JI, Peck SC, Rathjen JP. 2007.** The receptor-like kinase SERK3/BAK1 is a central regulator of innate immunity in plants. *Proceedings of the National Academy of Sciences of the United States of America* **104**(29): 12217-12222.
- Henry E, Toruno TY, Jauneau A, Deslandes L, Coaker G. 2017.** Direct and Indirect Visualization of Bacterial Effector Delivery into Diverse Plant Cell Types during Infection. *Plant Cell* **29**(7): 1555-+.
- Hille B. 2001.** *Ion channels of excitable membranes*. Sunderland, Mass.: Sinauer.
- Homann U, Thiel G. 1999.** Unitary exocytotic and endocytotic events in guard-cell protoplasts during osmotically driven volume changes. *FEBS letters* **460**(3): 495-499.
- Horak H, Sierla M, Toldsepp K, Wang C, Wang YS, Nuhkat M, Valk E, Pechter P, Merilo E, Salojarvi J, et al. 2016.** A Dominant Mutation in the HT1 Kinase Uncovers Roles of MAP Kinases and GHR1 in CO<sub>2</sub>-Induced Stomatal Closure. *Plant Cell* **28**(10): 2493-2509.
- Hosy E, Vavasseur A, Mouline K, Dreyer I, Gaymard F, Poree F, Boucherez J, Lebaudy A, Bouchez D, Very AA, et al. 2003.** The Arabidopsis outward K<sup>+</sup> channel GORK is

- involved in regulation of stomatal movements and plant transpiration. *Proc Natl Acad Sci U S A* **100**(9): 5549-5554.
- Hothorn M, Belkhadir Y, Dreux M, Dabi T, Noel JP, Wilson IA, Chory J. 2011.** Structural basis of steroid hormone perception by the receptor kinase BRI1. *Nature* **474**(7352): 467-471.
- Hrabak EM, Chan CW, Gribskov M, Harper JF, Choi JH, Halford N, Kudla J, Luan S, Nimmo HG, Sussman MR, et al. 2003.** The Arabidopsis CDPK-SnRK superfamily of protein kinases. *Plant physiology* **132**(2): 666-680.
- Hu HH, Boisson-Dernier A, Israelsson-Nordstrom M, Bohmer M, Xue SW, Ries A, Godoski J, Kuhn JM, Schroeder JI. 2010.** Carbonic anhydrases are upstream regulators of CO<sub>2</sub>-controlled stomatal movements in guard cells. *Nature Cell Biology* **12**(1): 87-U234.
- Hua DP, Wang C, He JN, Liao H, Duan Y, Zhu ZQ, Guo Y, Chen ZZ, Gong ZZ. 2012.** A Plasma Membrane Receptor Kinase, GHR1, Mediates Abscisic Acid- and Hydrogen Peroxide-Regulated Stomatal Movement in Arabidopsis. *Plant Cell* **24**(6): 2546-2561.
- Hurley B, Lee D, Mott A, Wilton M, Liu J, Liu YC, Angers S, Coaker G, Guttman DS, Desveaux D. 2014.** The *Pseudomonas syringae* Type III Effector HopF2 Suppresses Arabidopsis Stomatal Immunity. *PLoS one* **9**(12).
- Ichimura K, Shinozaki K, Tena G, Sheen J, Henry Y, Champion A, Kreis M, Zhang S, Hirt H, Wilson C, et al. 2002.** Mitogen-activated protein kinase cascades in plants: a new nomenclature. *Trends in plant science* **7**(7): 301-308.
- Imes D, Mumm P, Böhm J, Al-Rasheid KA, Marten I, Geiger D, Hedrich R. 2013.** Open stomata 1 (OST1) kinase controls R-type anion channel QUAC1 in Arabidopsis guard cells. *The Plant journal : for cell and molecular biology* **74**(3): 372-382.
- Inoue H, Hayashi N, Matsushita A, Liu XQ, Nakayama A, Sugano S, Jiang CJ, Takatsuji H. 2013.** Blast resistance of CC-NB-LRR protein Pb1 is mediated by WRKY45 through protein-protein interaction. *Proceedings of the National Academy of Sciences of the United States of America* **110**(23): 9577-9582.
- Inoue S, Kinoshita T, Matsumoto M, Nakayama KI, Doi M, Shimazaki K. 2008.** Blue light-induced autophosphorylation of phototropin is a primary step for signaling. *Proceedings of the National Academy of Sciences of the United States of America* **105**(14): 5626-5631.
- Inoue S, Takahashi K, Okumura-Noda H, Kinoshita T. 2016.** Auxin Influx Carrier AUX1 Confers Acid Resistance for Arabidopsis Root Elongation Through the Regulation of Plasma Membrane H<sup>+</sup>-ATPase. *Plant and Cell Physiology* **57**(10): 2194-2201.
- Iyer LM, Koonin EV, Aravind L. 2001.** Adaptations of the helix-grip fold for ligand binding and catalysis in the START domain superfamily. *Proteins-Structure Function and Genetics* **43**(2): 134-144.
- Jahn T, Fuglsang AT, Olsson A, Bruntrup IM, Collinge DB, Volkmann D, Sommarin M, Palmgren MG, Larsson C. 1997.** The 14-3-3 protein interacts directly with the C-terminal region of the plant plasma membrane H<sup>+</sup>-ATPase. *Plant Cell* **9**(10): 1805-1814.
- Jalakas P, Yarmolinsky D, Kollist H, Brosche M. 2017.** Isolation of Guard-cell Enriched Tissue for RNA Extraction. *Bio-protocol* **7**(15): e2447.

- Jane B, Michael AV, Michael RB. 1997.** The effect of elevated CO<sub>2</sub> concentrations on K<sup>+</sup> and anion channels of *Vicia faba* L. guard cells. *Planta* **203**(2).
- Jia Y, McAdams SA, Bryan GT, Hershey HP, Valent B. 2000.** Direct interaction of resistance gene and avirulence gene products confers rice blast resistance. *Embo Journal* **19**(15): 4004-4014.
- Jiang SS, Yao J, Ma KW, Zhou HB, Song JK, He SY, Ma WB. 2013.** Bacterial Effector Activates Jasmonate Signaling by Directly Targeting JAZ Transcriptional Repressors. *Plos Pathogens* **9**(10).
- Jossier M, Kroniewicz L, Dalmas F, Le Thiec D, Ephritikhine G, Thomine S, Barbier-Brygoo H, Vavasseur A, Filleur S, Leonhardt N. 2010.** The Arabidopsis vacuolar anion transporter, AtCLC<sub>c</sub>, is involved in the regulation of stomatal movements and contributes to salt tolerance. *Plant J* **64**(4): 563-576.
- Kadota Y, Sklenar J, Derbyshire P, Stransfeld L, Asai S, Ntoukakis V, Jones JD, Shirasu K, Menke F, Jones A, et al. 2014.** Direct regulation of the NADPH oxidase RBOHD by the PRR-associated kinase BIK1 during plant immunity. *Molecular cell* **54**(1): 43-55.
- Kanaoka MM, Pillitteri LJ, Fujii H, Yoshida Y, Bogenschutz NL, Takabayashi J, Zhu JK, Torii KU. 2008.** SCREAM/ICE1 and SCREAM2 specify three cell-state transitional steps leading to Arabidopsis stomatal differentiation. *Plant Cell* **20**(7): 1775-1785.
- Kinoshita T, Doi M, Suetsugu N, Kagawa T, Wada M, Shimazaki K. 2001.** phot1 and phot2 mediate blue light regulation of stomatal opening. *Nature* **414**(6864): 656-660.
- Kobayashi M, Ohura I, Kawakita K, Yokota N, Fujiwara M, Shimamoto K, Doke N, Yoshioka H. 2007.** Calcium-dependent protein kinases regulate the production of reactive oxygen species by potato NADPH oxidase. *Plant Cell* **19**(3): 1065-1080.
- Koers S, Guzel-Deger A, Marten I, Roelfsema MR. 2011.** Barley mildew and its elicitor chitosan promote closed stomata by stimulating guard-cell S-type anion channels. *Plant J* **68**(4): 670-680.
- Kolb HA, Marten I, Hedrich R. 1995.** Hodgkin-Huxley Analysis of a Gcac1 Anion Channel in the Plasma-Membrane of Guard-Cells. *Journal of Membrane Biology* **146**(3): 273-282.
- Kollist H, Jossier M, Laanemets K, Thomine S. 2011.** Anion channels in plant cells. *Febs Journal* **278**(22): 4277-4292.
- Kong Q, Sun TJ, Qu N, Ma JL, Li M, Cheng YT, Zhang Q, Wu D, Zhang ZB, Zhang YL. 2016.** Two Redundant Receptor-Like Cytoplasmic Kinases Function Downstream of Pattern Recognition Receptors to Regulate Activation of SA Biosynthesis. *Plant physiology* **171**(2): 1344-1354.
- Koornneef M, Jorna ML, Brinkhorst-van der Swan DL, Karssen CM. 1982.** The isolation of abscisic acid (ABA) deficient mutants by selection of induced revertants in non-germinating gibberellin sensitive lines of *Arabidopsis thaliana* (L.) heynh. *Theor Appl Genet* **61**(4): 385-393.
- Koornneef M, Reuling G, Karssen CM. 1984.** The Isolation and Characterization of Abscisic-Acid Insensitive Mutants of *Arabidopsis-Thaliana*. *Physiologia Plantarum* **61**(3): 377-383.
- Kroj T, Chanclud E, Michel-Romiti C, Grand X, Morel JB. 2016.** Integration of decoy domains derived from protein targets of pathogen effectors into plant immune receptors is widespread. *New Phytol* **210**(2): 618-626.

- Kwaaitaal M, Huisman R, Maintz J, Reinstadler A, Panstruga R. 2011.** Ionotropic glutamate receptor (iGluR)-like channels mediate MAMP-induced calcium influx in *Arabidopsis thaliana*. *Biochemical Journal* **440**(3): 355-365.
- Lange OL, Losch R, Schulze ED, Kappen L. 1971.** Responses of Stomata to Changes in Humidity. *Planta* **100**(1): 76-&.
- Larson ER, Van Zelm E, Roux C, Marion-Poll A, Blatta MR. 2017.** Clathrin Heavy Chain Subunits Coordinate Endo- and Exocytic Traffic and Affect Stomatal Movement. *Plant physiology* **175**(2): 708-720.
- Lawson T, Simkin AJ, Kelly G, Granot D. 2014.** Mesophyll photosynthesis and guard cell metabolism impacts on stomatal behaviour. *New Phytologist* **203**(4): 1064-1081.
- Le Roux C, Huet G, Jauneau A, Camborde L, Tremousaygue D, Kraut A, Zhou B, Levailant M, Adachi H, Yoshioka H, et al. 2015.** A receptor pair with an integrated decoy converts pathogen disabling of transcription factors to immunity. *Cell* **161**(5): 1074-1088.
- Lebaudy A, Hosy E, Simonneau T, Sentenac H, Thibaud JB, Dreyer I. 2008.** Heteromeric K<sup>+</sup> channels in plants. *Plant Journal* **54**(6): 1076-1082.
- Lebaudy A, Very AA, Sentenac H. 2007.** K<sup>+</sup> channel activity in plants: genes, regulations and functions. *FEBS Lett* **581**(12): 2357-2366.
- Lecourieux D, Ranjeva R, Pugin A. 2006.** Calcium in plant defence-signalling pathways. *New Phytol* **171**(2): 249-269.
- Lee D, Bourdais G, Yu G, Robatzek S, Coaker G. 2015.** Phosphorylation of the Plant Immune Regulator RPM1-INTERACTING PROTEIN4 Enhances Plant Plasma Membrane H<sup>+</sup>-ATPase Activity and Inhibits Flagellin-Triggered Immune Responses in *Arabidopsis*. *Plant Cell* **27**(7): 2042-2056.
- Lee JS, Kuroha T, Hnilova M, Khatayevich D, Kanaoka MM, McAbee JM, Sarikaya M, Tamerler C, Torii KU. 2012.** Direct interaction of ligand-receptor pairs specifying stomatal patterning. *Genes Dev* **26**(2): 126-136.
- Lee SC, Lan WZ, Buchanan BB, Luan S. 2009.** A protein kinase-phosphatase pair interacts with an ion channel to regulate ABA signaling in plant guard cells. *Proceedings of the National Academy of Sciences of the United States of America* **106**(50): 21419-21424.
- Leon-Kloosterziel KM, Gil MA, Ruijs GJ, Jacobsen SE, Olszewski NE, Schwartz SH, Zeevaart JA, Koornneef M. 1996.** Isolation and characterization of abscisic acid-deficient *Arabidopsis* mutants at two new loci. *Plant J* **10**(4): 655-661.
- Leung J, Bouvier-Durand M, Morris PC, Guerrier D, Cheddor F, Giraudat J. 1994.** *Arabidopsis* ABA response gene ABI1: features of a calcium-modulated protein phosphatase. *Science (New York, N.Y.)* **264**(5164): 1448-1452.
- Levchenko V, Konrad KR, Dietrich P, Roelfsema MRG, Hedrich R. 2005.** Cytosolic abscisic acid activates guard cell anion channels without preceding Ca<sup>2+</sup> signals. *Proceedings of the National Academy of Sciences of the United States of America* **102**(11): 4203-4208.
- Lewis JD, Lee AH, Hassan JA, Wan J, Hurley B, Jhingree JR, Wang PW, Lo T, Youn JY, Guttman DS, et al. 2013.** The *Arabidopsis* ZED1 pseudokinase is required for ZAR1-mediated immunity induced by the *Pseudomonas syringae* type III effector HopZ1a. *Proc Natl Acad Sci U S A* **110**(46): 18722-18727.

- Leyman B, Geelen D, Quintero FJ, Blatt MR. 1999.** A tobacco syntaxin with a role in hormonal control of guard cell ion channels. *Science* **283**(5401): 537-540.
- Li F, Wang J, Ma CL, Zhao YX, Wang YC, Hasi A, Qi Z. 2013.** Glutamate Receptor-Like Channel3.3 Is Involved in Mediating Glutathione-Triggered Cytosolic Calcium Transients, Transcriptional Changes, and Innate Immunity Responses in Arabidopsis. *Plant physiology* **162**(3): 1497-1509.
- Li L, Kim P, Yu L, Cai G, Chen S, Alfano JR, Zhou JM. 2016.** Activation-Dependent Destruction of a Co-receptor by a *Pseudomonas syringae* Effector Dampens Plant Immunity. *Cell Host Microbe* **20**(4): 504-514.
- Li L, Li M, Yu L, Zhou Z, Liang X, Liu Z, Cai G, Gao L, Zhang X, Wang Y, et al. 2014.** The FLS2-associated kinase BIK1 directly phosphorylates the NADPH oxidase RbohD to control plant immunity. *Cell Host Microbe* **15**(3): 329-338.
- Liang XX, Zhou JM. 2018.** Receptor-Like Cytoplasmic Kinases: Central Players in Plant Receptor Kinase-Mediated Signaling. *Annual Review of Plant Biology, Vol 69* **69**: 267-299.
- Liebrand TWH, van den Burg HA, Joosten MHAJ. 2014.** Two for all: receptor-associated kinases SOBIR1 and BAK1. *Trends in plant science* **19**(2): 123-132.
- Lin W, Ma X, Shan L, He P. 2013.** Big roles of small kinases: the complex functions of receptor-like cytoplasmic kinases in plant immunity and development. *J Integr Plant Biol* **55**(12): 1188-1197.
- Linder B, Raschke K. 1992.** A Slow Anion Channel in Guard-Cells, Activating at Large Hyperpolarization, May Be Principal for Stomatal Closing. *FEBS letters* **313**(1): 27-30.
- Liu J, Elmore JM, Fuglsang AT, Palmgren MG, Staskawicz BJ, Coaker G. 2009.** RIN4 functions with plasma membrane H<sup>+</sup>-ATPases to regulate stomatal apertures during pathogen attack. *PLoS Biol* **7**(6): e1000139.
- Liu J, Elmore JM, Lin ZJ, Coaker G. 2011.** A receptor-like cytoplasmic kinase phosphorylates the host target RIN4, leading to the activation of a plant innate immune receptor. *Cell Host Microbe* **9**(2): 137-146.
- Liu TT, Liu ZX, Song CJ, Hu YF, Han ZF, She J, Fan FF, Wang JW, Jin CW, Chang JB, et al. 2012.** Chitin-Induced Dimerization Activates a Plant Immune Receptor. *Science* **336**(6085): 1160-1164.
- Liu Z, Wu Y, Yang F, Zhang Y, Chen S, Xie Q, Tian X, Zhou JM. 2013.** BIK1 interacts with PEPRs to mediate ethylene-induced immunity. *Proc Natl Acad Sci U S A* **110**(15): 6205-6210.
- Lozano-Duran R, Bourdais G, He SY, Robatzek S. 2014.** The bacterial effector HopM1 suppresses PAMP-triggered oxidative burst and stomatal immunity. *New Phytologist* **202**(1): 259-269.
- Lu D, Lin W, Gao X, Wu S, Cheng C, Avila J, Heese A, Devarenne TP, He P, Shan L. 2011.** Direct ubiquitination of pattern recognition receptor FLS2 attenuates plant innate immunity. *Science (New York, N.Y.)* **332**(6036): 1439-1442.
- Lu D, Wu S, Gao X, Zhang Y, He P. 2010.** A receptor-like cytoplasmic kinase, BIK1, associates with a flagellin receptor complex to initiate plant innate immunity. *Proceedings of the National Academy of Sciences of the United States of America* **107**(1): 496-501.

- Lu D, Wu S, Gao X, Zhang Y, Shan L, He P. 2010.** A receptor-like cytoplasmic kinase, BIK1, associates with a flagellin receptor complex to initiate plant innate immunity. *Proc Natl Acad Sci U S A* **107**(1): 496-501.
- Lukasik E, Takken FLW. 2009.** STANDING strong, resistance proteins instigators of plant defence. *Current opinion in plant biology* **12**(4): 427-436.
- Ma X, Xu G, He P, Shan L. 2016.** SERKING Coreceptors for Receptors. *Trends Plant Sci* **21**(12): 1017-1033.
- Ma Y, Szostkiewicz I, Korte A, Moes D, Yang Y, Christmann A, Grill E. 2009.** Regulators of PP2C phosphatase activity function as abscisic acid sensors. *Science (New York, N.Y.)* **324**(5930): 1064-1068.
- MacAlister CA, Ohashi-Ito K, Bergmann DC. 2007.** Transcription factor control of asymmetric cell divisions that establish the stomatal lineage. *Nature* **445**(7127): 537-540.
- Macho AP, Schwessinger B, Ntoukakis V, Brutus A, Segonzac C, Roy S, Kadota Y, Oh MH, Sklenar J, Derbyshire P, et al. 2014.** A bacterial tyrosine phosphatase inhibits plant pattern recognition receptor activation. *Science* **343**(6178): 1509-1512.
- Macho AP, Zipfel C. 2014.** Plant PRRs and the Activation of Innate Immune Signaling. *Molecular cell* **54**(2): 263-272.
- Macho AP, Zipfel C. 2014.** Plant PRRs and the activation of innate immune signaling. *Mol Cell* **54**(2): 263-272.
- Mackey D, Belkhadir Y, Alonso JM, Ecker JR, Dangl JL. 2003.** Arabidopsis RIN4 is a target of the type III virulence effector AvrRpt2 and modulates RPS2-mediated resistance. *Cell* **112**(3): 379-389.
- Mackey D, Holt BF, 3rd, Wiig A, Dangl JL. 2002.** RIN4 interacts with *Pseudomonas syringae* type III effector molecules and is required for RPM1-mediated resistance in Arabidopsis. *Cell* **108**(6): 743-754.
- Maffi D, Bassi M, Brambilla A, Conti CG. 1998.** Possible role of chitosan in the interaction between barley and *Erysiphe graminis* after tetraconazole treatment. *Mycological Research* **102**: 599-606.
- Maierhofer T, Diekmann M, Offenborn JN, Lind C, Bauer H, Hashimoto K, Al-Rasheid KAS, Luan S, Kudla J, Geiger D, et al. 2014.** Site- and kinase-specific phosphorylation-mediated activation of SLAC1, a guard cell anion channel stimulated by abscisic acid. *Science signaling* **7**(342).
- Maqbool A, Saitoh H, Franceschetti M, Stevenson CE, Uemura A, Kanzaki H, Kamoun S, Terauchi R, Banfield MJ. 2015.** Structural basis of pathogen recognition by an integrated HMA domain in a plant NLR immune receptor. *Elife* **4**.
- Marten H, Konrad KR, Dietrich P, Roelfsema MRG, Hedrich R. 2007.** Ca<sup>2+</sup>-dependent and -independent abscisic acid activation of plasma membrane anion channels in guard cells of *Nicotiana tabacum*. *Plant physiology* **143**(1): 28-37.
- Marten I, Deeken R, Hedrich R, Roelfsema MRG. 2010.** Light-induced modification of plant plasma membrane ion transport. *Plant Biology* **12**: 64-79.
- Matrosova A, Bogireddi H, Mateo-Penas A, Hashimoto-Sugimoto M, Iba K, Schroeder JI, Israelsson-Nordstrom M. 2015.** The HT1 protein kinase is essential for red light-induced stomatal opening and genetically interacts with OST1 in red light and CO<sub>2</sub>-induced stomatal movement responses. *New Phytologist* **208**(4): 1126-1137.

- Mbengue M, Bourdais G, Gervasi F, Beck M, Zhou J, Spallek T, Bartels S, Boller T, Ueda T, Kuhn H, et al. 2016.** Clathrin-dependent endocytosis is required for immunity mediated by pattern recognition receptor kinases. *Proceedings of the National Academy of Sciences of the United States of America* **113**(39): 11034-11039.
- Mcainsh MR, Brownlee C, Hetherington AM. 1990.** Abscisic Acid-Induced Elevation of Guard-Cell Cytosolic Ca-2+ Precedes Stomatal Closure. *Nature* **343**(6254): 186-188.
- Meckel T, Gall L, Semrau S, Homann U, Thiel G. 2007.** Guard cells elongate: relationship of volume and surface area during stomatal movement. *Biophys J* **92**(3): 1072-1080.
- Melcher K, Ng LM, Zhou XE, Soon FF, Xu Y, Suino-Powell KM, Park SY, Weiner JJ, Fujii H, Chinnusamy V, et al. 2009.** A gate-latch-lock mechanism for hormone signalling by abscisic acid receptors. *Nature* **462**(7273): 602-U672.
- Melotto M, Underwood W, Koczan J, Nomura K, He SY. 2006.** Plant stomata function in innate immunity against bacterial invasion. *Cell* **126**(5): 969-980.
- Meng X, Chen X, Mang H, Liu C, Yu X, Gao X, Torii KU, He P, Shan L. 2015.** Differential Function of Arabidopsis SERK Family Receptor-like Kinases in Stomatal Patterning. *Curr Biol* **25**(18): 2361-2372.
- Meng X, Xu J, He Y, Yang KY, Mordorski B, Liu Y, Zhang S. 2013.** Phosphorylation of an ERF transcription factor by Arabidopsis MPK3/MPK6 regulates plant defense gene induction and fungal resistance. *Plant Cell* **25**(3): 1126-1142.
- Meng XZ, Zhang SQ. 2013.** MAPK Cascades in Plant Disease Resistance Signaling. *Annual Review of Phytopathology, Vol 51* **51**: 245-266.
- Merilo E, Laanemets K, Hu H, Xue S, Jakobson L, Tulva I, Gonzalez-Guzman M, Rodriguez PL, Schroeder JI, Brosche M, et al. 2013.** PYR/RCAR receptors contribute to ozone-, reduced air humidity-, darkness-, and CO<sub>2</sub>-induced stomatal regulation. *Plant Physiol* **162**(3): 1652-1668.
- Merlot S, Leonhardt N, Fenzi F, Valon C, Costa M, Piette L, Vavasseur A, Genty B, Boivin K, Muller A, et al. 2007.** Constitutive activation of a plasma membrane H<sup>+</sup>-ATPase prevents abscisic acid-mediated stomatal closure. *Embo Journal* **26**(13): 3216-3226.
- Meszaros T, Helfer A, Hatzimasoura E, Magyar Z, Serazetdinova L, Rios G, Bardoczky V, Teige M, Koncz C, Peck S, et al. 2006.** The Arabidopsis MAP kinase kinase MKK1 participates in defence responses to the bacterial elicitor flagellin. *Plant Journal* **48**(4): 485-498.
- Meyer K, Leube MP, Grill E. 1994.** A Protein Phosphatase 2c Involved in ABA Signal-Transduction in Arabidopsis-Thaliana. *Science* **264**(5164): 1452-1455.
- Meyer S, Mumm P, Imes D, Endler A, Weder B, Al-Rasheid KAS, Geiger D, Marten I, Martinoia E, Hedrich R. 2010.** AtALMT12 represents an R-type anion channel required for stomatal movement in Arabidopsis guard cells. *Plant Journal* **63**(6): 1054-1062.
- Miller G, Schlauch K, Tam R, Cortes D, Torres MA, Shulaev V, Dangl JL, Mittler R. 2009.** The plant NADPH oxidase RBOHD mediates rapid systemic signaling in response to diverse stimuli. *Science signaling* **2**(84).
- Miyazono K, Miyakawa T, Sawano Y, Kubota K, Kang HJ, Asano A, Miyauchi Y, Takahashi M, Zhi Y, Fujita Y, et al. 2009.** Structural basis of abscisic acid signalling. *Nature* **462**(7273): 609-614.

- Montillet J-LL, Leonhardt N, Mondy S, Tranchimand S, Rumeau D, Boudsocq M, Garcia AV, Douki T, Bigeard J, Laurière C, et al. 2013.** An abscisic acid-independent oxylipin pathway controls stomatal closure and immune defense in Arabidopsis. *PLoS biology* **11**(3).
- Morth JP, Pedersen BP, Buch-Pedersen MJ, Andersen JP, Vilsen B, Palmgren MG, Nissen P. 2011.** A structural overview of the plasma membrane Na<sup>+</sup>, K<sup>+</sup>-ATPase and H<sup>+</sup>-ATPase ion pumps. *Nature Reviews Molecular Cell Biology* **12**(1): 60-70.
- Mott KA. 2009.** Opinion: Stomatal responses to light and CO<sub>2</sub> depend on the mesophyll. *Plant Cell and Environment* **32**(11): 1479-1486.
- Mott KA, Sibbersen ED, Shope JC. 2008.** The role of the mesophyll in stomatal responses to light and CO<sub>2</sub>. *Plant Cell and Environment* **31**(9): 1299-1306.
- Mucyn TS, Clemente A, Andriotis VM, Balmuth AL, Oldroyd GE, Staskawicz BJ, Rathjen JP. 2006.** The tomato NBARC-LRR protein Prf interacts with Pto kinase in vivo to regulate specific plant immunity. *Plant Cell* **18**(10): 2792-2806.
- Mustilli A-CC, Merlot S, Vavasseur A, Fenzi F, Giraudat J. 2002.** Arabidopsis OST1 protein kinase mediates the regulation of stomatal aperture by abscisic acid and acts upstream of reactive oxygen species production. *The Plant cell* **14**(12): 3089-3099.
- Na JK, Metzger JD. 2014.** Chimeric promoter mediates guard cell-specific gene expression in tobacco under water deficit. *Biotechnol Lett* **36**(9): 1893-1899.
- Narusaka M, Shirasu K, Noutoshi Y, Kubo Y, Shiraishi T, Iwabuchi M, Narusaka Y. 2009.** RRS1 and RPS4 provide a dual Resistance-gene system against fungal and bacterial pathogens. *Plant J* **60**(2): 218-226.
- Negi J, Matsuda O, Nagasawa T, Oba Y, Takahashi H, Kawai-Yamada M, Uchimiya H, Hashimoto M, Iba K. 2008.** CO<sub>2</sub> regulator SLAC1 and its homologues are essential for anion homeostasis in plant cells. *Nature* **452**(7186): 483-U413.
- Niittylä T, Fuglsang AT, Palmgren MG, Frommer WB, Schulze WX. 2007.** Temporal analysis of sucrose-induced phosphorylation changes in plasma membrane proteins of Arabidopsis. *Mol Cell Proteomics* **6**(10): 1711-1726.
- Nishimura MT, Anderson RG, Cherkis KA, Law TF, Liu QL, Machius M, Nimchuk ZL, Yang L, Chung EH, El Kasmi F, et al. 2017.** TIR-only protein RBA1 recognizes a pathogen effector to regulate cell death in Arabidopsis. *Proc Natl Acad Sci U S A* **114**(10): E2053-E2062.
- Nishimura N, Hitomi K, Arvai AS, Rambo RP, Hitomi C, Cutler SR, Schroeder JI, Getzoff ED. 2009.** Structural mechanism of abscisic acid binding and signaling by dimeric PYR1. *Science (New York, N.Y.)* **326**(5958): 1373-1379.
- Nomura K, Debroy S, Lee YH, Pumplin N, Jones J, He SY. 2006.** A bacterial virulence protein suppresses host innate immunity to cause plant disease. *Science* **313**(5784): 220-223.
- Ntoukakis V, Saur IM, Conlan B, Rathjen JP. 2014.** The changing of the guard: the Pto/Prf receptor complex of tomato and pathogen recognition. *Curr Opin Plant Biol* **20**: 69-74.
- Nühse TS, Bottrill AR, Jones AM, Peck SC. 2007.** Quantitative phosphoproteomic analysis of plasma membrane proteins reveals regulatory mechanisms of plant innate immune responses. *The Plant journal : for cell and molecular biology* **51**(5): 931-940.

- Obulareddy N, Panchal S, Melotto M. 2013.** Guard Cell Purification and RNA Isolation Suitable for High-Throughput Transcriptional Analysis of Cell-Type Responses to Biotic Stresses. *Molecular Plant-Microbe Interactions* **26**(8): 844-849.
- Oecking C, Piotrowski M, Hagemeyer J, Hagemann K. 1997.** Topology and target interaction of the fusicoccin-binding 14-3-3 homologs of *Commelina communis*. *Plant Journal* **12**(2): 441-453.
- Ogasawara Y, Kaya H, Hiraoka G, Yumoto F, Kimura S, Kadota Y, Hishinuma H, Senzaki E, Yamagoe S, Nagata K, et al. 2008.** Synergistic activation of the Arabidopsis NADPH oxidase AtrbohD by Ca<sup>2+</sup> and phosphorylation. *J Biol Chem* **283**(14): 8885-8892.
- Ohashi-Ito K, Bergmann DC. 2006.** Arabidopsis FAMA controls the final proliferation/differentiation switch during stomatal development. *Plant Cell* **18**(10): 2493-2505.
- Okumura M, Inoue S, Kuwata K, Kinoshita T. 2016.** Photosynthesis Activates Plasma Membrane H<sup>+</sup>-ATPase via Sugar Accumulation. *Plant Physiol* **171**(1): 580-589.
- Okumura M, Inoue S, Takahashi K, Ishizaki K, Kohchi T, Kinoshita T. 2012.** Characterization of the plasma membrane H<sup>+</sup>-ATPase in the liverwort *Marchantia polymorpha*. *Plant Physiol* **159**(2): 826-834.
- Ortiz D, de Guillen K, Cesari S, Chalvon V, Gracy J, Padilla A, Kroj T. 2017.** Recognition of the Magnaporthe oryzae Effector AVR-Pia by the Decoy Domain of the Rice NLR Immune Receptor RGA5. *Plant Cell* **29**(1): 156-168.
- Osakabe Y, Watanabe T, Sugano SS, Ueta R, Ishihara R, Shinozaki K, Osakabe K. 2016.** Optimization of CRISPR/Cas9 genome editing to modify abiotic stress responses in plants. *Scientific Reports* **6**.
- Palevitz BA, Hepler PK. 1985.** Changes in dye coupling of stomatal cells of *Allium* and *Commelina* demonstrated by microinjection of Lucifer yellow. *Planta* **164**(4): 474-479.
- Park S-YY, Fung P, Nishimura N, Jensen DR, Fujii H, Zhao Y, Lumba S, Santiago J, Rodrigues A, Chow T-FF, et al. 2009.** Abscisic acid inhibits type 2C protein phosphatases via the PYR/PYL family of START proteins. *Science (New York, N.Y.)* **324**(5930): 1068-1071.
- Pecher P, Eschen-Lippold L, Herklotz S, Kuhle K, Naumann K, Bethke G, Uhrig J, Weyhe M, Scheel D, Lee J. 2014.** The Arabidopsis thaliana mitogen-activated protein kinases MPK3 and MPK6 target a subclass of 'VQ-motif'-containing proteins to regulate immune responses. *The New phytologist* **203**(2): 592-606.
- Peterson KM, Rychel AL, Torii KU. 2010.** Out of the Mouths of Plants: The Molecular Basis of the Evolution and Diversity of Stomatal Development. *Plant Cell* **22**(2): 296-306.
- Petutschnig EK, Jones AME, Serazetdinova L, Lipka U, Lipka V. 2010.** The Lysin Motif Receptor-like Kinase (LysM-RLK) CERK1 Is a Major Chitin-binding Protein in Arabidopsis thaliana and Subject to Chitin-induced Phosphorylation. *Journal of Biological Chemistry* **285**(37): 28902-28911.
- Pillitteri LJ, Torii KU. 2012.** Mechanisms of stomatal development. *Annu Rev Plant Biol* **63**: 591-614.
- Poncini L, Wyrsh I, Tendon VD, Vorley T, Boller T, Geldner N, Mettraux JP, Lehmann S. 2017.** In roots of Arabidopsis thaliana, the damage-associated molecular pattern

AtPep1 is a stronger elicitor of immune signalling than flg22 or the chitin heptamer. *PLoS one* **12**(10).

- Qi Z, Verma R, Gehring C, Yamaguchi Y, Zhao YC, Ryan CA, Berkowitz GA. 2010.** Ca<sup>2+</sup> signaling by plant *Arabidopsis thaliana* Pep peptides depends on AtPepR1, a receptor with guanylyl cyclase activity, and cGMP-activated Ca<sup>2+</sup> channels. *Proceedings of the National Academy of Sciences of the United States of America* **107**(49): 21193-21198.
- Radauer C, Lackner P, Breiteneder H. 2008.** The Bet v 1 fold: an ancient, versatile scaffold for binding of large, hydrophobic ligands. *Bmc Evolutionary Biology* **8**.
- Rairdan GJ, Moffett P. 2006.** Distinct domains in the ARC region of the potato resistance protein Rx mediate LRR binding and inhibition of activation. *Plant Cell* **18**(8): 2082-2093.
- Ranf S, Eschen-Lippold L, Frhlich K, Westphal L, Scheel D, Lee J. 2014.** Microbe-associated molecular pattern-induced calcium signaling requires the receptor-like cytoplasmic kinases, PBL1 and BIK1. *Bmc Plant Biology* **14**.
- Ranf S, Eschen-Lippold L, Pecher P, Lee J, Scheel D. 2011.** Interplay between calcium signalling and early signalling elements during defence responses to microbe- or damage-associated molecular patterns. *Plant J* **68**(1): 100-113.
- Ravensdale M, Bernoux M, Ve T, Kobe B, Thrall PH, Ellis JG, Dodds PN. 2012.** Intramolecular interaction influences binding of the Flax L5 and L6 resistance proteins to their AvrL567 ligands. *PLoS Pathog* **8**(11): e1003004.
- Robatzek S, Chinchilla D, Boller T. 2006.** Ligand-induced endocytosis of the pattern recognition receptor FLS2 in *Arabidopsis*. *Genes & development* **20**(5): 537-542.
- Rodrigues O, Reshetnyak G, Grondin A, Saijo Y, Leonhardt N, Maurel C, Verdoucq L. 2017.** Aquaporins facilitate hydrogen peroxide entry into guard cells to mediate ABA- and pathogen-triggered stomatal closure. *Proceedings of the National Academy of Sciences of the United States of America* **114**(34): 9200-9205.
- Roelfsema MRG, Prins HBA. 1995.** Effect of abscisic acid on stomatal opening in isolated epidermal strips of *abi* mutants of *Arabidopsis thaliana*. *Physiologia Plantarum* **95**(3): 373-378.
- Ronzier E, Corratgé-Faillie C, Sanchez F, Prado K, Brière C, Leonhardt N, Thibaud J-BB, Xiong TC. 2014.** CPK13, a Noncanonical Ca<sup>2+</sup>-Dependent Protein Kinase, Specifically Inhibits KAT2 and KAT1 Shaker K<sup>+</sup> Channels and Reduces Stomatal Opening. *Plant physiology* **166**(1): 314-326.
- Ruiz MT, Voinnet O, Baulcombe DC. 1998.** Initiation and maintenance of virus-induced gene silencing. *Plant Cell* **10**(6): 937-946.
- Rusconi F, Simeoni F, Francia P, Cominelli E, Conti L, Riboni M, Simoni L, Martin CR, Tonelli C, Galbiati M. 2013.** The *Arabidopsis thaliana* MYB60 promoter provides a tool for the spatio-temporal control of gene expression in stomatal guard cells. *Journal of experimental botany* **64**(11): 3361-3371.
- Santiago J, Rodrigues A, Saez A, Rubio S, Antoni R, Dupeux F, Park S, Márquez J, Cutler SR, Rodriguez PL. 2009.** Modulation of drought resistance by the abscisic acid receptor PYL5 through inhibition of clade A PP2Cs. *The Plant Journal* **60**(4): 575-588.

- Sarris PF, Cevik V, Dagdas G, Jones JD, Krasileva KV. 2016.** Comparative analysis of plant immune receptor architectures uncovers host proteins likely targeted by pathogens. *BMC Biol* **14**: 8.
- Sarris PF, Duxbury Z, Huh SU, Ma Y, Segonzac C, Sklenar J, Derbyshire P, Cevik V, Rallapalli G, Saucet SB, et al. 2015.** A Plant Immune Receptor Detects Pathogen Effectors that Target WRKY Transcription Factors. *Cell* **161**(5): 1089-1100.
- Sasaki T, Mori IC, Furuichi T, Munemasa S, Toyooka K, Matsuoka K, Murata Y, Yamamoto Y. 2010.** Closing Plant Stomata Requires a Homolog of an Aluminum-Activated Malate Transporter. *Plant and Cell Physiology* **51**(3): 354-365.
- Sato A, Sato Y, Fukao Y, Fujiwara M, Umezawa T, Shinozaki K, Hibi T, Taniguchi M, Miyake H, Goto DB, et al. 2009.** Threonine at position 306 of the KAT1 potassium channel is essential for channel activity and is a target site for ABA-activated SnRK2/OST1/SnRK2.6 protein kinase. *Biochemical Journal* **424**: 439-448.
- Saucet SB, Ma Y, Sarris PF, Furzer OJ, Sohn KH, Jones JD. 2015.** Two linked pairs of Arabidopsis TNL resistance genes independently confer recognition of bacterial effector AvrRps4. *Nat Commun* **6**: 6338.
- Saur IM, Conlan BF, Rathjen JP. 2015.** The N-terminal domain of the tomato immune protein Prf contains multiple homotypic and Pto kinase interaction sites. *J Biol Chem* **290**(18): 11258-11267.
- Scherzer S, Maierhofer T, Al-Rasheid KAS, Geiger D, Hedrich R. 2012.** Multiple Calcium-Dependent Kinases Modulate ABA-Activated Guard Cell Anion Channels. *Molecular Plant* **5**(6): 1409-1412.
- Schroeder JI. 1989.** Quantitative analysis of outward rectifying K<sup>+</sup> channel currents in guard cell protoplasts from *Vicia faba*. *J Membr Biol* **107**(3): 229-235.
- Schroeder JI, Hagiwara S. 1989.** Cytosolic Calcium Regulates Ion Channels in the Plasma-Membrane of *Vicia-Faba* Guard-Cells. *Nature* **338**(6214): 427-430.
- Schwessinger B, Roux M, Kadota Y, Ntoukakis V, Sklenar J, Jones A, Zipfel C. 2011.** Phosphorylation-dependent differential regulation of plant growth, cell death, and innate immunity by the regulatory receptor-like kinase BAK1. *PLoS genetics* **7**(4).
- Segonzac C, Feike D, Gimenez-Ibanez S, Hann DR, Zipfel C, Rathjen JP. 2011.** Hierarchy and Roles of Pathogen-Associated Molecular Pattern-Induced Responses in *Nicotiana benthamiana*. *Plant physiology* **156**(2): 687-699.
- Segonzac C, Macho AP, Sanmartin M, Ntoukakis V, Sanchez-Serrano J, Zipfel C. 2014.** Negative control of BAK1 by protein phosphatase 2A during plant innate immunity. *The EMBO journal* **33**(18): 2069-2079.
- Sela H, Spiridon LN, Ashkenazi H, Bhullar NK, Brunner S, Petrescu AJ, Fahima T, Keller B, Jordan T. 2014.** Three-dimensional modeling and diversity analysis reveals distinct AVR recognition sites and evolutionary pathways in wild and domesticated wheat Pm3 R genes. *Mol Plant Microbe Interact* **27**(8): 835-845.
- Shan L, He P, Li J, Heese A, Peck SC, Nurnberger T, Martin GB, Sheen J. 2008.** Bacterial effectors target the common signaling partner BAK1 to disrupt multiple MAMP receptor-signaling complexes and impede plant immunity. *Cell Host Microbe* **4**(1): 17-27.
- Shao F, Golstein C, Ade J, Stoutemyer M, Dixon JE, Innes RW. 2003.** Cleavage of Arabidopsis PBS1 by a bacterial type III effector. *Science* **301**(5637): 1230-1233.

- Shao ZQ, Xue JY, Wu P, Zhang YM, Wu Y, Hang YY, Wang B, Chen JQ. 2016.** Large-Scale Analyses of Angiosperm Nucleotide-Binding Site-Leucine-Rich Repeat Genes Reveal Three Anciently Diverged Classes with Distinct Evolutionary Patterns. *Plant physiology* **170**(4): 2095-2109.
- Sharma R, Rawat V, Suresh CG. 2017.** Genome-wide identification and tissue-specific expression analysis of nucleotide binding site-leucine rich repeat gene family in *Cicer arietinum* (kabuli chickpea). *Genomics Data* **14**: 24-31.
- Sheriff DW. 1979.** Stomatal aperture and the sensing of the environment by guard cells. *Plant, Cell and Environment* **2**: 15-22.
- Shi H, Shen Q, Qi Y, Yan H, Nie H, Chen Y, Zhao T, Katagiri F, Tang D. 2013.** BR-SIGNALING KINASE1 physically associates with FLAGELLIN SENSING2 and regulates plant innate immunity in *Arabidopsis*. *The Plant cell* **25**(3): 1143-1157.
- Shimada TL, Shimada T, Hara-Nishimura I. 2010.** A rapid and non-destructive screenable marker, FAST, for identifying transformed seeds of *Arabidopsis thaliana*. *Plant J* **61**(3): 519-528.
- Shimazaki K, Doi M, Assmann SM, Kinoshita T. 2007.** Light regulation of stomatal movement. *Annual review of plant biology* **58**: 219-247.
- Shimazaki K, Iino M, Zeiger E. 1986.** Blue Light-Dependent Proton Extrusion by Guard-Cell Protoplasts of *Vicia-Faba*. *Nature* **319**(6051): 324-326.
- Shinya T, Yamaguchi K, Desaki Y, Yamada K, Narisawa T, Kobayashi Y, Maeda K, Suzuki M, Tanimoto T, Takeda J, et al. 2014.** Selective regulation of the chitin-induced defense response by the *Arabidopsis* receptor-like cytoplasmic kinase PBL27. *Plant Journal* **79**(1): 56-66.
- Shiu SH, Bleecker AB. 2001.** Receptor-like kinases from *Arabidopsis* form a monophyletic gene family related to animal receptor kinases. *Proc Natl Acad Sci U S A* **98**(19): 10763-10768.
- Shope JC, DeWald DB, Mott KA. 2003.** Changes in surface area of intact guard cells are correlated with membrane internalization. *Plant physiology* **133**(3): 1314-1321.
- Shpak ED, McAbee JM, Pillitteri LJ, Torii KU. 2005.** Stomatal patterning and differentiation by synergistic interactions of receptor kinases. *Science* **309**(5732): 290-293.
- Sinapidou E, Williams K, Nott L, Bahkt S, Tor M, Crute I, Bittner-Eddy P, Beynon J. 2004.** Two TIR:NB:LRR genes are required to specify resistance to *Peronospora parasitica* isolate Cala2 in *Arabidopsis*. *Plant J* **38**(6): 898-909.
- Sirichandra C, Gu D, Hu H-CC, Davanture M, Lee S, Djaoui M, Valot B, Zivy M, Leung J, Merlot S, et al. 2009.** Phosphorylation of the *Arabidopsis* AtrbohF NADPH oxidase by OST1 protein kinase. *FEBS letters* **583**(18): 2982-2986.
- Smirnova OG, Ibragimova SS, Kochetov AV. 2012.** Simple database to select promoters for plant transgenesis. *Transgenic Res* **21**(2): 429-437.
- Sohn KH, Segonzac C, Rallapalli G, Sarris PF, Woo JY, Williams SJ, Newman TE, Paek KH, Kobe B, Jones JDG. 2014.** The Nuclear Immune Receptor RPS4 Is Required for RRS1(SLH1)-Dependent Constitutive Defense Activation in *Arabidopsis thaliana*. *PLoS genetics* **10**(10).
- Spallek T, Beck M, Ben Khaled S, Salomon S, Bourdais G, Schellmann S, Robatzek S. 2013.** ESCRT-I mediates FLS2 endosomal sorting and plant immunity. *PLoS genetics* **9**(12).

- Steinbrenner AD, Goritschnig S, Staskawicz BJ. 2015.** Recognition and activation domains contribute to allele-specific responses of an Arabidopsis NLR receptor to an oomycete effector protein. *PLoS Pathog* **11**(2): e1004665.
- Suarez-Rodriguez MC, Adams-Phillips L, Liu YD, Wang HC, Su SH, Jester PJ, Zhang SQ, Bent AF, Krysan PJ. 2007.** MEKK1 is required for flg22-induced MPK4 activation in Arabidopsis plants. *Plant physiology* **143**(2): 661-669.
- Sun Y, Li L, Macho AP, Han Z, Hu Z, Zipfel C, Zhou J-MM, Chai J. 2013.** Structural basis for flg22-induced activation of the Arabidopsis FLS2-BAK1 immune complex. *Science (New York, N.Y.)* **342**(6158): 624-628.
- Sutter JU, Sieben C, Hartel A, Eisenach C, Thiel G, Blatt MR. 2007.** Abscisic acid triggers the endocytosis of the Arabidopsis KAT1 K<sup>+</sup> channel and its recycling to the plasma membrane. *Current Biology* **17**(16): 1396-1402.
- Takahashi K, Hayashi K, Kinoshita T. 2012.** Auxin activates the plasma membrane H<sup>+</sup>-ATPase by phosphorylation during hypocotyl elongation in Arabidopsis. *Plant Physiol* **159**(2): 632-641.
- Takahashi Y, Ebisu Y, Kinoshita T, Doi M, Okuma E, Murata Y, Shimazaki K. 2013.** bHLH Transcription Factors That Facilitate K<sup>+</sup> Uptake During Stomatal Opening Are Repressed by Abscisic Acid Through Phosphorylation. *Science signaling* **6**(280).
- Takahashi Y, Kinoshita T, Matsumoto M, Shimazaki K. 2016.** Inhibition of the Arabidopsis bHLH transcription factor by monomerization through abscisic acid-induced phosphorylation. *Plant Journal* **87**(6): 559-567.
- Takemiya A, Kinoshita T, Asanuma M, Shimazaki K. 2006.** Evidence for the involvement of protein phosphatase 1 in the blue light signaling of stomatal opening. *Plant and Cell Physiology* **47**: S207-S207.
- Takemiya A, Shimazaki K. 2010.** Phosphatidic Acid Inhibits Blue Light-Induced Stomatal Opening via Inhibition of Protein Phosphatase. *Plant physiology* **153**(4): 1555-1562.
- Takemiya A, Shimazaki K. 2016.** Arabidopsis phot1 and phot2 phosphorylate BLUS1 kinase with different efficiencies in stomatal opening. *Journal of Plant Research* **129**(2): 167-174.
- Takemiya A, Sugiyama N, Fujimoto H, Tsutsumi T, Yamauchi S, Hiyama A, Tada Y, Christie JM, Shimazaki KI. 2013a.** Phosphorylation of BLUS1 kinase by phototropins is a primary step in stomatal opening. *Nature Communications* **4**.
- Takemiya A, Yamauchi S, Yano T, Ariyoshi C, Shimazaki K. 2013b.** Identification of a Regulatory Subunit of Protein Phosphatase 1 Which Mediates Blue Light Signaling for Stomatal Opening. *Plant and Cell Physiology* **54**(1): 24-35.
- Takken FLW, Albrecht M, Tameling WIL. 2006.** Resistance proteins: molecular switches of plant defence. *Current opinion in plant biology* **9**(4): 383-390.
- Takken FLW, Goverse A. 2012.** How to build a pathogen detector: structural basis of NB-LRR function. *Current opinion in plant biology* **15**(4): 375-384.
- Tameling WIL, Vossen JH, Albrecht M, Lengauer T, Berden JA, Haring MA, Cornelissen BJC, Takken FLW. 2006.** Mutations in the NB-ARC domain of I-2 that impair ATP hydrolysis cause autoactivation. *Plant physiology* **140**(4): 1233-1245.
- Tamnanloo F, Damen H, Jangra R, Lee JS. 2018.** MAP KINASE PHOSPHATASE1 controls cell fate transition during stomatal development. *Plant Physiol*.

- Tan XP, Meyers BC, Kozik A, Al West M, Morgante M, St Clair DA, Bent AF, Michelmore RW. 2007.** Global expression analysis of nucleotide binding site-leucine rich repeat-encoding and related genes in Arabidopsis. *Bmc Plant Biology* **7**.
- Thiele K, Wanner G, Kindzierski V, Jurgens G, Mayer U, Pahl F, Assaad FF. 2009.** The timely deposition of callose is essential for cytokinesis in Arabidopsis. *Plant Journal* **58**(1): 13-26.
- Thor K, Peiter E. 2014.** Cytosolic calcium signals elicited by the pathogen-associated molecular pattern flg22 in stomatal guard cells are of an oscillatory nature. *New Phytologist* **204**(4): 873-881.
- Tian W, Hou CC, Ren ZJ, Pan YJ, Jia JJ, Zhang HW, Bai FL, Zhang P, Zhu HF, He YK, et al. 2015.** A molecular pathway for CO<sub>2</sub> response in Arabidopsis guard cells. *Nature Communications* **6**.
- Vahisalu T, Kollist H, Wang YF, Nishimura N, Chan WY, Valerio G, Lamminmaki A, Brosche M, Moldau H, Desikan R, et al. 2008.** SLAC1 is required for plant guard cell S-type anion channel function in stomatal signalling. *Nature* **452**(7186): 487-U415.
- Vahisalu T, Puzorjova I, Brosche M, Valk E, Lepiku M, Moldau H, Pechter P, Wang YS, Lindgren O, Salojarvi J, et al. 2010.** Ozone-triggered rapid stomatal response involves the production of reactive oxygen species, and is controlled by SLAC1 and OST1. *Plant Journal* **62**(3): 442-453.
- van der Hoorn RA, Kamoun S. 2008.** From Guard to Decoy: a new model for perception of plant pathogen effectors. *Plant Cell* **20**(8): 2009-2017.
- Virlouvet L, Fromm M. 2015.** Physiological and transcriptional memory in guard cells during repetitive dehydration stress. *New Phytol* **205**(2): 596-607.
- Vlad F, Rubio S, Rodrigues A, Sirichandra C, Belin C, Robert N, Leung J, Rodriguez PL, Laurière C, Merlot S. 2009.** Protein phosphatases 2C regulate the activation of the Snf1-related kinase OST1 by abscisic acid in Arabidopsis. *The Plant cell* **21**(10): 3170-3184.
- Waadt R, Manalansan B, Rauniyar N, Munemasa S, Booker MA, Brandt B, Waadt C, Nusinow DA, Kay SA, Kunz HH, et al. 2015.** Identification of Open Stomata1-Interacting Proteins Reveals Interactions with Sucrose Non-fermenting1-Related Protein Kinases2 and with Type 2A Protein Phosphatases That Function in Abscisic Acid Responses. *Plant Physiol* **169**(1): 760-779.
- Wan JR, Tanaka K, Zhang XC, Son GH, Brechenmacher L, Tran HNN, Stacey G. 2012.** LYK4, a Lysin Motif Receptor-Like Kinase, Is Important for Chitin Signaling and Plant Innate Immunity in Arabidopsis. *Plant physiology* **160**(1): 396-406.
- Wang C, Hu HH, Qin X, Zeise B, Xu DY, Rappel WJ, Boron WF, Schroeder JI. 2016.** Reconstitution of CO<sub>2</sub> Regulation of SLAC1 Anion Channel and Function of CO<sub>2</sub>-Permeable PIP2;1 Aquaporin as CARBONIC ANHYDRASE4 Interactor. *Plant Cell* **28**(2): 568-582.
- Wang G, Roux B, Feng F, Guy E, Li L, Li N, Zhang X, Lautier M, Jardinaud MF, Chabannes M, et al. 2015.** The Decoy Substrate of a Pathogen Effector and a Pseudokinase Specify Pathogen-Induced Modified-Self Recognition and Immunity in Plants. *Cell Host Microbe* **18**(3): 285-295.

- Wang Y, Li J, Hou S, Wang X, Li Y, Ren D, Chen S, Tang X, Zhou JM. 2010.** A *Pseudomonas syringae* ADP-ribosyltransferase inhibits Arabidopsis mitogen-activated protein kinase kinases. *Plant Cell* **22**(6): 2033-2044.
- Wang Y, Noguchi K, Ono N, Inoue S, Terashima I, Kinoshita T. 2014.** Overexpression of plasma membrane H<sup>+</sup>-ATPase in guard cells promotes light-induced stomatal opening and enhances plant growth. *Proceedings of the National Academy of Sciences of the United States of America* **111**(1): 533-538.
- Wang Y, Yang J, Yi J. 2012.** Redox Sensing by Proteins: Oxidative Modifications on Cysteines and the Consequent Events. *Antioxidants & Redox Signaling* **16**(7): 649-657.
- Werner S, Engler C, Weber E, Gruetzner R, Marillonnet S. 2011.** A Modular Cloning System for Standardized Assembly of Multigene Constructs. *PloS one* **6**(2).
- Wille AC, Lucas WJ. 1984.** Ultrastructural and histochemical studies on guard cells. *Planta* **160**(2): 129-142.
- Williams SJ, Sohn KH, Wan L, Bernoux M, Sarris PF, Segonzac C, Ve T, Ma Y, Saucet SB, Ericsson DJ, et al. 2014.** Structural basis for assembly and function of a heterodimeric plant immune receptor. *Science* **344**(6181): 299-303.
- Wong SC, Cowan IR, Farquhar GD. 1979.** Stomatal Conductance Correlates with Photosynthetic Capacity. *Nature* **282**(5737): 424-426.
- Wu CH, Abd-El-Haliem A, Bozkurt TO, Belhaj K, Terauchi R, Vossen JH, Kamoun S. 2017.** NLR network mediates immunity to diverse plant pathogens. *Proc Natl Acad Sci U S A* **114**(30): 8113-8118.
- Wyrsh I, Dominguez-Ferreras A, Geldner N, Boller T. 2015.** Tissue-specific FLAGELLIN-SENSING 2 (FLS2) expression in roots restores immune responses in Arabidopsis fls2 mutants. *New Phytologist* **206**(2): 774-784.
- Xiang T, Zong N, Zou Y, Wu Y, Zhang J, Xing W, Li Y, Tang X, Zhu L, Chai J, et al. 2008.** *Pseudomonas syringae* effector AvrPto blocks innate immunity by targeting receptor kinases. *Curr Biol* **18**(1): 74-80.
- Xin XF, Nomura K, Aung K, Velasquez AC, Yao J, Boutrot F, Chang JH, Zipfel C, He SY. 2016.** Bacteria establish an aqueous living space in plants crucial for virulence. *Nature* **539**(7630): 524-529.
- Xue SW, Hu HH, Ries A, Merilo E, Kollist H, Schroeder JI. 2011.** Central functions of bicarbonate in S-type anion channel activation and OST1 protein kinase in CO<sub>2</sub> signal transduction in guard cell. *Embo Journal* **30**(8): 1645-1658.
- Yamada K, Yamaguchi K, Shirakawa T, Nakagami H, Mine A, Ishikawa K, Fujiwara M, Narusaka M, Narusaka Y, Ichimura K, et al. 2016.** The Arabidopsis CERK1-associated kinase PBL27 connects chitin perception to MAPK activation. *Embo Journal* **35**(22): 2468-2483.
- Yamauchi S, Takemiya A, Sakamoto T, Kurata T, Tsutsumi T, Kinoshita T, Shimazaki K. 2016.** The Plasma Membrane H<sup>+</sup>-ATPase AHA1 Plays a Major Role in Stomatal Opening in Response to Blue Light. *Plant physiology* **171**(4): 2731-2743.
- Yang Y, Costa A, Leonhardt N, Siegel RS, Schroeder JI. 2008.** Isolation of a strong Arabidopsis guard cell promoter and its potential as a research tool. *Plant methods* **4**: 6.

- Yin P, Fan H, Hao Q, Yuan XQ, Wu D, Pang YX, Yan CY, Li WQ, Wang JW, Yan N. 2009.** Structural insights into the mechanism of abscisic acid signaling by PYL proteins. *Nature Structural & Molecular Biology* **16**(12): 1230-U1242.
- Yoshida R, Hobo T, Ichimura K, Mizoguchi T, Takahashi F, Aronso J, Ecker JR, Shinozaki K. 2002.** ABA-activated SnRK2 protein kinase is required for dehydration stress signaling in Arabidopsis. *Plant & cell physiology* **43**(12): 1473-1483.
- Yoshida R, Umezawa T, Mizoguchi T, Takahashi S, Takahashi F, Shinozaki K. 2006.** The regulatory domain of SRK2E/OST1/SnRK2.6 interacts with ABI1 and integrates abscisic acid (ABA) and osmotic stress signals controlling stomatal closure in Arabidopsis. *The Journal of biological chemistry* **281**(8): 5310-5318.
- Yoshimura S, Yamanouchi U, Katayose Y, Toki S, Wang ZX, Kono I, Kurata N, Yano M, Iwata N, Sasaki T. 1998.** Expression of Xa1, a bacterial blight-resistance gene in rice, is induced by bacterial inoculation. *Proc Natl Acad Sci U S A* **95**(4): 1663-1668.
- Zhang A, Ren HM, Tan YQ, Qi GN, Yao FY, Wu GL, Yang LW, Hussain J, Sun SJ, Wang YF. 2016.** S-Type Anion Channels SLAC1 and SLAH3 Function as Essential Negative Regulators of Inward K<sup>+</sup> Channels and Stomatal Opening in Arabidopsis. *Plant Cell* **28**(4): 949-965.
- Zhang J, Li W, Xiang T, Liu Z, Laluk K, Ding X, Zou Y, Gao M, Zhang X, Chen S, et al. 2010.** Receptor-like cytoplasmic kinases integrate signaling from multiple plant immune receptors and are targeted by a *Pseudomonas syringae* effector. *Cell host & microbe* **7**(4): 290-301.
- Zhang J, Li W, Xiang TT, Liu ZX, Laluk K, Ding XJ, Zou Y, Gao MH, Zhang XJ, Chen S, et al. 2010.** Receptor-like Cytoplasmic Kinases Integrate Signaling from Multiple Plant Immune Receptors and Are Targeted by a *Pseudomonas syringae* Effector. *Cell host & microbe* **7**(4): 290-301.
- Zhang J, Shao F, Li Y, Cui H, Chen L, Li H, Zou Y, Long C, Lan L, Chai J, et al. 2007.** A *Pseudomonas syringae* effector inactivates MAPKs to suppress PAMP-induced immunity in plants. *Cell Host Microbe* **1**(3): 175-185.
- Zhang S, Klessig DF. 2001.** MAPK cascades in plant defense signaling. *Trends in plant science* **6**(11): 520-527.
- Zhang X, Bernoux M, Bentham AR, Newman TE, Ve T, Casey LW, Raaymakers TM, Hu J, Croll TI, Schreiber KJ, et al. 2017.** Multiple functional self-association interfaces in plant TIR domains. *Proc Natl Acad Sci U S A* **114**(10): E2046-E2052.
- Zhang X, Takemiya A, Kinoshita T, Shimazaki KI. 2007.** Nitric oxide inhibits blue light-specific stomatal opening via abscisic acid signaling pathways in *Vicia* guard cells. *Plant and Cell Physiology* **48**(5): 715-723.
- Zhang Z, Wu Y, Gao M, Zhang J, Kong Q, Liu Y, Ba H, Zhou J, Zhang Y. 2012.** Disruption of PAMP-induced MAP kinase cascade by a *Pseudomonas syringae* effector activates plant immunity mediated by the NB-LRR protein SUMM2. *Cell Host Microbe* **11**(3): 253-263.
- Zheng X, Kang S, Jing Y, Ren Z, Li L, Zhou JM, Berkowitz G, Shi J, Fu A, Lan W, et al. 2018.** Danger-Associated Peptides Close Stomata by OST1-Independent Activation of Anion Channels in Guard Cells. *Plant Cell* **30**(5): 1132-1146.
- Zheng XY, Spivey NW, Zeng WQ, Liu PP, Fu ZQ, Klessig DF, He SY, Dong XN. 2012.** Coronatine Promotes *Pseudomonas syringae* Virulence in Plants by Activating a

Signaling Cascade that Inhibits Salicylic Acid Accumulation. *Cell host & microbe* **11**(6): 587-596.

**Zhou ZY, Wu YJ, Yang YQ, Du MM, Zhang XJ, Guo Y, Li CY, Zhou JM. 2015.** An Arabidopsis Plasma Membrane Proton ATPase Modulates JA Signaling and Is Exploited by the *Pseudomonas syringae* Effector Protein AvrB for Stomatal Invasion. *Plant Cell* **27**(7): 2032-2041.

**Zhu XY, Dunand C, Snedden W, Galaud JP. 2015.** CaM and CML emergence in the green lineage. *Trends in plant science* **20**(8): 483-489.

**Zipfel C, Robatzek S, Navarro L, Oakeley EJ, Jones JD, Felix G, Boller T. 2004.** Bacterial disease resistance in Arabidopsis through flagellin perception. *Nature* **428**(6984): 764-767.